The Abdus Salam International Centre for Theoretical Physics

United Nations Educational, Scientific and Cultural Organization

IAEA International Atomic Energy Agency

2332-15

School on Synchrotron and FEL Based Methods and their Multi-Disciplinary Applications

19 - 30 March 2012

ARPES

Andrea Goldoni

Sincrotrone Trieste

Angle resolved photoemission: Interacting electrons

Part III

Papers: S. Hüfner et al., J. Electron Spectroscopy Rel. Phenom. 100 (1999)
A. Damascelli et al., Rev. Modern Phys. (2005)
F. Reinert et al., New J. Phys. 7 (2005)
X.J. Zhou et al., J. Electron Spectroscopy Rel. Phenom. 126 (2002)

Thanks to: A. Damascelli, Z.X. Shen, R. Claessen, Ph. Hofmann and E. Rotemberg from whose I have taken slides and figures

Outline

- Interacting electrons: many-body physics
- Single particle spectral density function $A(k, \omega)$
- The self-energy
- The “kinky” physics: electron-phonon interactions
- 1D System: Luttinger liquid. Spinon and holon dispersion
- Mott-Hubbard insulator
- Fullerenes

Interaction effects between electrons: "Many-body Physics"

Many body effects are due to the interactions between the electrons and each other, or with excitations inside the crystal :

1) A "many-body" problem: intrinsically hard to calculate and understand

2) Responsible for many surprising phenomena:
Superconductivity, Magnetism, Density Waves, ...

Non-Interacting

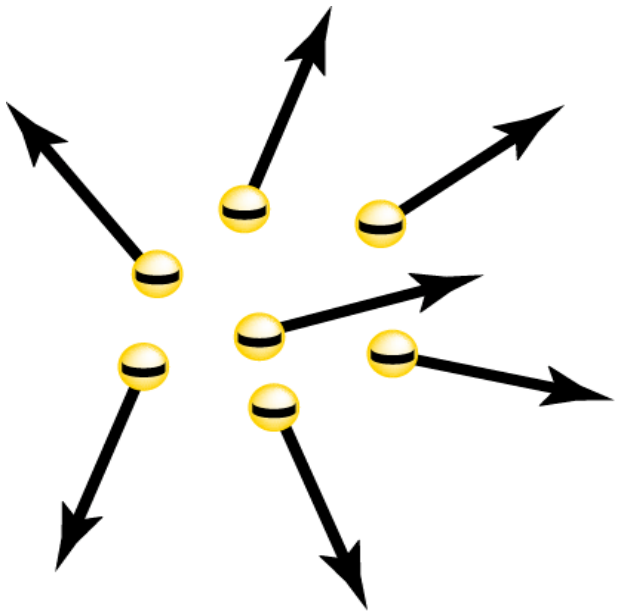

Interacting

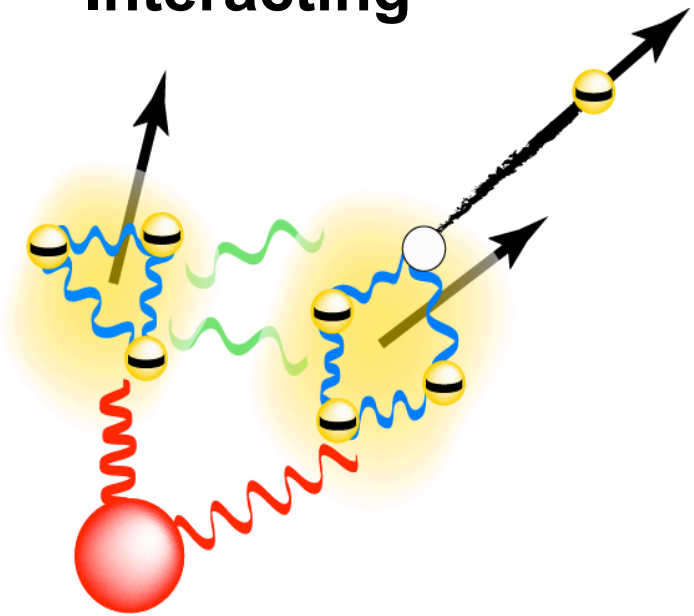

Interacting Electrons: many-body physics

$$\sum_{j=1}^{N} A(r_j)\cdot p_j = A\cdot p$$

$$I(E_{kin}) = \frac{2e^2\pi}{m^2\hbar}\sum_f \left|\langle N, f|A\cdot p|N, i\rangle\right|^2 \rho\left(E_f^N\right)\delta\left(E_f^N - E_i^N - h\nu\right)$$

$$I(E_{kin}) = \sum_f \left|M_{fi}\right|^2 \rho\left(E_f^N\right)\delta\left(E_f^N - E_i^N - h\nu\right)$$

The final state relevant for photoemission must contain a free electron with wave vector **k** and energy E_{kin}.

$$I(E_{kin}) = \frac{2e^2\pi}{m^2\hbar}\sum_x \left|\langle k, N-1, x|A\cdot p|N, i\rangle\right|^2 \rho\left(E_x^{N-1}\right)\rho\left(E_{kin}\right)\delta\left(E_{kin} + E_x^{N-1} - E_i^N - h\nu\right)$$

Now the sum is over all the possible final excited states x of the (N-1)-electrons system left behind by the photoelectron. The essential step in simplifying this expression consists in the factorization of the final state wave function $|k, N\text{-}1, x\rangle$ as the product of the photoelectron ϕ_k and the $\phi_x(N\text{-}1)$ electrons wave functions.

In second quantization $|k, N-1, x\rangle \approx \phi_k \phi_x (N-1) = c_k^+ |N-1, x\rangle$

This involves two assumptions:

1) Sudden approx.: The photoelectron decuples immediately from the photohole left behind and carries no information on the relaxation of the (N-1) system

2) We neglect inelastic losses of the photoelectron on its travel inside the crystal

$$I(E_{kin}) = \frac{2e^2\pi}{m^2\hbar} \sum_{j=1}^{N} |M_{k,kj}|^2 \sum_x |\langle N-1, x | c_{kj} | N, i\rangle|^2 \rho\left(E_x^{N-1}\right) \rho\left(E_{kin}\right) \delta\left(E_{kin} + E_x^{N-1} - E_i^N - h\nu\right)$$

where

$$|N, i\rangle = \frac{1}{N} c_{kj}^+ c_{kj} |N, i\rangle \qquad M_{k,kj} = \frac{1}{N} c_k A(r_j) p_j c_{kj}^+ = \frac{1}{N} \langle k | A(r_j) p_j | kj\rangle$$

Transition probability for interacting electrons

$$I(E_{kin}) = \frac{2e^2\pi}{m^2\hbar}\sum_{j=1}^{N}\left|M_{k,kj}\right|^2\sum_{x}\left|\langle N-1,x|c_{kj}|N,i\rangle\right|^2\rho\left(E_x^{N-1}\right)\rho\left(E_{kin}\right)\delta\left(E_{kin}+E_x^{N-1}-E_i^N-h\nu\right)$$

c_{kj} destroys an electron with momentum kj from the initial state $|N,i\rangle$

$|N\text{-}1,x\rangle$ is an eigenstate of the (N-1) Hamiltonian,
while the (N-1) wave function $c_{kj}|N,i\rangle$ is not

We can write $E_i^N - E_x^{N-1} = (E_i^N - E_0^{N-1}) - (E_x^{N-1} - E_0^{N-1}) = \varepsilon_0^i - \Delta\varepsilon_x$

Interpretation: The photon absorption suddenly creates an (N-1)-electron state $c_{kj}|N,i\rangle$ that is not an eigenstate of the (N-1) Hamiltonian (frozen state). The spectrum is the projection of this frozen states over the "fully relaxed" eigenstates $|N\text{-}1,x\rangle$ of the (N-1) Hamiltonian. We call "fundamental peak" (or "elastic peak", or "coherent peak") the transition leaving the (N-1)-system in the ground state $|N\text{-}1,0\rangle$ that correspond to a photoelectron with kinetic energy $E_{kin} = (E_i^N - E_0^{N-1}) + h\nu = \varepsilon_0^i + h\nu$
The spectrum also exhibits peaks at lower kinetic energies by quantities $-\Delta\varepsilon_x$ when the system is left in an excited $|N\text{-}1,x\rangle$ state.

Interacting electrons

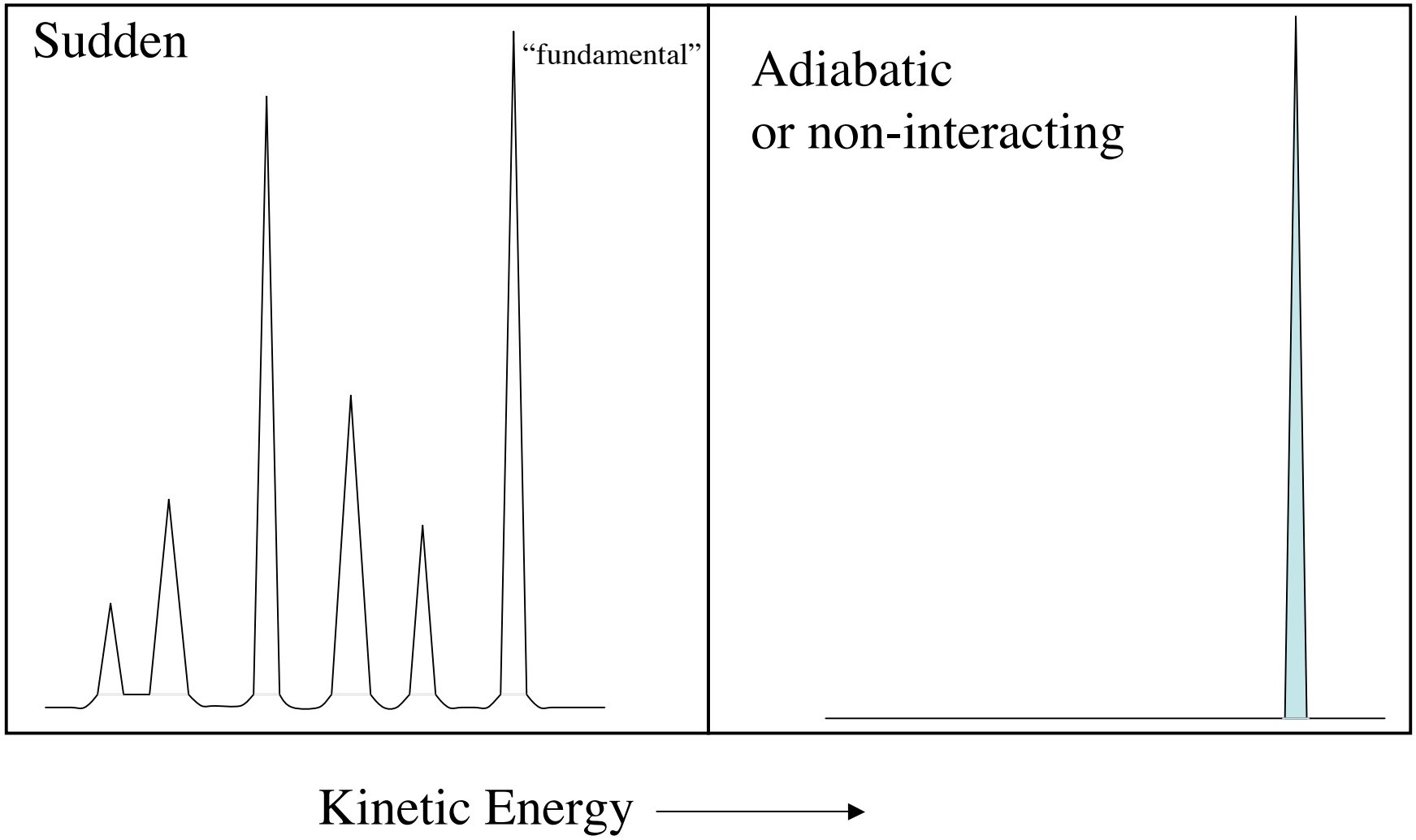

non-interacting system

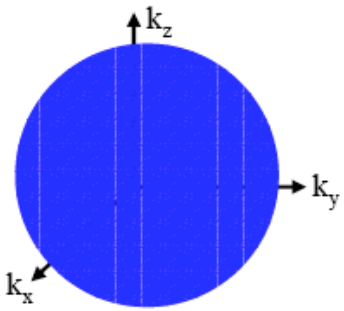

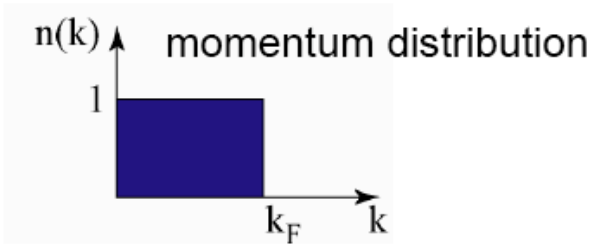

interacting system

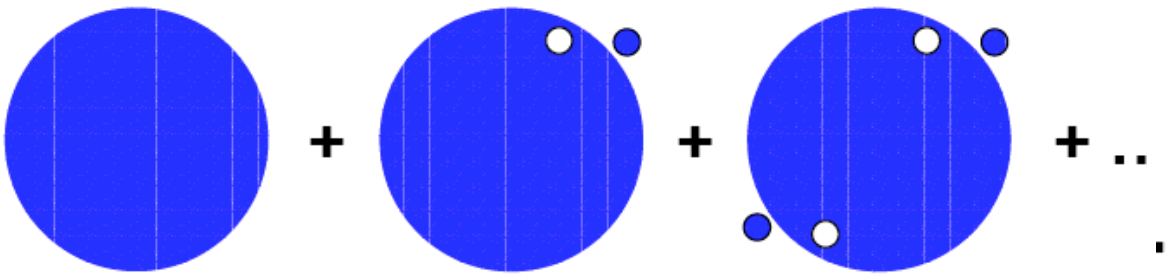

quasiparticle weight $Z < 1$

1:1 mapping

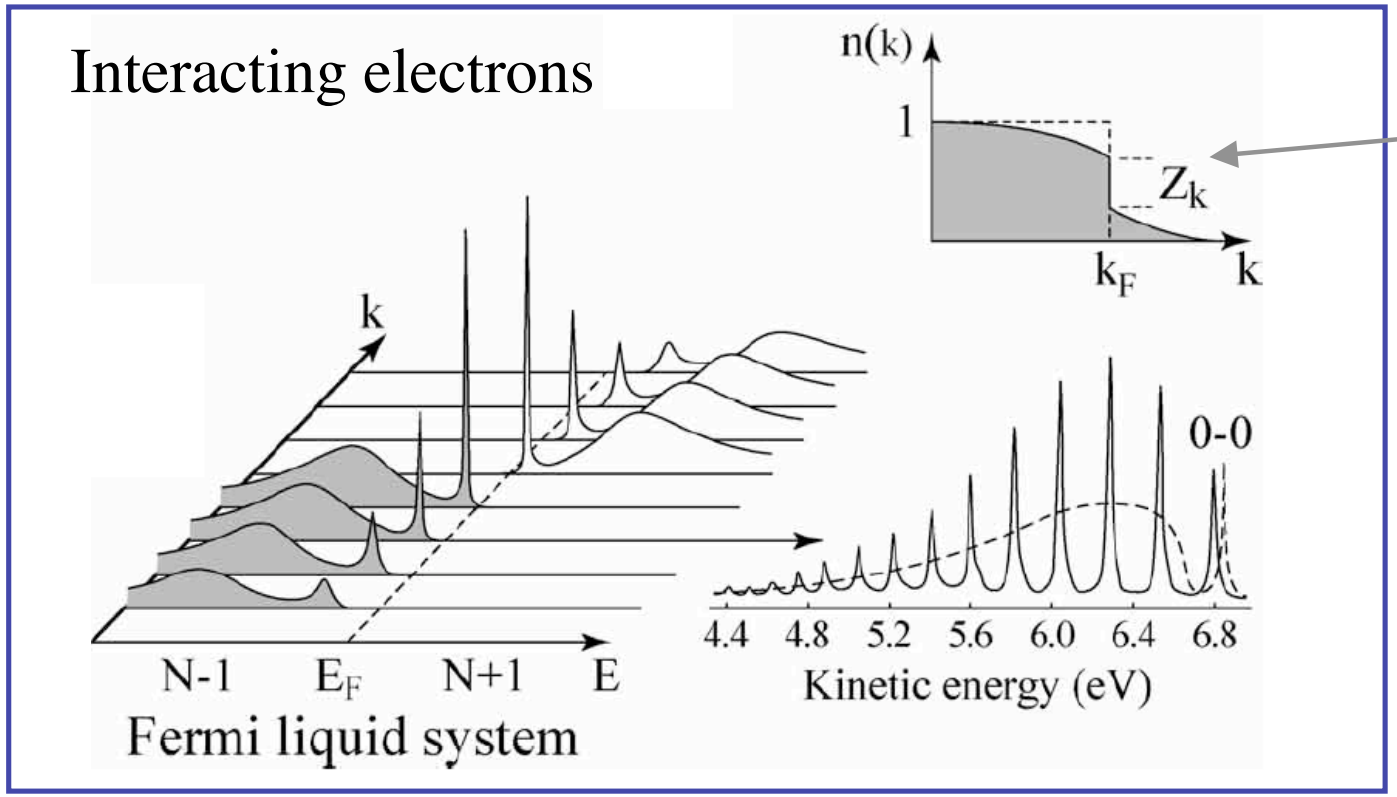

?

Still no information on the lifetime of the states (width of the peaks)

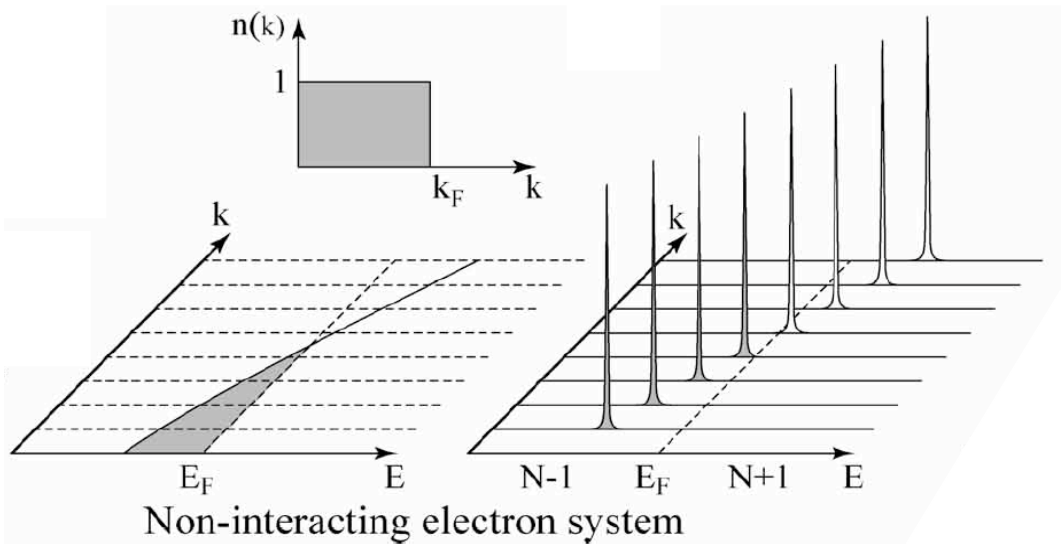

A bit of math and the quasi-particles

It is useful to introduce the one-electron removal Green function formalism:

$$G(kj,\omega j) = \sum_x \frac{\left|\langle N-1,x|c_{kj}|N,i\rangle\right|^2}{\omega j - E_x^{N-1} + E_i^N - i\eta}$$

η can be infinitesimally small

c_{kj} destroys an electron with momentum kj and energy ωj from the initial state $|N,i\rangle$

… and the corresponding spectral density function $A(kj,\omega j)=(1/\pi)\mathrm{Im}G(kj,\omega j)$
In the limit $\eta \to 0$:

$$A(kj,\omega j) = \frac{1}{\pi}\sum_x \left|\langle N-1,x|c_{kj}|N,i\rangle\right|^2 \delta\left(\omega j - E_x^{N-1} + E_i^N\right) = \frac{1}{\pi}\mathrm{Im}\,G(kj,\omega j)$$

Comparing to:

$$I(E_{kin}) = \frac{2e^2\pi}{m^2\hbar}\sum_{j=1}^{N}\left|M_{k,kj}\right|^2 \sum_x \left|\langle N-1,x|c_{kj}|N,i\rangle\right|^2 \rho\left(E_x^{N-1}\right)\rho\left(E_{kin}\right)\delta\left(E_{kin} + E_x^{N-1} - E_i^N - h\nu\right)$$

We have $$I(E_{kin}) = \frac{2e^2\pi^2}{m^2\hbar}\sum_{j=1}^{N}\left|M_{k,kj}\right|^2 A(kj,\omega j)$$

Where $A(kj,\omega j) \neq 0$ only when $\omega j = h\nu - E_{kin} = \left|E_i^N - E_x^{N-1}\right|$

Rewriting in terms of the electron binding energy ω, considering the momentum conservation and including the Fermi-Dirac distribution:

$$I(k,\omega) = I_{if}(k,\mathbf{A},\nu)A(k,\ \omega)\ fd(\omega,\ T)$$

Fermi-Dirac

Proportional to
Matrix elements

Spectral function

This is the most important result: in the sudden approx. the photoemission spectrum is proportional to the single particle spectral density function $A(k,\ \omega)$

This relationship has been obtained in the limit $\eta \rightarrow 0$ (η is the peak width), i.e. the peaks are Dirac's δ. It can be extended to "real systems" where the width Γ is finite.

$$G(k,\omega) = \sum_x \frac{|\langle N-1, x|c_k|N,i\rangle|^2}{\omega - E_x^{N-1} + E_i^N - i\Gamma}$$

$$A(k,\omega) = \frac{1}{\pi}\mathrm{Im}\,G(k,\omega) = \frac{\Gamma}{\pi}\sum_x \frac{|\langle N-1, x|c_k|N,i\rangle|^2}{(\omega - E_x^{N-1} + E_i^N)^2 + \Gamma^2}$$

Quasi-particle: when one hole is added adiabatically forming an (N-1)-electron system the coulomb interaction is screened by the formation of an electron cloud around the hole. At equilibrium, the hole+the screening cloud is a quasi-particle.

An eigenstate $|N-1, x\rangle$ of the (N-1)-electron system can be obtained by adding a quasi-particle to the N-electron system (quasi-particle state).

If instead we suddenly simply add a bare hole of momentum k (or we remove an electron of momentum k) we obtain the state $c_k|N,i\rangle$, that in general is not an eigenstate of the (N-1)-system, but it will have a finite overlap with the corresponding quasi-particle state.

The spectral density function A(k, ω) gives the probability that the original system plus the bare hole will be found in an exact eigenstate of the (N-1)-system

non-interacting
electrons

interacting
electrons

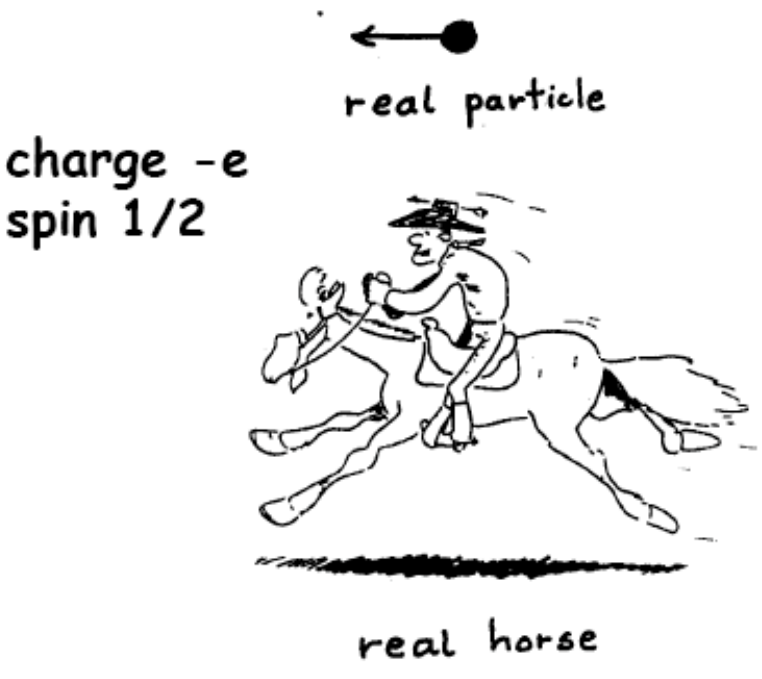

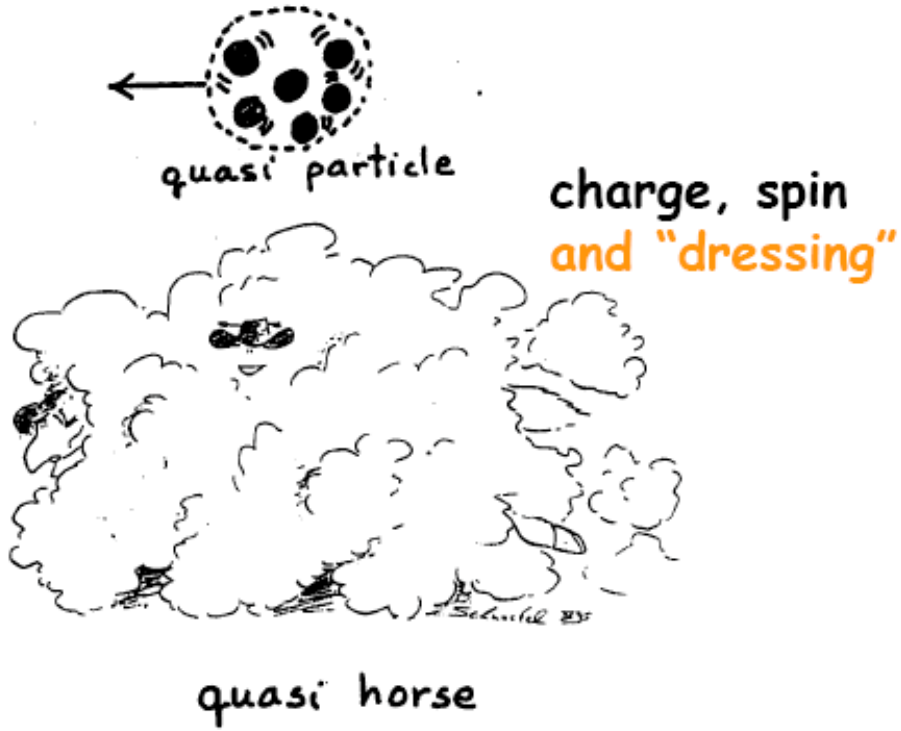

band structure

$\varepsilon_0(\mathbf{k})$

quasiparticle band structure

$\varepsilon(\mathbf{k}) = \varepsilon_0(\mathbf{k}) + \Sigma(\mathbf{k}, \varepsilon)$

self-energy

$$G(k,\omega) = \overbrace{\frac{\left|\langle N-1, i|c_k|N, i\rangle\right|^2}{\omega - \varepsilon(k) - i\Gamma}}^{Z_k} + \sum_{x\neq i} \frac{\left|\langle N-1, x|c_k|N, i\rangle\right|^2}{\omega - \varepsilon_x(k) - i\Gamma} = G_{coh.}(k,\omega) + G_{incoh.}(k,\omega)$$

$$A(k,\omega) = -\frac{1}{\pi}\,\mathrm{Im}\,G(k,\omega) = \frac{\Gamma}{\pi}\frac{\left|\langle N-1, i|c_k|N, i\rangle\right|^2}{(\omega - \varepsilon(k))^2 + \Gamma^2} + \frac{\Gamma}{\pi}\sum_{x\neq i}\frac{\left|\langle N-1, x|c_k|N, i\rangle\right|^2}{(\omega - \varepsilon_x(k))^2 + \Gamma^2}$$

$$= A(k,\omega)_{coh.} + A(k,\omega)_{incoh}$$

Where $\varepsilon(k)$ is the quasi-particle energy referred to the Fermi level $\mu=0$

As $\varepsilon(k) \rightarrow \mu$, $\Gamma \propto (\varepsilon - \mu)^2 \rightarrow 0$

The quasi-particle is well-defined only at (or very close to) the Fermi level, where its lifetime $1/\Gamma \rightarrow \infty$

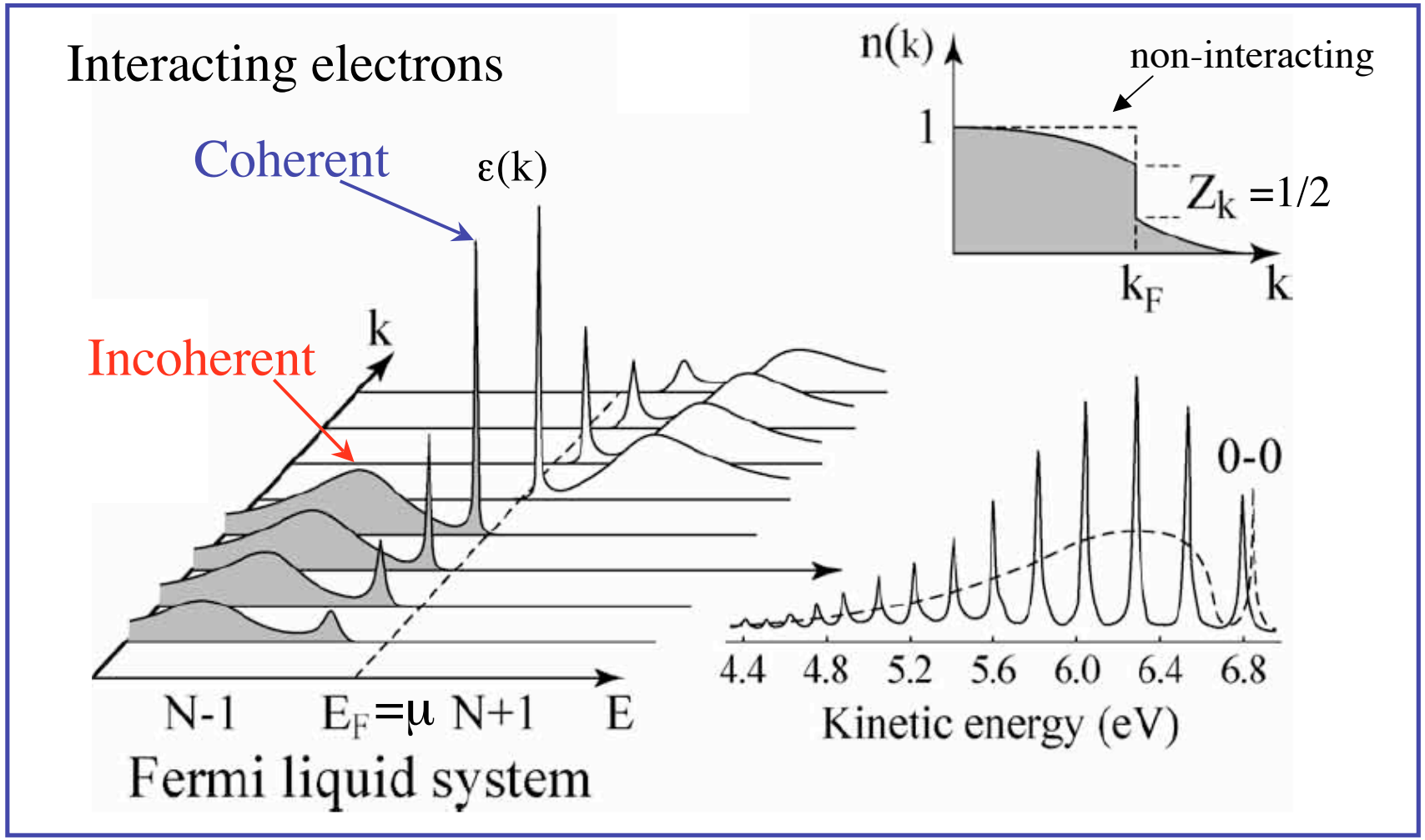

$$A(k,\omega)=\frac{\Gamma}{\pi}\frac{Z_k}{(\omega-\varepsilon(k))^2+\Gamma^2}+\frac{\Gamma}{\pi}\sum_{x\neq i}\frac{|\langle N-1,x|c_k|N,i\rangle|^2}{(\omega-\varepsilon_x(k))^2+\Gamma^2}=A(k,\omega)_{coh.}+A(k,\omega)_{incoh}$$

Example: $TiTe_2$

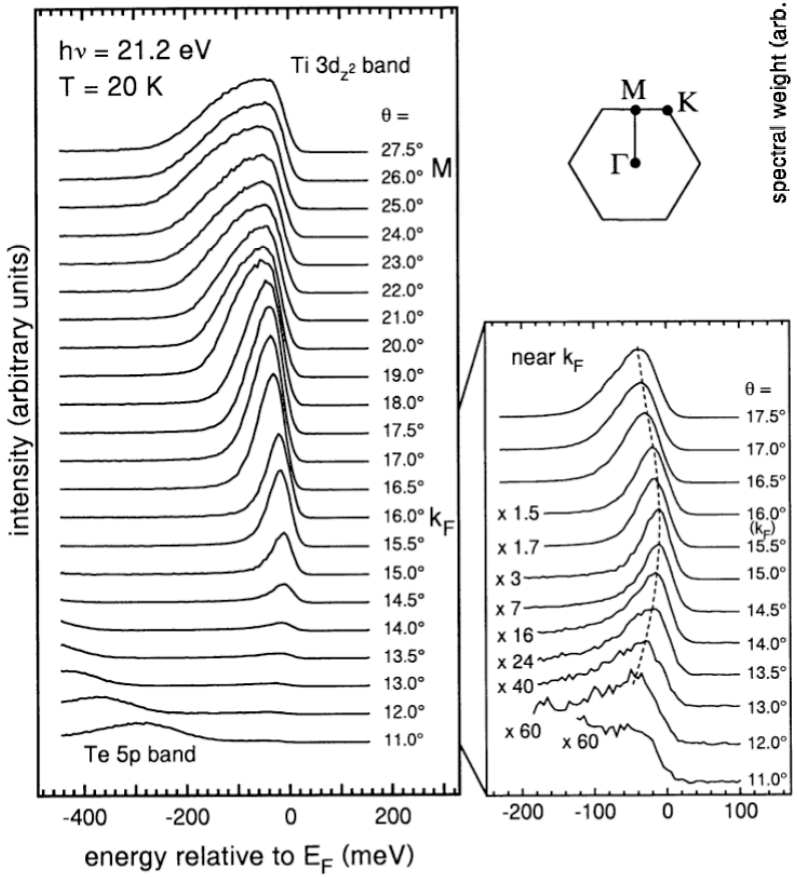

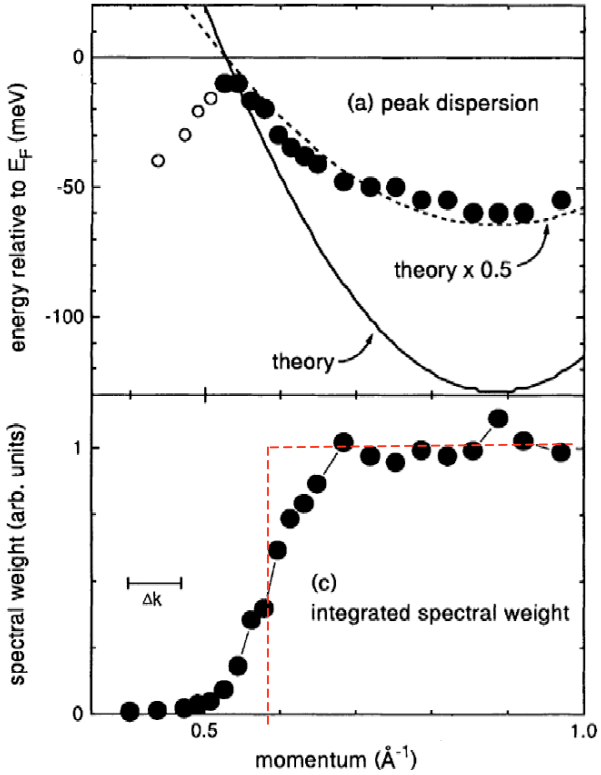

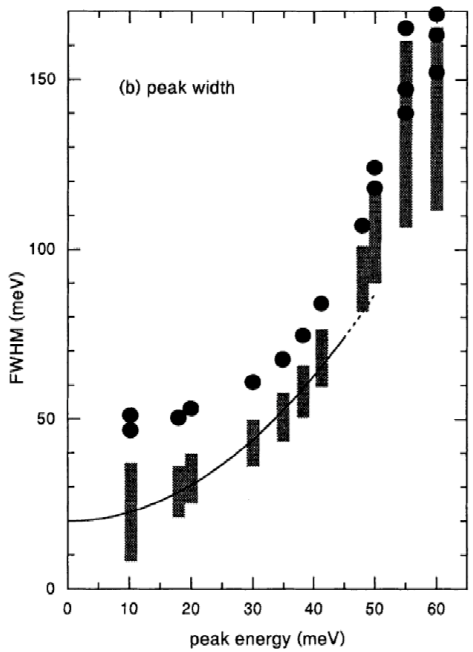

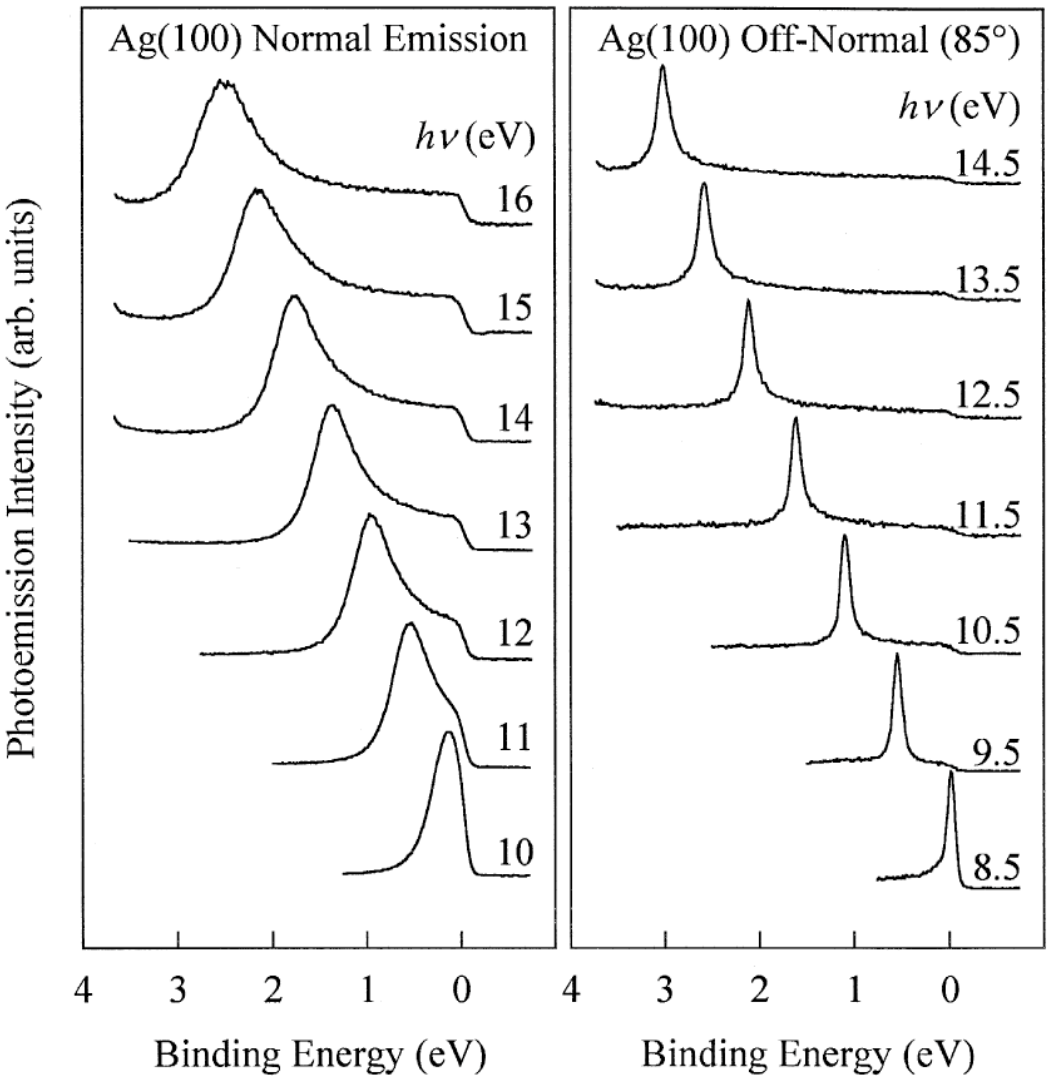

Fig. 1. Angle resolved photoemission spectra taken with a normal emission geometry (left panel) and a grazing emission geometry (right panel). The photon energies are indicated in the figure.

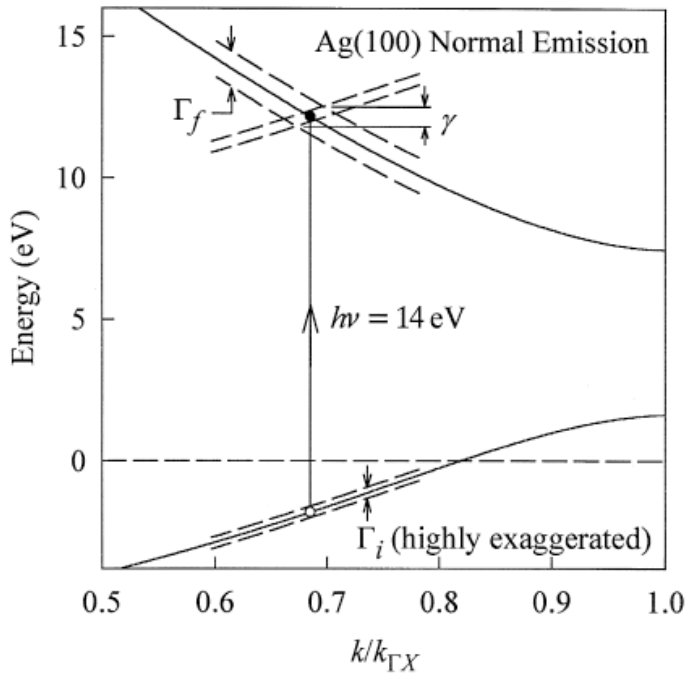

The total width γ (overlapping region) depends on the slopes, or group velocities.
γ is dominated by Γ_f (much larger than Γ_i).
Difficult to obtain the true quasiparticle inverse lifetime.

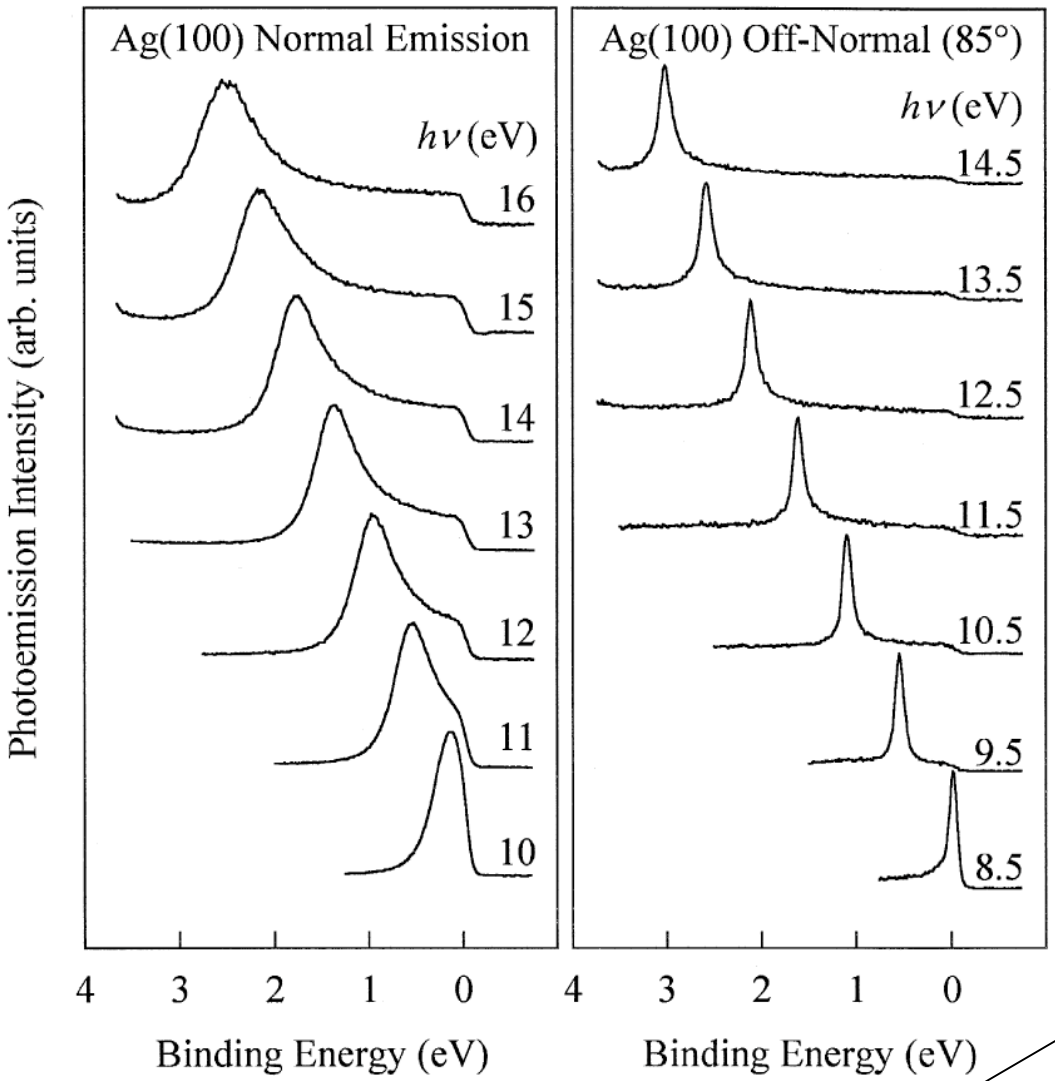

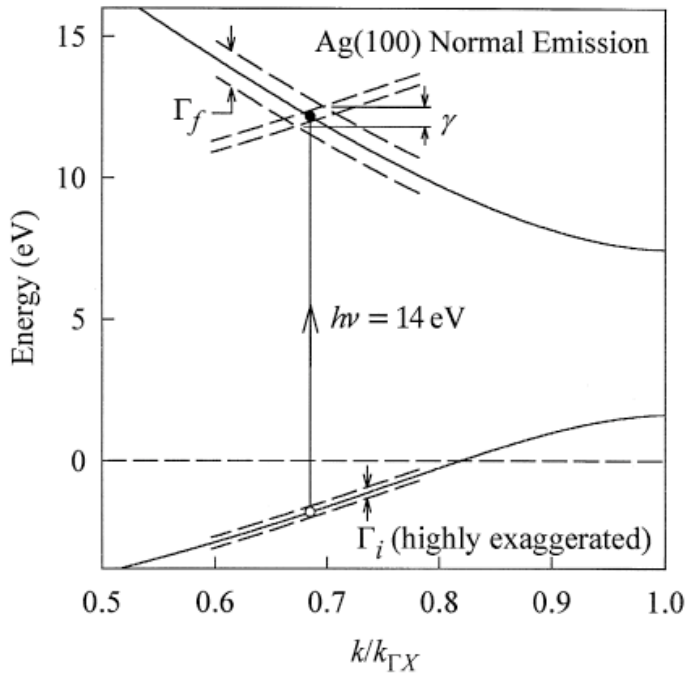

$$\gamma = \frac{\dfrac{\Gamma_i}{|v_{i\perp}|} + \dfrac{\Gamma_f}{|v_{f\perp}|}}{\left|\dfrac{1}{v_{i\perp}} - \dfrac{1}{v_{f\perp}}\right|}$$

Normal emission

Interesting when $v_i = v_f$ and $v_i/v_f = 0$

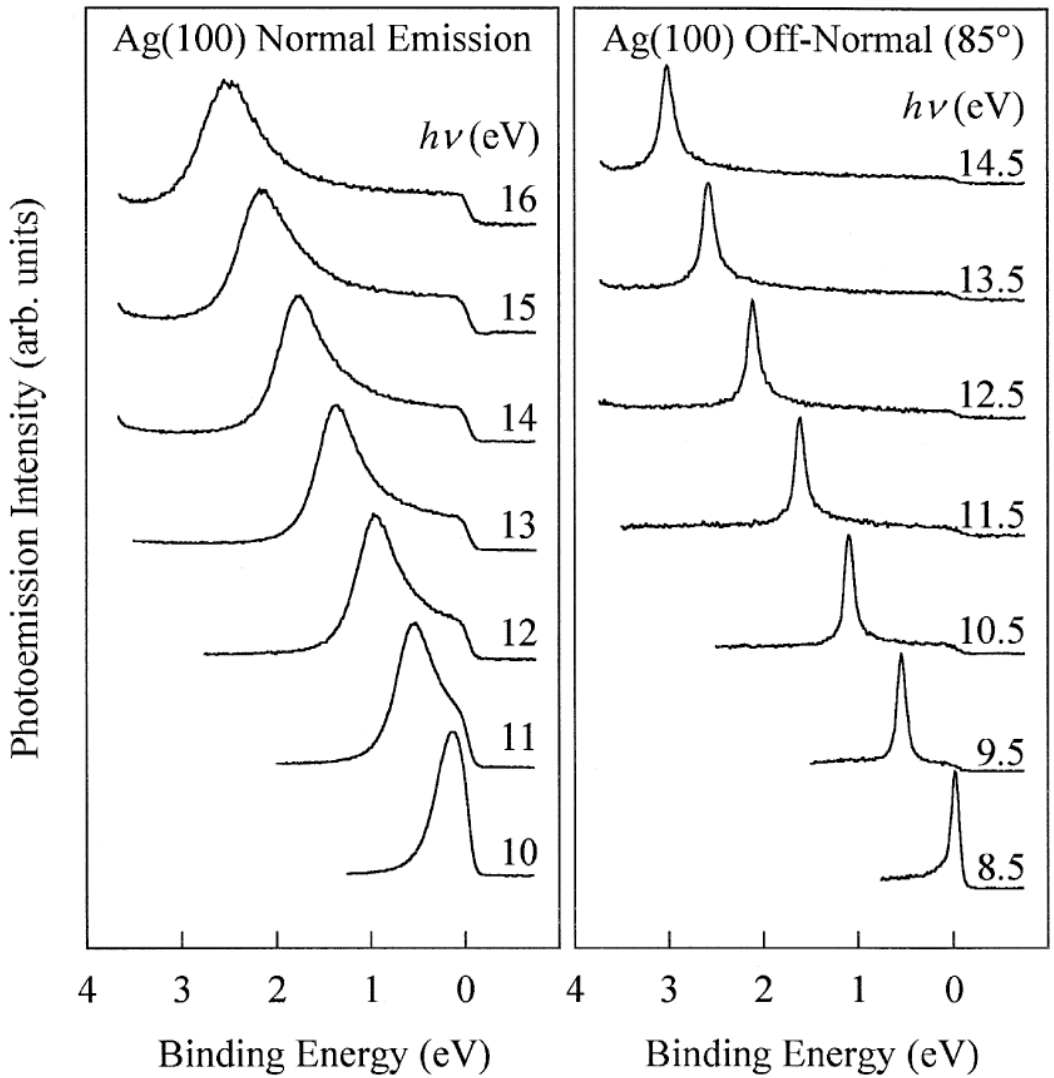

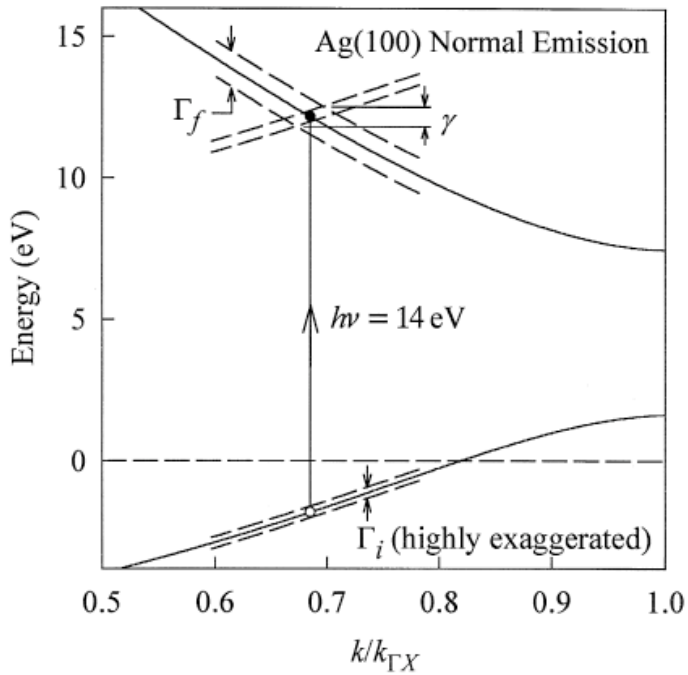

When $v_i/v_f=0$ $\gamma = C\cdot\Gamma_i$

$$C = \left|1 - \frac{m v_{i\parallel} \sin^2\theta}{\hbar k_\parallel}\right|^{-1}$$

Grazing emission

$$\gamma = \frac{\dfrac{\Gamma_i}{|v_{i\perp}|} + \dfrac{\Gamma_f}{|v_{f\perp}|}}{\left|\dfrac{1}{v_{i\perp}}\left(1 - \dfrac{m v_{i\parallel}\sin^2\theta}{\hbar k_\parallel}\right) - \dfrac{1}{v_{f\perp}}\left(1 - \dfrac{m v_{f\parallel}\sin^2\theta}{\hbar k_\parallel}\right)\right|}$$

ARPES: FWHM and Inverse Lifetime

FWHM of an ARPES peak

$$\Gamma = \frac{\frac{\Gamma_i}{|v_{i\perp}|} + \frac{\Gamma_f}{|v_{f\perp}|}}{\left| \frac{1}{v_{i\perp}} \left[1 - \frac{m v_{i\parallel} \sin^2 \vartheta}{\hbar k_\parallel} \right] - \frac{1}{v_{f\perp}} \left[1 - \frac{m v_{f\parallel} \sin^2 \vartheta}{\hbar k_\parallel} \right] \right|}$$

Hansen *et al.*, PRL **80**, 1766 (1998)

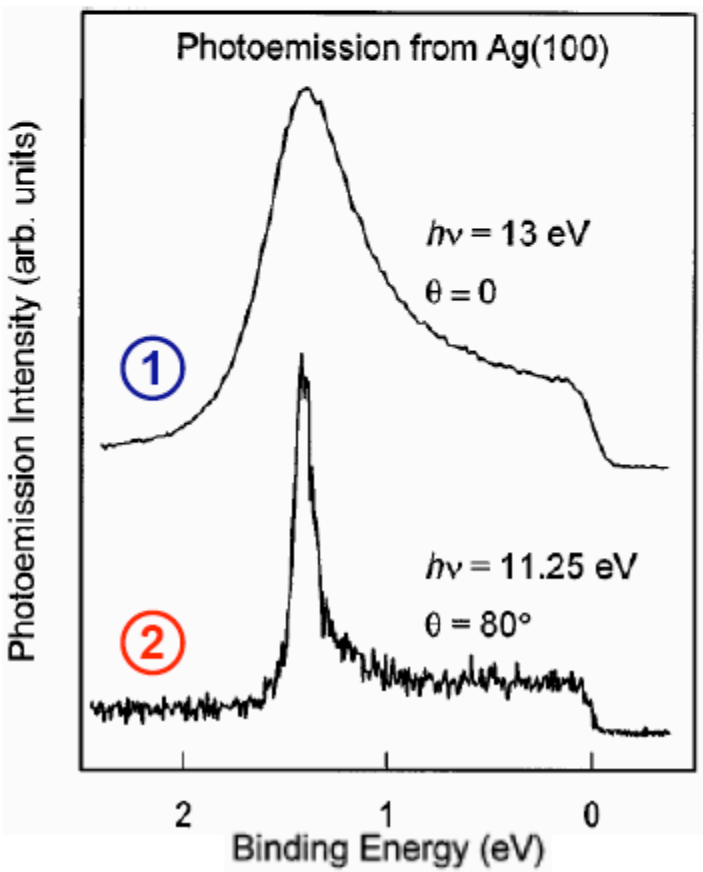

1 if $E_i \simeq E_F$

$\rightarrow \Gamma_i \longrightarrow 0 \rightarrow \boxed{\Gamma \propto \Gamma_f}$

2 if $|v_{i\perp}| \simeq 0$

$$\rightarrow \Gamma = \frac{\Gamma_i}{\left| 1 - \frac{m v_{i\parallel} \sin^2 \vartheta}{\hbar k_\parallel} \right|} \equiv C\,\Gamma_i$$

if $v_{i\parallel} < 0$, large; θ large; $k_\parallel$ small

$\rightarrow C < 1$, and $\boxed{\Gamma < \Gamma_i}$

The self-energy

It is useful to express the effects of the electron interactions in terms of the "electron self energy" defined as:

$$\Sigma(k,\omega) = \Sigma_1(k,\omega) + i\Sigma_2(k,\omega)$$

$\Sigma(\mathbf{k},\omega)$: the *"self-energy"* - captures the effects of interactions

$$\Gamma = \Sigma_2$$

$$\varepsilon(k) = \varepsilon_0(k) + \Sigma_1(k,\omega) = Z_k \varepsilon_0(k)$$

$$Z_k = \left(1 - \frac{\partial \Sigma_1}{\partial \omega}\right)^{-1}_{\omega = \varepsilon_0(k)}$$

… rewriting G(k,ω) and A(k,ω):

$$G(k,\omega) = \frac{Z_K}{\omega - \left[\varepsilon_0(k) + \Sigma(k,\omega)\right]} + G_{inch.}(k,\omega)$$

$$A(k,\omega) = \frac{\Sigma_2}{\pi} \frac{Z_k}{\left[\omega - \varepsilon_0(k) - \Sigma_1\right]^2 + \Sigma_2^2} + A_{inch.}(k,\omega)$$

$$\lambda = \left(-\frac{\partial \Sigma_1}{\partial \omega}\right)_{\omega = E_F}$$

Coupling constant

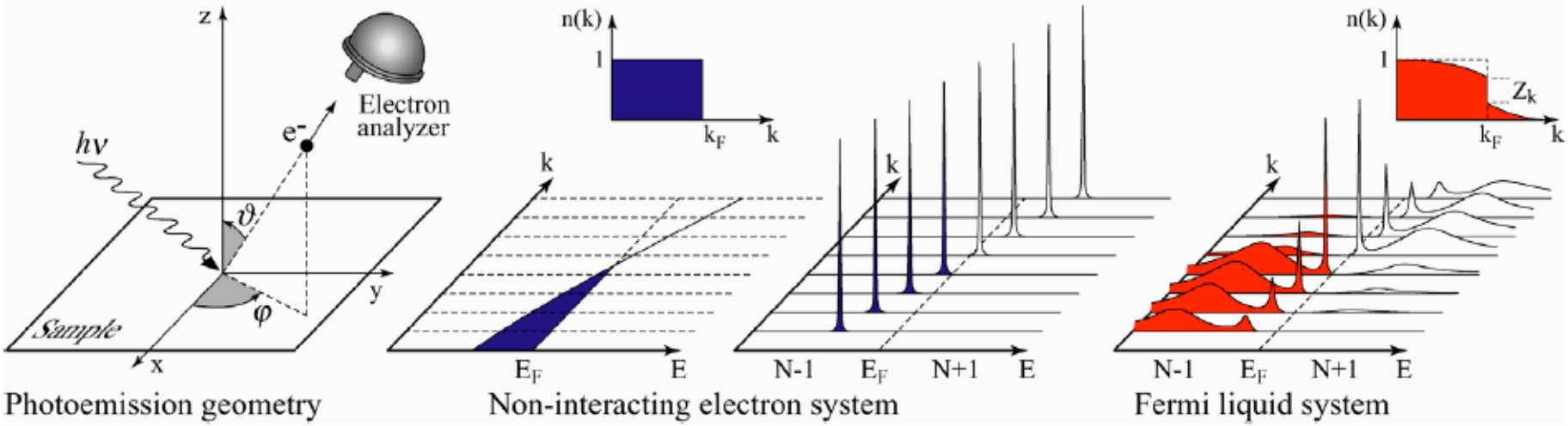

non-interacting

$$A(\vec{k},\omega) = -\frac{1}{\pi}\mathrm{Im}\frac{1}{\omega-\varepsilon_{\vec{k}}+0^+}$$

$$= \delta(\omega-\varepsilon_{\vec{k}})$$

Fermi liquid

$$A(\vec{k},\omega) = -\frac{1}{\pi}\mathrm{Im}\frac{1}{\omega-\varepsilon_{\vec{k}}-\Sigma(\vec{k},\omega)+0^+}$$

$$= -\frac{1}{\pi}\mathrm{Im}\frac{Z_{\vec{k}}}{\omega-E_{\vec{k}}-i\Gamma_{\vec{k}}} + A_{inc}$$

→ **energy renormalization:** $E_{\vec{k}} = \varepsilon_{\vec{k}} + \mathrm{Re}\,\Sigma = Z_k \cdot \varepsilon_{\vec{k}}$

→ **lifetime broadening:** $\Gamma_{\vec{k}} = \mathrm{Im}\,\Sigma$

→ **quasiparticle weight:** $Z_{\vec{k}} = (1-\frac{\partial\Sigma}{\partial\omega})^{-1} \le 1$

The “Kinky” physics

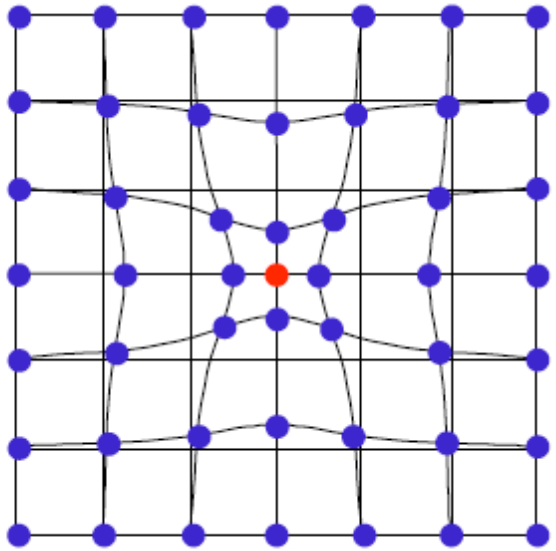

- Clear-cut case of a quasiparticle picture
- The quasiparticle mass near E_F is renormalized and the density of state increased

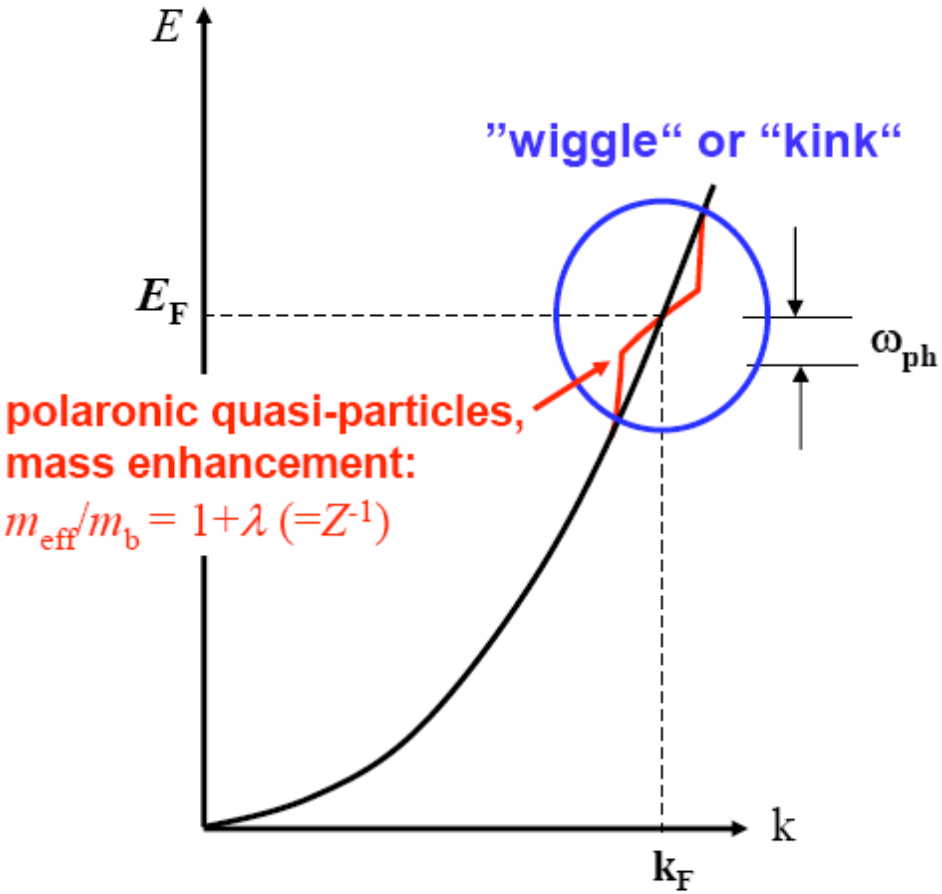

electron + (dynamical) lattice polarization
= polaronic quasiparticle

Electron-phonon coupling

$$A(k,\omega) = \frac{\Sigma_2}{\pi} \frac{Z_k}{\left[\omega - \varepsilon_0(k) - \Sigma_1\right]^2 + \Sigma_2^2} + A_{inch.}(k,\omega)$$

Spectral function:
excitation spectrum

electronic self-energy

$$\mathrm{Im}\Sigma(\omega) \propto \int_0^{\omega} \alpha^2 F(\Omega) d\Omega = \lambda \int_0^{\omega} \rho_{ph}(\Omega) d\Omega$$

λ -
electron-phonon coupling constant

$\mathrm{Re}\Sigma(\omega)$ **from Kramers-Kronig relation**

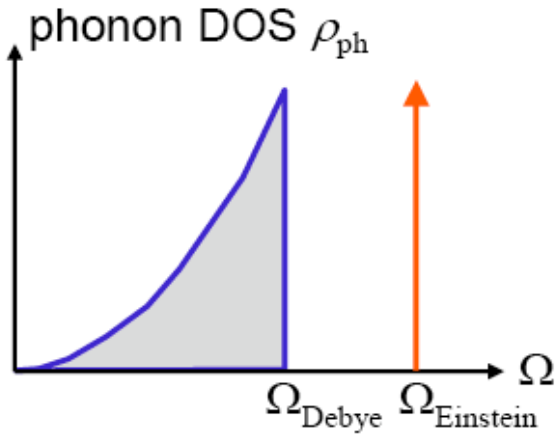

example: Einstein model:

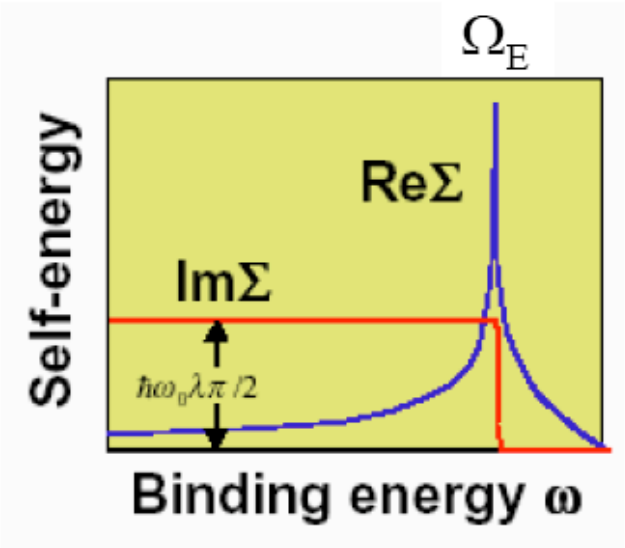

$$\left|\varepsilon_{\vec{k}} - E_F\right| > \omega_0$$

hole emits (decays into)
***real* phonon**

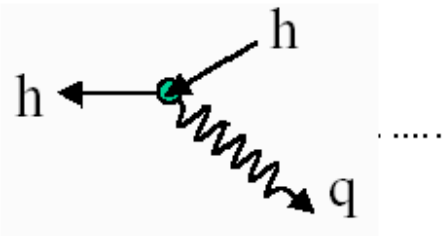

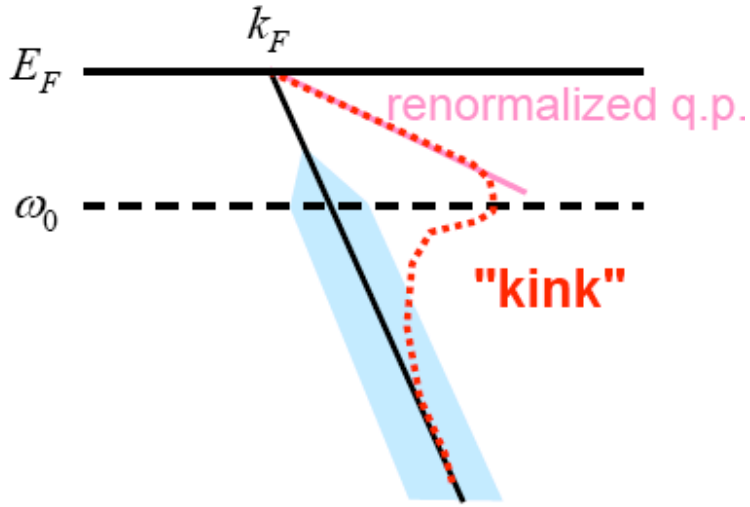

$$\left|\varepsilon_{\vec{k}} - E_F\right| < \omega_0$$

hole emits and reabsorbs phonon,
dressed with cloud of *virtual* phonons

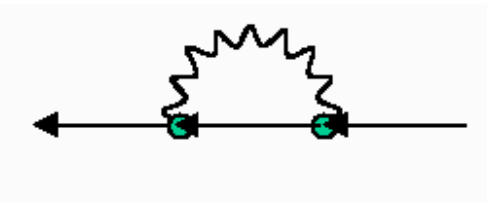

example: Einstein model:

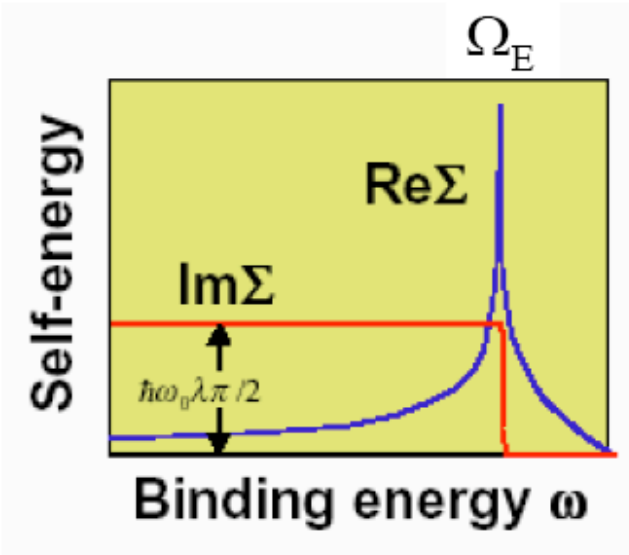

Debye Model (λ = 1)

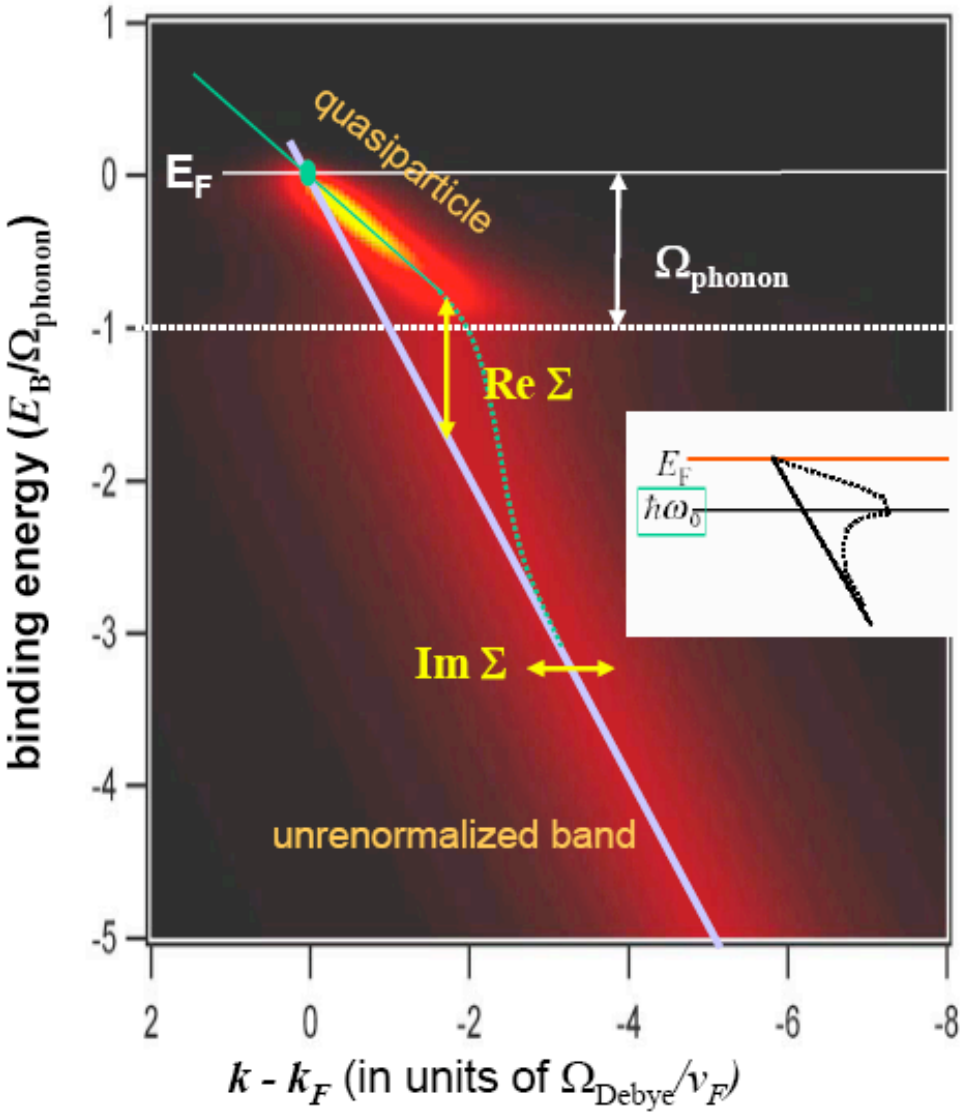

theoretical energy distribution curves (EDCs)

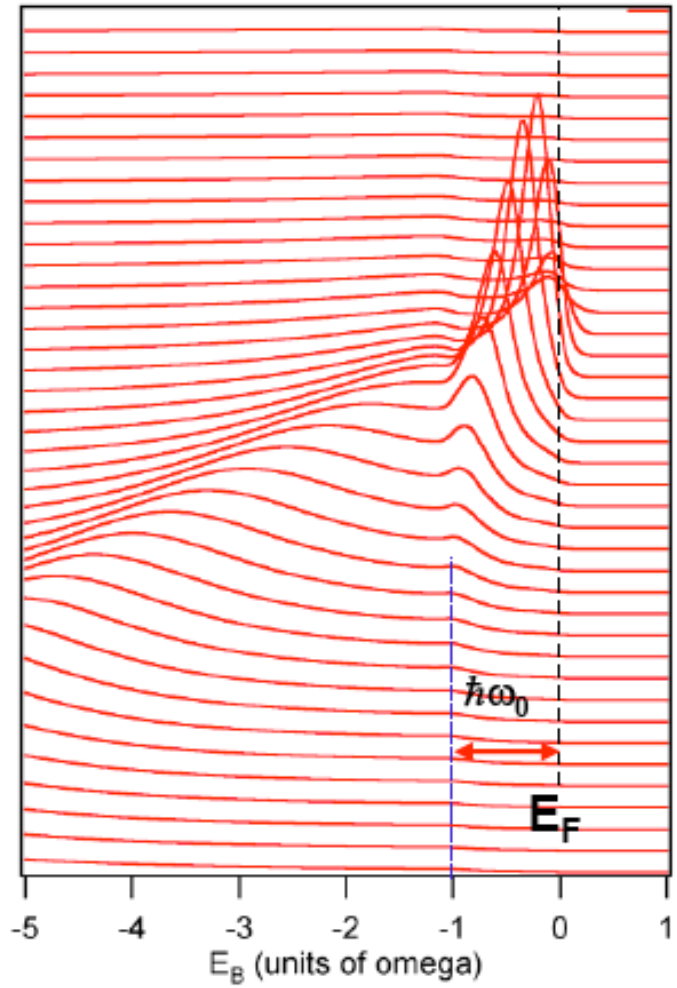

Coupling to adsorbate vibrations on a surface

hydrogen adsorbed on W(110) – an Einstein-type system

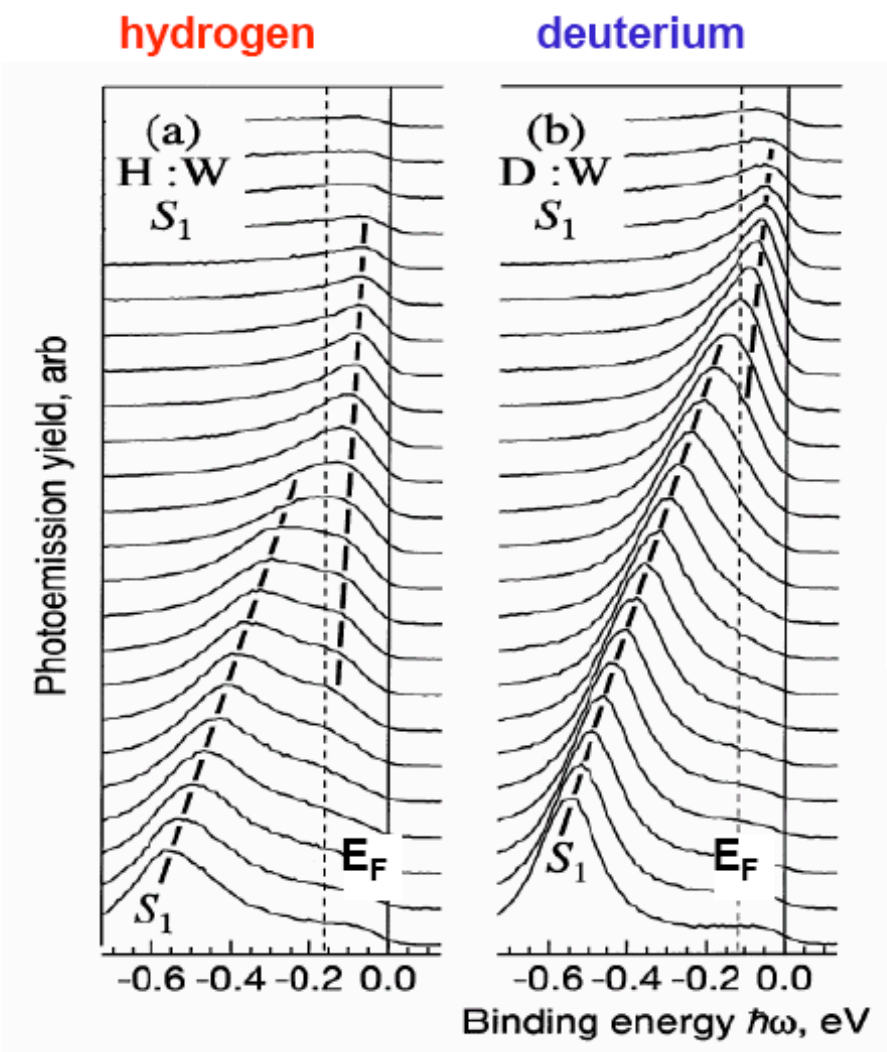

E. Rotenberg, J. Schäfer et al., PRL ***84****, 2925 (2000)*

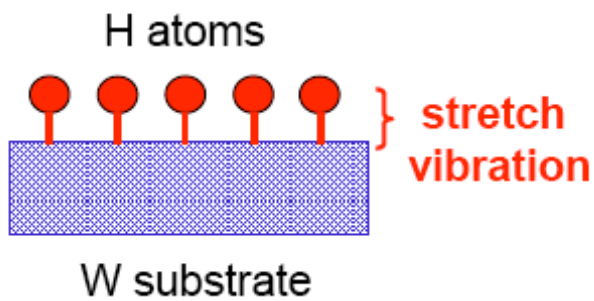

quantitative analysis:

- **energy scale:** ω_0 = 160 meV for H,
  115 meV for D (isotope effect $1/\sqrt{2}$)
- **coupling constant:** λ = 1.4 for H/W(110)
- **significant mass renormalization**
- **isotope effect H → D**
  $(\omega_0 \sim 1/\sqrt{M})$

Intrinsic electron-phonon coupling on a surface: Debye model

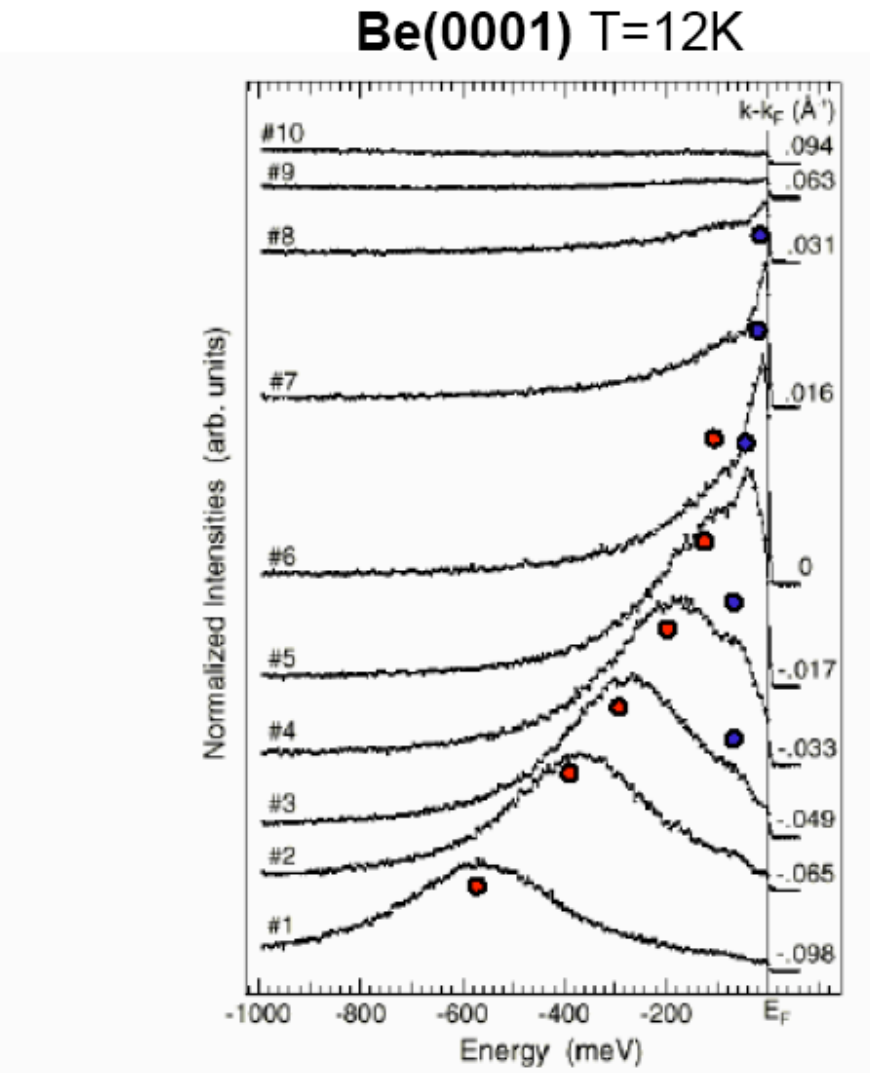

Hengsberger et al, PRL 83,592 (1999).

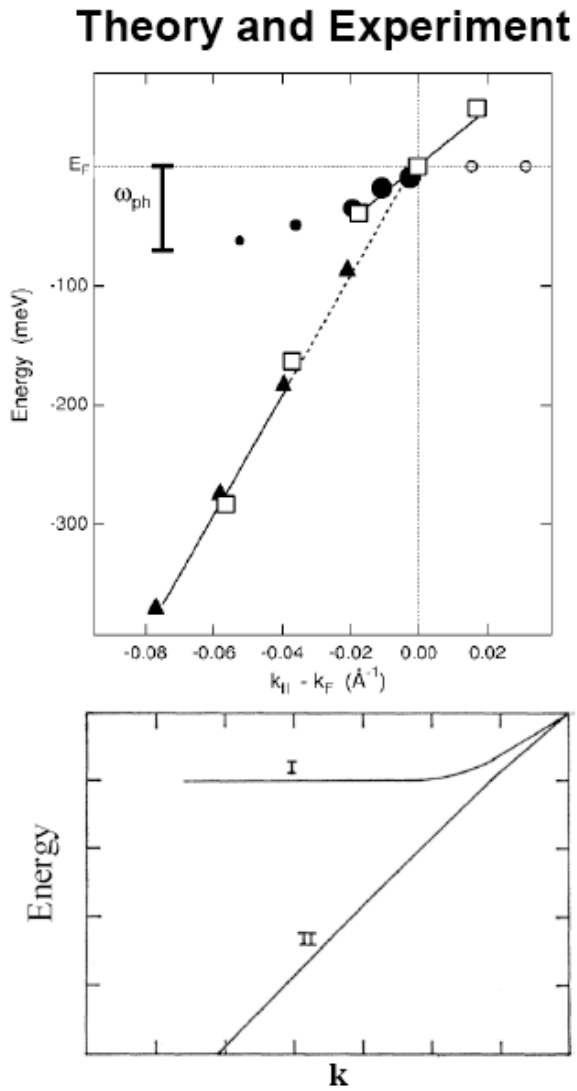

S. Engelsberg and J.R. Schrieffer, **PR** 131, 993 (1963)

How to get λ?: real part of Σ

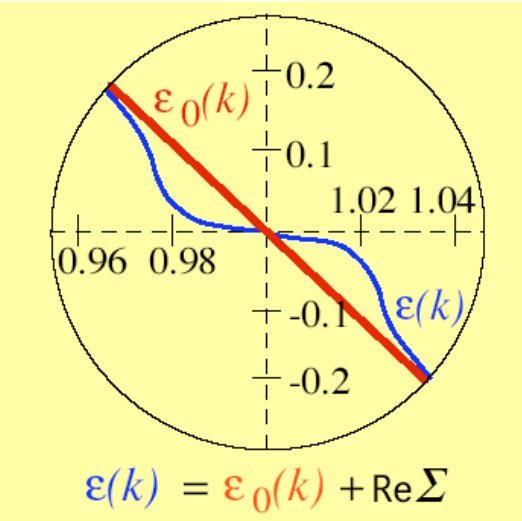

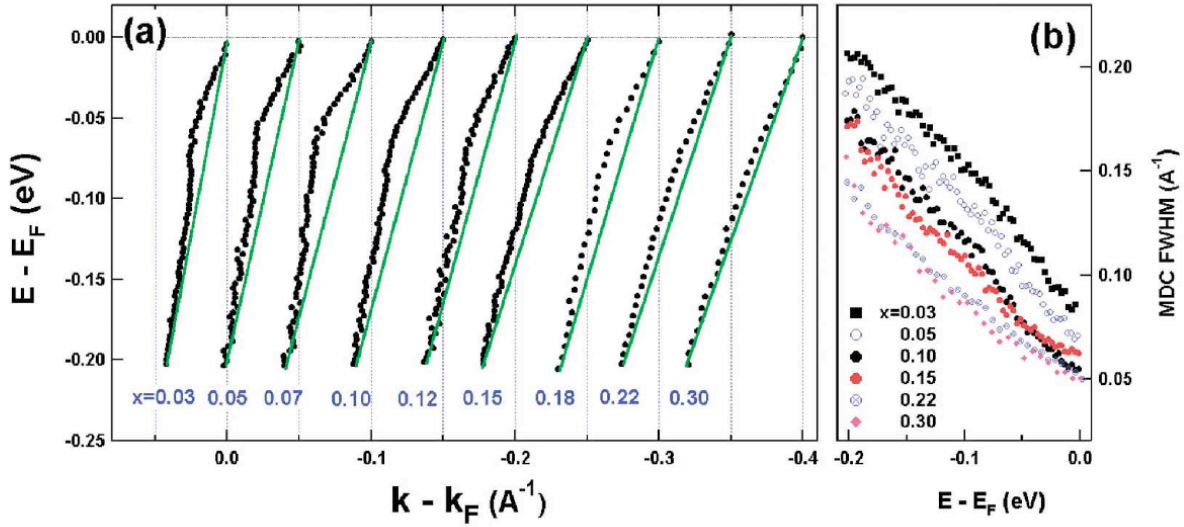

Fig. 13. Dispersion (a) and MDC width (FWHM)(b) of LSCO samples ($x = 0.03 \sim 0.30$) measured along the nodal direction, as determined from fitting MDCs. For clarity, the dispersion in (a) is offset horizontally along the momentum axis. The green lines in (a) connect the points in dispersion at E_F and 0.2 eV which approximately represents the bare band; they also serve as guides to the eye to identify the kink in dispersion. The MDC width (b) shows an overall decrease with increasing doping. A slight drop in MDC width is discernible at a binding energy of ~80 meV, particularly obvious for lower doping samples.

$$\lambda = \frac{d\Re\Sigma}{d\epsilon}\Big|_{\epsilon_F}$$

but this may also be caused by something else....

- yields directly λ when measured at 0 K.
- the effect has to be large in order to be observable
- the un-renormalized dispersion has to be known

How to get λ?: imag. part of Σ

EDC linewidth $\Gamma = \Gamma_{e-e}(T) + \Gamma_{e-i}(T) + \Gamma_{e-ph}(T)$

$$\Gamma_{e-ph}(T) = 2\pi\hbar \int_0^{\omega_m} d\omega' \alpha^2 F(\omega')[1 - f(\omega - \omega') + 2n(\omega') + f(\omega + \omega')] \simeq 2\pi\lambda k_B T$$

- In most cases, the temperature dependence of the lifetime is dominated by the electron-phonon coupling.
- The T-dependence of the linewidth can be used to extract λ.
- The T-dependence is **independent of binding energy** (not too close to the Fermi level).
- several practical problems when the binding energy is very close to the Fermi level

$$\alpha^2 F(\omega) = \lambda(\frac{\omega}{\omega_D})^2 \quad , \omega < \omega_D$$

$$\alpha^2 F(\omega) = 0, \omega > \omega_D$$

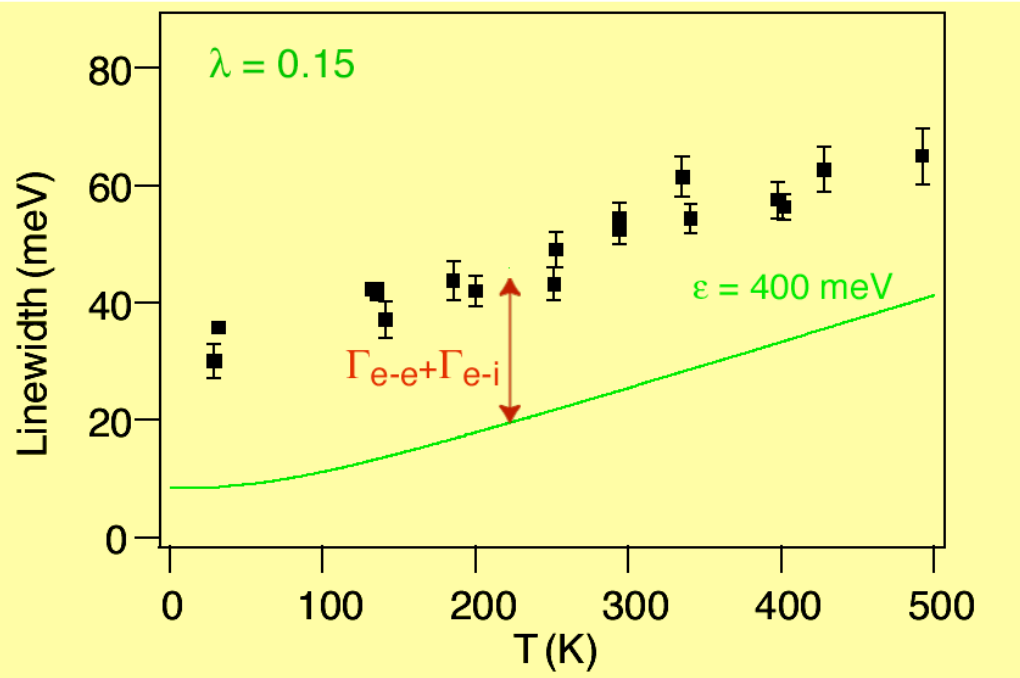

B.A. McDougall, T. Balasubmaranian and E. Jensen PRB 51, 13891 (1995).

How to get λ?: imag. part of Σ

EDC linewidth $\Gamma = \Gamma_{e-e}(\cancel{T}) + \Gamma_{e-i}(\cancel{T}) + \Gamma_{e-ph}(T)$

$$\Gamma_{e-ph}(T) = 2\pi\hbar \int_0^{\omega_m} d\omega' \alpha^2 F(\omega')[1 - f(\omega - \omega') + 2n(\omega') + f(\omega + \omega')] \simeq 2\pi\lambda k_B T$$

- In most cases, the temperature dependence of the lifetime is dominated by the electron-phonon coupling.
- The T-dependence of the linewidth can be used to extract λ.
- The T-dependence is **independent of binding energy** (not too close to the Fermi level).
- several practical problems when the binding energy is very close to the Fermi level

$$\alpha^2 F(\omega) = \lambda(\frac{\omega}{\omega_D})^2 \quad , \omega < \omega_D$$

$$\alpha^2 F(\omega) = 0, \omega > \omega_D$$

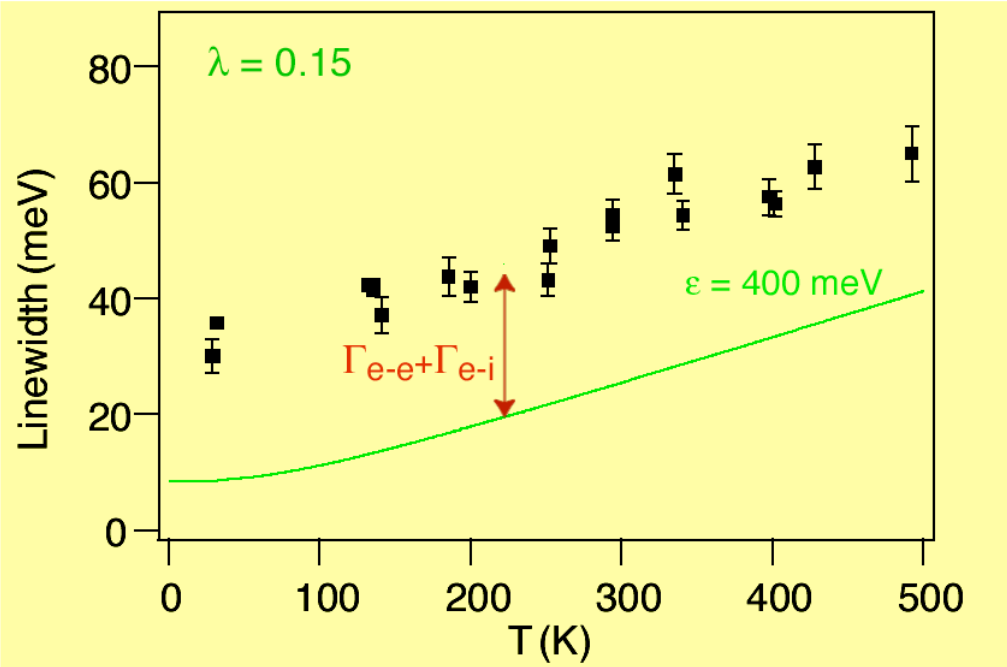

B.A. McDougall, T. Balasubmaranian and E. Jensen PRB 51, 13891 (1995).

Electron-phonon coupling constant and superconductivity

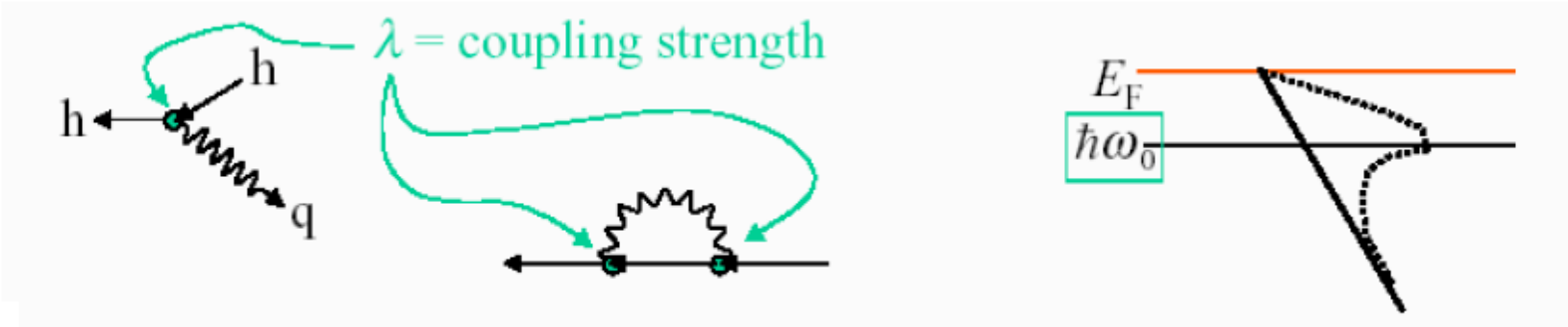

Strong-coupling theory of superconductivity

	Matl	λ	w0 [K]	Tc(theory)	Tc(expt)
	W	0.28	390	0.01	0.012
	Mo	0.41	460	0.84	0.92
	Be	0.24	1000	**0.02**	0.026
3-D	Hg	1	72	3.56	4.16
	Pb	1.12	105	6.25	7.19
	Nb	0.82	277	9.20	9.22
	Pd	0.15	274	0.00	not SC
	PdH	0.75	475	12.67	10
2-D	H:W	0.5-1.4	1932	**50-150**	?
	Be surf	1.15	1000	**70.21**	?

$$T_c \propto \omega_0 \exp(-\frac{1}{\lambda})$$

table by Eli Rotenberg

Coupling to other bosons

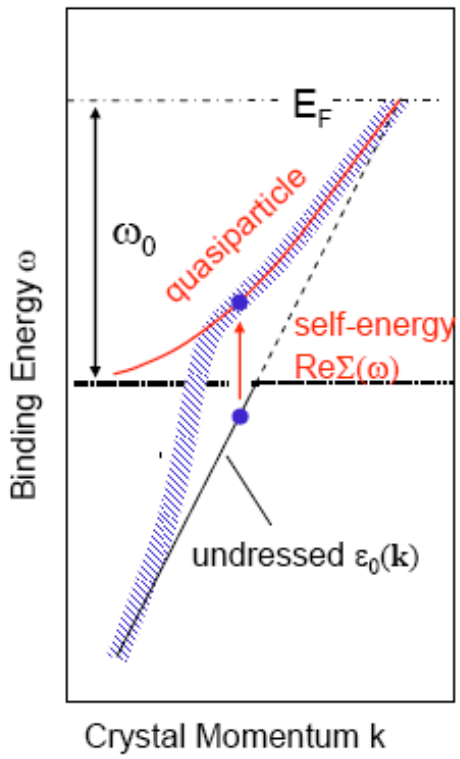

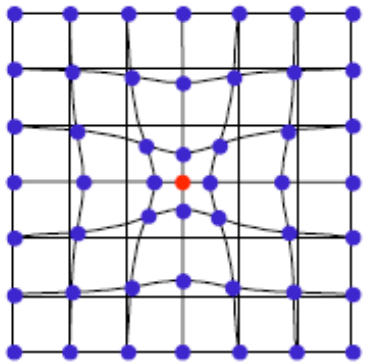

e-ph

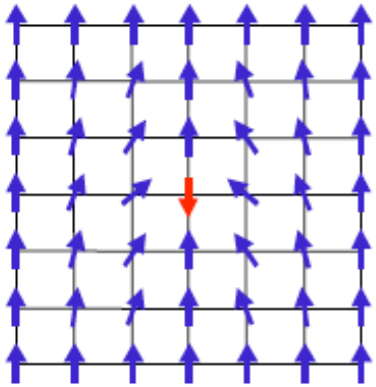

e-spin

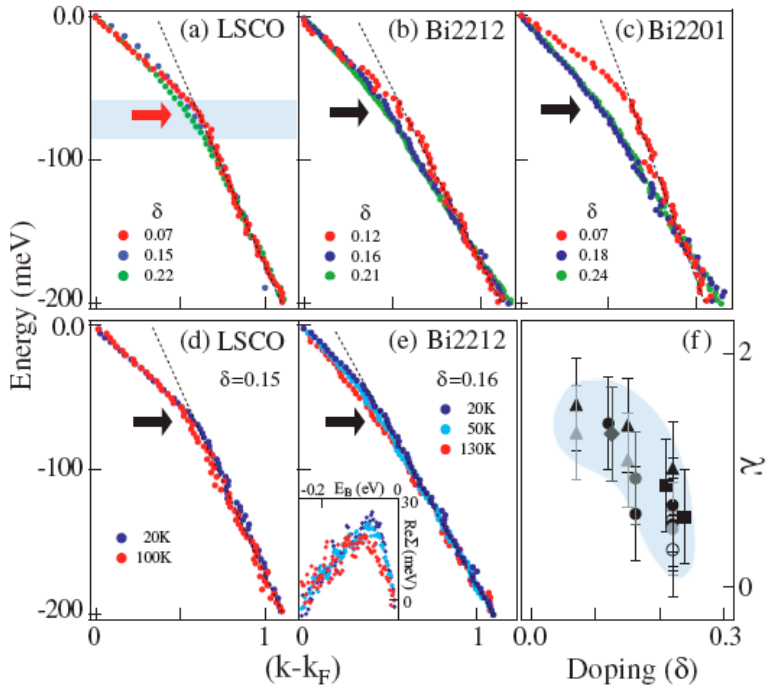

formation of quasiparticles by coupling to spin excitations ?

kink observed in the cuprates :

- Cooper-pairing mediated by spin fluctuations ?
- problem: energy scales for phonons and magnetic modes very similar

Fe(001) surface state: dispersion and lifetime width

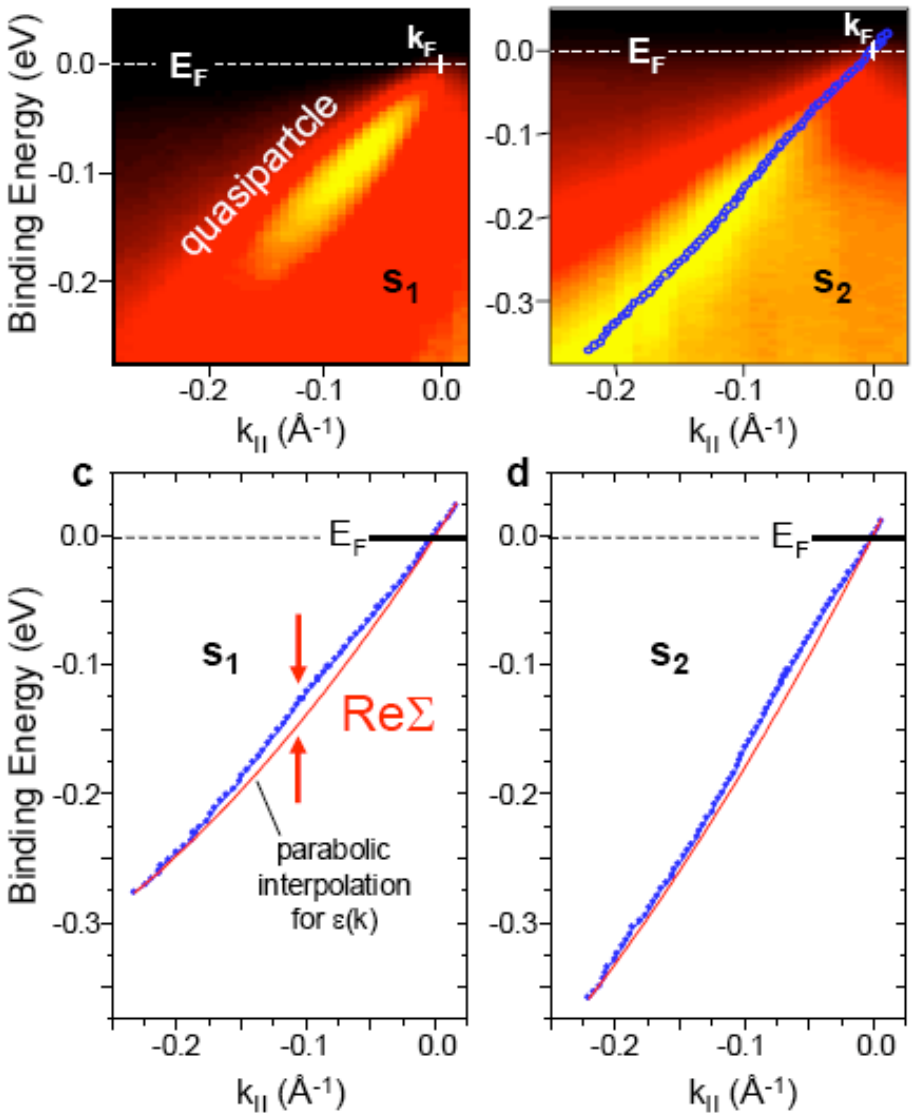

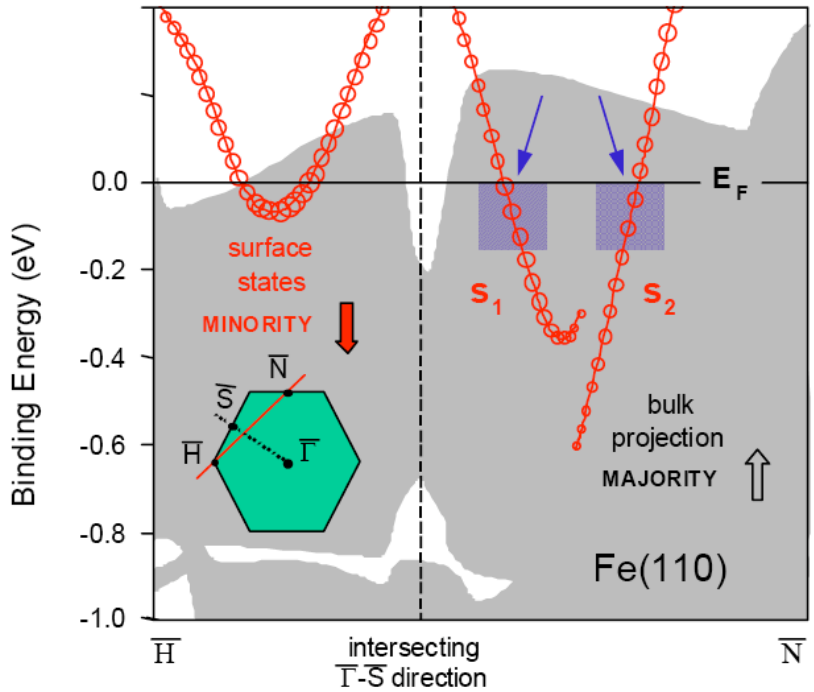

self-energy $\Sigma(\omega)$ derived from momentum distribution curves (MDCs)

peak maximum $\rightarrow \varepsilon_k + \mathrm{Re}\,\Sigma(\omega)$

renormalization @ 100-200 meV
(>> ω_{Debye} ~ 30 meV)

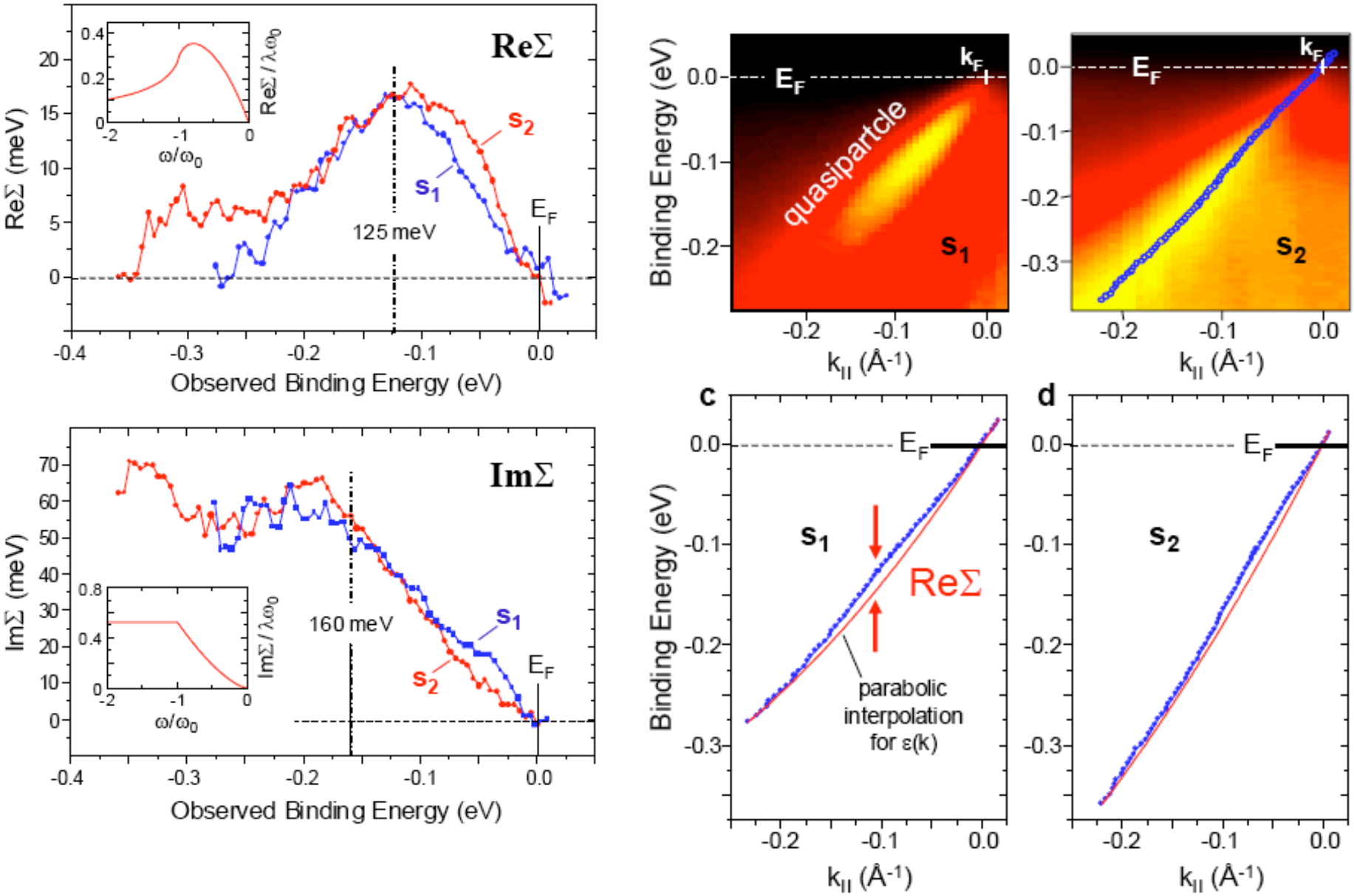
ReΣ
ReΣ (meV)
Observed Binding Energy (eV)
125 meV
E_F
s_1
s_2
ReΣ / λω0
ω/ω0
ImΣ
ImΣ (meV)
160 meV
ImΣ / λω0
Binding Energy (eV)
k_F
quasipartcle
$k_{||}$ (Å-1)
c
d
ReΣ
parabolic interpolation for ε(k)

1D System: breakdown of the Fermi liquid
Spinon and holon dispersion

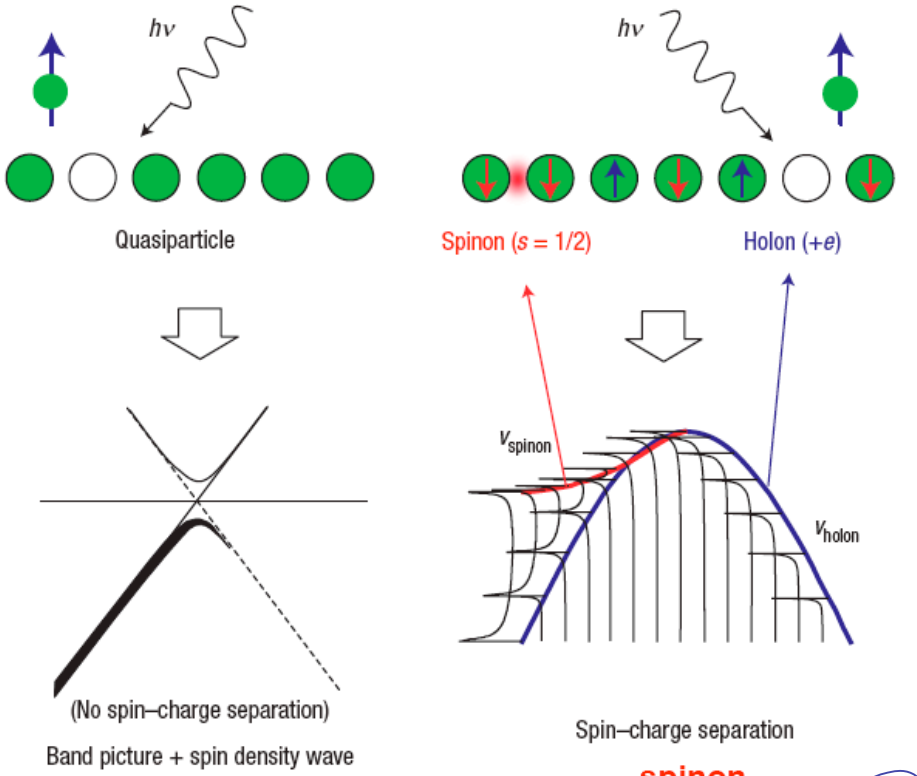

t - hopping integral

$J \propto t^2/U$ - magnetic exchange

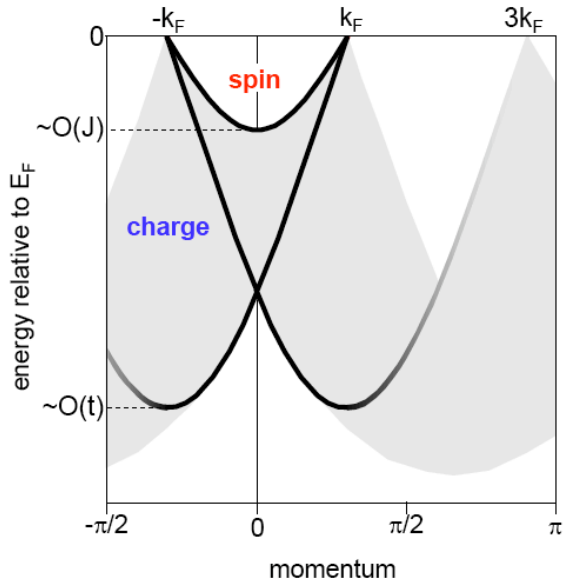

U >> t
strong
coupling

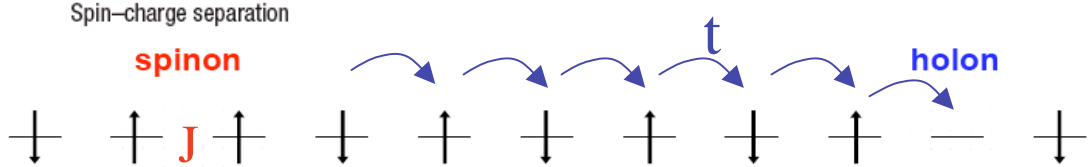

spin-charge separation in 1D

K. Penc et al. (1996): tJ-model
J.M.P. Carmelo et al. (2002 / 2003): Bethe ansatz
E. Jeckelmann et al. (2003): dynamical DMRG

Distinct spinon and holon dispersions in photoemission spectral functions from one-dimensional $SrCuO_2$

B.J. Kim at al., Nature Physics 2 (2006)

$$H = t \sum_{\langle ij \rangle, \sigma} c^{+}_{i\sigma} c_{j\sigma} + U \sum_{i} n_{i\uparrow} n_{i\downarrow}$$

t – hopping integral

U – local Coulomb energy

strong coupling $U >> t$

$J \propto t^2/U$ - magnetic exchange energy

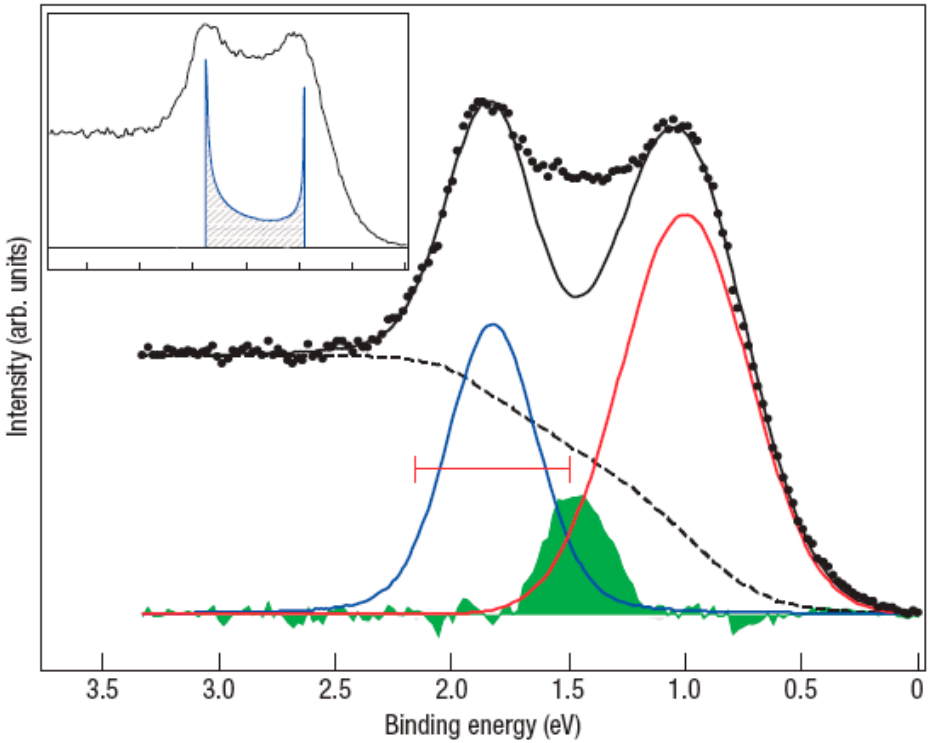

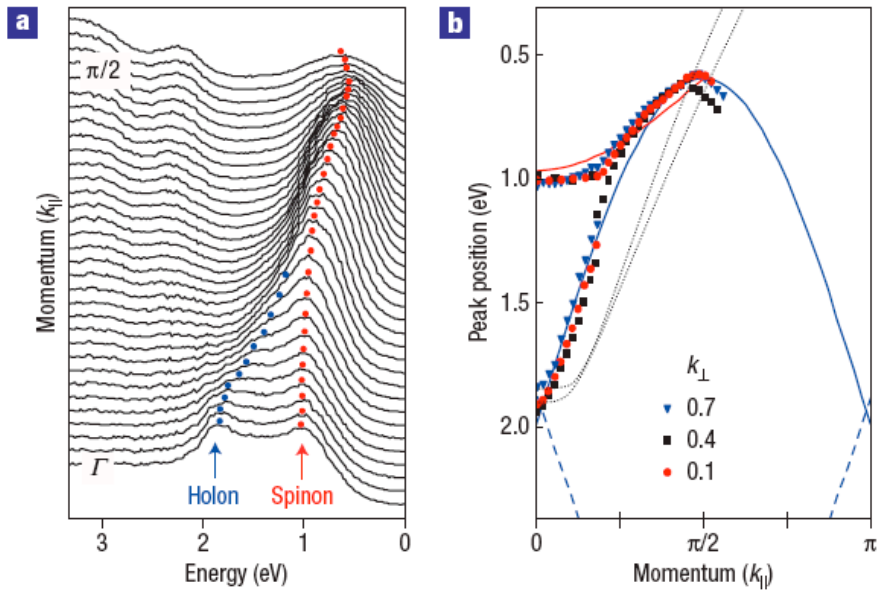

Figure 3 EDCs and dispersions. a, EDCs for $k_{\parallel}$ between Γ and 0.6π at $k_{\perp} = 0.7$ Å^{-1}. Each EDC is curve-fitted to find the peak positions. Two peaks were used in the region between $k_{\parallel} = \Gamma$ and $\pi/4$, whereas a single peak was used for the rest. The results are marked by red and blue circles. **b**, Experimental (symbols) and theoretical (solid and dashed lines) dispersions. The theoretical dispersions are obtained by taking the nearest-neighbour hopping of $t = 0.65$ eV and the exchange coupling of $J = 0.23$ eV. Dispersions from the band theory are also shown as two dotted lines[22].

TTF-TCNQ: an organic 1D metal

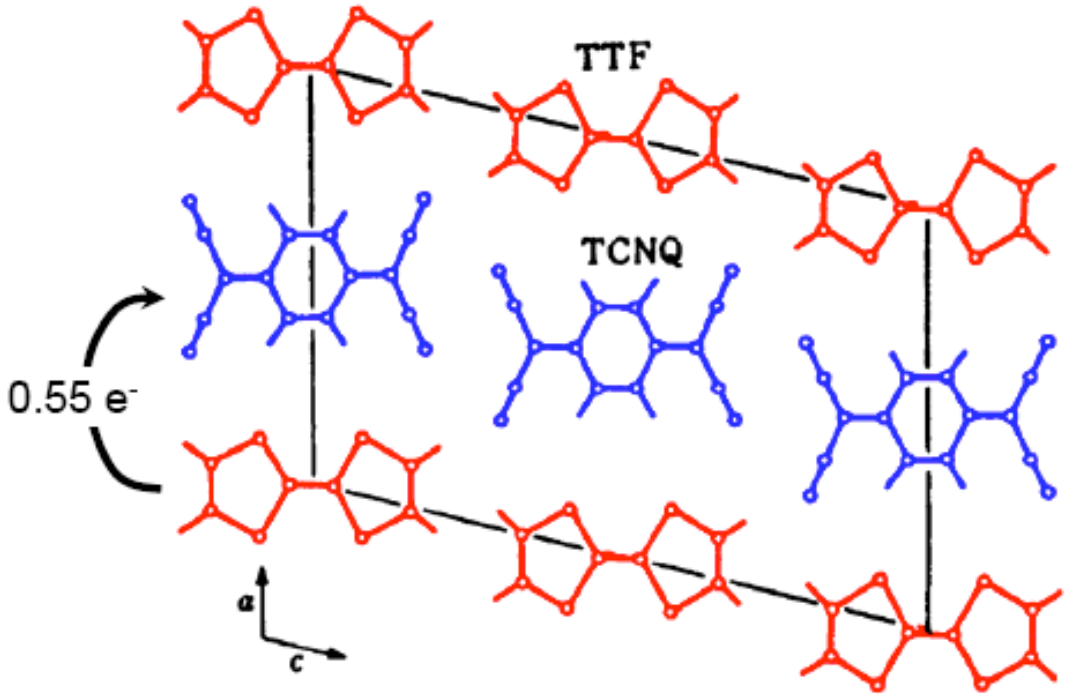

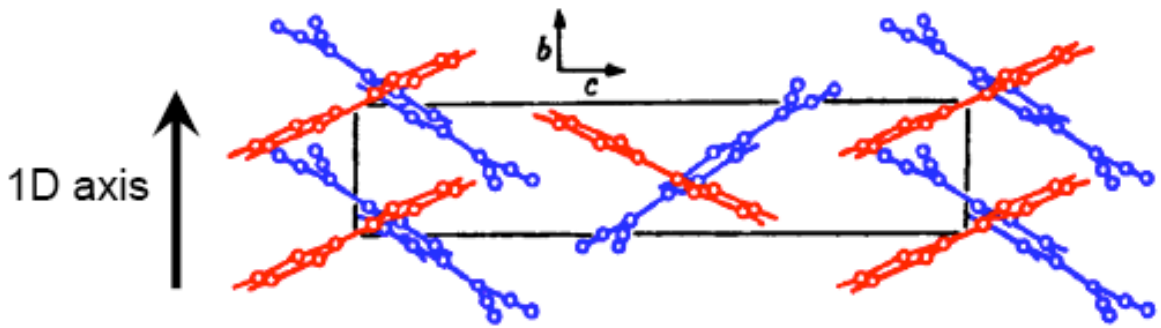

strongly anisotropic conductivity
$\sigma_b/\sigma_a \approx \sigma_b/\sigma_c \sim 1000$

Peierls instability @ $T_P = 54$ K, incommensurate CDWs on TCNQ stacks

electronic correlation effects:

- $4k_F$-fluctuations (on TTF stacks ?) observed up to 300 K
- enhanced magnetic susceptibility
- enhanced NMR relaxation rate

$\Rightarrow$ **estimate for Hubbard model parameters:**

U ~ 4t ~ 1 eV

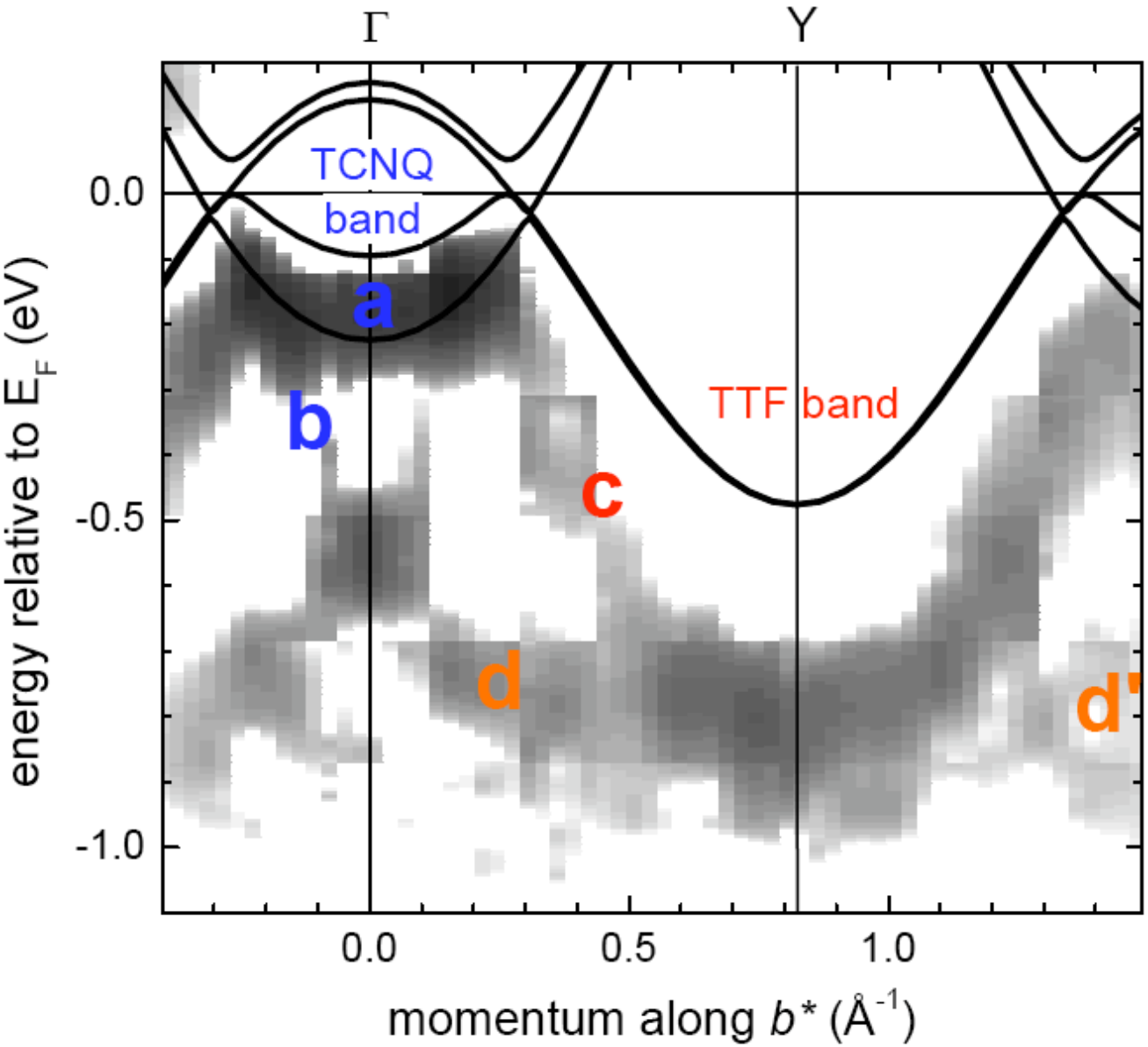

$-d^2I/dE^2$ vs. **k**

experimental band width doubled relative to theory

→ **molecular surface relaxation**

PRB ***67****, 125402 (2003)*

spectral structure (**d**) not explained by band theory

→ **1D correlation effects**

PRL ***88****, 096402 (2002);*
PRB ***68****, 125111 (2003)*

E. Jeckelmann et al.,
*PRL **92**, 256401 (2004)*

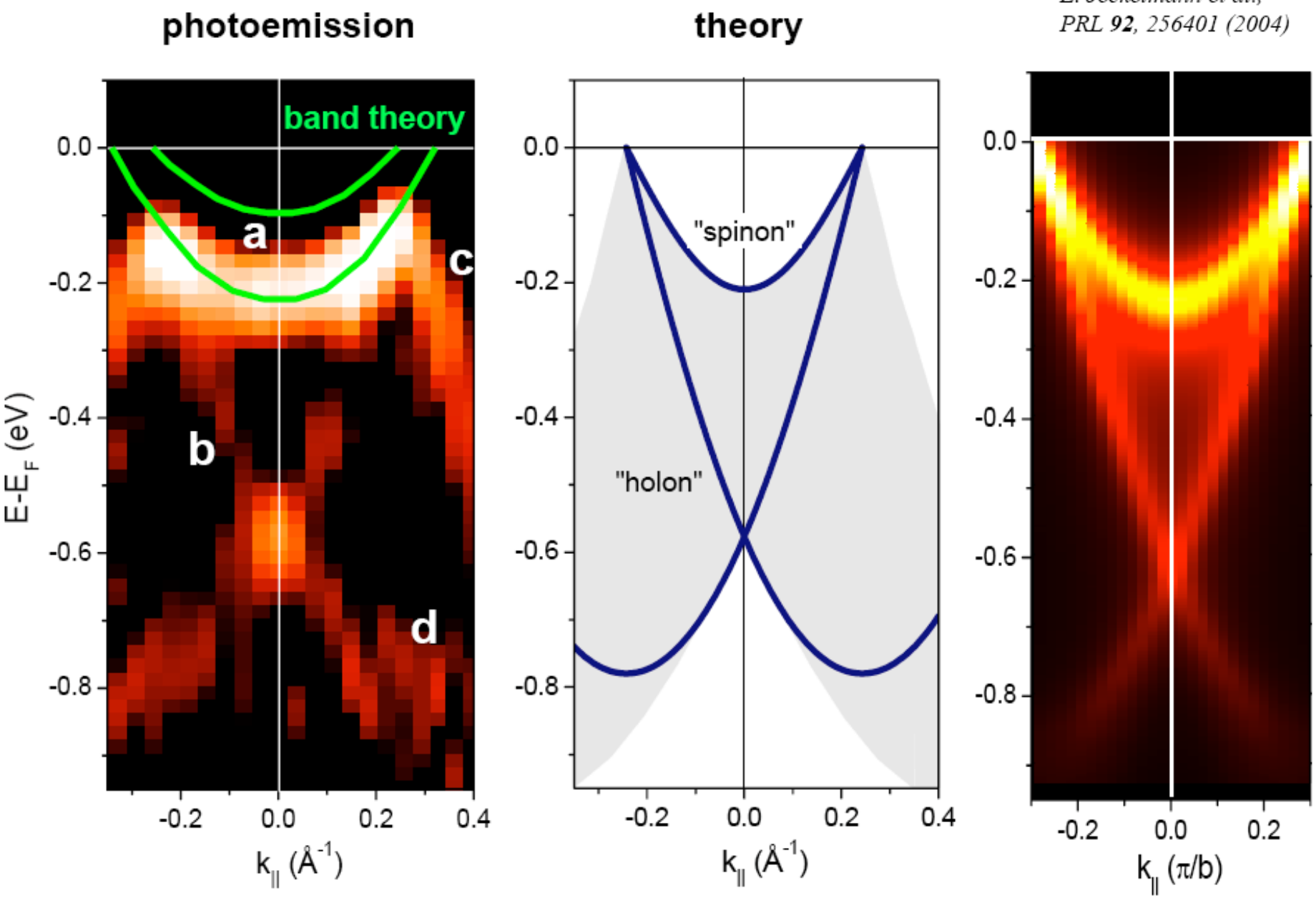

1D System: breakdown of the Fermi liquid
The Tomonaga-Luttinger liquid

Tomonaga-Luttinger model:

spectral function $A(\mathbf{k},\omega)$

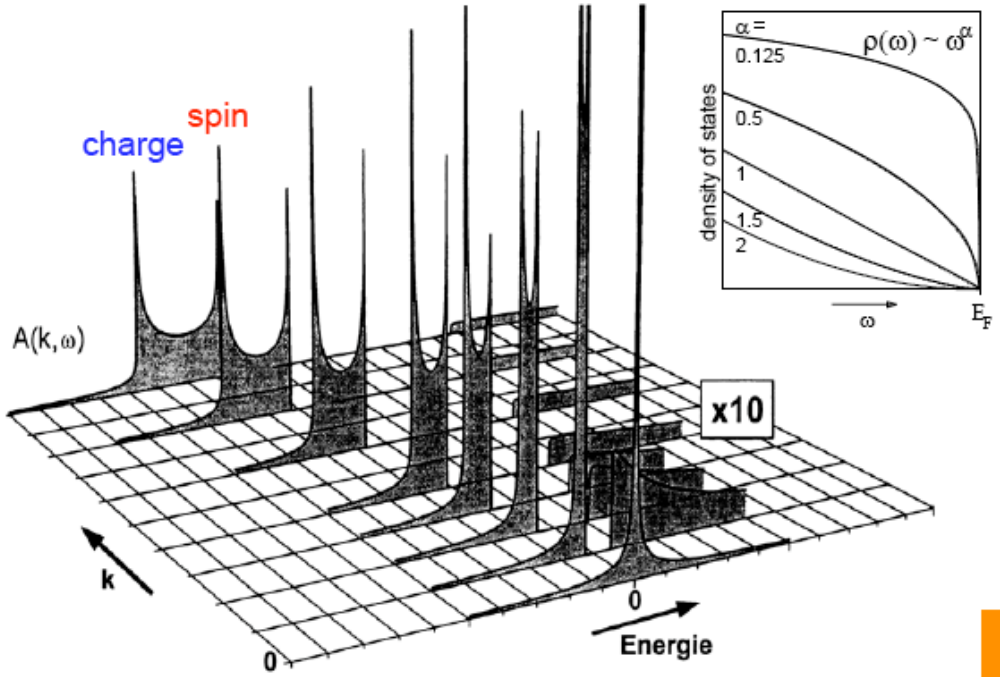

Voit (1995)
Schönhammer and Meden (1995)

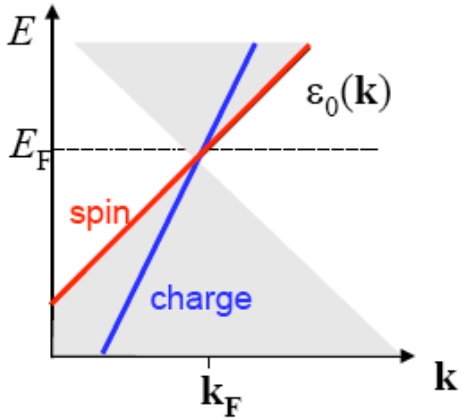

- **spin-charge "separation"**
- **failure of the quasiparticle concept**
- **power law onset in DOS (no Fermi edge !)**

generic low-energy physics of interacting 1D metals: LUTTINGER LIQUID

SWCNTs: an example of Tomonaga-Luttinger liquid

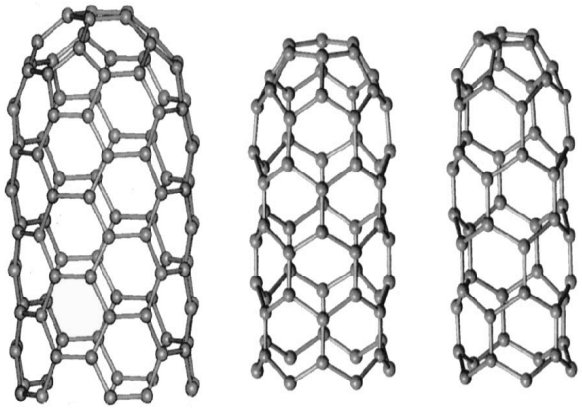

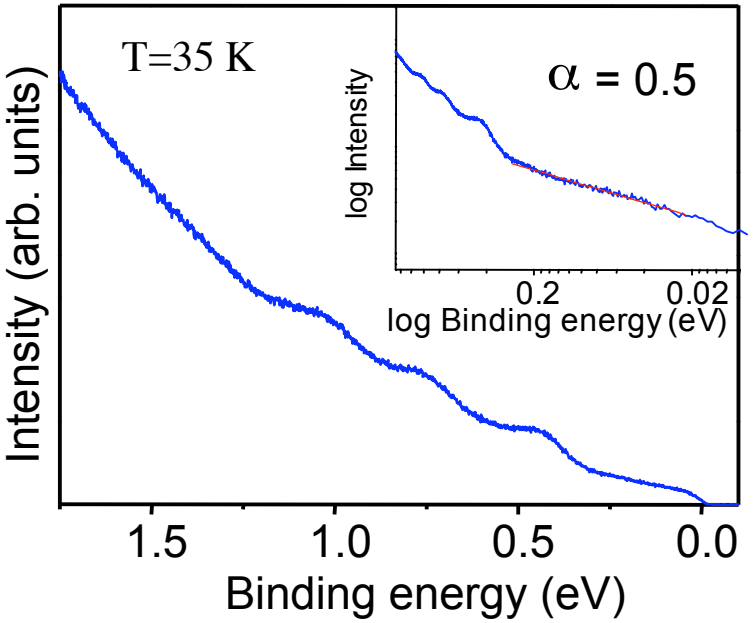

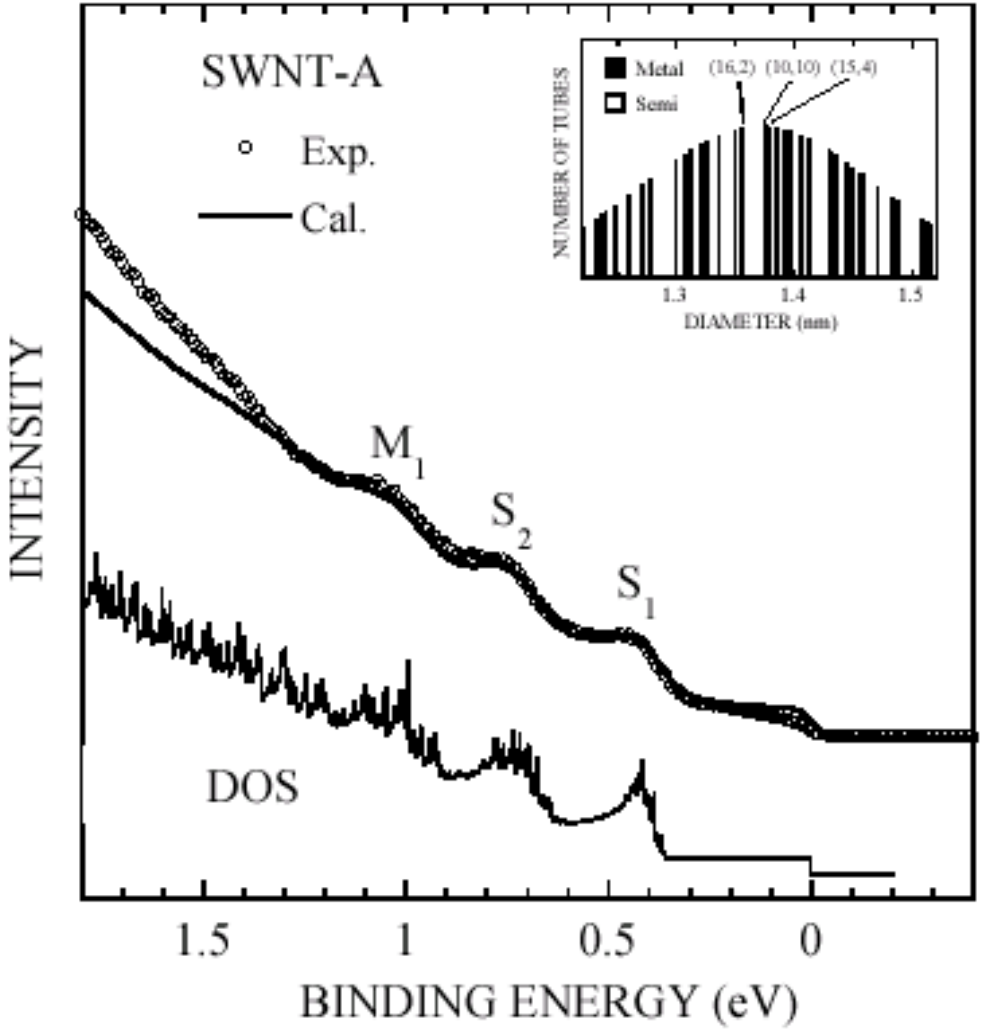

H. Ishii et al, Nature, 426, 540 (2003)

log-log plot

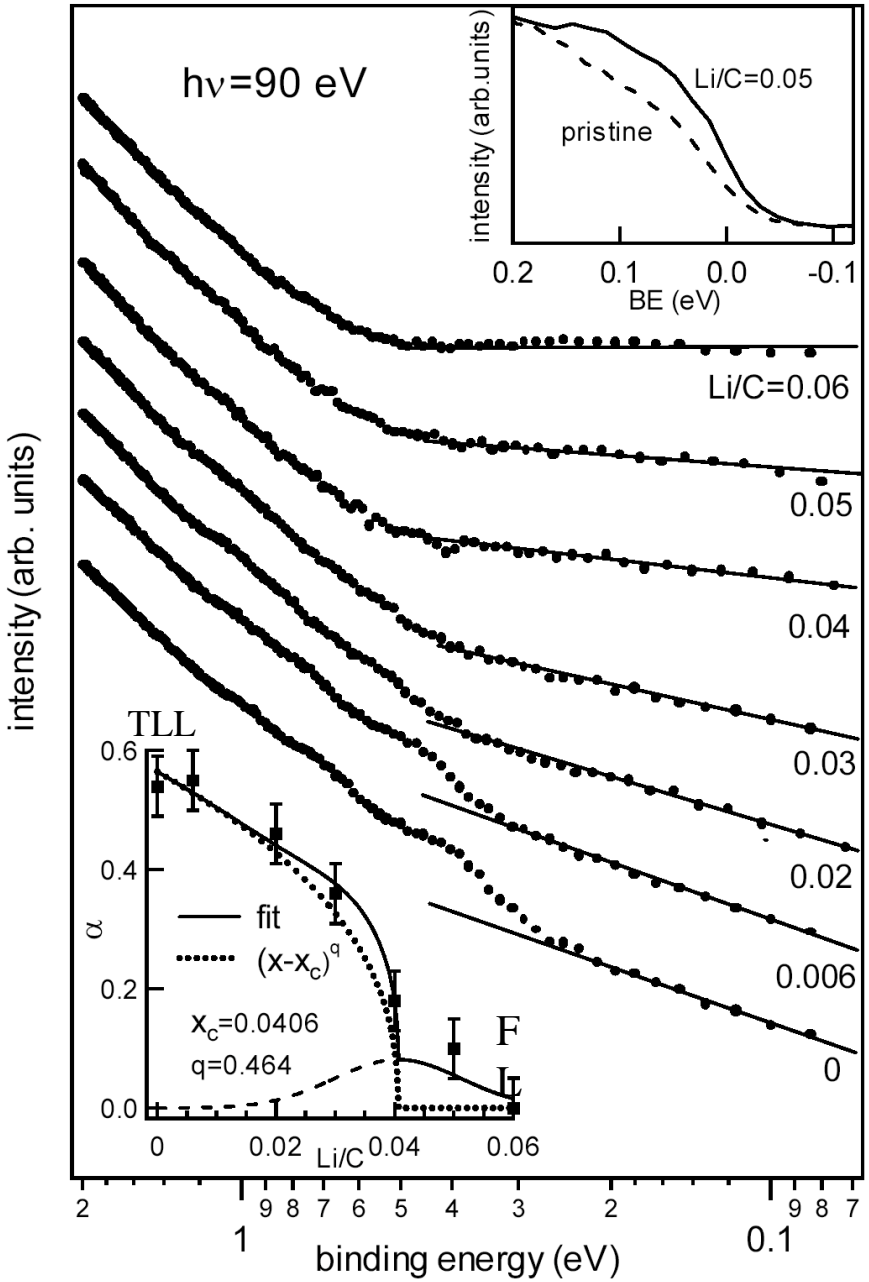

Transition from a Tomonaga-Luttinger liquid to a Fermi liquid

$n(E) \propto |E-E_F|^{\alpha}$, where $\alpha=(g+g^{-1}-2)/8$ depends on the size of the Coulomb interaction and g is the Luttinger parameter

$\alpha \sim 0.53 \pm 0.05$ for pristine SWCNTs in agreement with other estimations

$\alpha=0$ Fermi liquid

R. Larciprete, S. Lizzit, L. Petaccia, A. Goldoni, PRB 71, (2005)

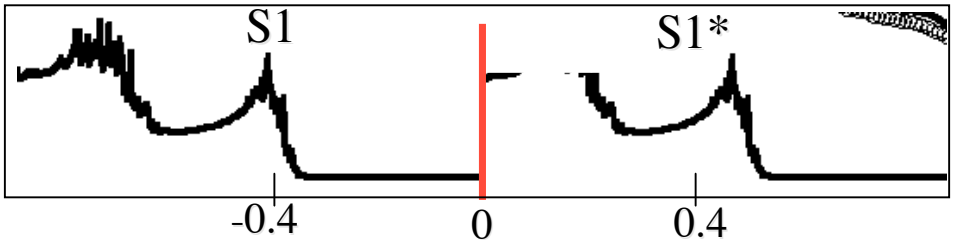

Mott-Hubbard insulator

Non-interacting Limit

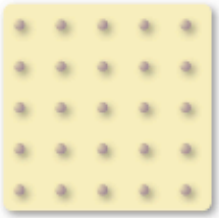

- metallic
- bandwidth ~ 8*t* ~ 3 eV

Metal

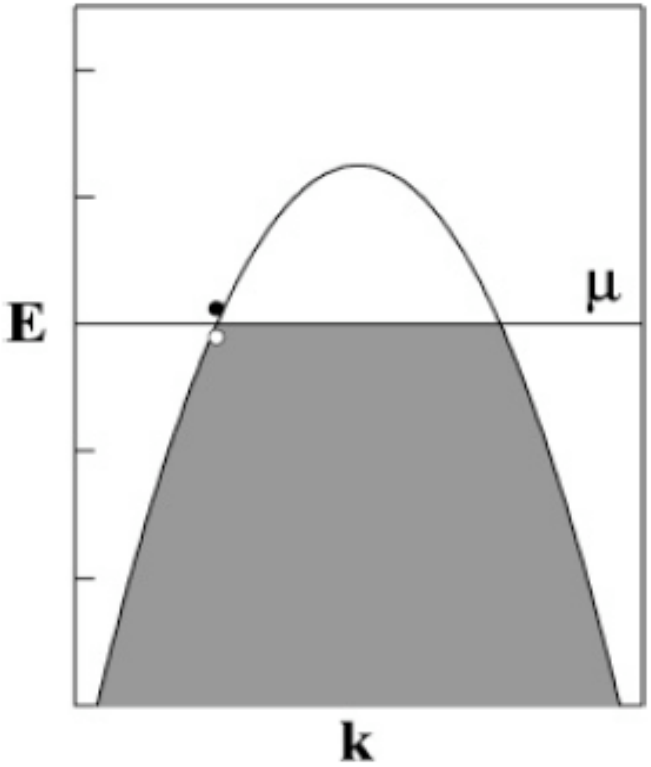

Strongly Interacting (Mott) Limit

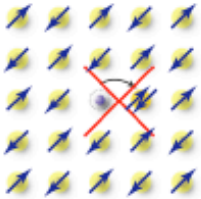

- insulating (Δ ~ 2 eV)
- antiferromagnetic
- bandwidth ~ 2*J* ~ 0.3 eV

Insulator

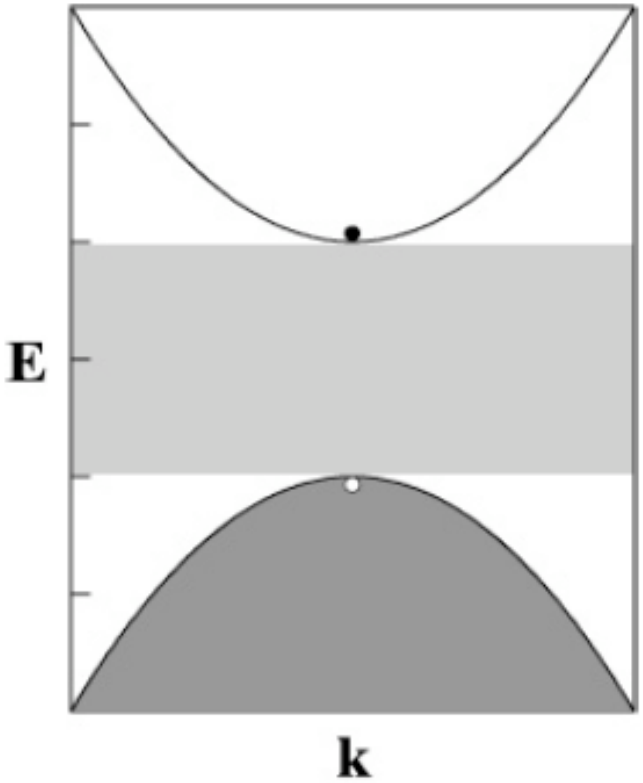

$Ca_{2-x}Na_xCuO_2Cl_2$: at x=0 Mott-Hubbard insulator

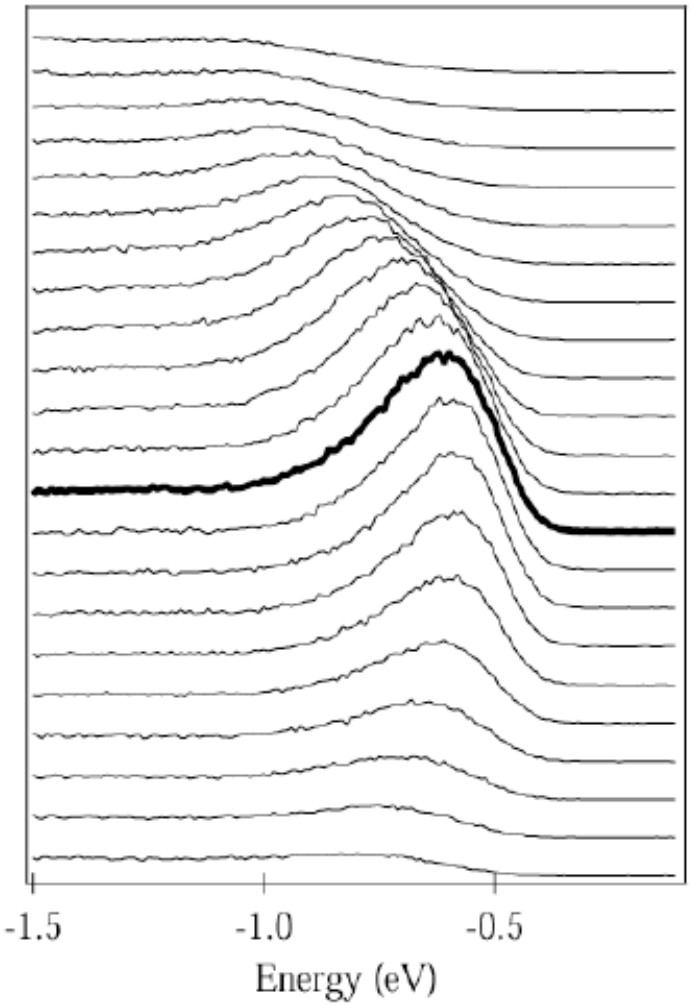

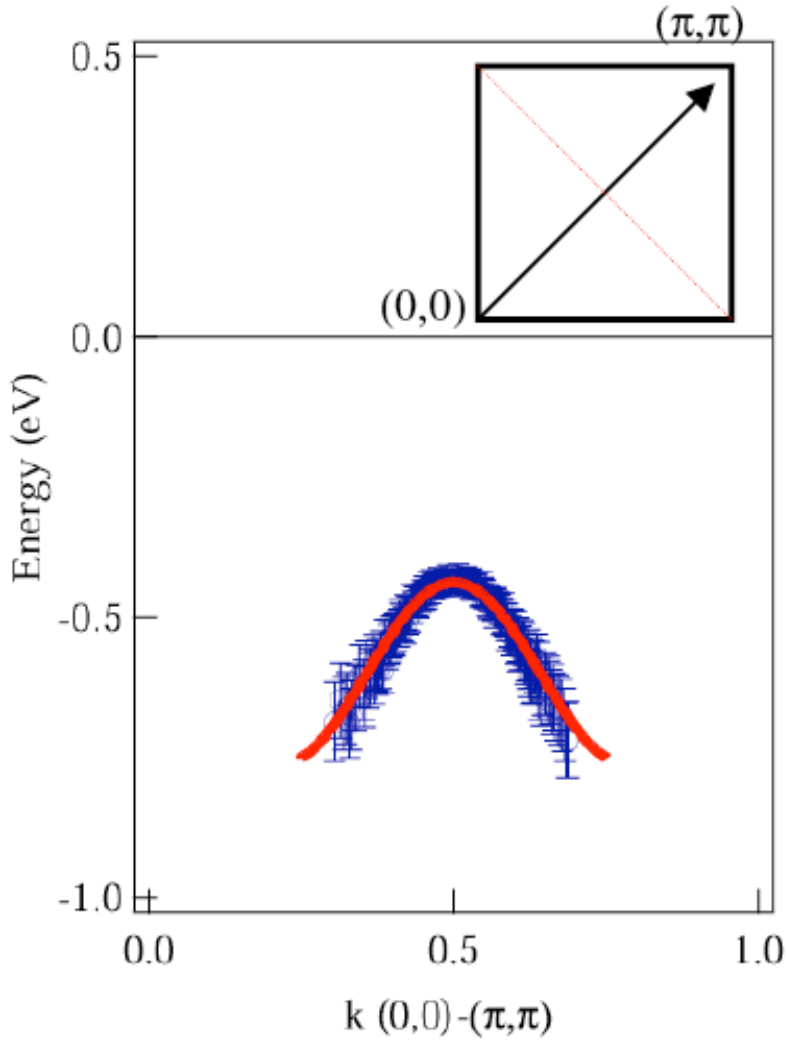

- Dispersion of peak intensity follows *t-J* model well
- Suggests quasiparticle excitations from *t-J* model are appropriate
- However, this is not the end of the story....

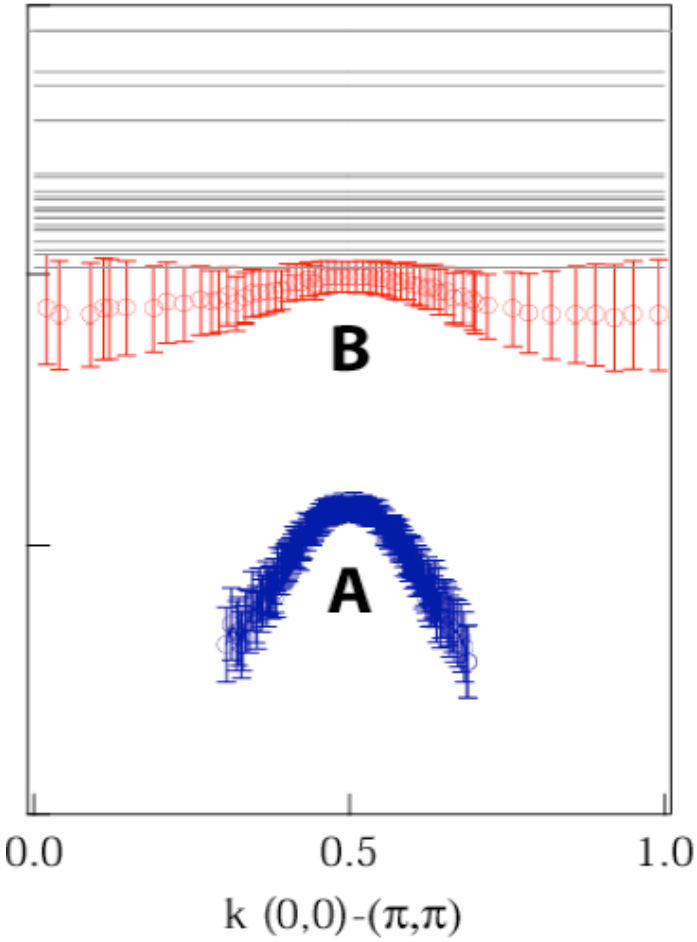

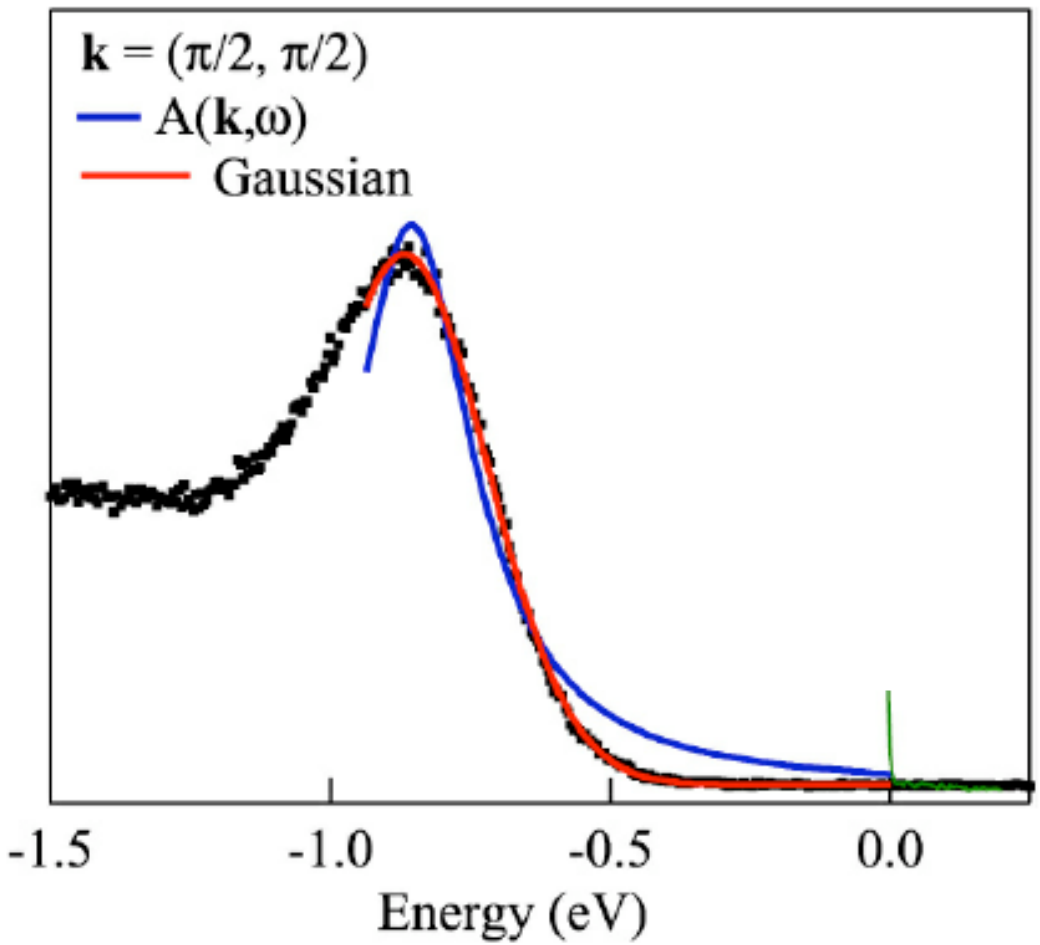

$$A(\mathbf{k},\omega) \propto \frac{\mathrm{Im}\Sigma(\mathbf{k},\omega)}{[\omega - \varepsilon_k - \mathrm{Re}\Sigma(\mathbf{k},\omega)]^2 + [\mathrm{Im}\Sigma(\mathbf{k},\omega)]^2}$$

- Spectral function formalism **FAILS** to qualitatively describe lineshape
- Linewidth far too broad

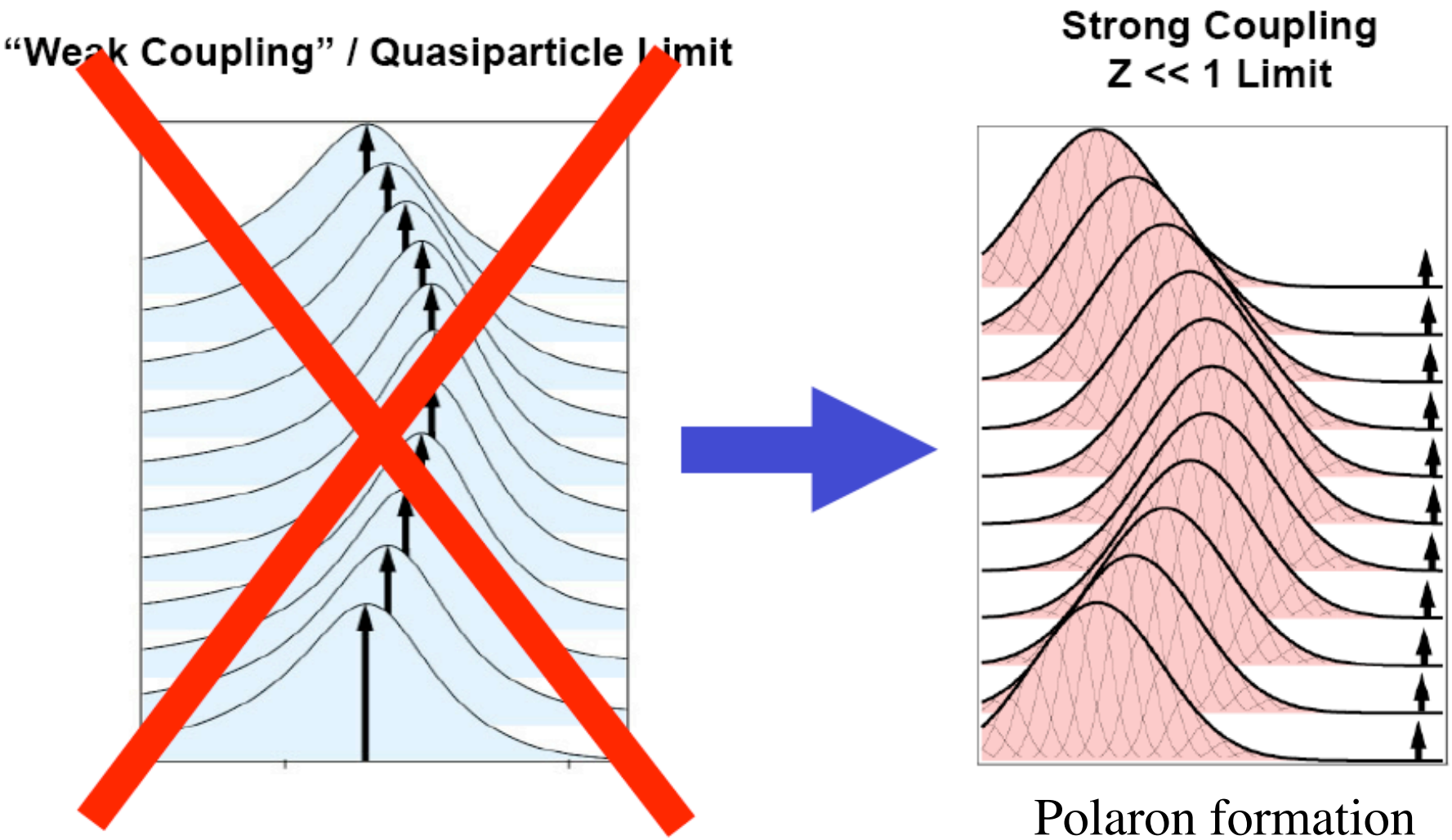

- Consistent with extreme width
- Explains anomalous lineshape
- Justifies positions of chemical potential
- Vast majority of spectral weight in *incoherent* transitions

$Ca_{2-x}Na_xCuO_2Cl_2$: doping dependence

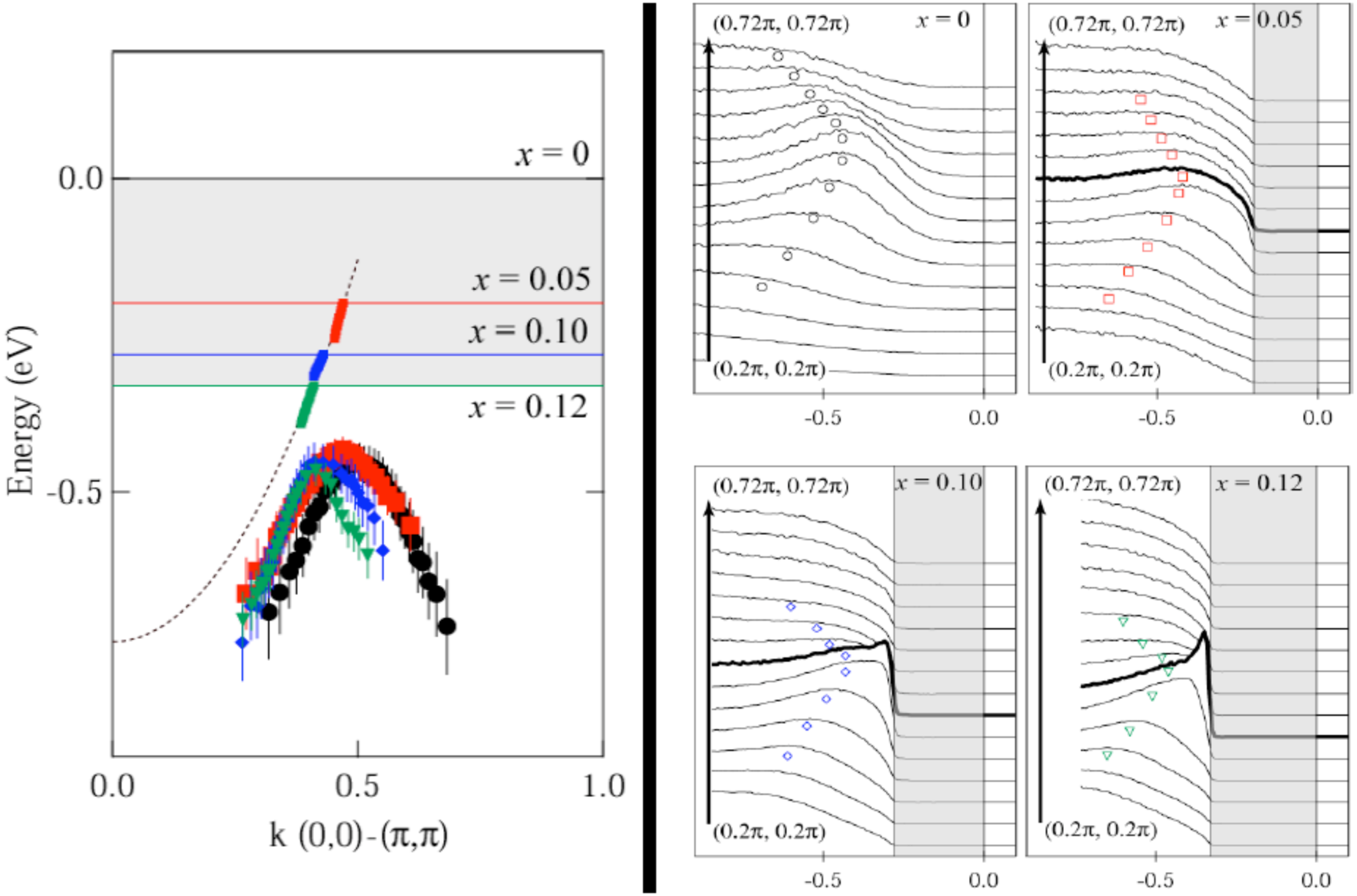

$Ca_{2-x}Na_xCuO_2Cl_2$: doping dependence

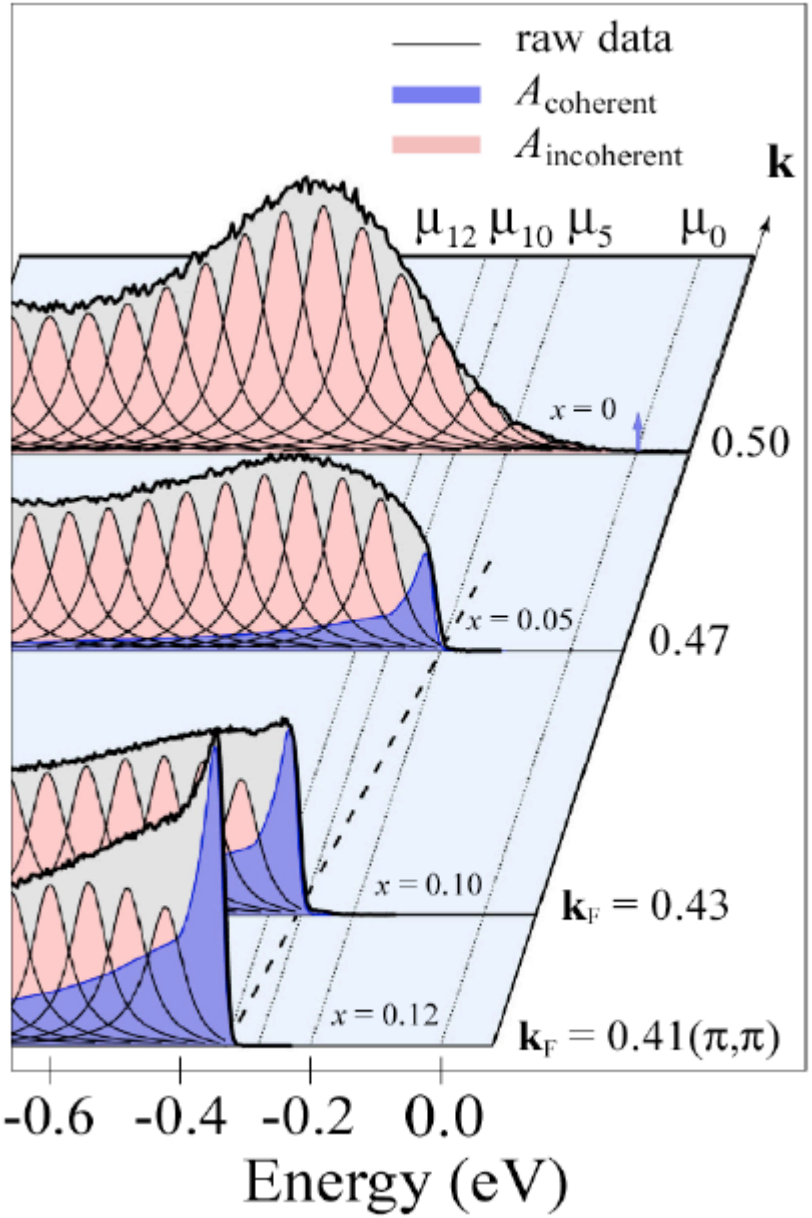

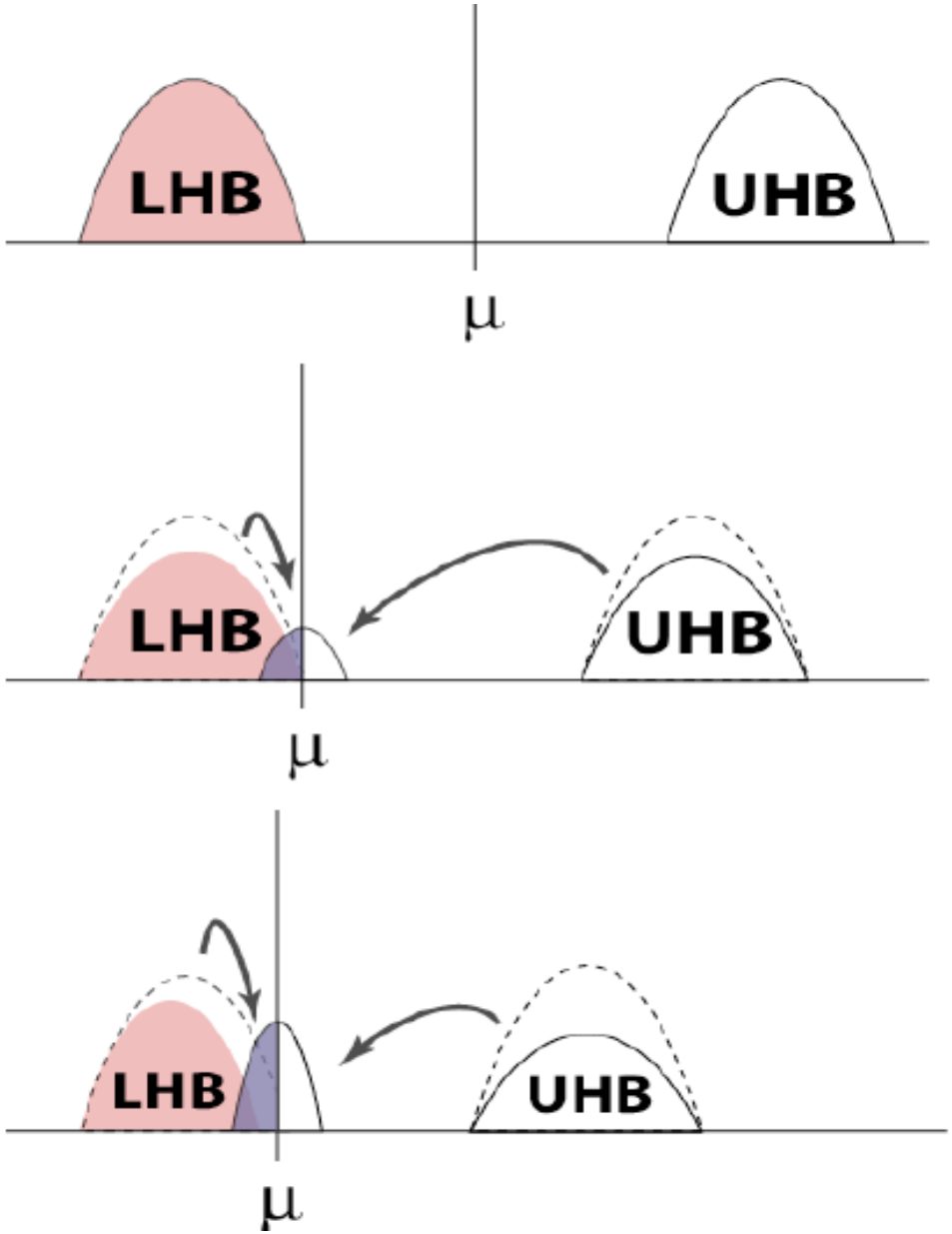

Fullerenes

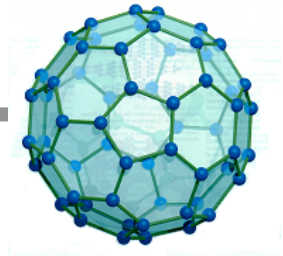

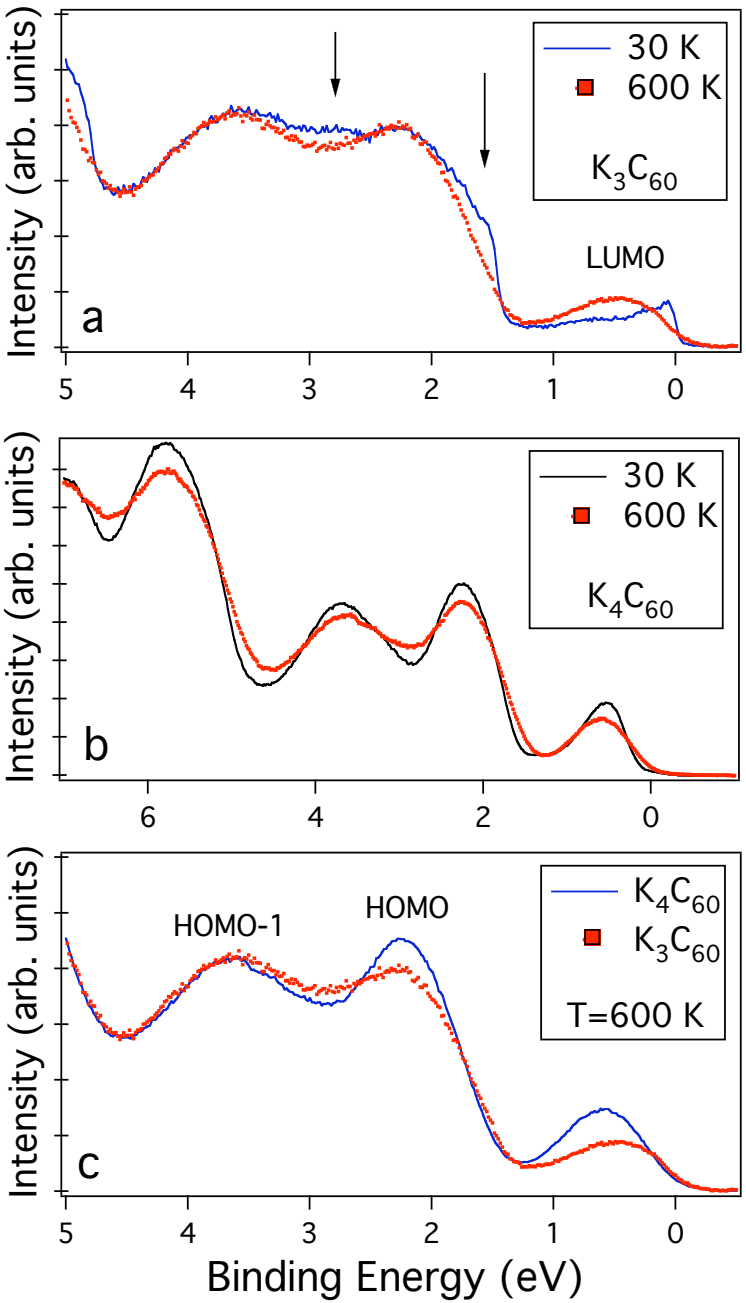

A. Goldoni, L. Sangaletti, S.L. Friedmann, Z.-X. Shen, M. Peloi, F. Parmigiani, G. Comelli and G. Paolucci, J. Chem. Phys. 113, 8266 (2000)

Strongly correlated metal

Strong correlations U ~ 1 - 1.3 eV
Small band dispersion W ~ 0.5 - 0.6 eV
Orbital degeneracy (HOMO 5 fold, LUMO 3 fold)
Small Fermi energy ~ 0.25 eV
Phonon spectrum up to 0.2 eV
Jahn-Teller distortions in charged C_{60}
E_{JT}~ 0.03-0.18 eV for C_{60}^{n-}

Mott-Hubbard insulator

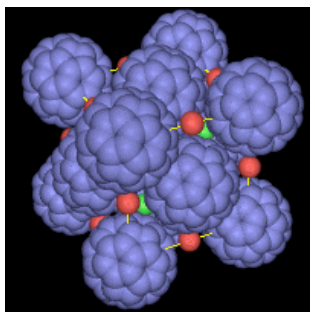

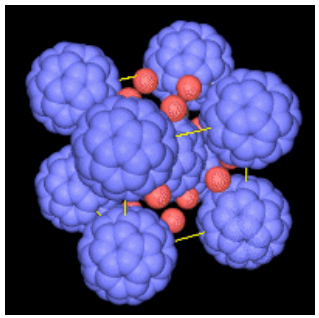

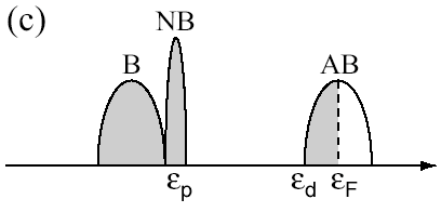

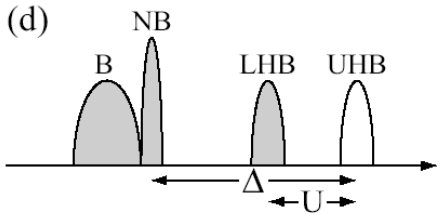

Band dispersion of $K_3C_{60}(111)$

Dispersion < 100 meV

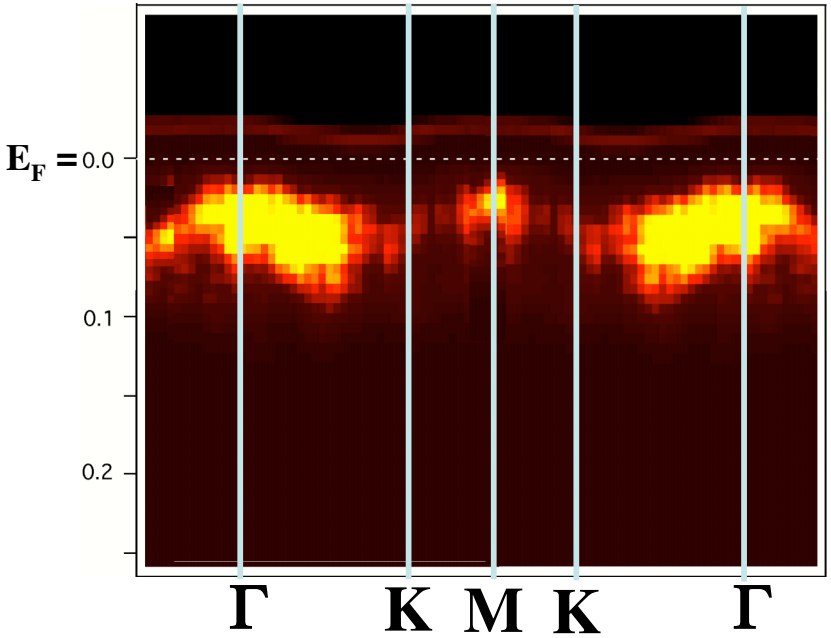

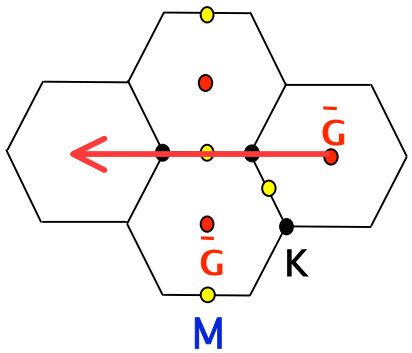

Spectrum dominated by phonon and plasmon excitations; quasi-particle coherent peak confined near E_F

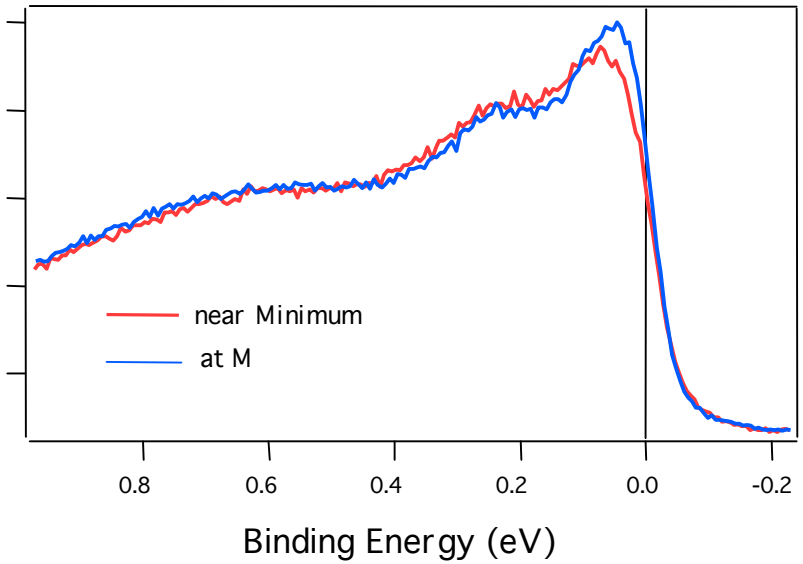

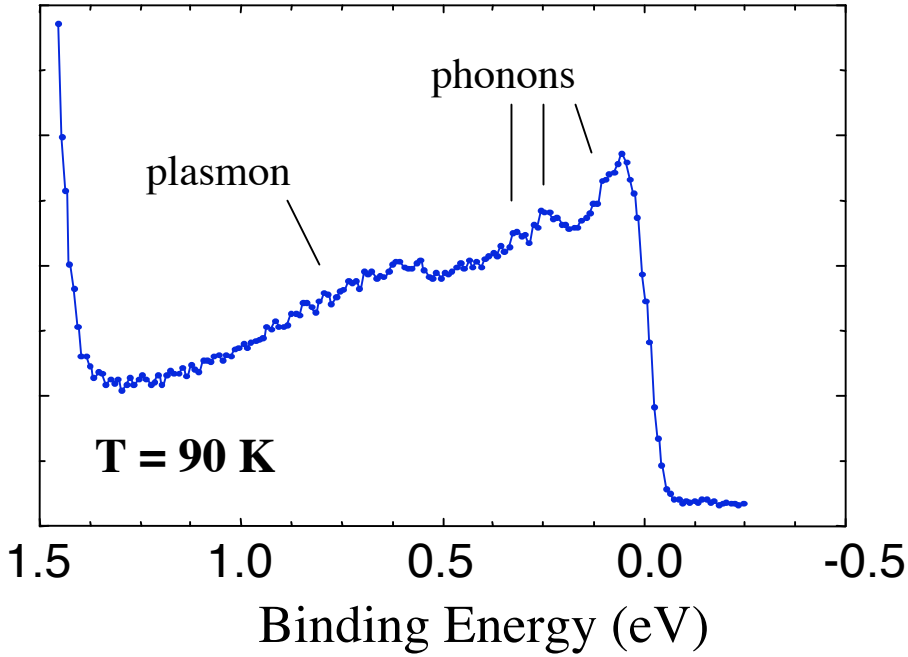

K_6C_{60} (Ionic Crystal)

bcc lattice

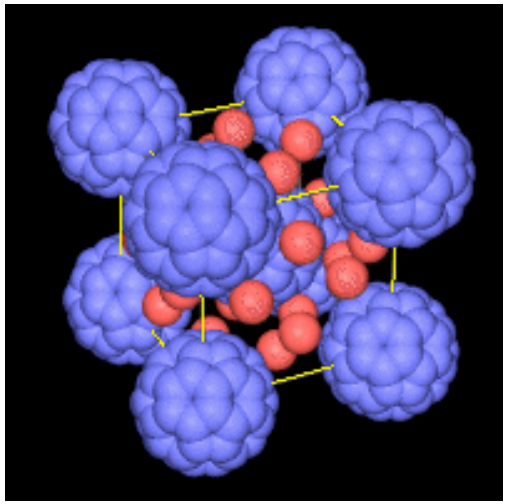

LUMO bands completely filled:
band insulator
Ground state trivial

No molecular motion
No J-T distortion
No correlation effects
No screening
Coupling also to K^+ modes

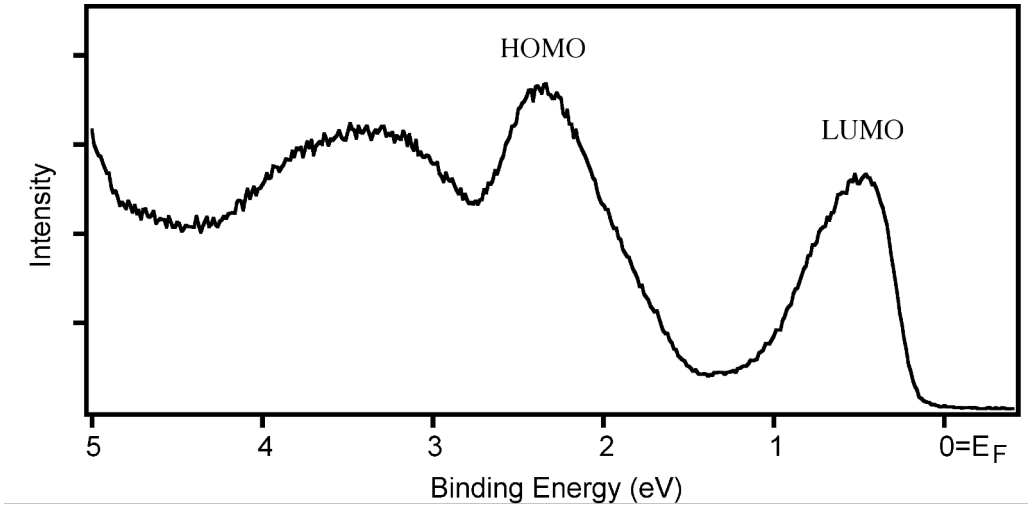

Photoemission creates a single hole in a full band,
that couple to phonons ===> POLARON PROBLEM

Predictions for K_6C_{60} (Ionic Crystal)

Contributions to the convolution:

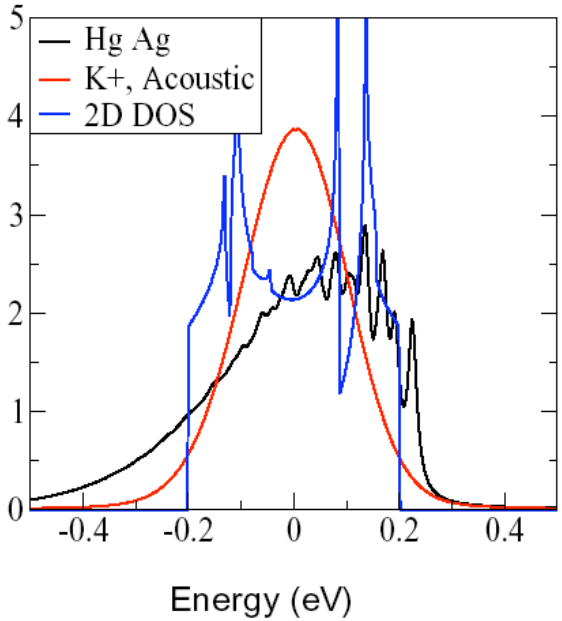

What we should expect ?

Comparison with experiment:

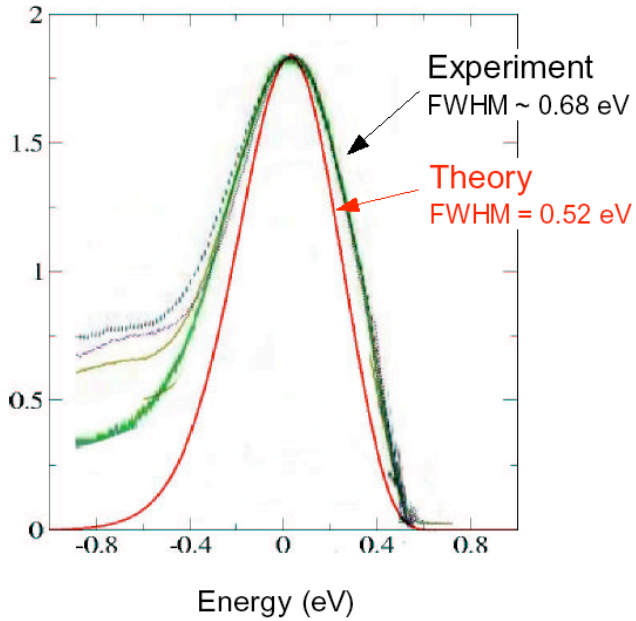

K^+, $C60^{6-}$ phonons are strongly coupled ($g >> \omega$).
⇒ Smooth spectra (convolution with gaussian)

The width is dominated by the on-ball phonons.
⇒ The width is independent of the system
⇒ The width should be similar in K4C40 (?)

The first moment $\mu_1(k)$ in ARPES is the band structure.
⇒ The mean value of the broad peak should be k-dependent.

S. Wehrli *et al.*, Phys. Rev. B **70**, 233412 (2004)

Band dispersion of $K_6C_{60}(110)$

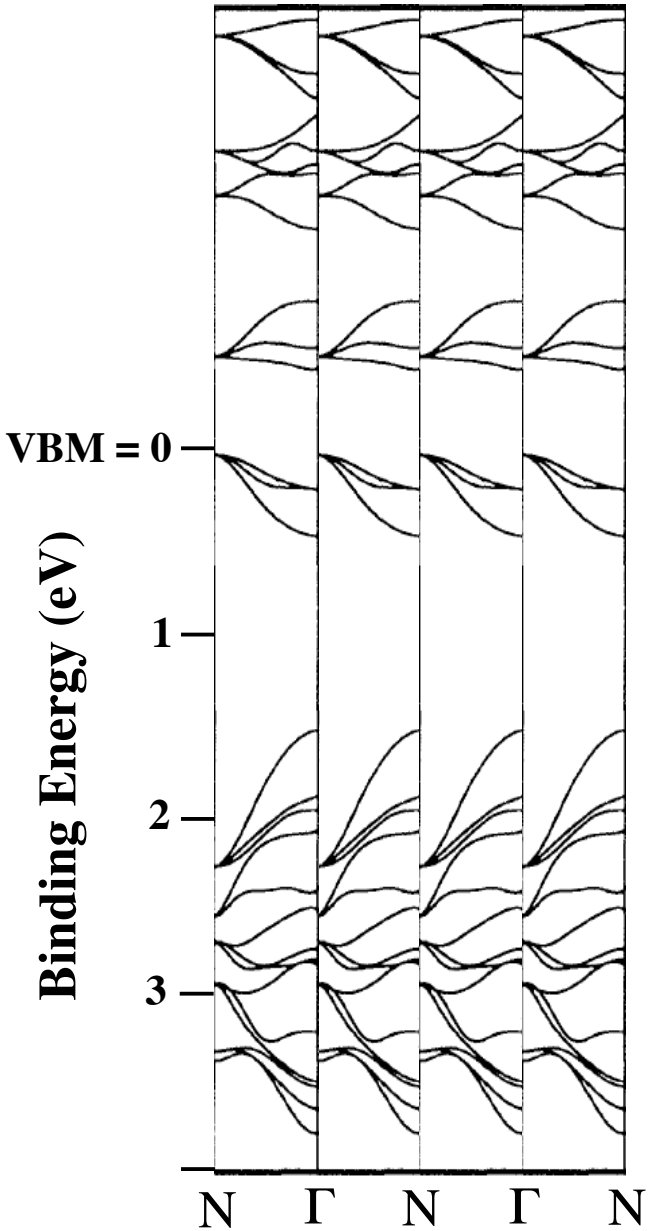

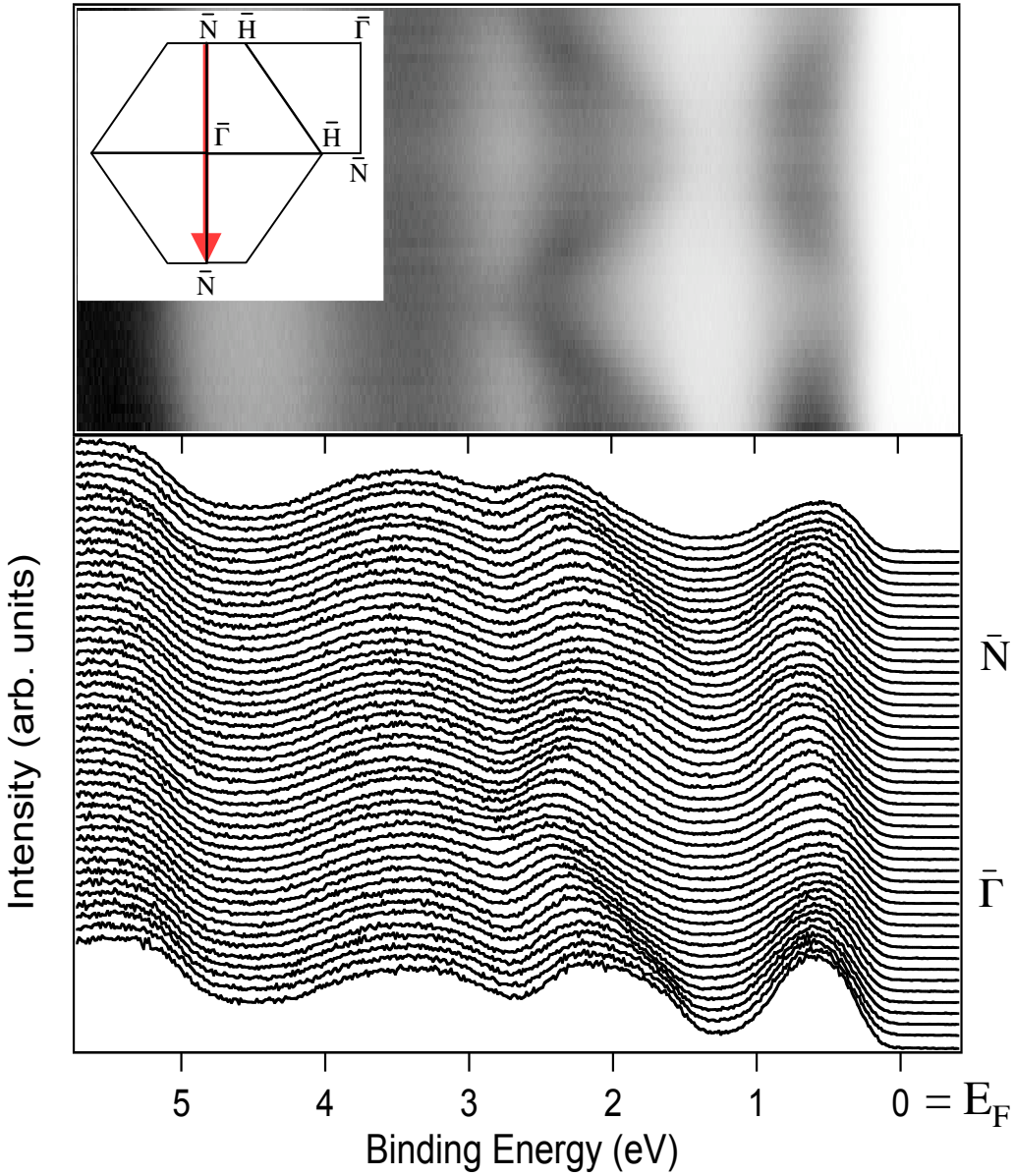

Band dispersion of $K_6C_{60}(110)$

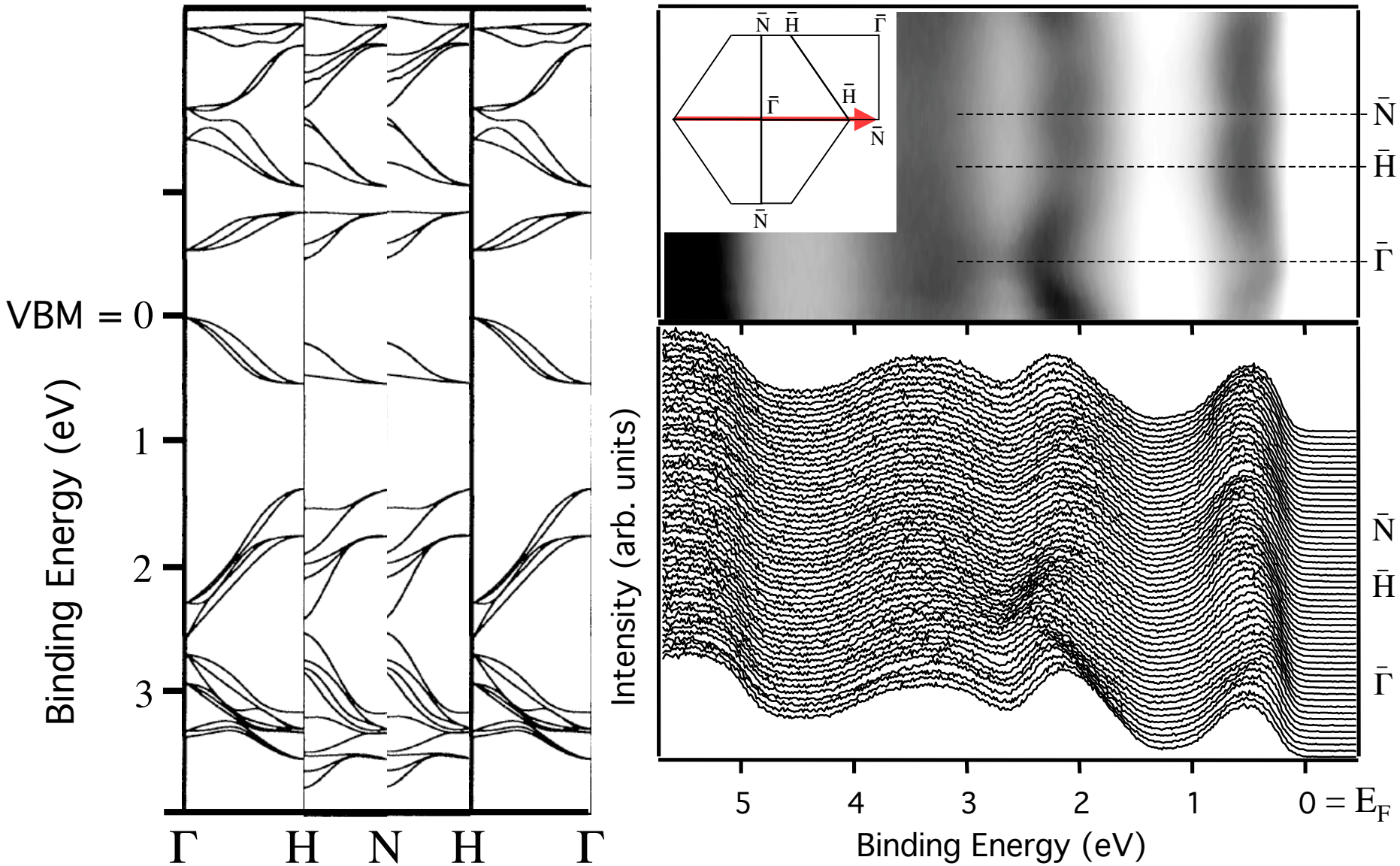

Band dispersion of $K_6C_{60}(110)$

At Γ the bandwidth due to the presence of the three LUMO bands should be very sharp and, even considering our integration in $K_\perp$, in the worst case we must expect a width of the photoemission feature of 0.25 eV **=> difference more than a factor of 2**

Phonon contribution to the LUMO width

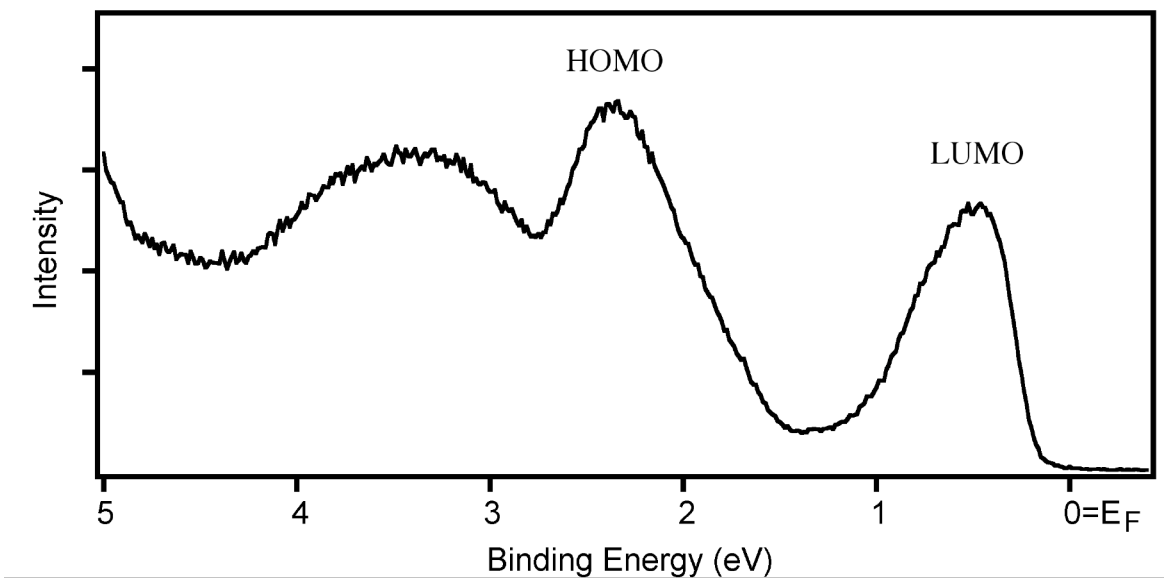

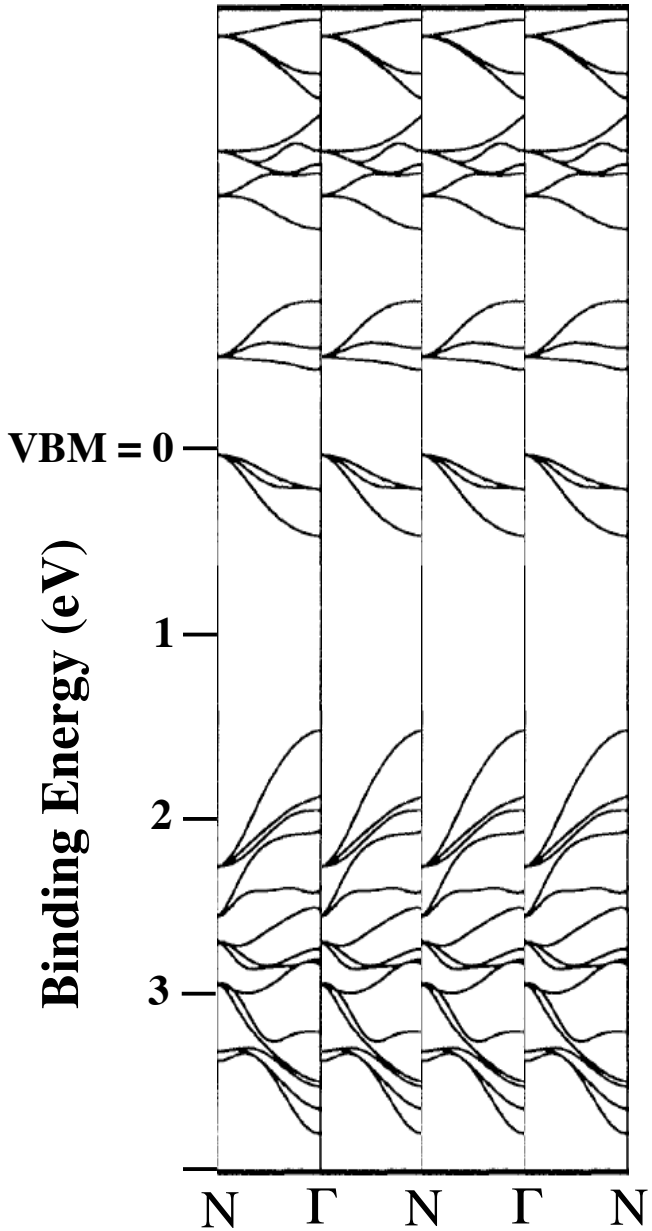

Temperature dependence of $K_6C_{60}(110)$ LUMO width at $\bar{\Gamma}$

$$FWHM = W_0 + 2\pi\hbar \int_0^{\omega_D} \alpha^2 F(\omega)\left[1 + 2n(\omega, T)\right] d\omega$$

Debye Model

$$\begin{cases} \alpha^2F(\omega)=[\lambda\omega/\sqrt{(\omega_D^2-\omega^2)}]/\pi \text{ (2D model)} \\ \alpha^2F(\omega)=\lambda(\omega/\omega_D)^2 \text{ (3D model)} \end{cases}$$

B. Hellsing et al.,
J. Phys.: Condens. Matter **14**, 5959 (2002)

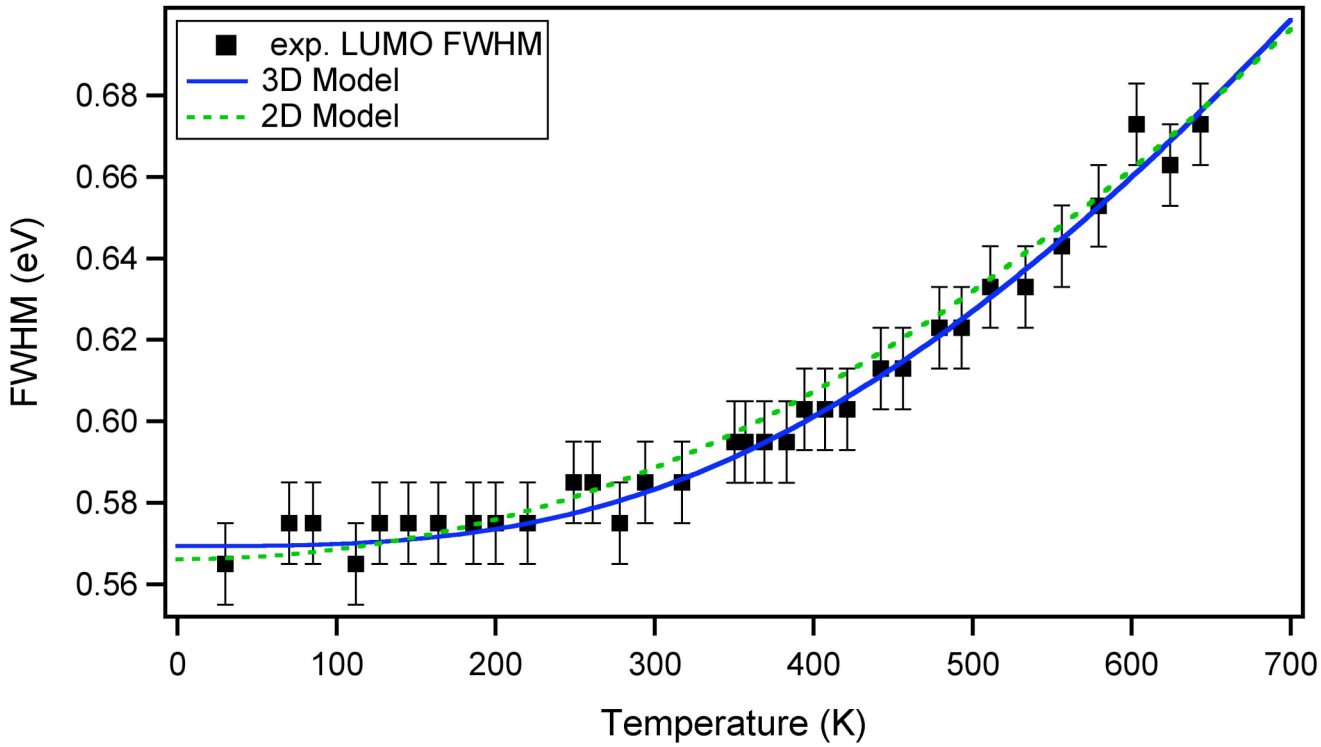

ω_D= 200 meV
W_0=0.11±0.04 eV

λ=1.15±0.05
Intermediate polaron regime

Calculations explain why the el-ph coupling leads to a broadening of spectra calculated by neglecting el-ph coupling, with minor influence on the dispersion.
O. Rösch and O. Gunnarsson, Eur. Phys. J. B **43**, 11 (2005)

In the intermediate polaron regime the dispersion of the incoherent spectral function (that dominates the spectrum) is weakly affected compared to the weak-coupling regime (spectrum dominated by the coherent part and bear a close resemblance with the free-electron case), but with a much more broadened lineshape reflecting the stronger coupling to the phonon distribution. M. Hohenadler *et al.*, Phys. Rev. B **71**, 245111 (2005)

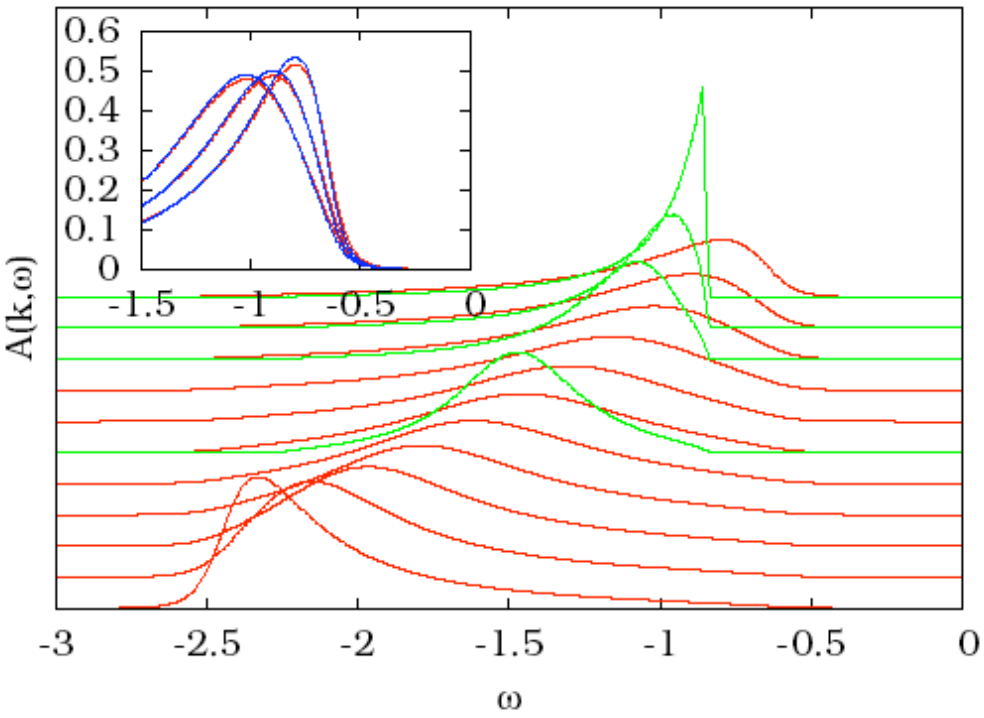

Similar results obtained for a Mott-Hubbard insulator with intermediate coupling to phonons
S. Fratini and S. Ciuchi, PRB 72 235107 (2005)

Very low-energy photoemission spectroscopy

Andrea Goldoni
Sincrotrone Trieste S.C.p.A.

elettra

Outline

- How low photon energy are produced
- The Bad ElPh beamline
- Reasons for low photon energy: bulk sensitivity, higher momentum resolution, good energy resolution easier
- Sudden Approx still valid?
- Final state effects?
- Other problems

How low photon energies can be obtained ?

1) Gas discharge lamp (He=21.22 eV, Ne=16.85 eV, Ar= 11.62-11.83 eV, H_2= 10.2 eV)

Large spot size (several mm), ~ 10^{14} photons/s, intrinsic linewidth ~ 1-2meV satellite lines

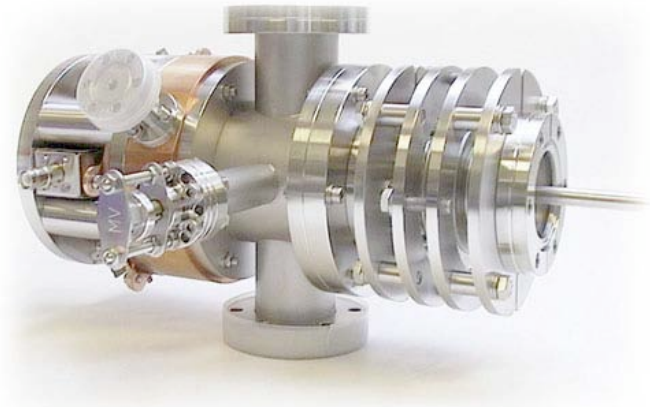

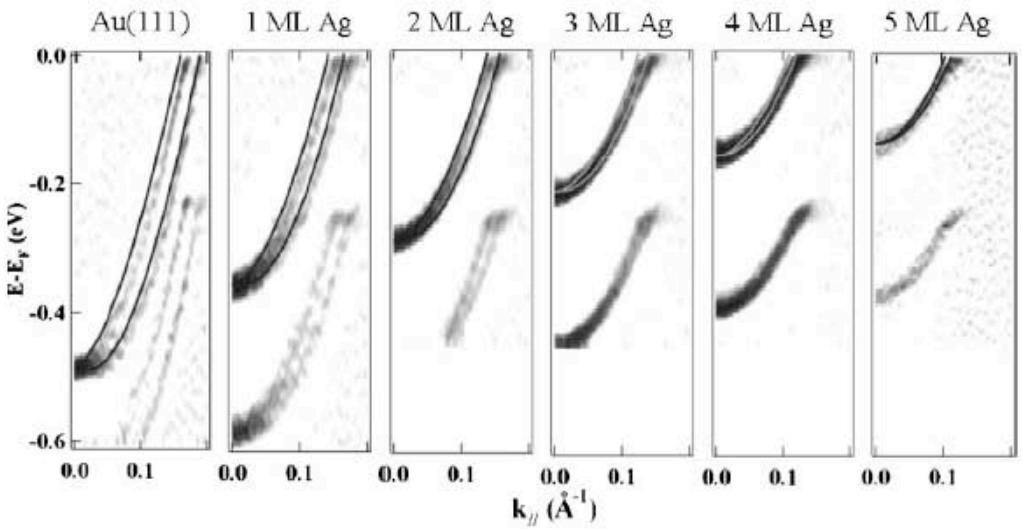

FIG. 2. Surface state dispersion changes with silver coverage taken with Ar I. The grey-scale maps represent the second derivative of the measured intensity. The calculations of the Shockley state (black lines) have been shifted for each coverage to fit the measured binding energies. The replica at higher BEs is due to the Ar satellite.

How low photon energies can be obtained ?

2) Laser systems (6 - 7 eV)

Spot size 1-500μm, > 10^{15} photons/s on the sample, intrinsic linewidth 0.26-0.1meV, only one energy

S. Shin, RIKEN, Tokyo Univ. (Jap)
D.S. Dessau, Univ. Colorado (USA)

Schematic of a system for performing photoemission spectroscopy based on a frequency quadrupled Ti:sapphire oscillator (6 eV) running at 100 MHz.

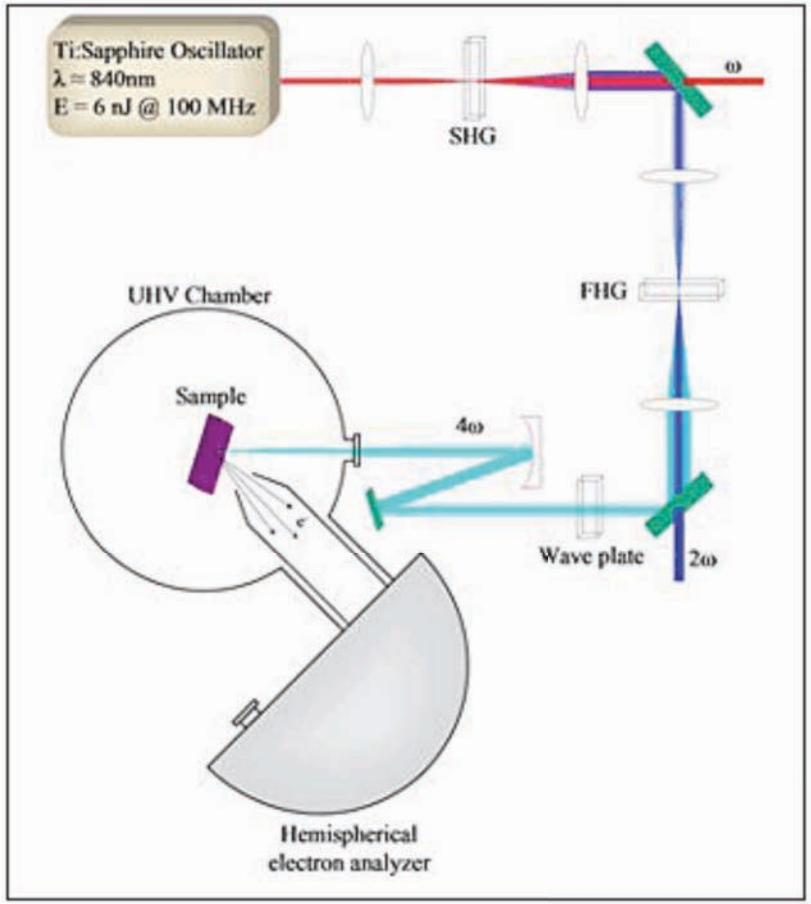

Note the high repetition rate:
Needed for a high signal to noise while keeping the instantaneous electron emission rate low.

This last aspect is critical for keeping the electronic response of the sample in the linear regime and to minimize space-charge and other spurious effects.

Laser excitation photoemission spectrometer

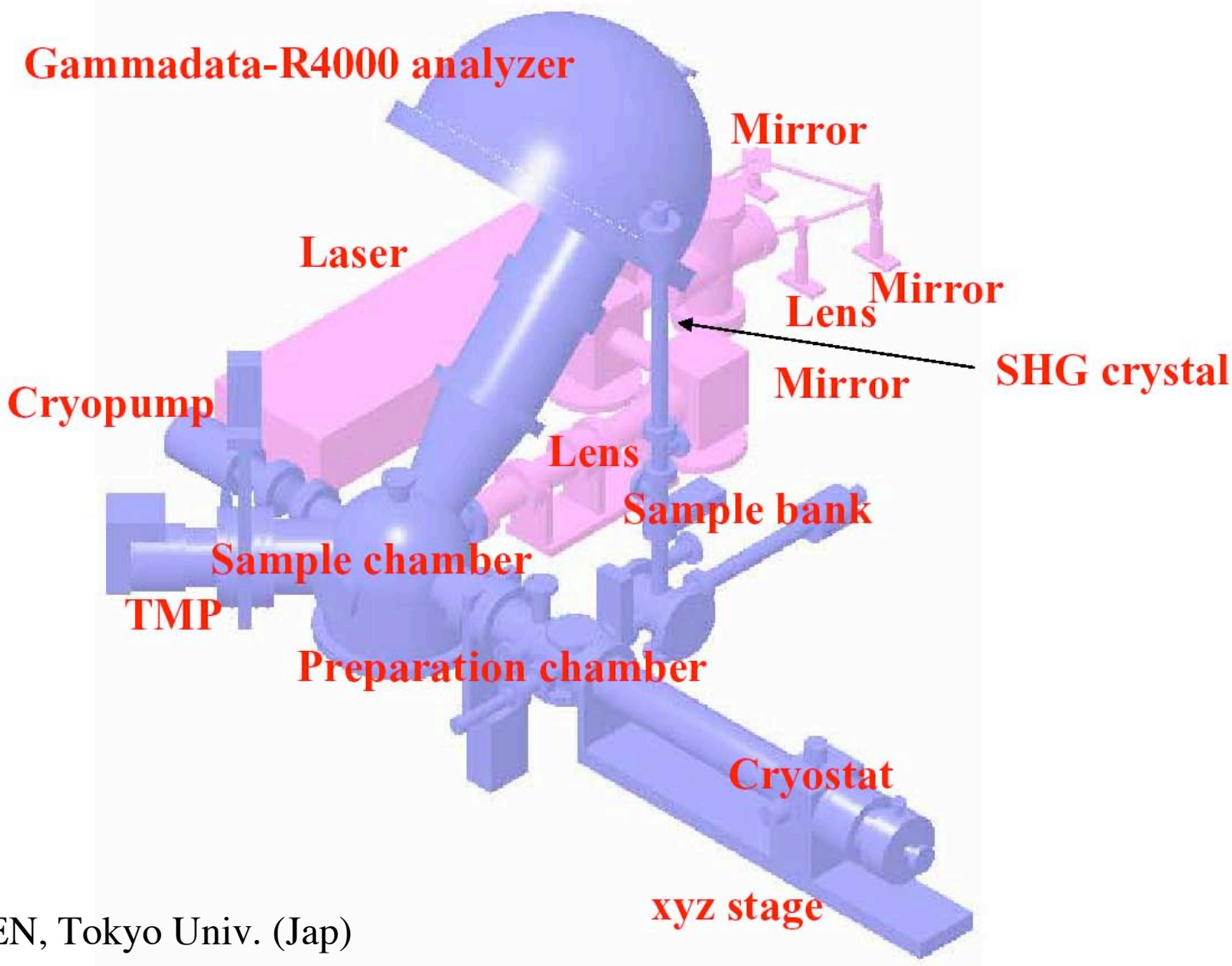

S. Shin, RIKEN, Tokyo Univ. (Jap)

How low photon energies can be obtained ?

3) Synchrotron radiation

Spot size 10-400μm, > 10^{12} photons/s on the sample, intrinsic linewidth < 1meV, continuous energy range

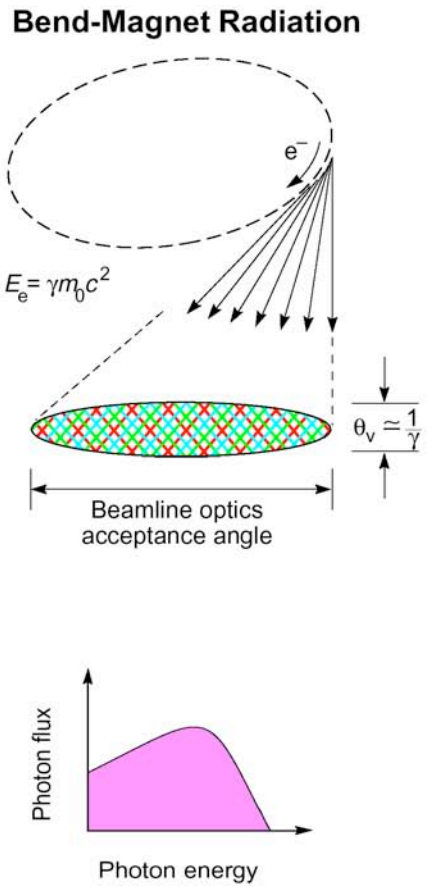

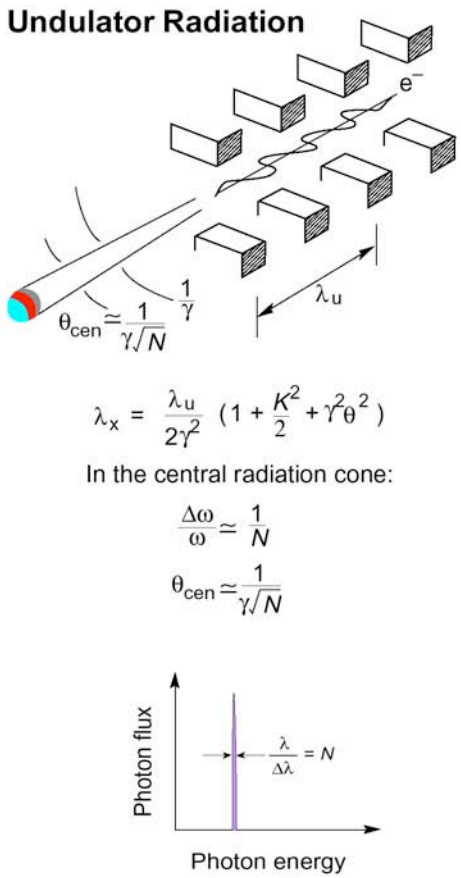

BaD ElPh Layout

4m Normal Incidence Monochromator: 5°

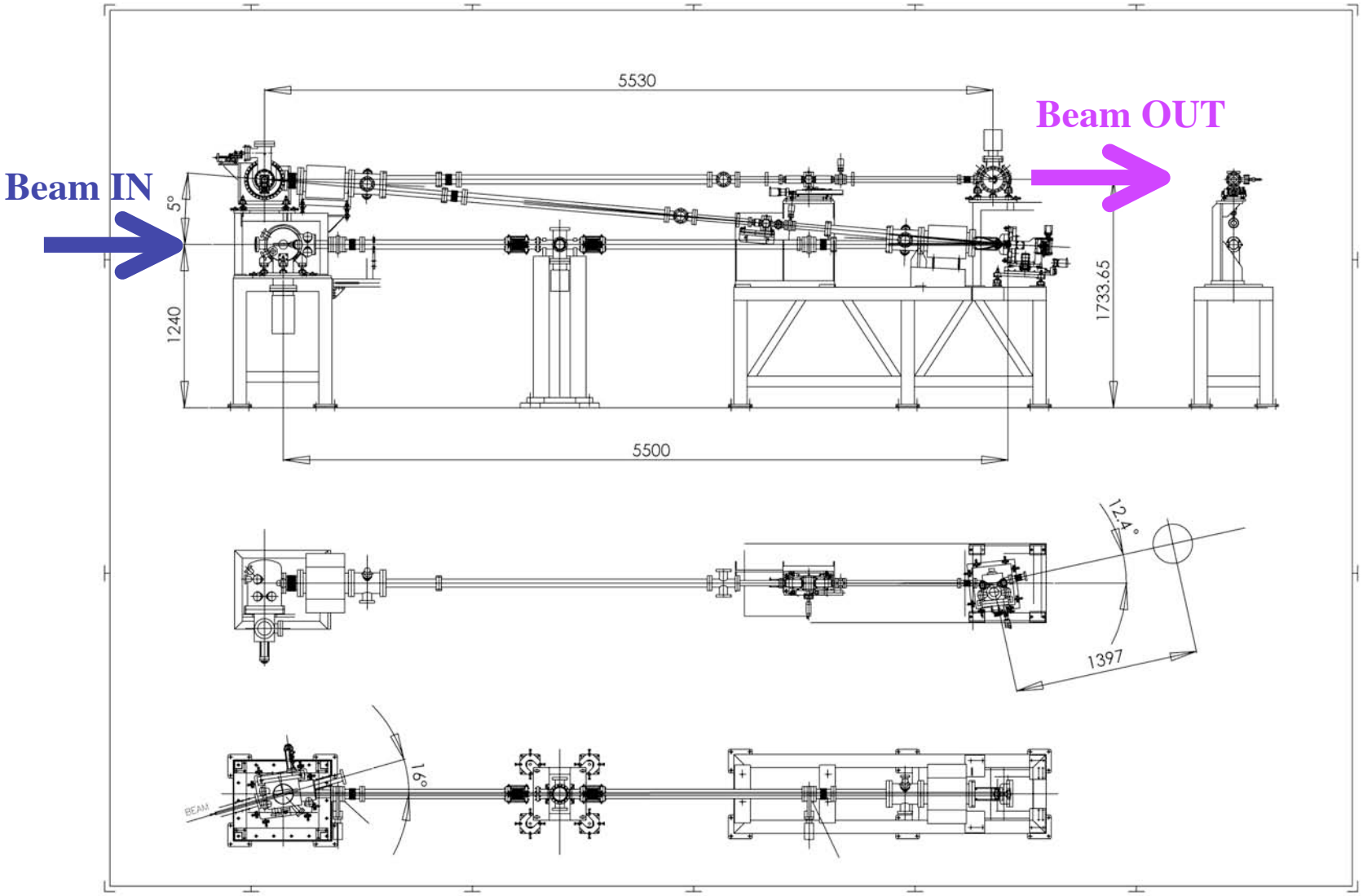

Energy range: 5 - 23 eV with two gratings, a third grating foreseen for 23-35 eV

The monochromator performances

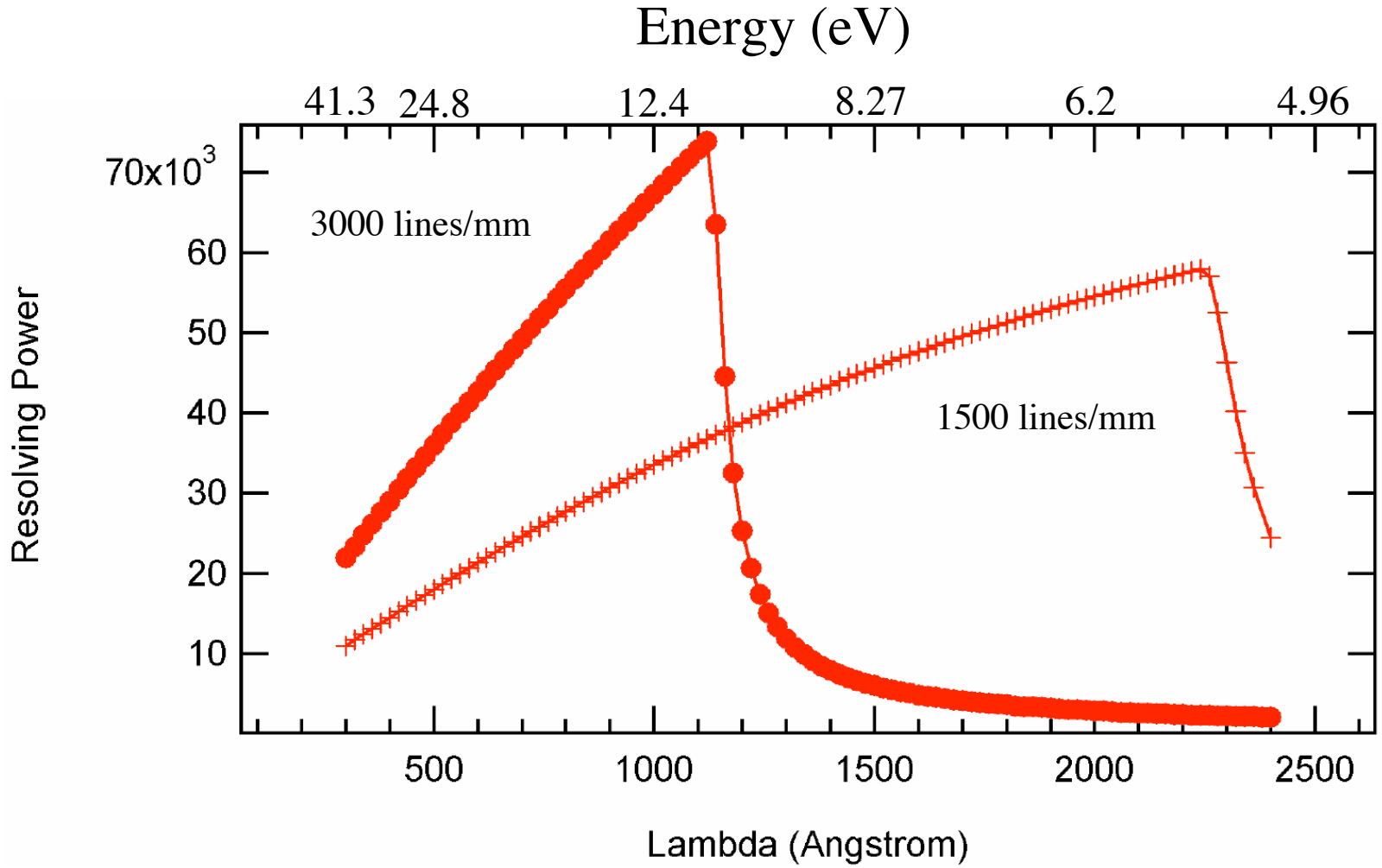

20 eV, resolving power 45000 (10 μm)
12 eV, resolving power 75000 (10 μm)
8 eV, resolving power 50000 (10 μm)

Expected performances:

Cryostat/manipulator
T ~ 4 K

Total energy resolution
~ 3 meV

Momentum resolution
< 0.005 Å^{-1}

Actual performances:

Cryostat/manipulator
T ~ 11 K (on the sample)

Total energy resolution
~ 5.7 meV

Momentum resolution
< 0.005 Å^{-1}

GAMMADATA —SCIENTA—

ELECTRON SPECTROMETER

SCIENTA SES 50

Features:

- < 3 meV energy resolution
- Angle multiplexing recording from small area samples
- Extremely low noise, high stability power supplies
- Customized lens design
- Multi-channel resistive anode detector

Main application:

- High resolution electron spectroscopy
- High resolution photo-electron diffractionion
- High resolution angular resolved spectroscopy

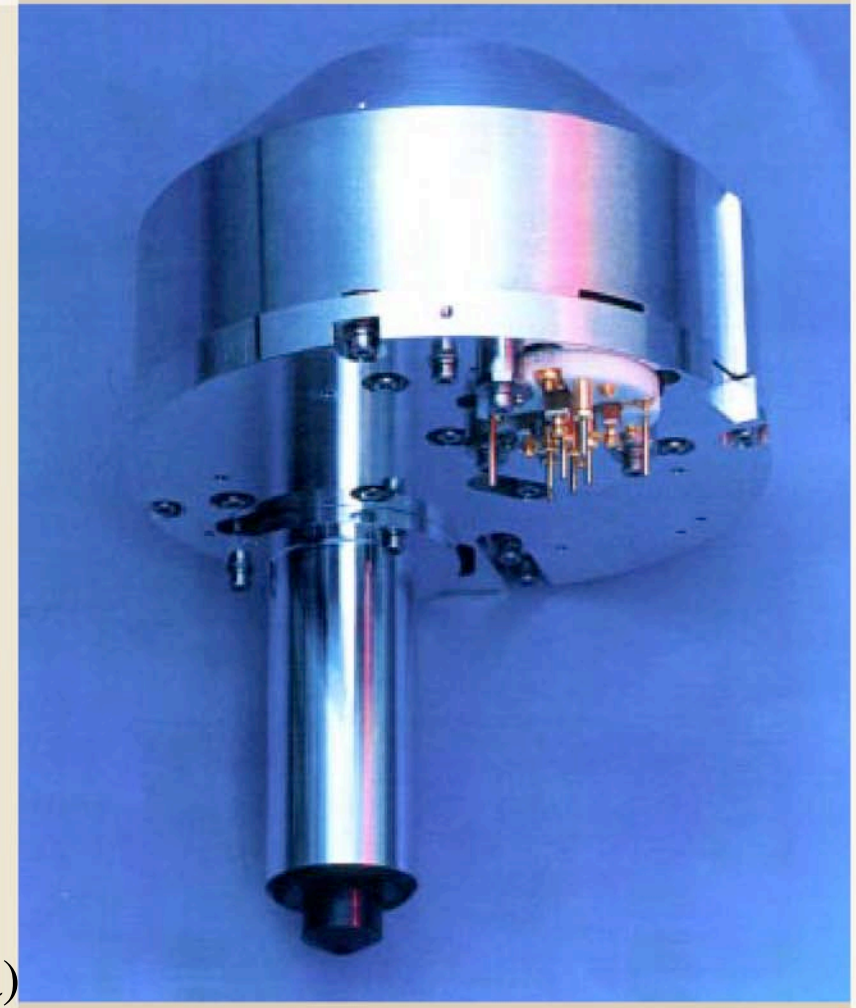

256x256 pixels
128 slices (spectra)
3 MHz count-rate

Mounted on a two-axis goniometer

Courtesy of R. Claessen (Univ. of Wuerzburg)

hν = 9 eV

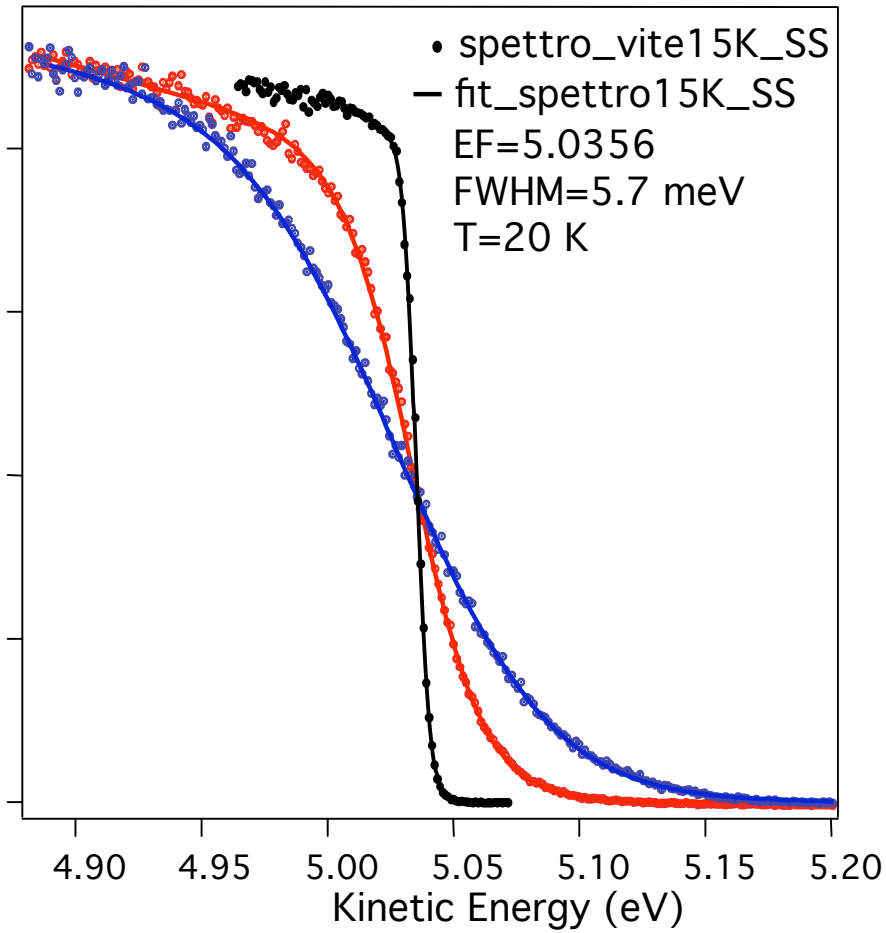

• somma_vite 160K

— fit_somma_vite 160K

EF=5.03563; FWHM:5.8meV; T=164 K

• somma_vite 300K

— fit_somma_vite 300K

EF=5.0356; FWHM:5.8meV; T=300 K

PE=2 eV

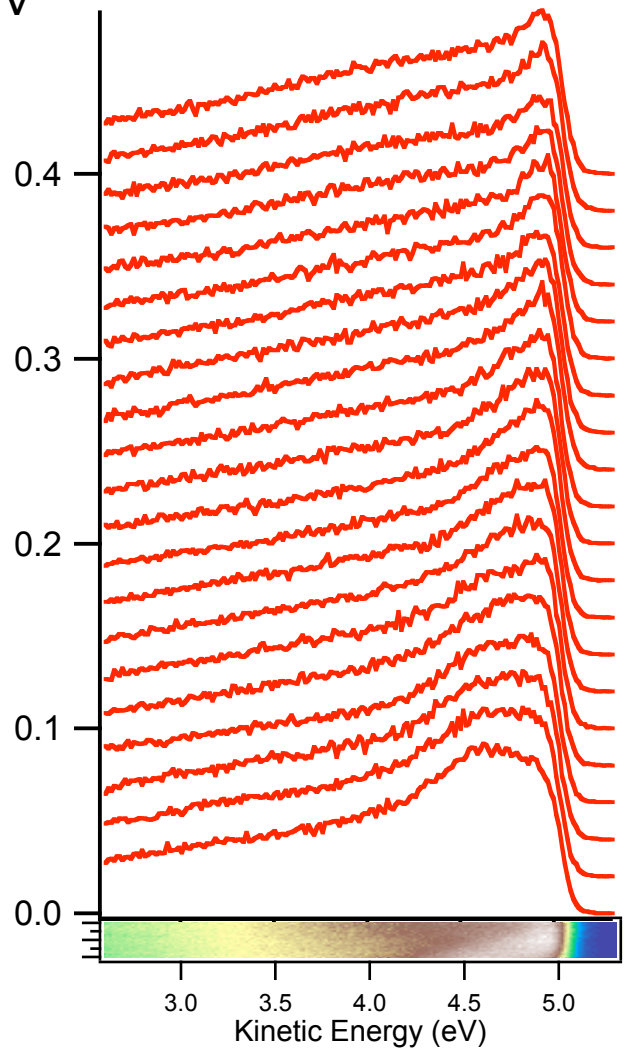

θ range = 5°

21 slices; Δθ ~ 0.25°

ΔK < 0.005 Å^{-1}

A. Goldoni et al., unpublished

Why going to very low photon energies?

$$4\ \text{eV} < h\nu < 20\ \text{eV}$$

1) Bulk sensitivity
2) Higher momentum resolution
3) Good energy resolution easier

Why going to very low photon energies?

$$4\ \text{eV} < h\nu < 20\ \text{eV}$$

1) **Bulk sensitivity**
2) Higher momentum resolution
3) Good energy resolution easier

Electrons photoemitted with low photon energies are the most bulk sensitive

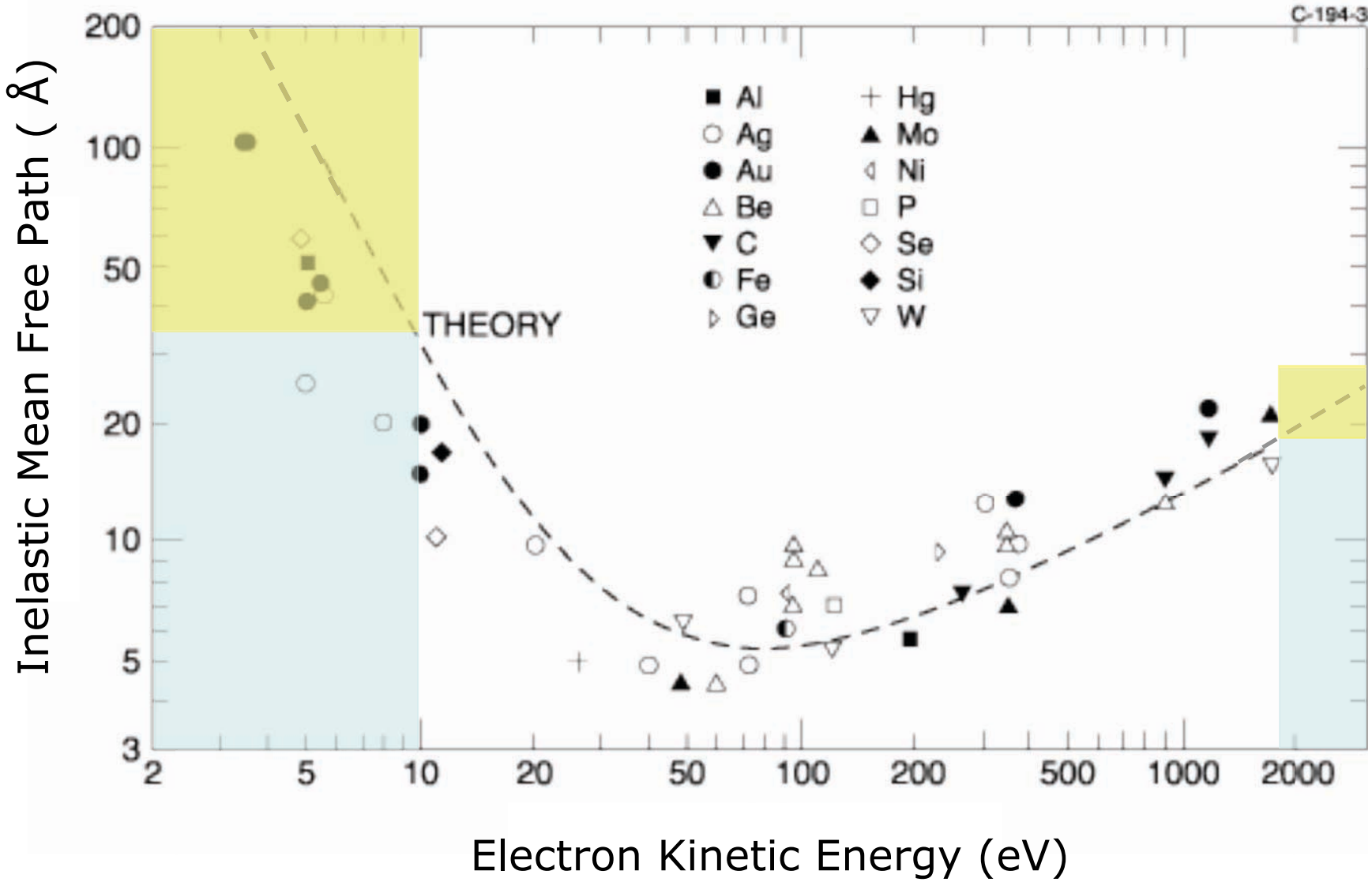

Superconducting gap of Nb

Chainani et.al., PRL, 85(2000)1966

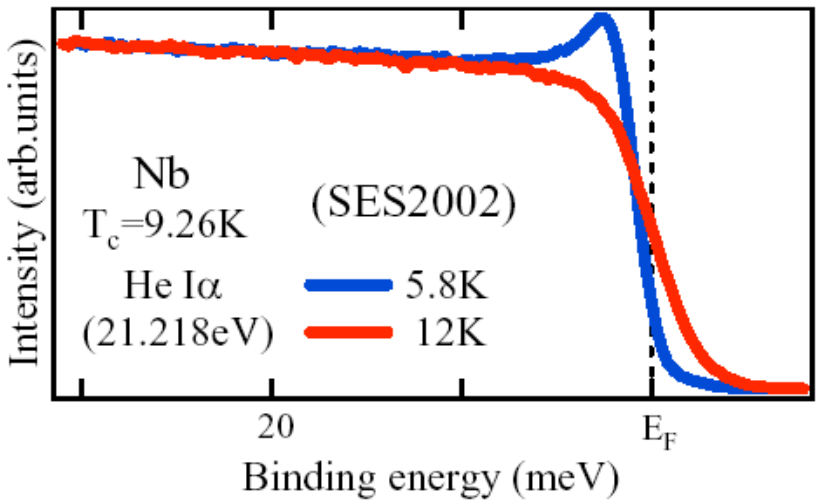

clean surface(scraped)

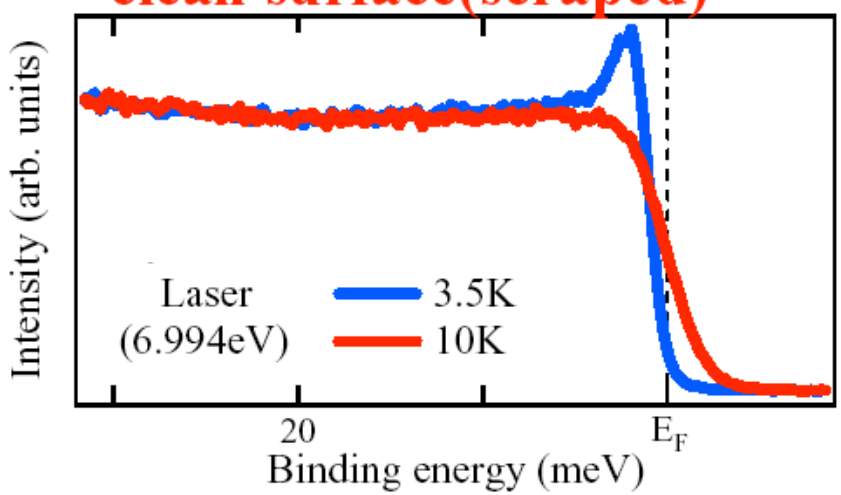

dirty surface(non scraped)

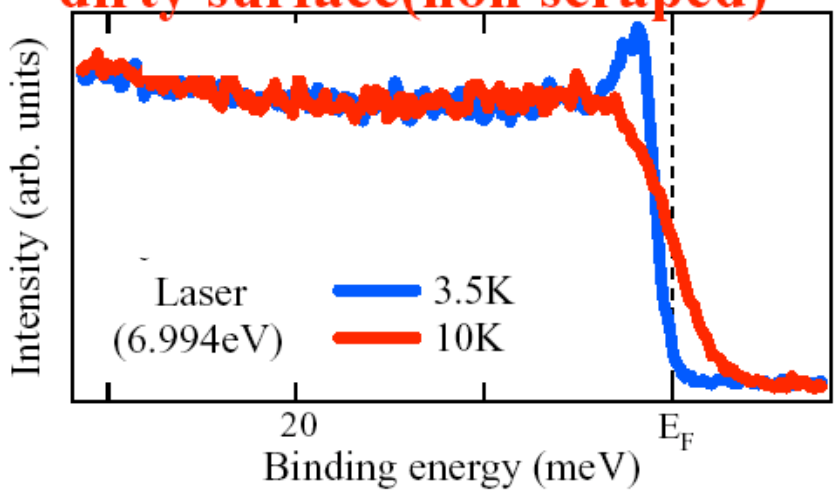

We can measure superconducting gap without clean surface

T. Kiss et al.,JESRP 144-147, 953 (2005)

Fermi surface of Bi(111): Bulk vs Surface states

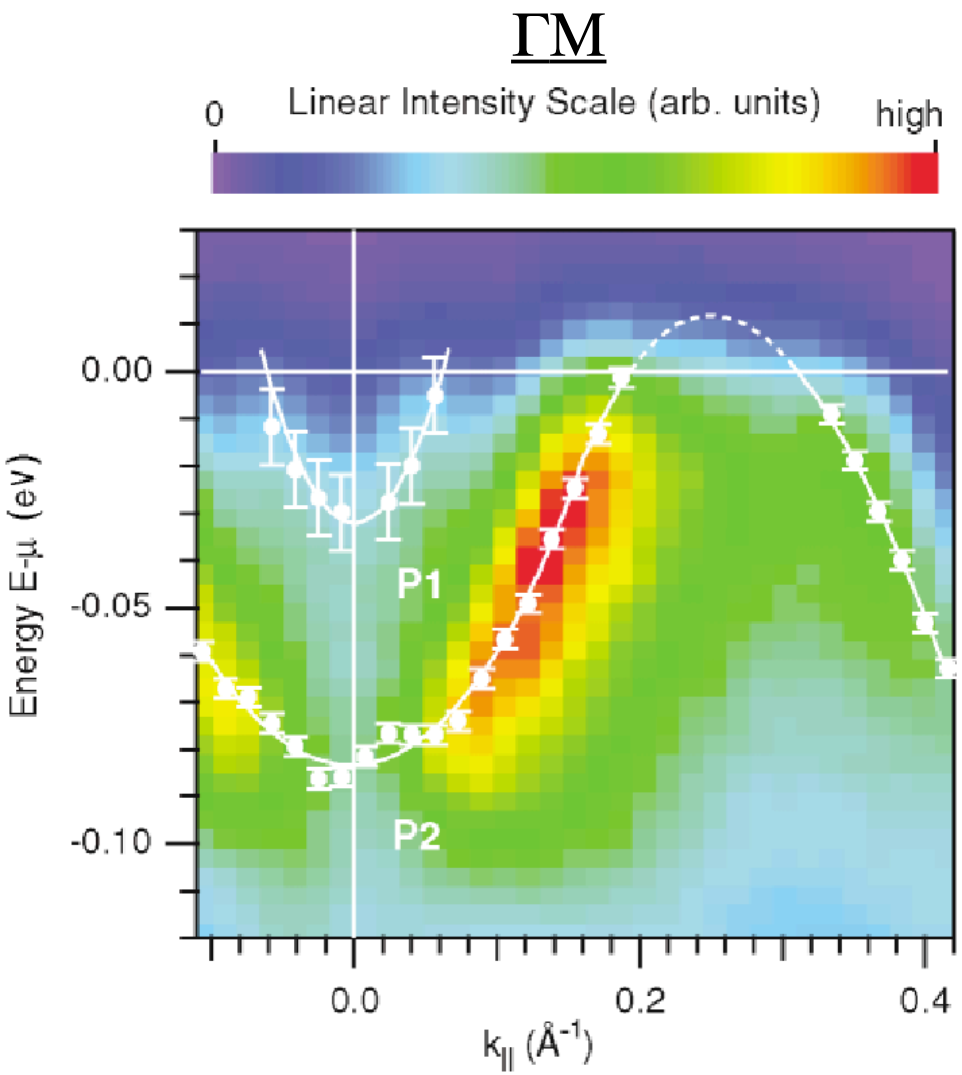

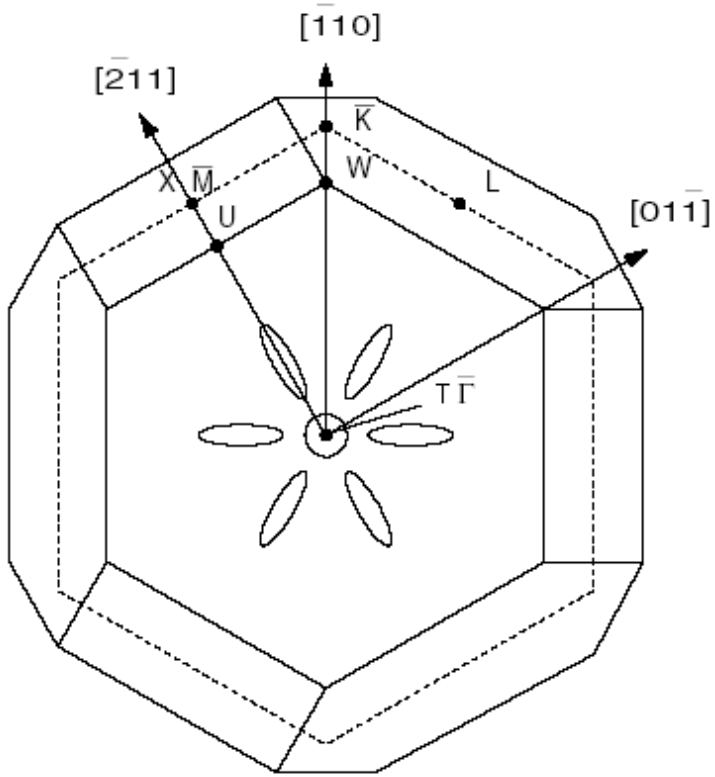

FIG. 4 (color). Band structure of Bi(111) at $h\nu = 18$ eV. $k_{\parallel}$ along $\overline{\Gamma M}$. Solid lines: Polynomial fit to peak positions. Energies relative to chemical potential μ.

C.R. Ast, H. Hochst, PRL 87, 177602 (2001)

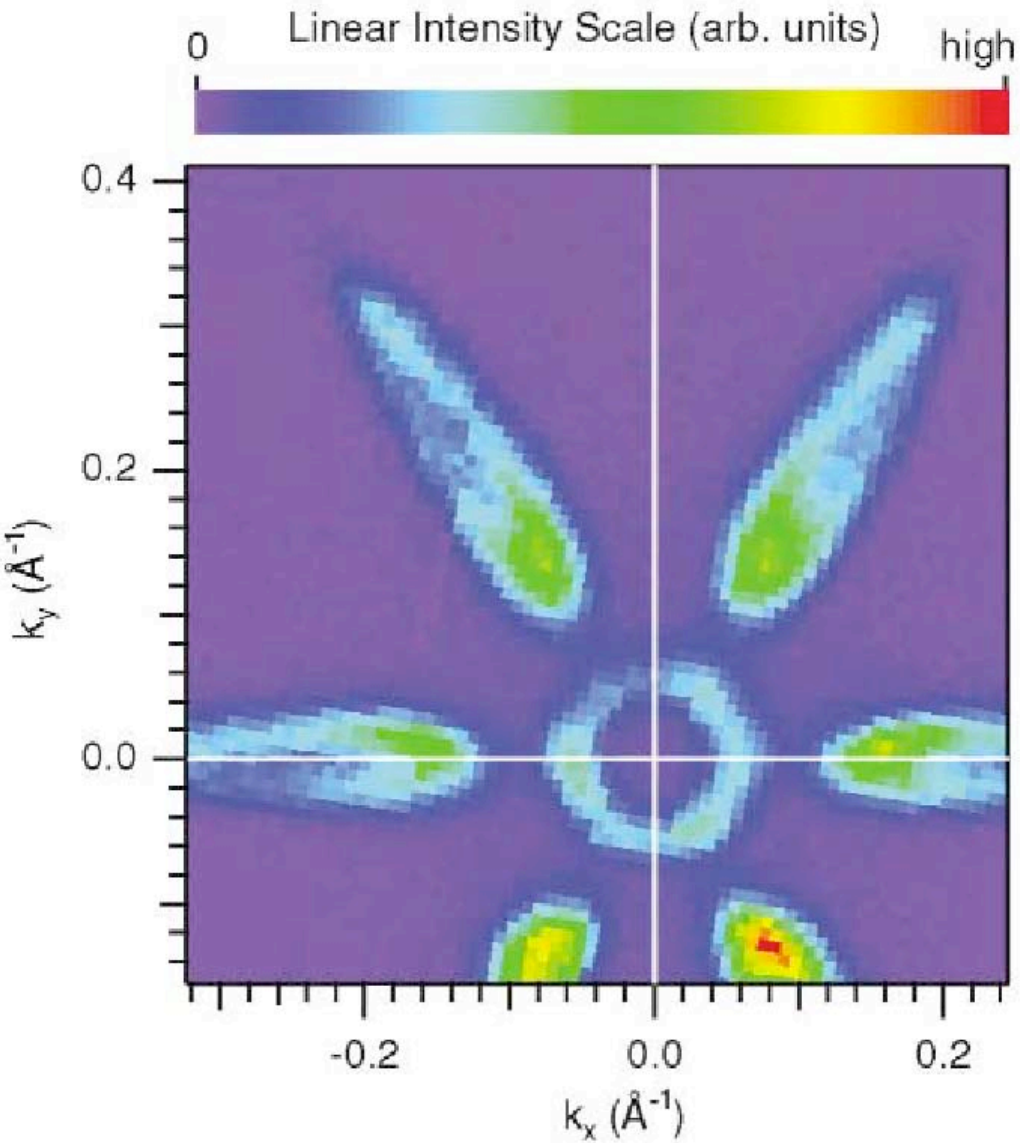

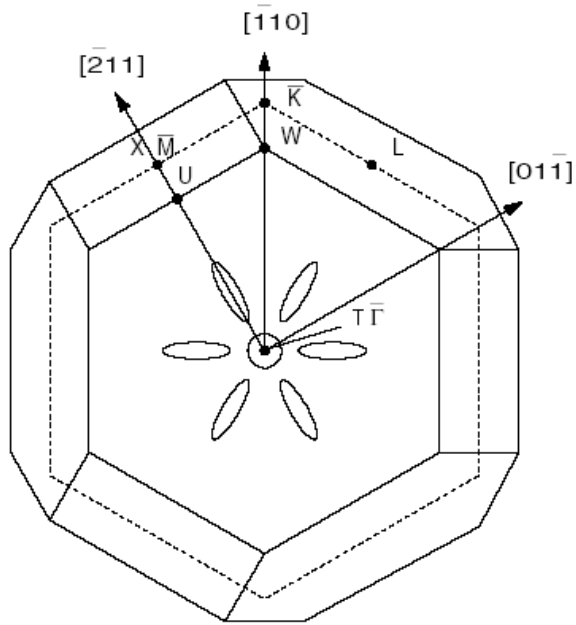

FIG. 1 (color). Intensity map at the Fermi level of Bi(111) measured at $h\nu = 18$ eV. The angular steps were 0.25°. k_x and k_y are the parallel components of the electron momentum along the $\overline{\Gamma M}$ and the $\overline{\Gamma K}$ direction, respectively.

C.R. Ast, H. Hochst, PRL 87, 177602 (2001)

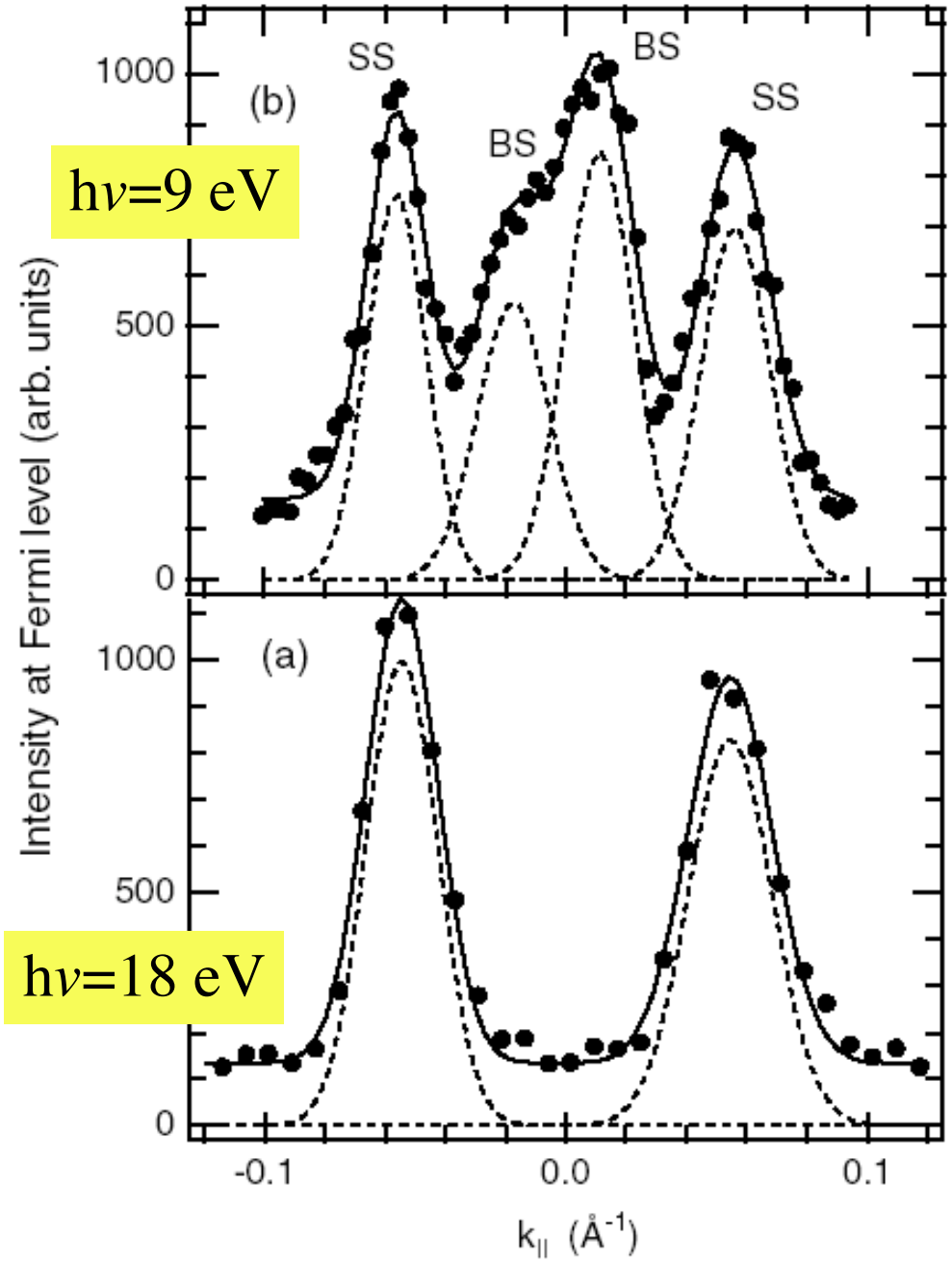

Momentum Distribution Curves at E_F for Bi(111) along the <u>ΓK</u>

Note:
bulk states (BS) appear at low photon energies

C.R. Ast, H. Hochst, PRL 87, 177602 (2001)

Photoemission from Mg(0001): surface *vs* bulk states

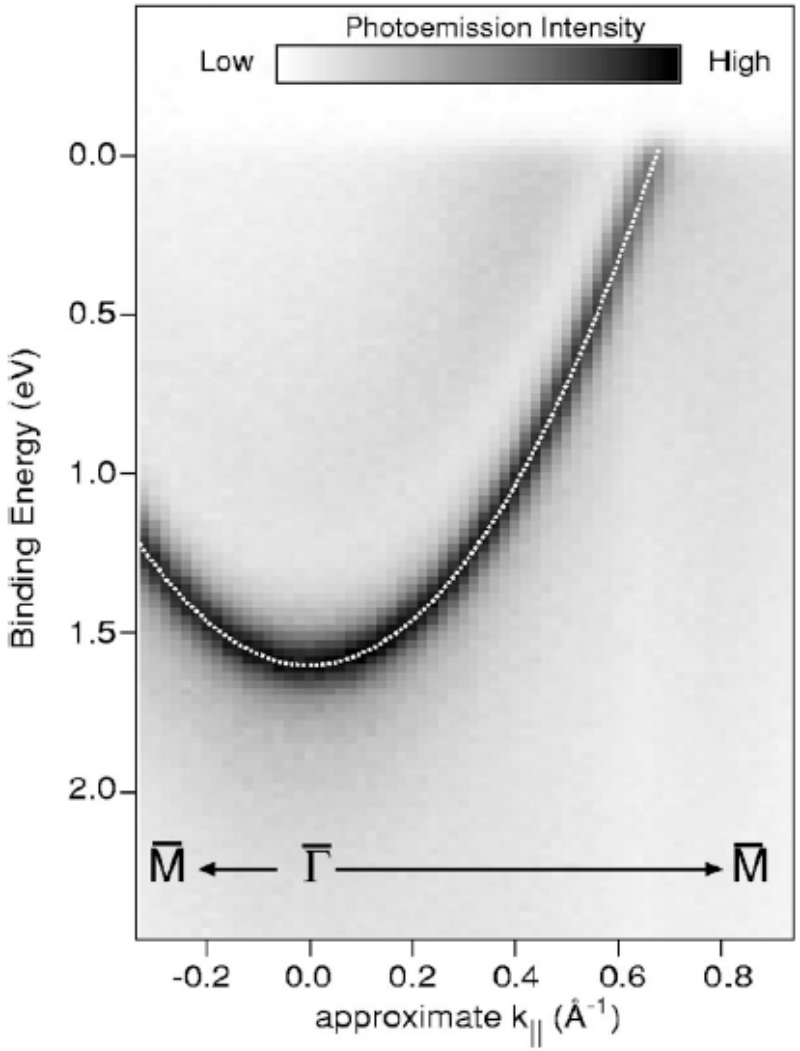

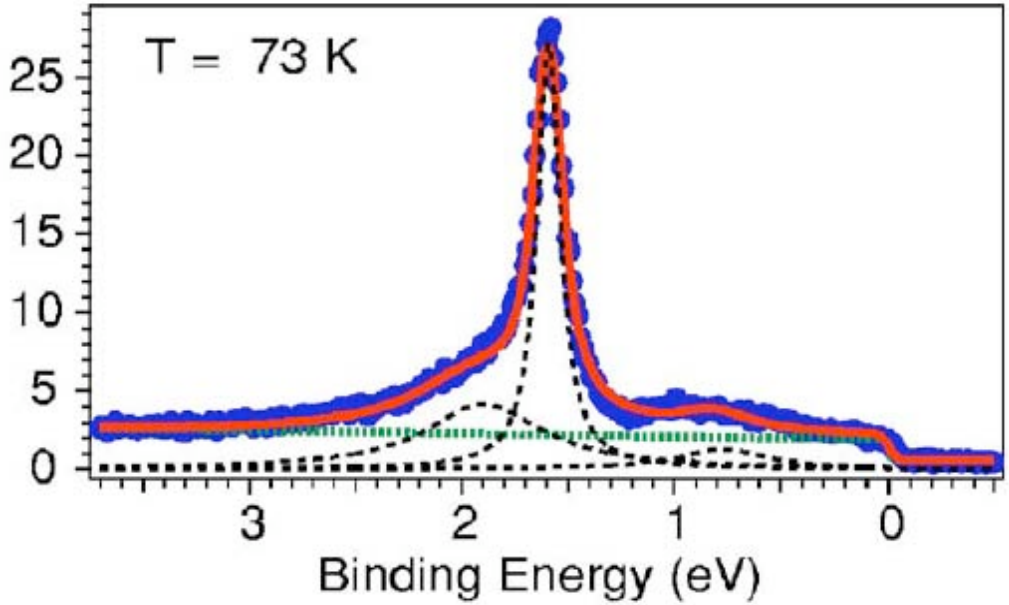

Measured at hν=44 eV
Bulk states intensity very very small

T. Kim et al., PRB 72, 075422 (2005)

Mg(0001) measured at hν = 9 eV

Enhanced bulk sensitivity at low photon energy

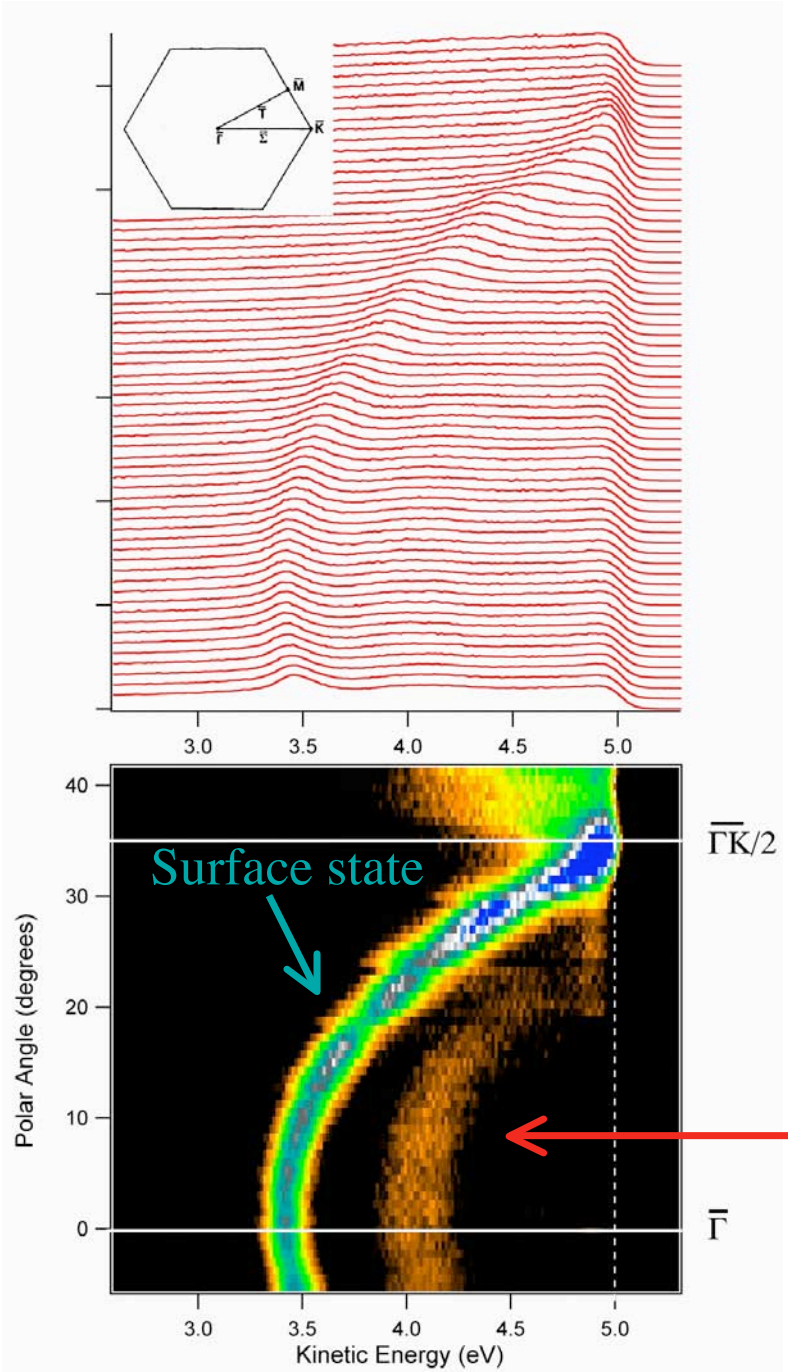

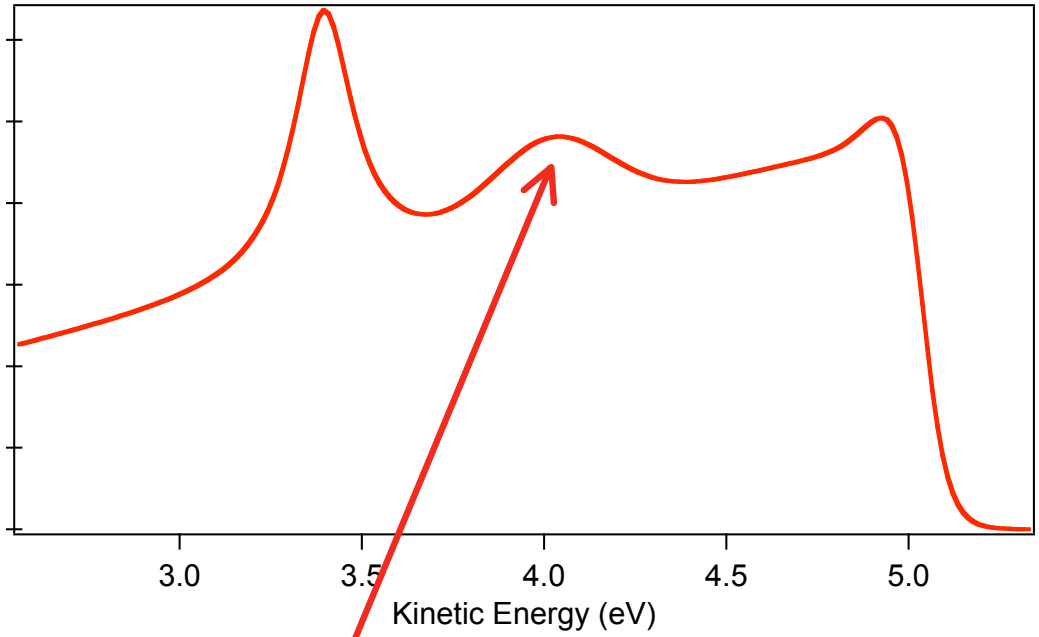

Bulk band
(now well visible)

P. Vilmercati et al., Notiziario Neutroni e Luce di Sincrotrone (2008)

Mott transition in V_2O_3

M. Marsi et al., submitted to PRB
(similar experiment made by R. Claessen et al.)

$(V_{1-x}Cr_x)_2O_3$ prototype system for isostructural metal-insulator transition induced by electron correlations

$(V_{1-x}Cr_x)_2O_3$ x =0,011

T=300K paramagnetic insulator
T=200K paramagnetic metal

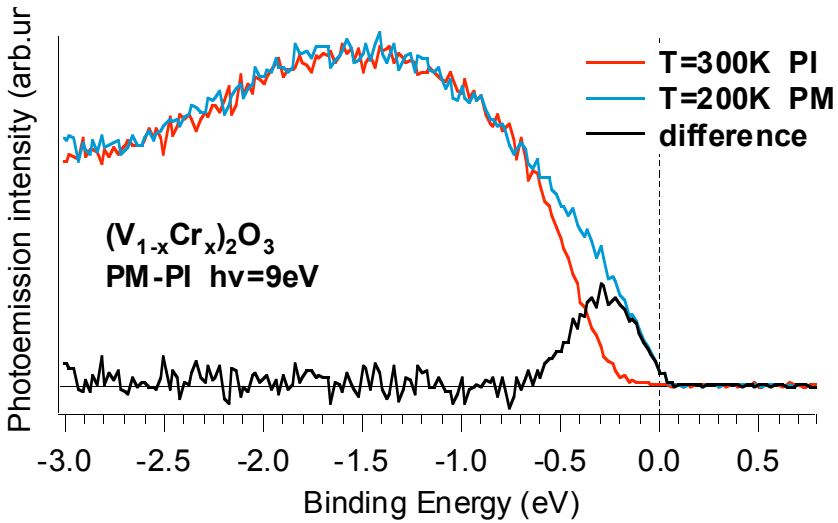

Mott transition in V_2O_3

M. Marsi et al., submitted to PRB

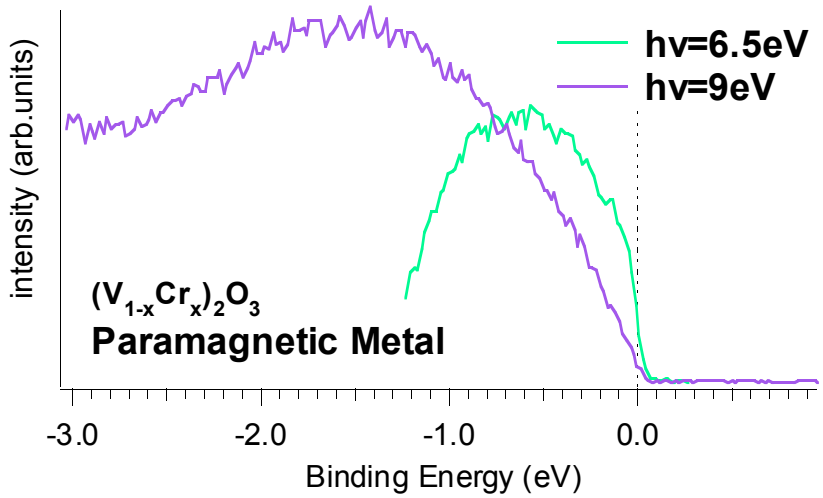

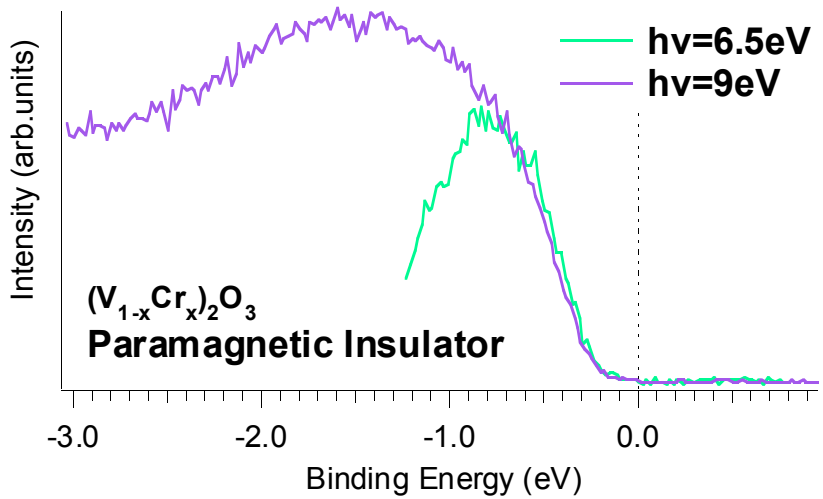

Photoemission on BaD ElPh
Low photon energy
Normal emission

metallic phase shows larger difference between surface and bulk

- Surface is more correlated than bulk
- True also for other strongly correlated systems ?

Coronene ($C_{24}H_{12}$) on Au(110), intercalated with Rb

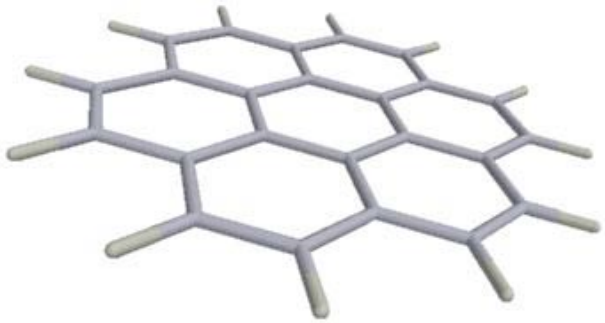

Petra Rudolf et al.

University of Groningen
Zernike Institute
for Advanced Materials

$h\nu = 21$ eV

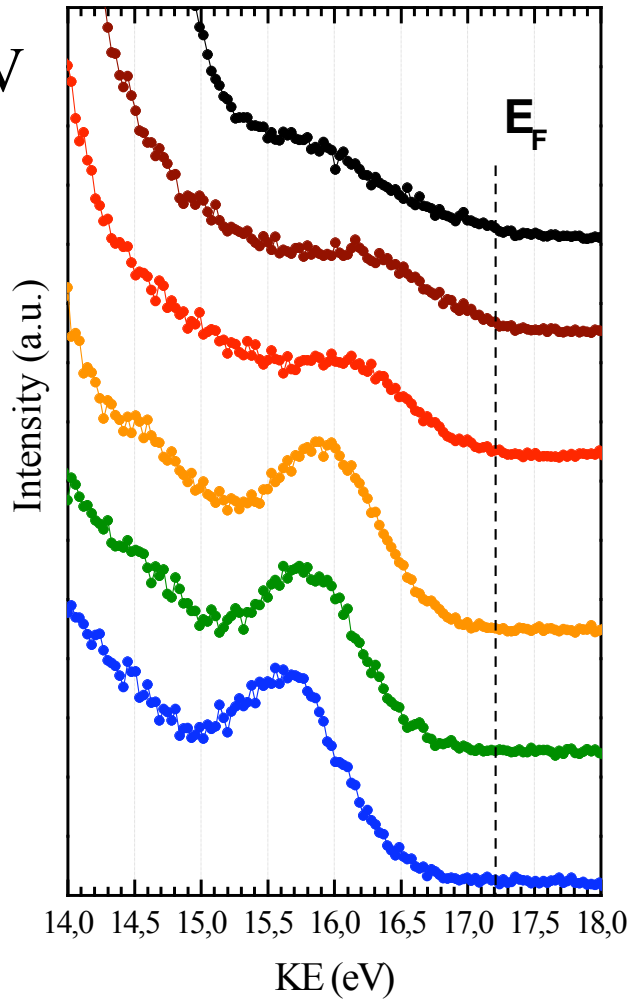

As the LUMO fills no states near E_F: always insulating

Plenty of similar photoemission examples in the literature: phtalocynins, porphyrins, …

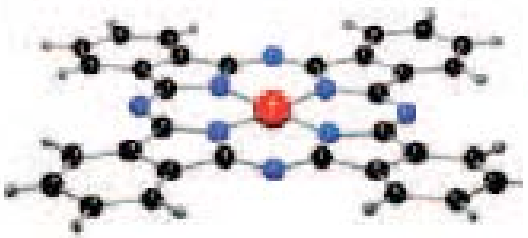

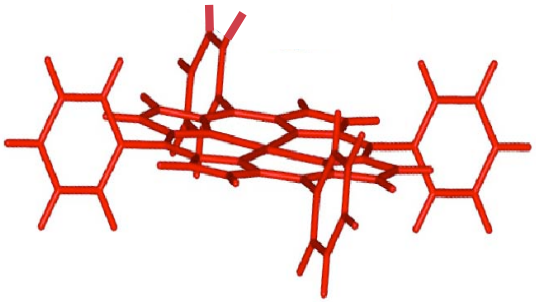

Rb-Coronene: Fermi region with hν < 10 eV

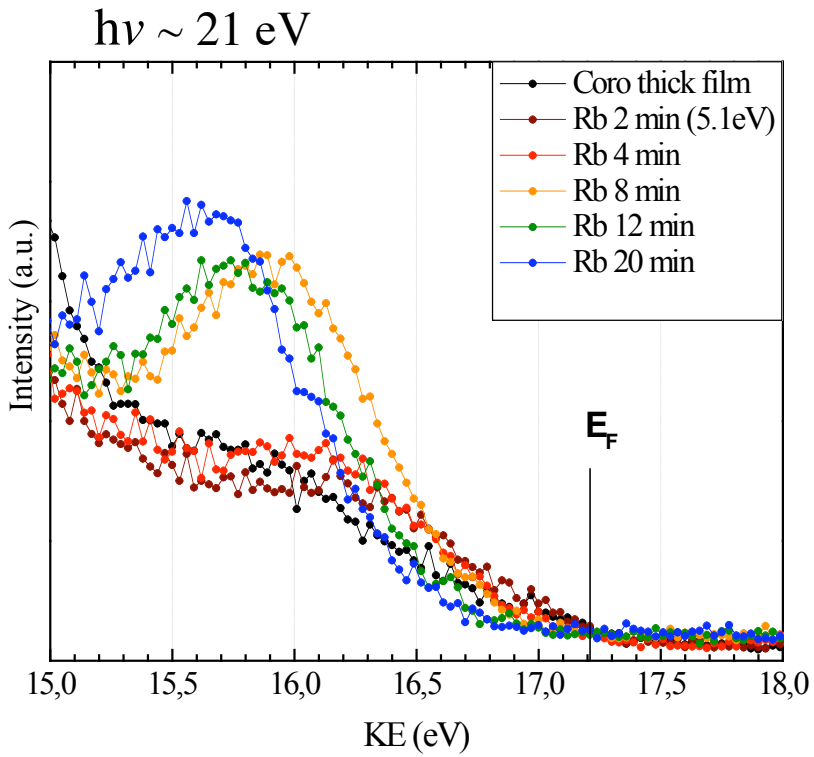

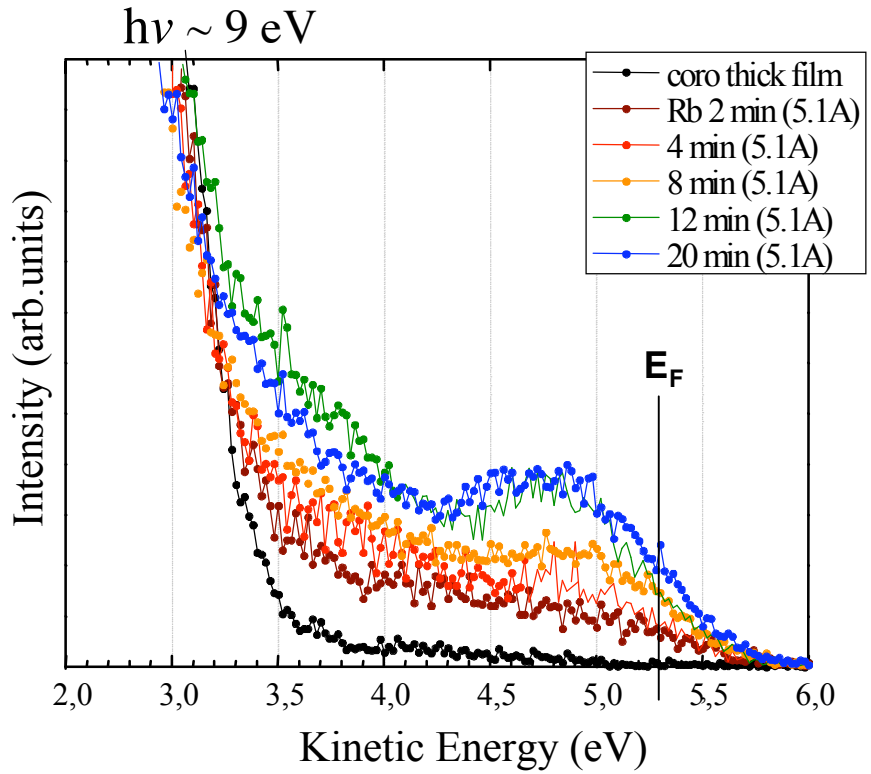

At hν =9 eV the evolution is completely different:
density of states crossing Fermi

The LUMO states are closer to Fermi and crosses E_F

Petra Rudolf et al.

University of Groningen
Zernike Institute
for Advanced Materials

Attenuation length of low electron in solids: CoO/Ag and C_{60}/Ag

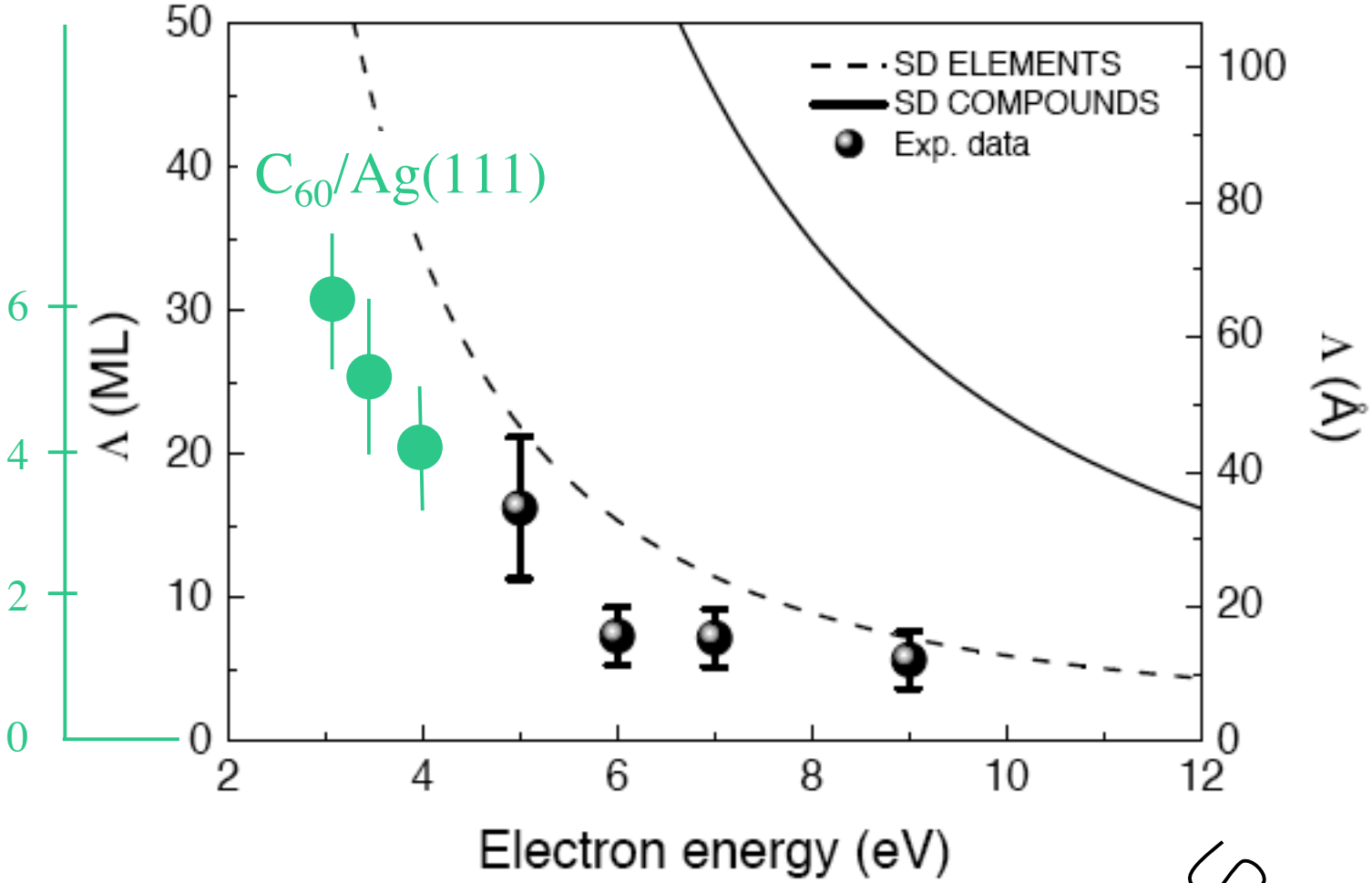

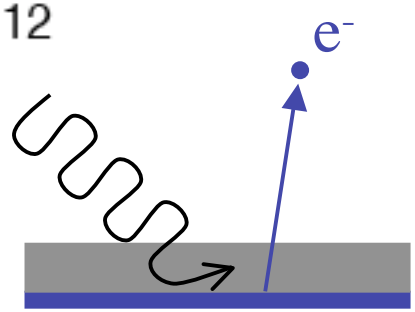

F. Offi et al., PRB Rapid Comm. (in press); A. Goldoni et al., in preparation

Why going to very low photon energies?
4 eV< hν < 20 eV

1) Bulk sensitivity

2) Higher momentum resolution

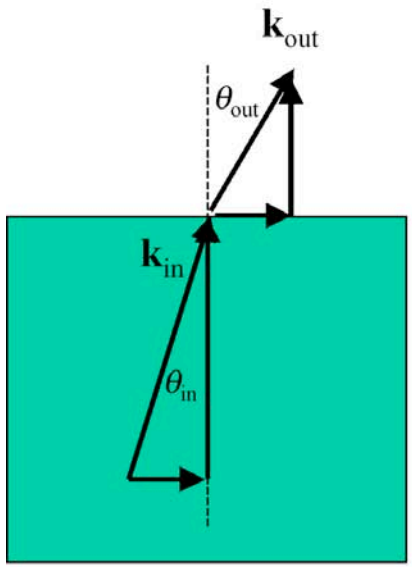

Kinematic relations

$$k_{out} = \sqrt{\frac{2m}{\hbar^2} E_{kin}}$$

$$k_{in} = \sqrt{\frac{2m}{\hbar^2}(E_{kin} + V_0)}$$

$$k_{out,\parallel} = k_{in,\parallel} \equiv k_{\parallel}$$

"Snell's Law"

$$k_{\parallel} = \sin\theta_{out}\sqrt{\frac{2m}{\hbar^2} E_{kin}} = \sin\theta_{in}\sqrt{\frac{2m}{\hbar^2}(E_{kin} + V_0)}$$

Critical angle for emission

$$(\sin\theta_{out})_{\max} = \sqrt{\frac{E_{kin}}{E_{kin} + V_0}}$$

At the surface the crystal symmetry is conserved in the surface plane but is broken perpendicularly to the surface: the component of the electron momentum parallel to the surface plane ($k_{//}$) is conserved, but $k_{\perp}$ is not

$$k_{//} = \sqrt{\frac{2m^* E_k}{\hbar^2}} \sin\theta_{out} \approx 0.512\sqrt{E_k}\,\sin\theta_{out}$$

The angular resolution is defined by the electron energy analyzer. Suppose it is 0.5° and the BZ boundary is ~ 0.25 Å^{-1}.

At E_k=25 eV the BZ boundary is reached after ~ 5.5°
We have 11 sampling points → $\Delta k_{//}$ ~ 0.025 Å^{-1}

At E_k=9 eV the BZ boundary is reached after ~ 9.5°
We have 19 sampling points → $\Delta k_{//}$ ~ 0.014 Å^{-1}

GOOD for systems with small BZ

Example: Band structure in fullerides

Typical hexagonal surface lattice parameter > 10 Å

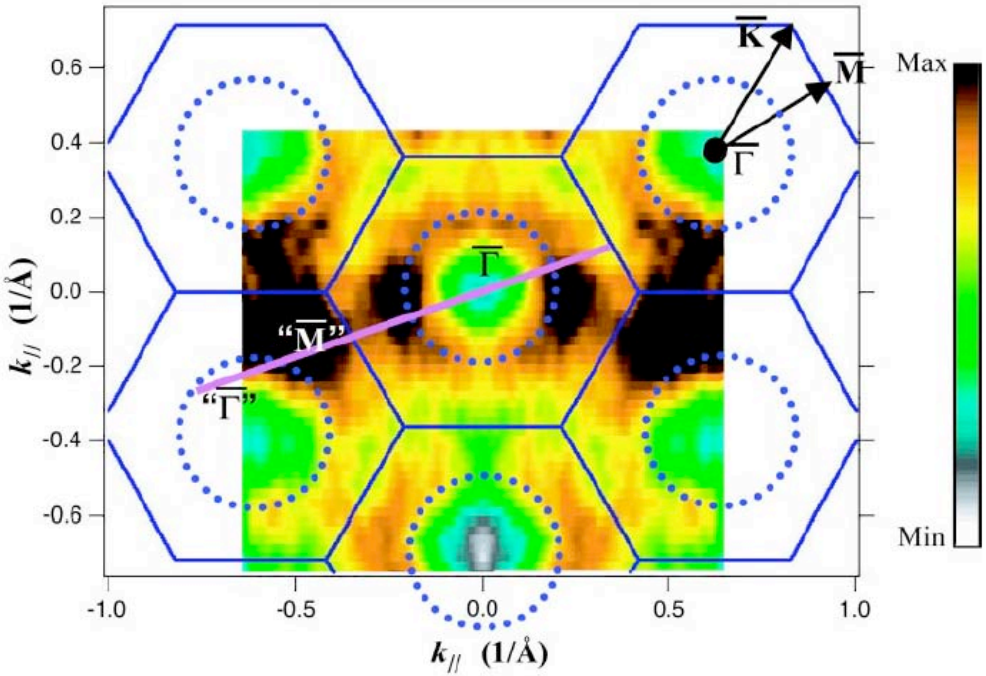

Measured at 22 eV. Lower photon energy should allow better Fermi surface mapping.

W. Yang et al., Science **300,** 303 (2003);
V. Brouet et al., PRL (2004)

1ML-K_xC_{60}/Ag(**100**)

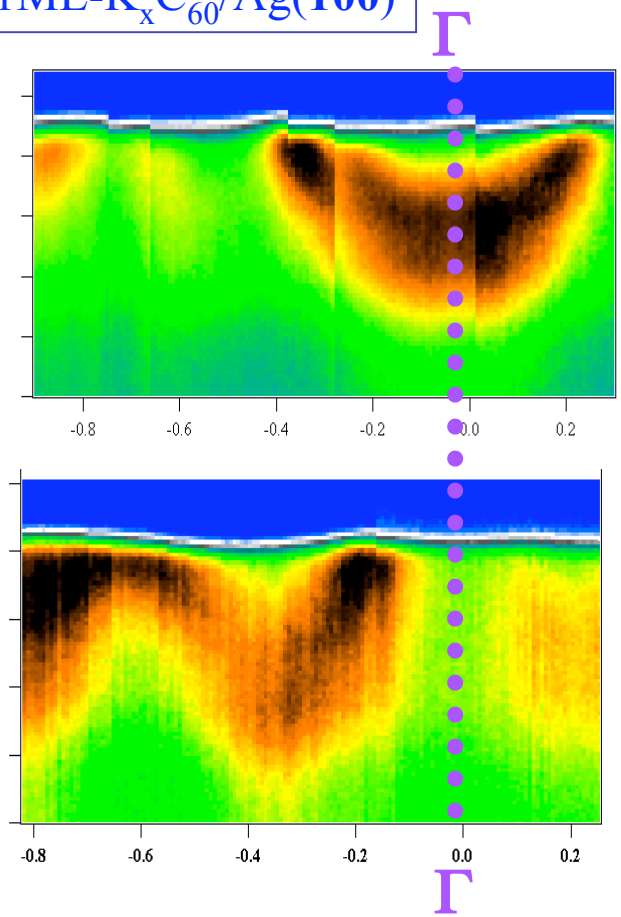

1ML-K_3C_{60}/Ag(**111**)

Why going to very low photon energies?

4 eV< hν < 20 eV

1) Bulk sensitivity
2) Higher momentum resolution
3) **Good energy resolution easier**

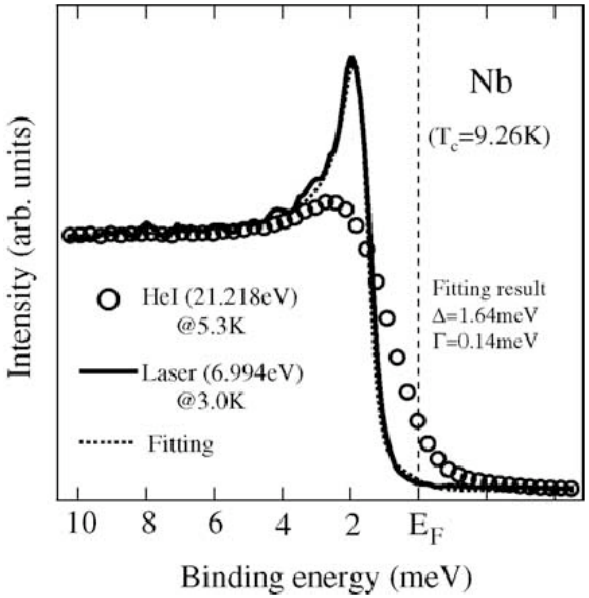

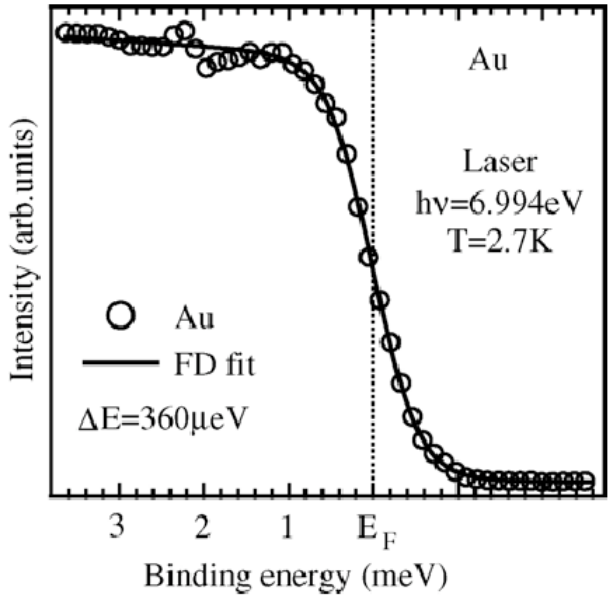

T. Kiss et al.,JESRP 144-147, 953 (2005)

Angle Resolved Photoemission Spectroscopy of MgB_2 Single Crystals

S. Souma et al. Nature **423**, 65 (2003)

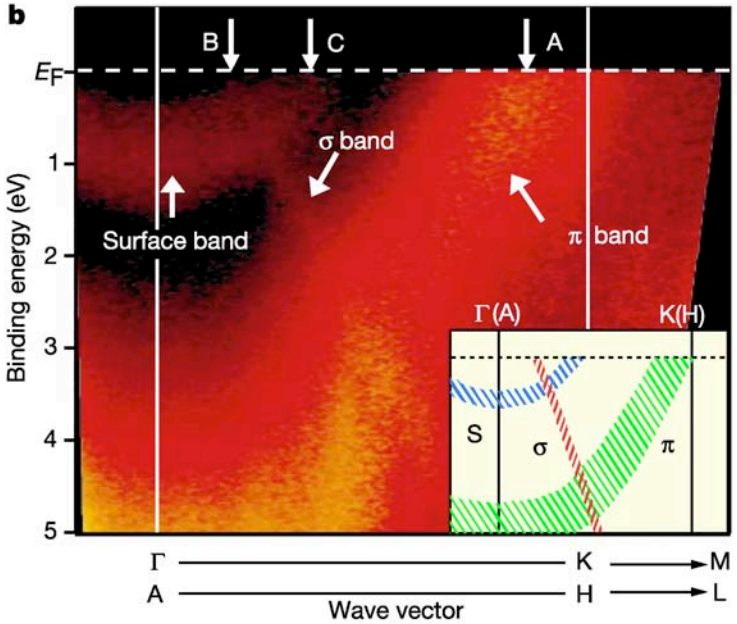

s and p superconducting gaps

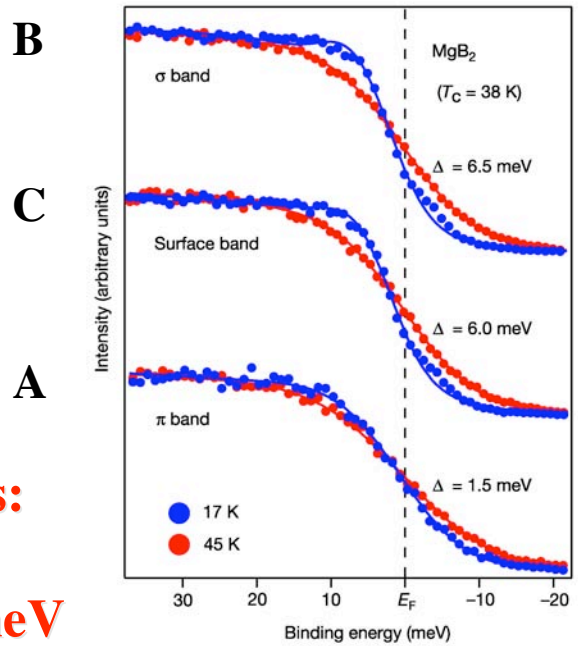

Two superconducting gaps:

D_s=5.5 meV D_p=2.2 meV

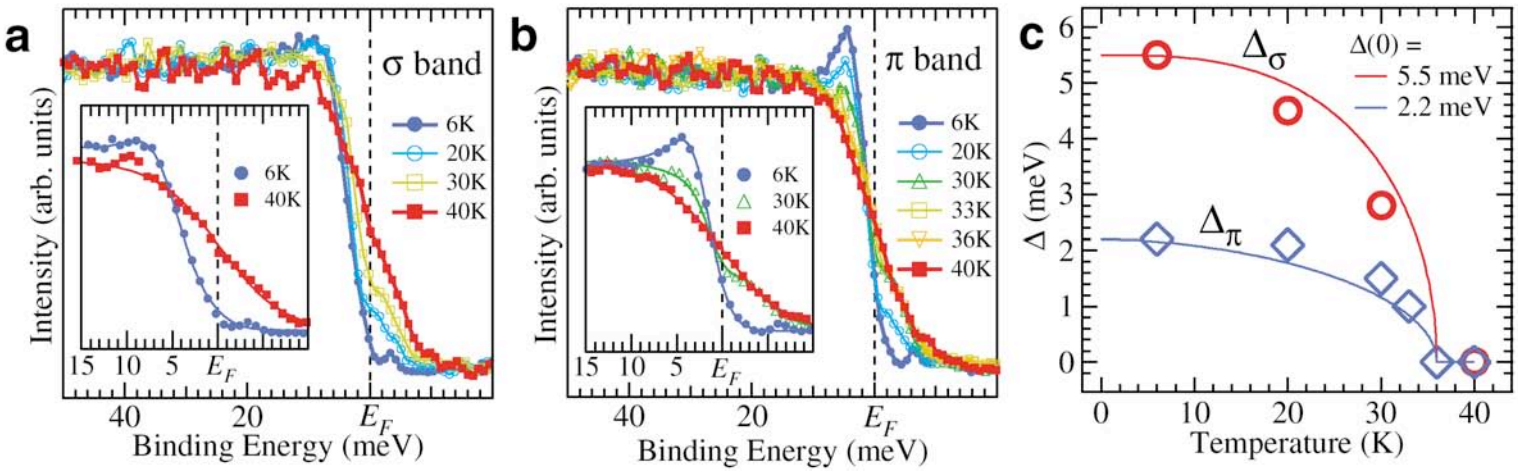

S. Tsuda et al. Phys. Rev. Lett. **91**, 127001 (2003)

"sub meV" resolution spectra on MgB_2 by laser-PES

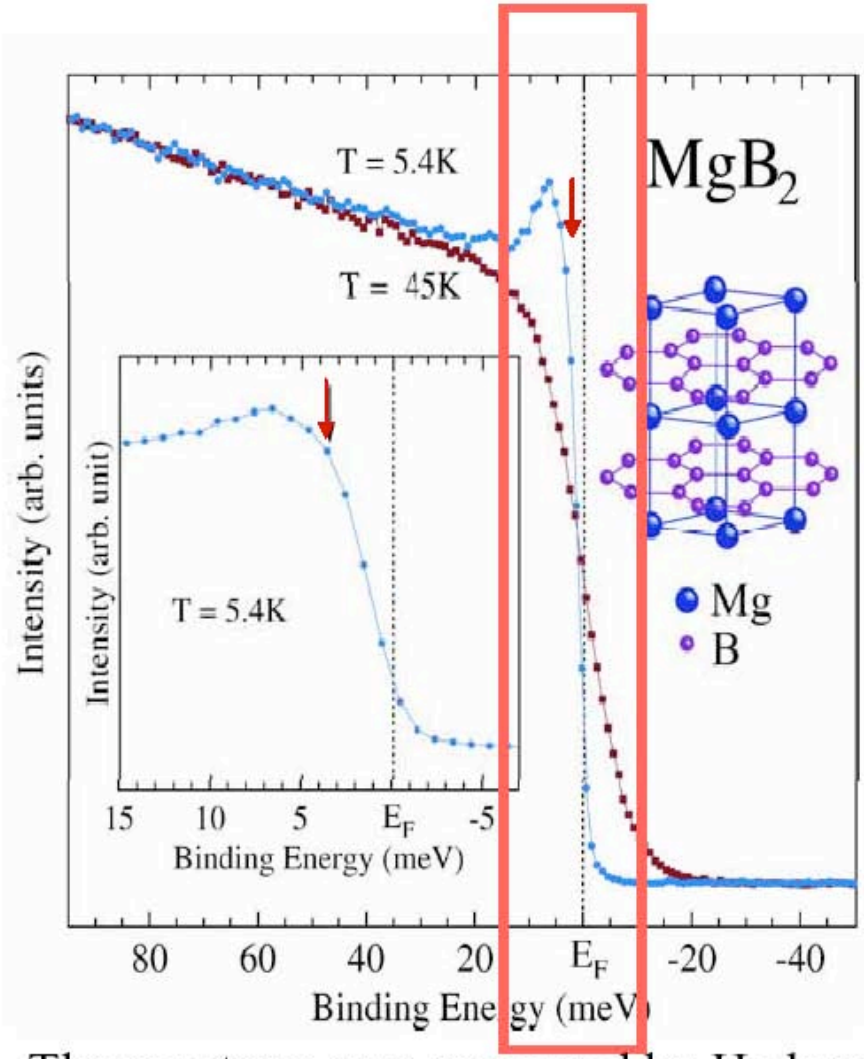

The spectrum was measured by He lamp and show the two gap structure for the first time

Tsuda et al., PRL**87**,17006(2001)

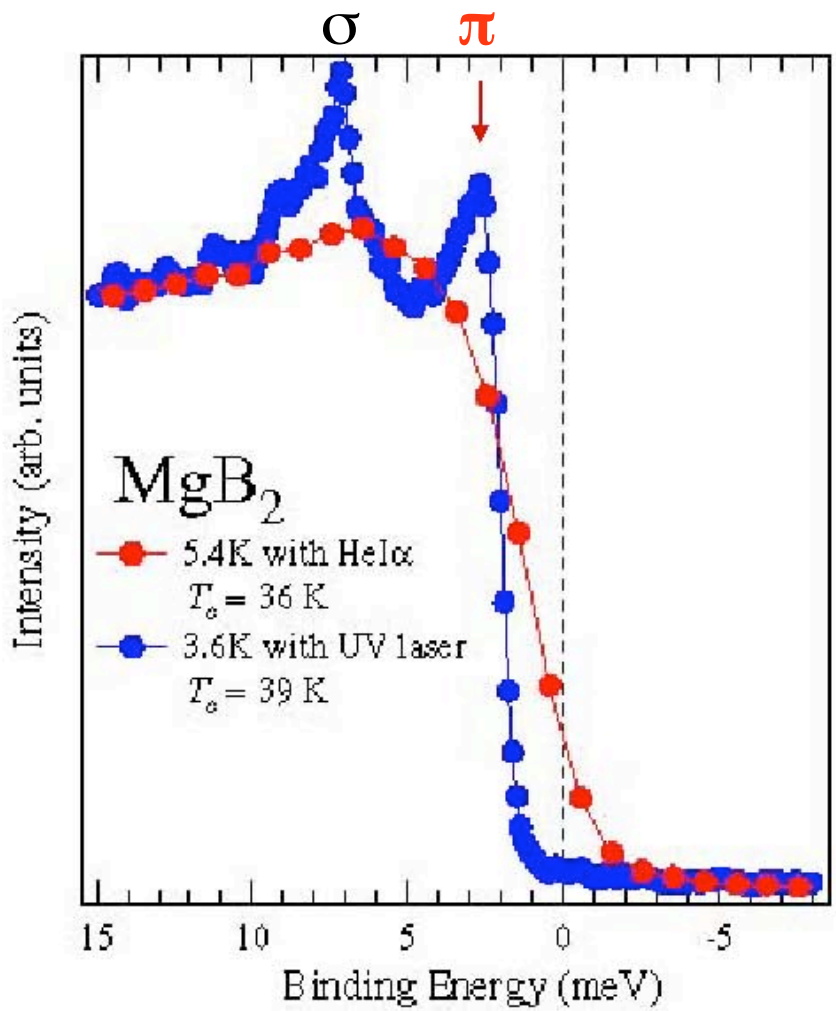

Laser-PES

Tsuda et al.

Superconducting gap of $CeRu_2$

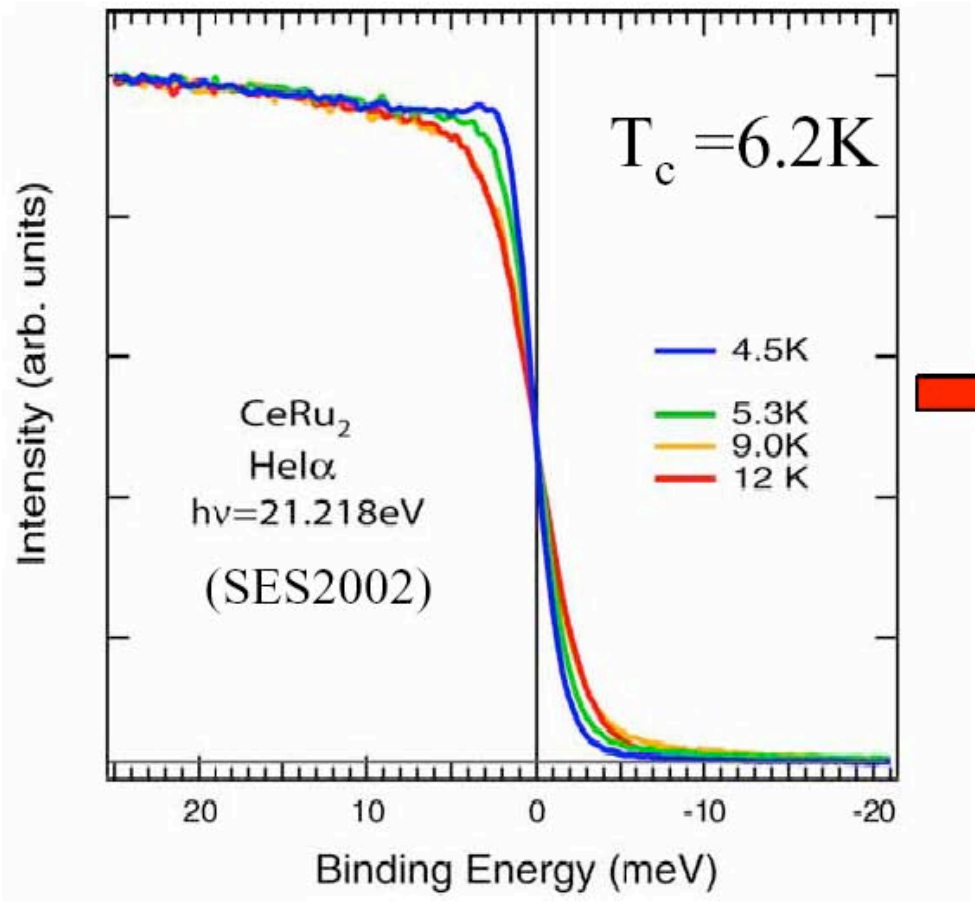

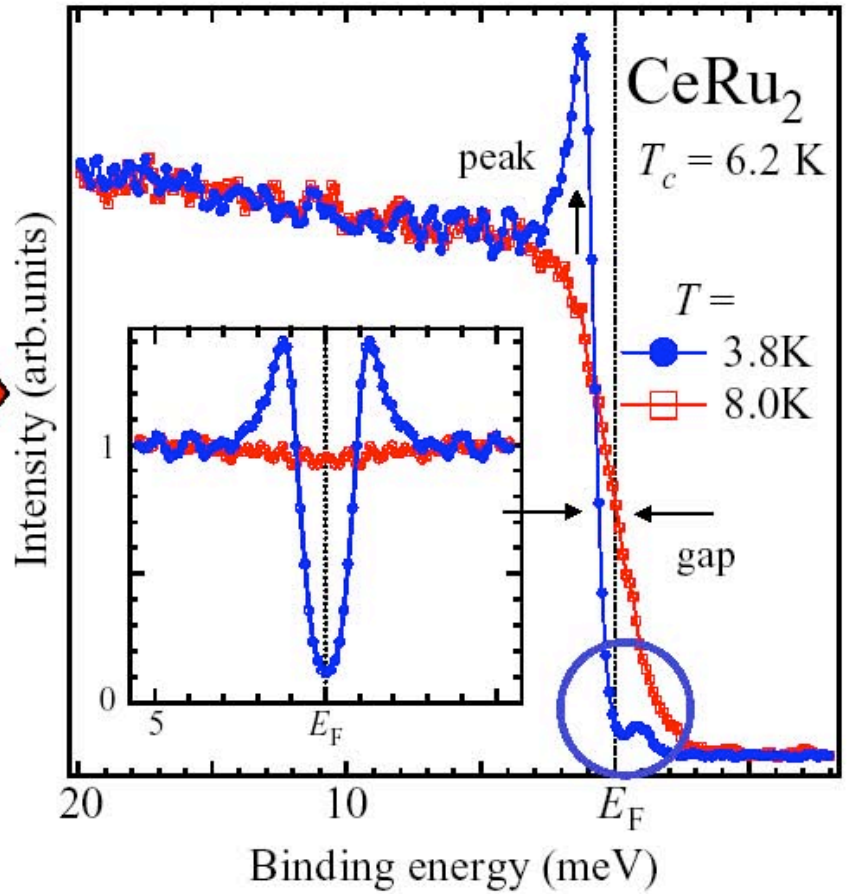

Superconducting gap was clearly observed by laser-PES

Kiss et al., PRL **94** (2005)57001

Pseudo-gap opening in FeSi

K. Ishizaka et al., PRB 72, 233202 (2005)

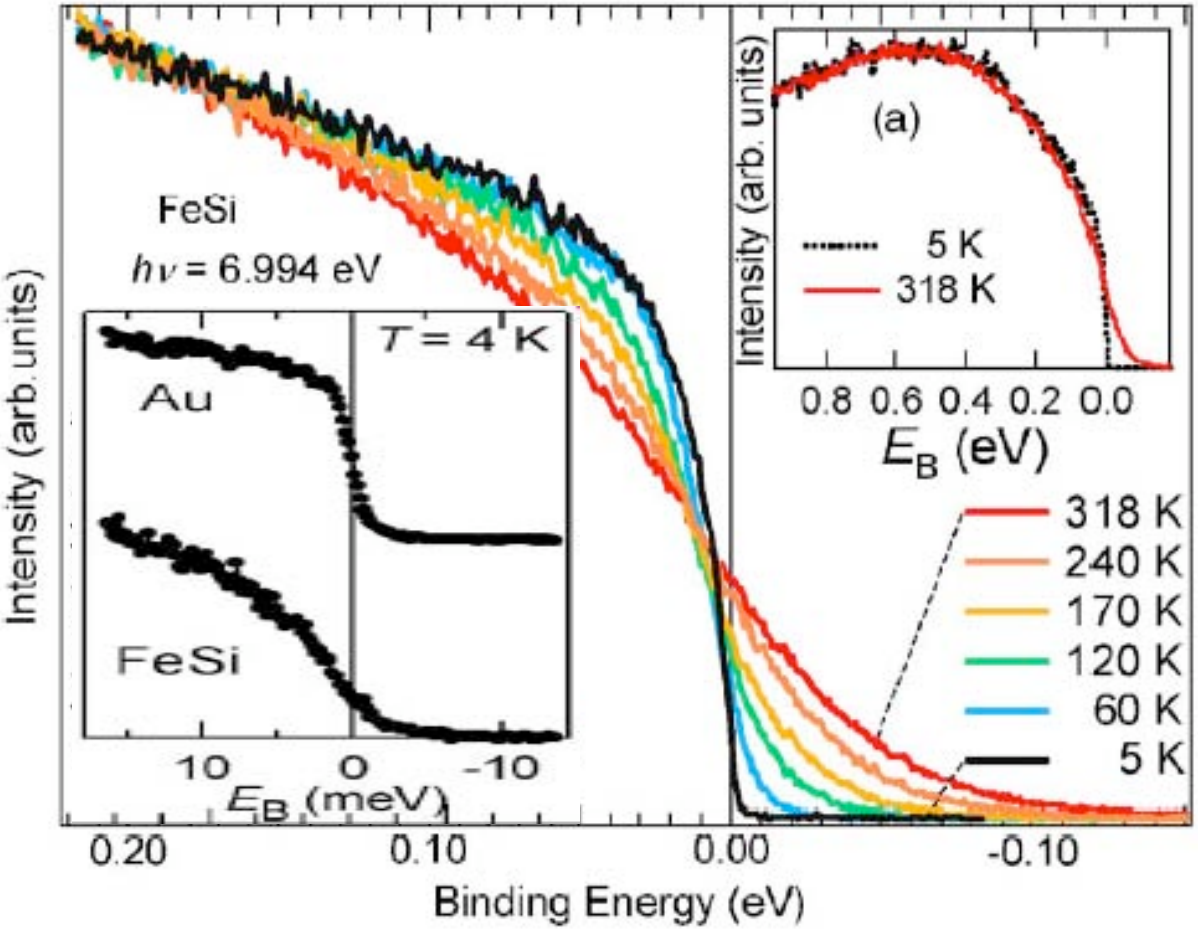

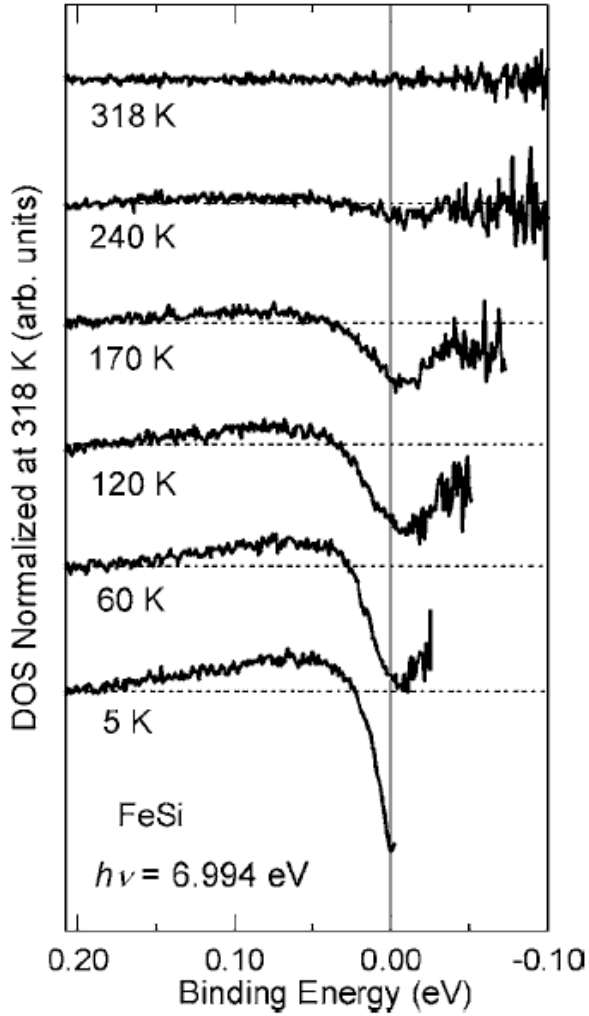

Critical question for ARPES at such low energies: is the Sudden Approx still valid?

Fermi´s Golden Rule for N-particle states:

$$I(\vec{k},\varepsilon) \propto \sum_s \left| \left\langle \Psi_{f,s} \middle| \hat{\Delta} \middle| \Psi_{i,0} \right\rangle \right|^2 \delta(E_{N,s} - E_{N,0} - h\nu)$$

SUDDEN APPROXIMATION:

$$\left| \Psi_{f,s} \right\rangle = \left| \vec{k}, N-1, s \right\rangle = c_{\vec{k}}^{+} \left| N-1, s \right\rangle$$

Factorization !

photoelectron

sth eigenstate of remaining N-1 electron system

<u>Physical meaning</u>:
photoelectron decouples from remaining system immediately after photoexcitation, *before* relaxation sets in

This is the most important result: in the sudden approx. the photoemission spectrum is proportional to the single particle spectral density function *A(k, ω)*

$$I(k,\omega) = I_{if}(k,\mathbf{A},\nu)A(k,\omega)\, fd(\omega, T)$$

Proportional to Matrix elements

Spectral function

Fermi-Dirac

$$A(k,\omega) = \frac{1}{\pi}\mathrm{Im}\, G(k,\omega) = \frac{\Gamma}{\pi}\sum_s \frac{|\langle N-1,s|c_k|N,i\rangle|^2}{(\omega - E_s^{N-1} + E_i^N)^2 + \Gamma^2}$$

The single particle spectral function A(k, ω) gives the probability that the original system plus the bare hole (electron suddenly removed) will be found in an exact eigenstate of the (N-1)-system

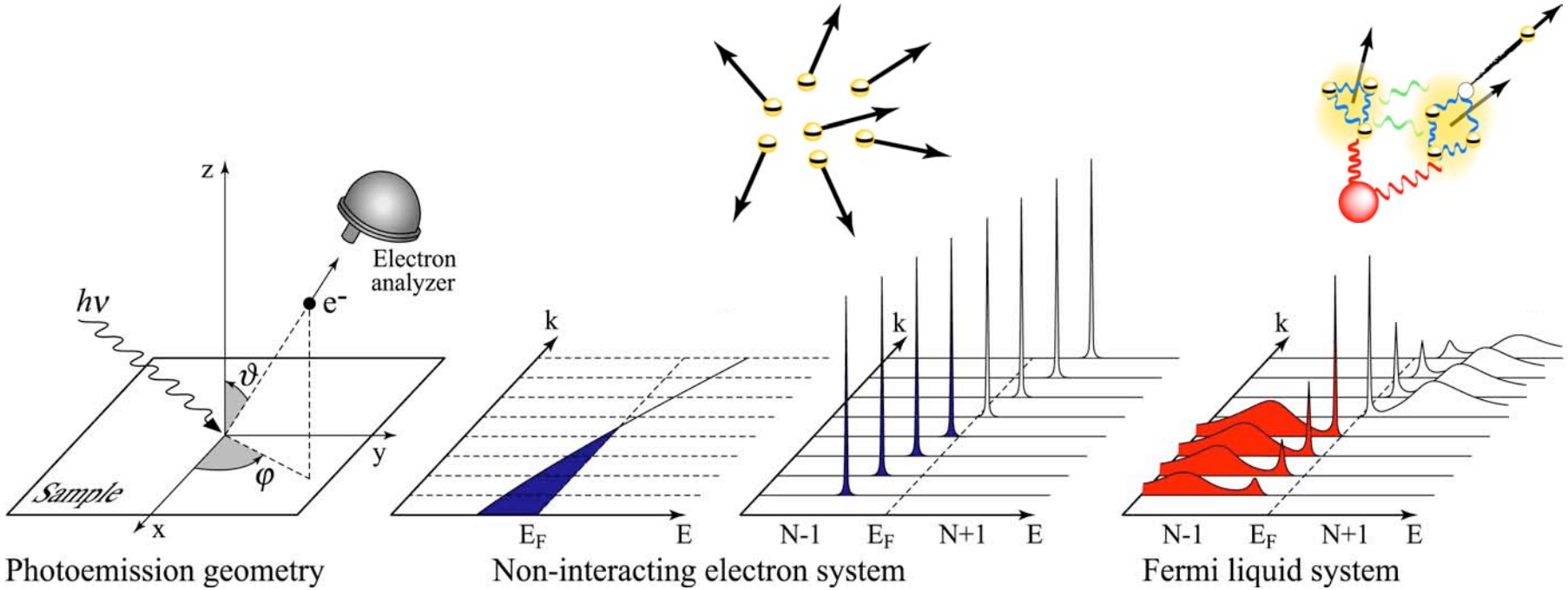

non-interacting system

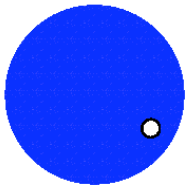

$$A(k,\omega) = -\frac{1}{\pi}\,\mathrm{Im}\,G(k,\omega) = \frac{\Gamma}{\pi}\frac{\left|\langle N-1,i|c_k|N,i\rangle\right|^2}{(\omega-\varepsilon(k))^2+\Gamma^2} = \frac{\Gamma}{\pi}\frac{1}{(\omega-\varepsilon_0(k))^2+\Gamma^2}$$

interacting system

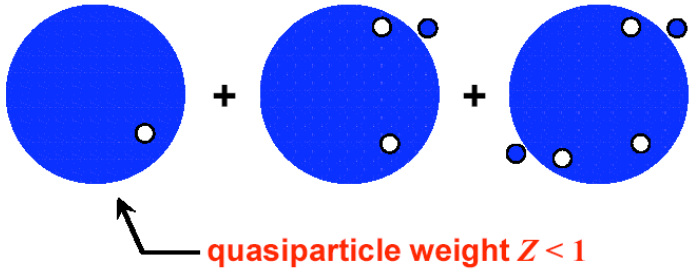

$$A(k,\omega) = -\frac{1}{\pi}\,\mathrm{Im}\,G(k,\omega) = \frac{\Gamma}{\pi}\frac{\left|\langle N-1,i|c_k|N,i\rangle\right|^2}{(\omega-\varepsilon(k))^2+\Gamma^2} + \frac{\Gamma}{\pi}\sum_{s\neq i}\frac{\left|\langle N-1,s|c_k|N,i\rangle\right|^2}{(\omega-\varepsilon_s(k))^2+\Gamma^2}$$

$$= A(k,\omega)_{\mathrm{coh.}} + A(k,\omega)_{\mathrm{incoh}}$$

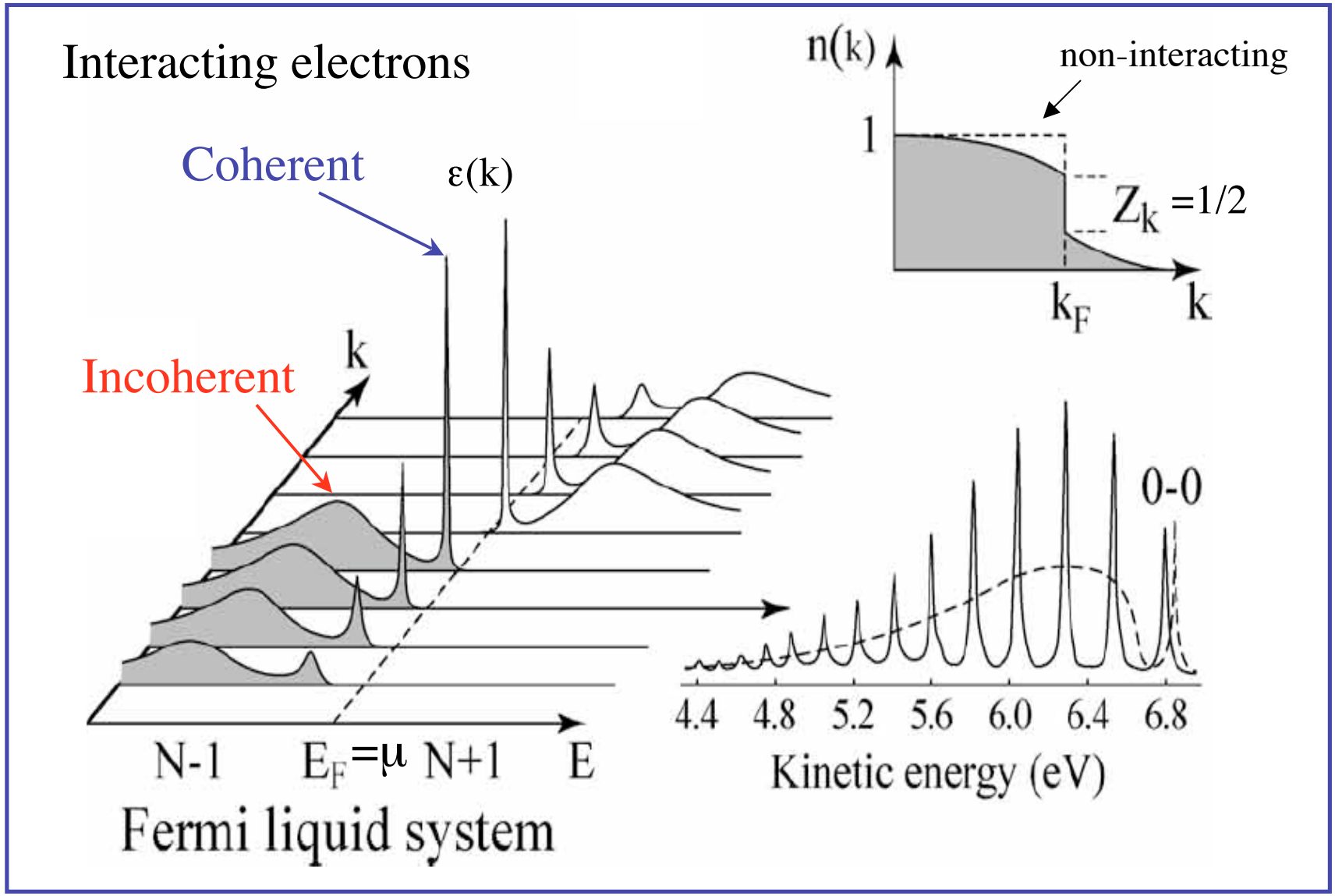

$$A(k,\omega) = \frac{\Gamma}{\pi}\frac{Z_k}{(\omega-\varepsilon(k))^2+\Gamma^2} + \frac{\Gamma}{\pi}\sum_{s\neq i}\frac{|\langle N-1,s|c_k|N,i\rangle|^2}{(\omega-\varepsilon_s(k))^2+\Gamma^2} = A(k,\omega)_{coh.} + A(k,\omega)_{incoh}$$

non-interacting electrons

interacting electrons

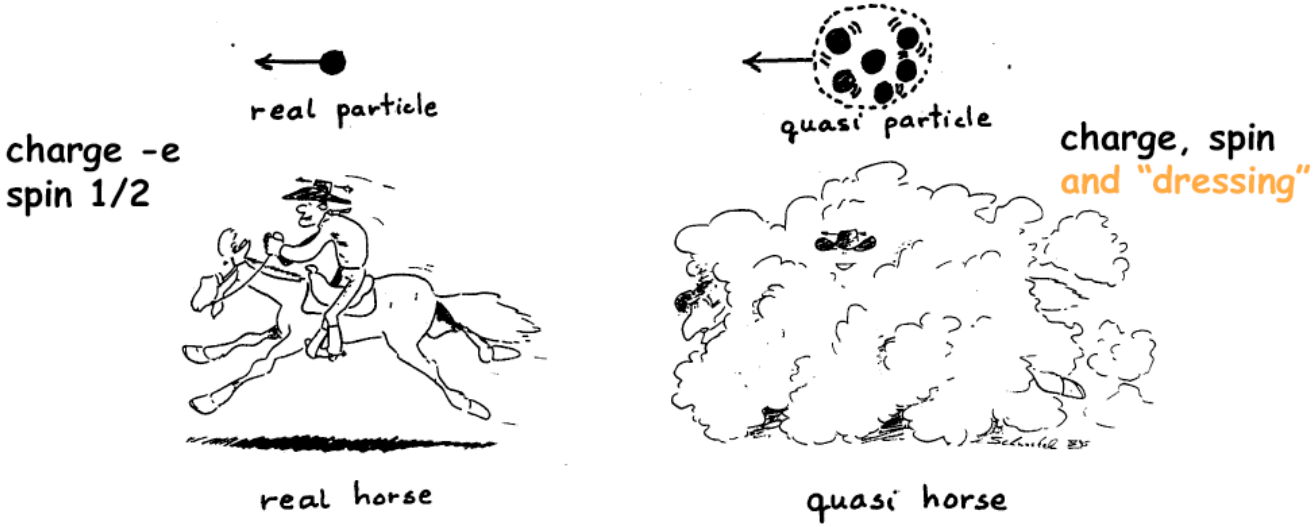

band structure

$\varepsilon_0(\mathbf{k})$

quasiparticle band structure

$$\varepsilon(k) = [\varepsilon_0(k) + \Sigma_1(k,\omega)]$$

$$\Sigma(\mathrm{k},\omega) = \Sigma_1(\mathrm{k},\omega) + \mathrm{i}\Sigma_2(\mathrm{k},\omega)$$ Self Energy

- **photohole probes interactions** between electrons and with other dynamical degrees of freedom
  - → energy shifts
  - → shake-up satellites
  - → line broadening
  - → line shape
  - *(generalized Franck-Condon effect)*

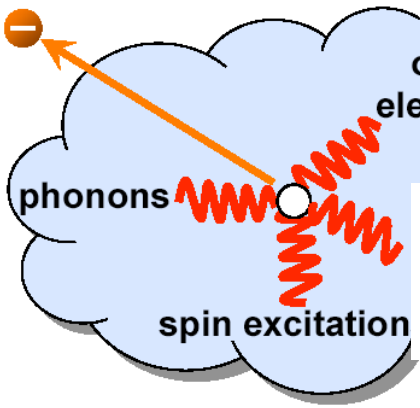

→ **lifetime broadening:** $\Gamma_{\vec{k}} = \mathrm{Im}\,\Sigma$

→ **quasiparticle weight:** $Z_{\vec{k}} = (1 - \frac{\partial \Sigma}{\partial \omega})^{-1} \leq 1$

$= m_o/m_{eff}$

Debye Model (λ = 1)

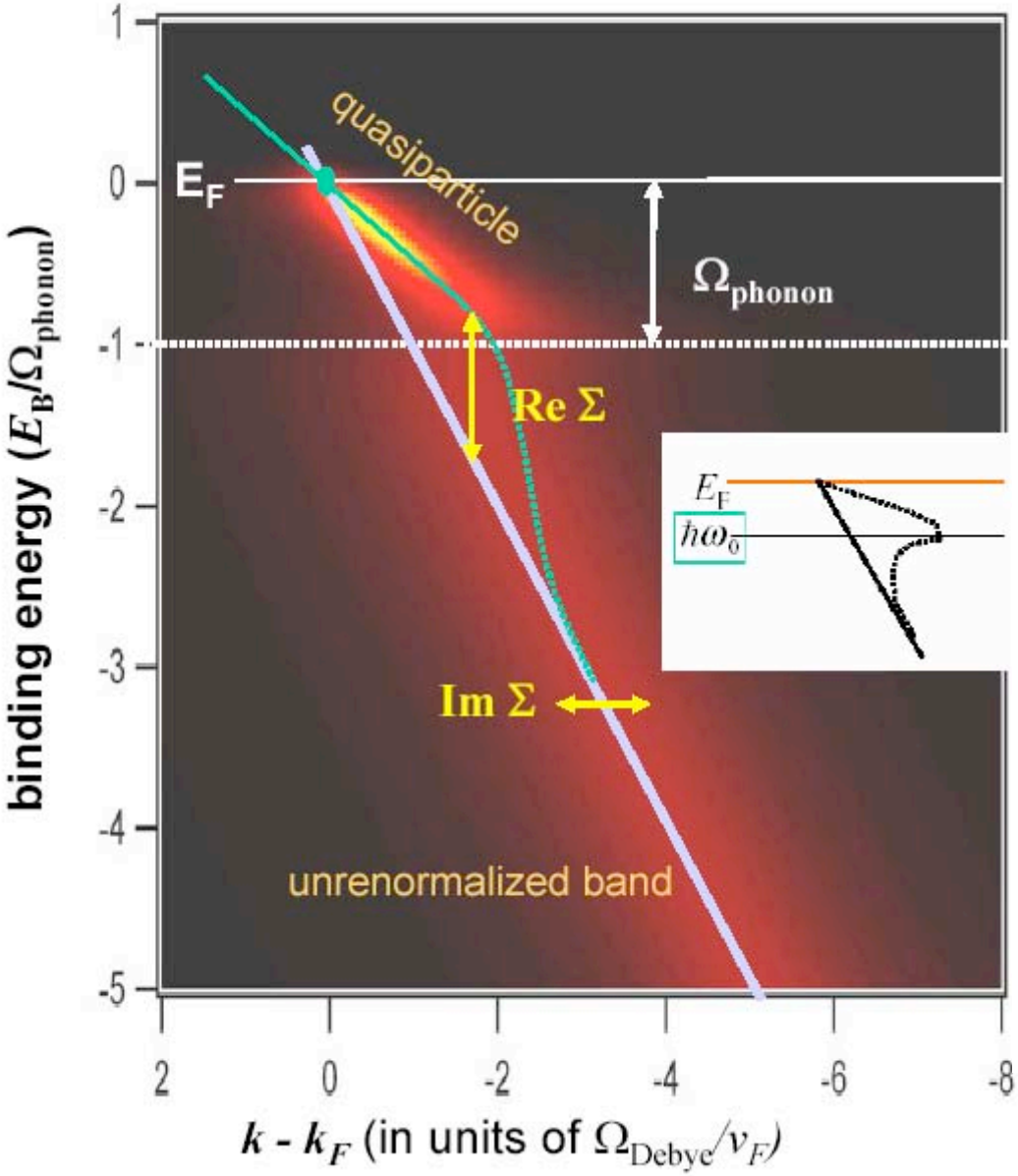

$$\mathrm{Im}\,\Sigma(\omega) \propto \lambda \int_0^{\omega} \rho_{phonon}(\Omega)\, d\Omega$$

energy scale Ω_{phonon}:

separates between *virtual* and *real* scattering processes

coupling constant λ:

effective Fermi velocity
$v_F^* = v_F^0/(1+\lambda)$

effective mass $m^* = (1+\lambda)m_0$

i.e. $Z = (1+\lambda)^{-1}$

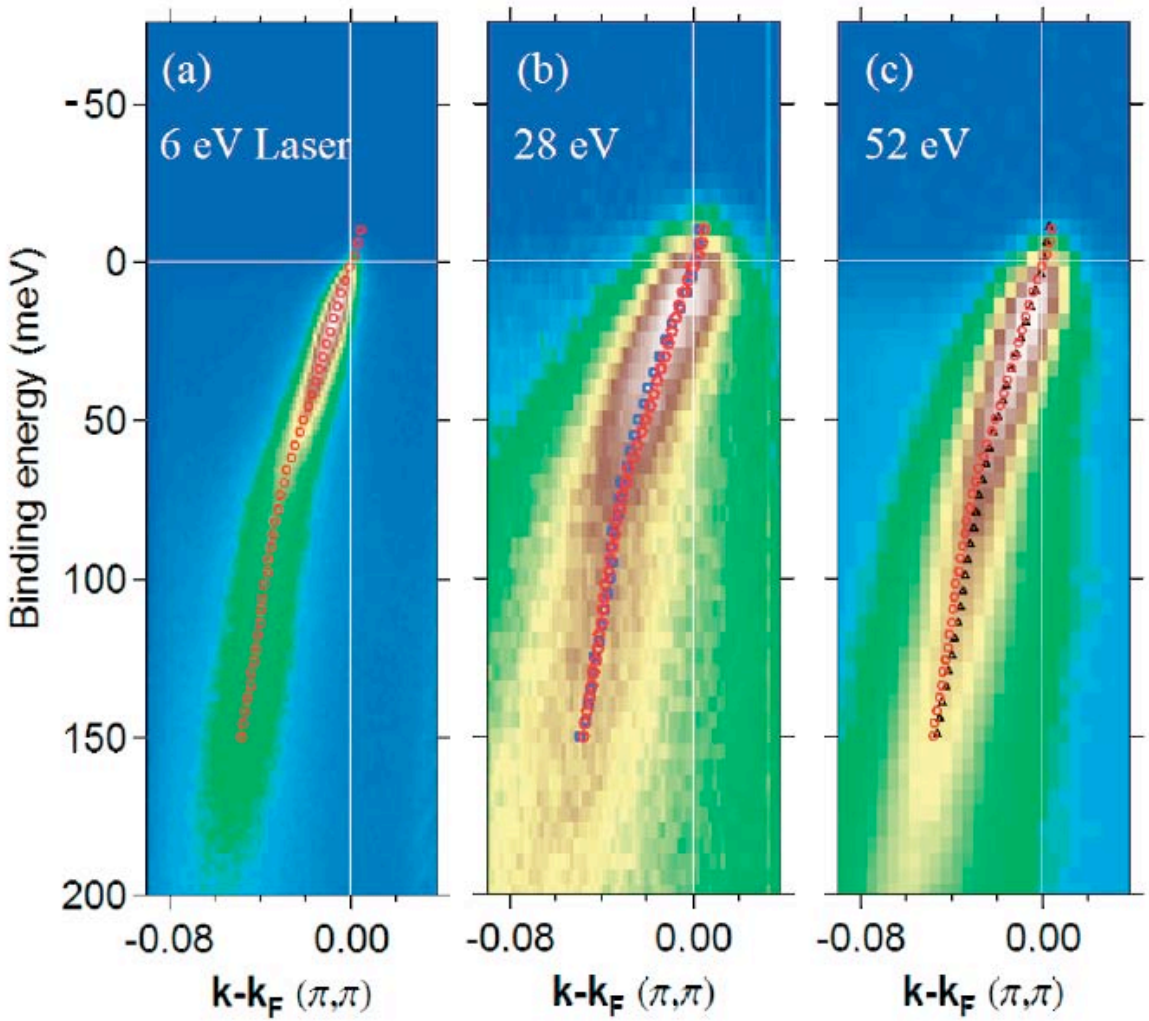

No dramatic changes in the electronic spectra near the Fermi surface. The sudden approx seems to be still valid or its breakdown may be not so important for the states near E_F.

J.D. Koralek et al., PRL76, 017005 (2005)

Another critical point for ARPES at low energies: "Final state" effects

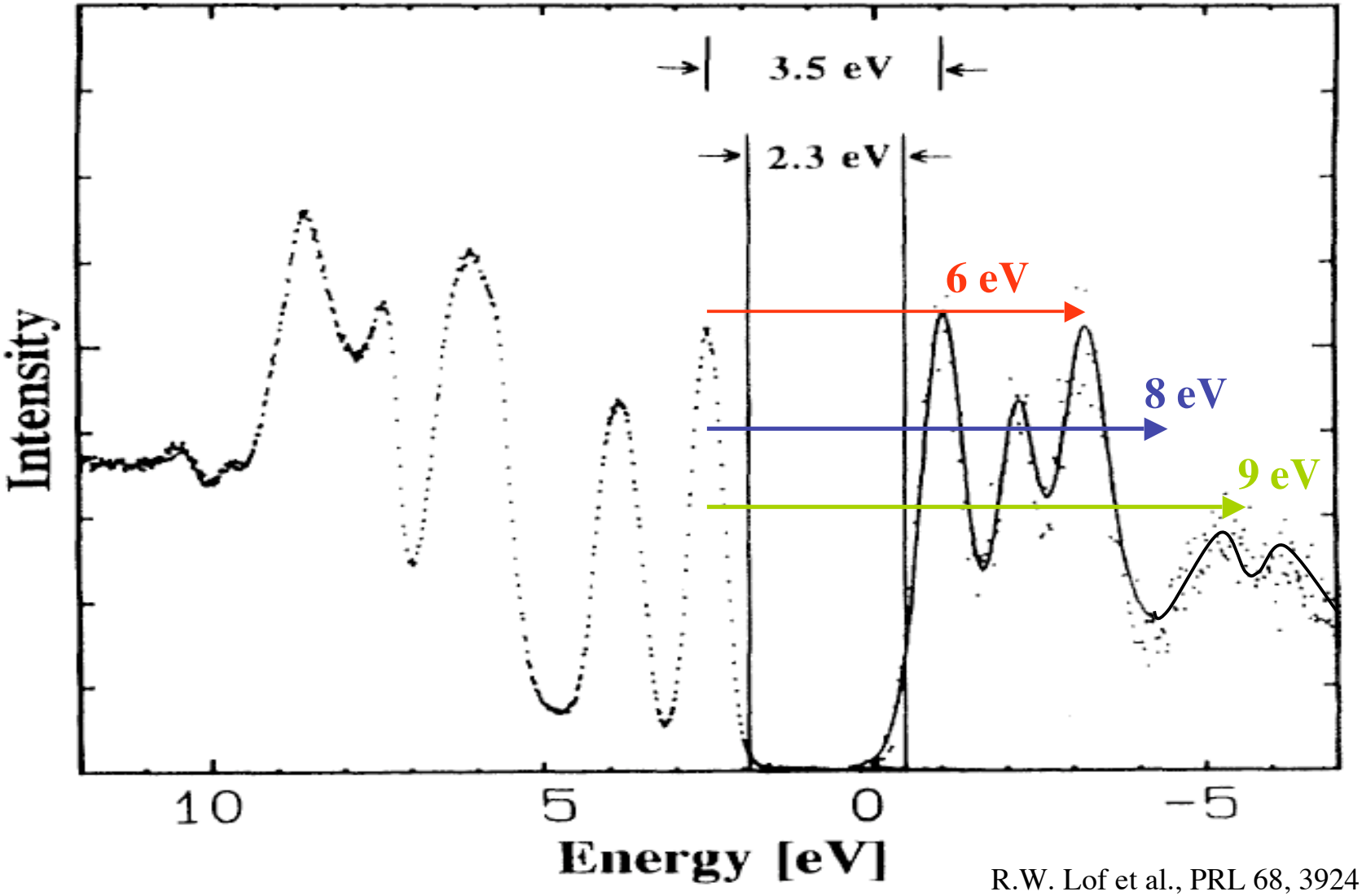

R.W. Lof et al., PRL 68, 3924 (1992)

C_{60}(111) multilayer @ RT

A. Goldoni et al.

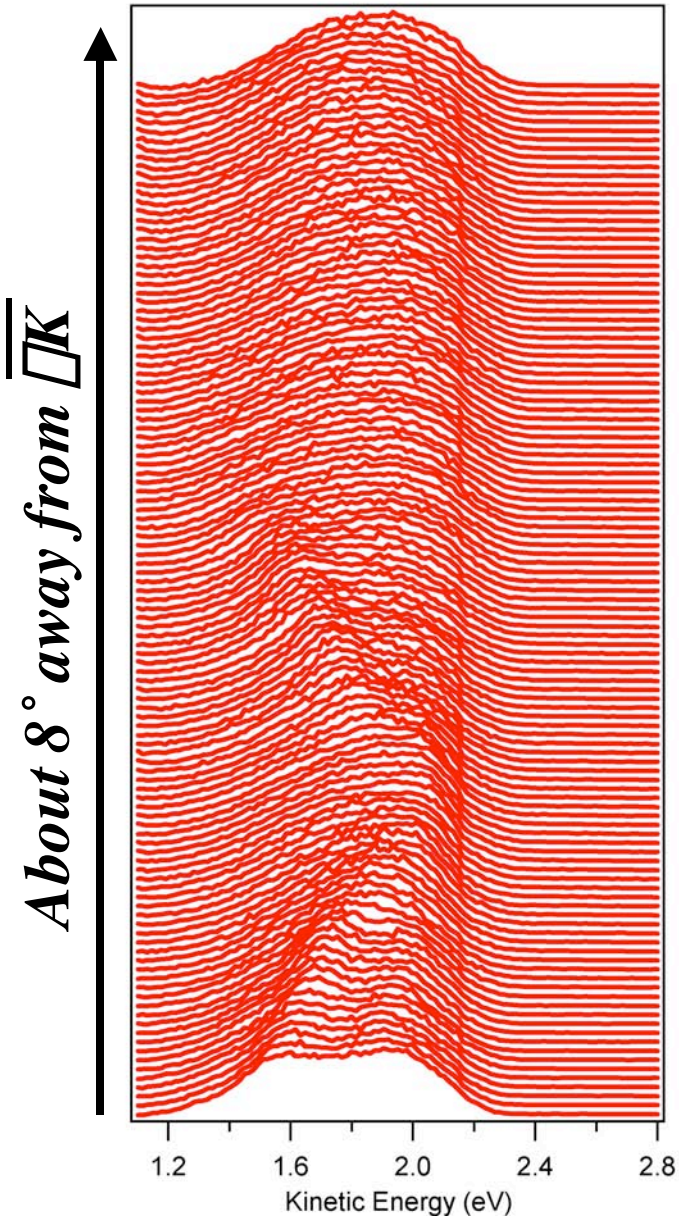

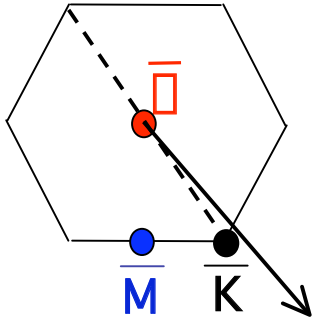

HOMO band dispersion ~ 0.6 eV

No difference @ 77 K

hν = 8 eV

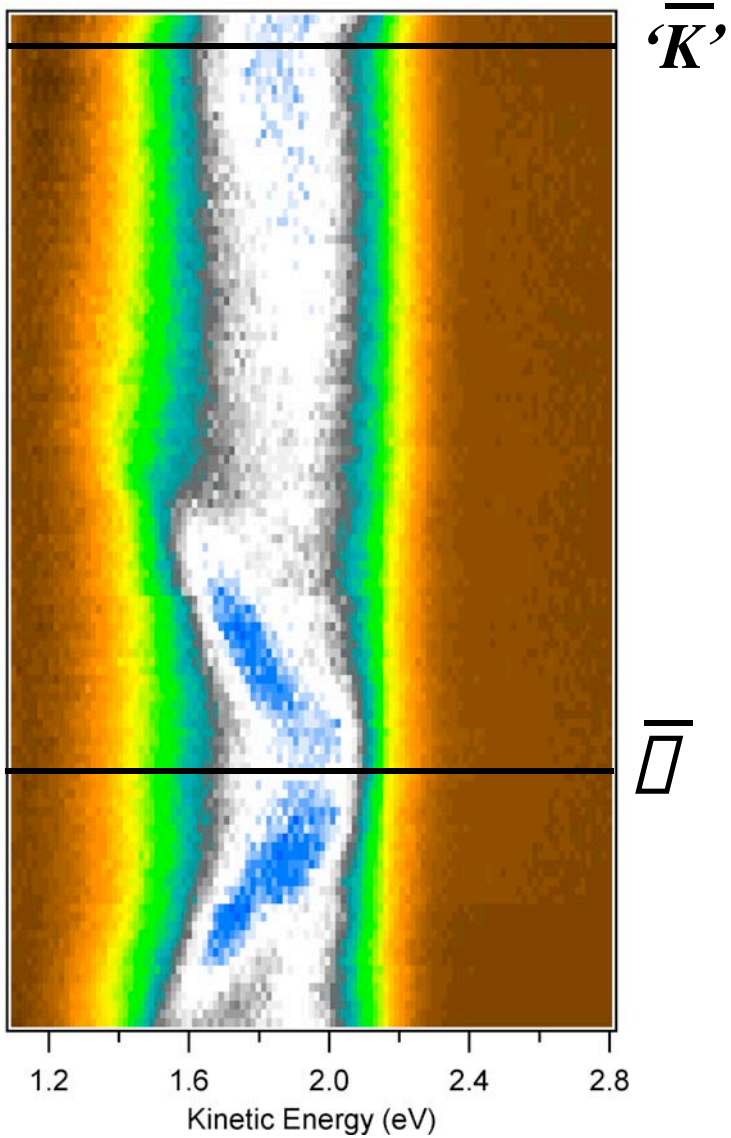

C_{60}(111) multilayer @ RT

A. Goldoni et al.

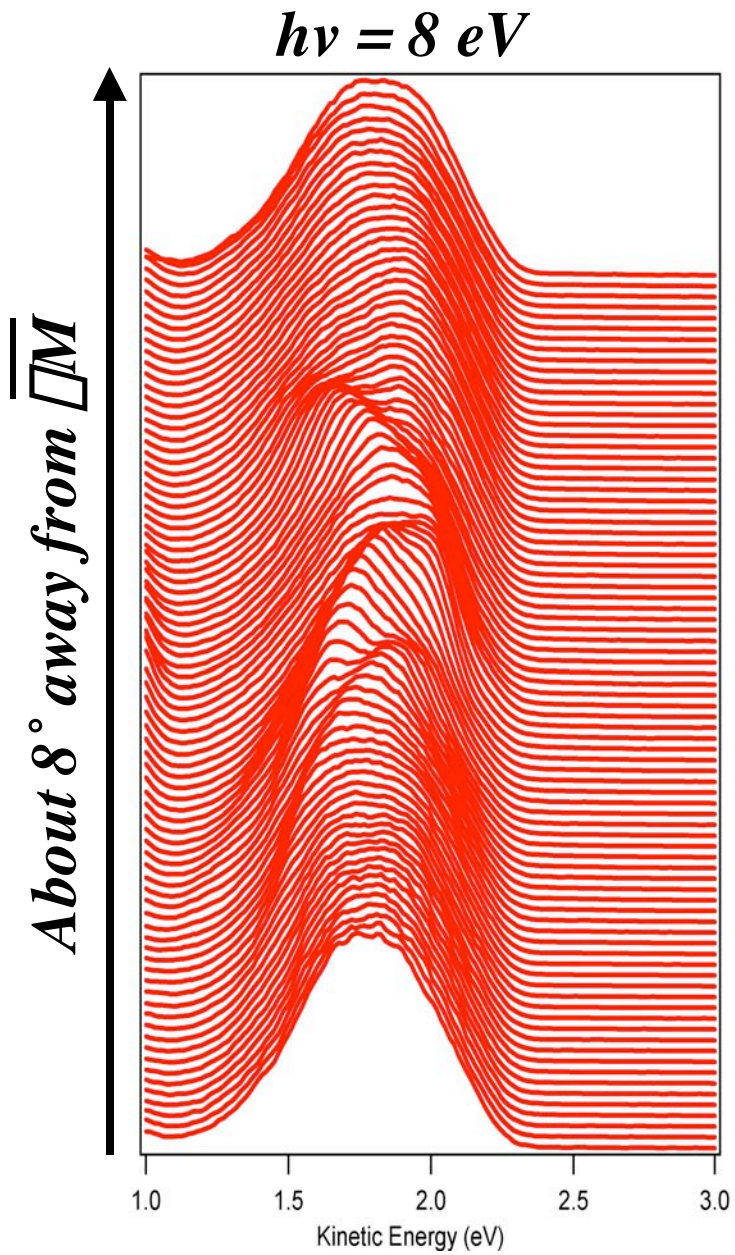

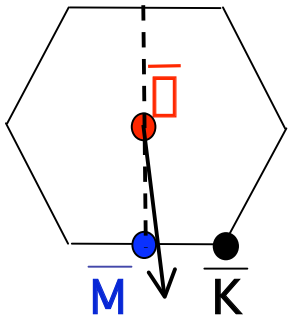

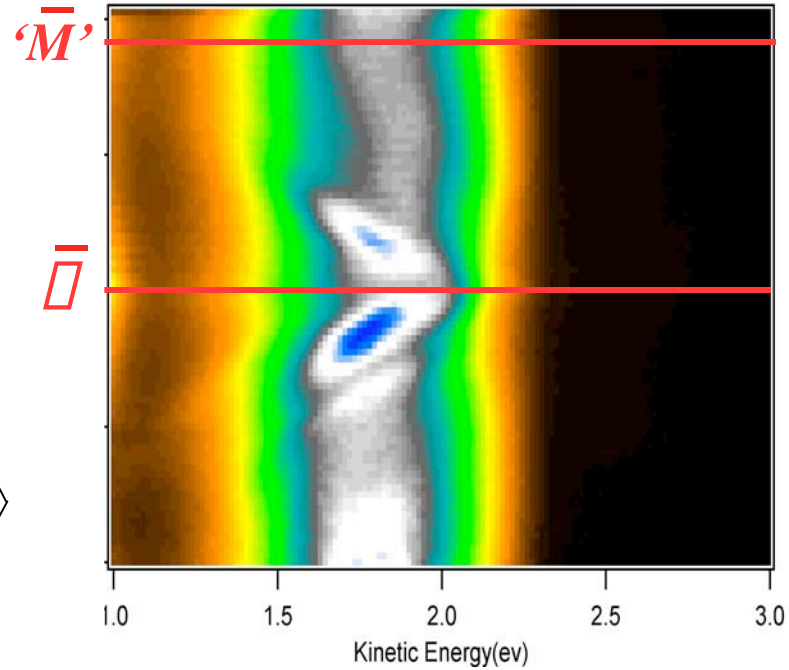

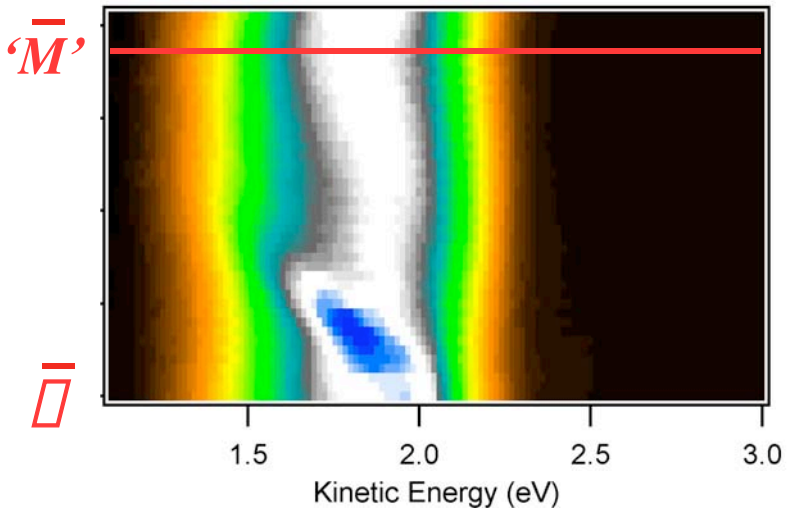

C_{60}(111) multilayer @ RT

A. Goldoni et al.

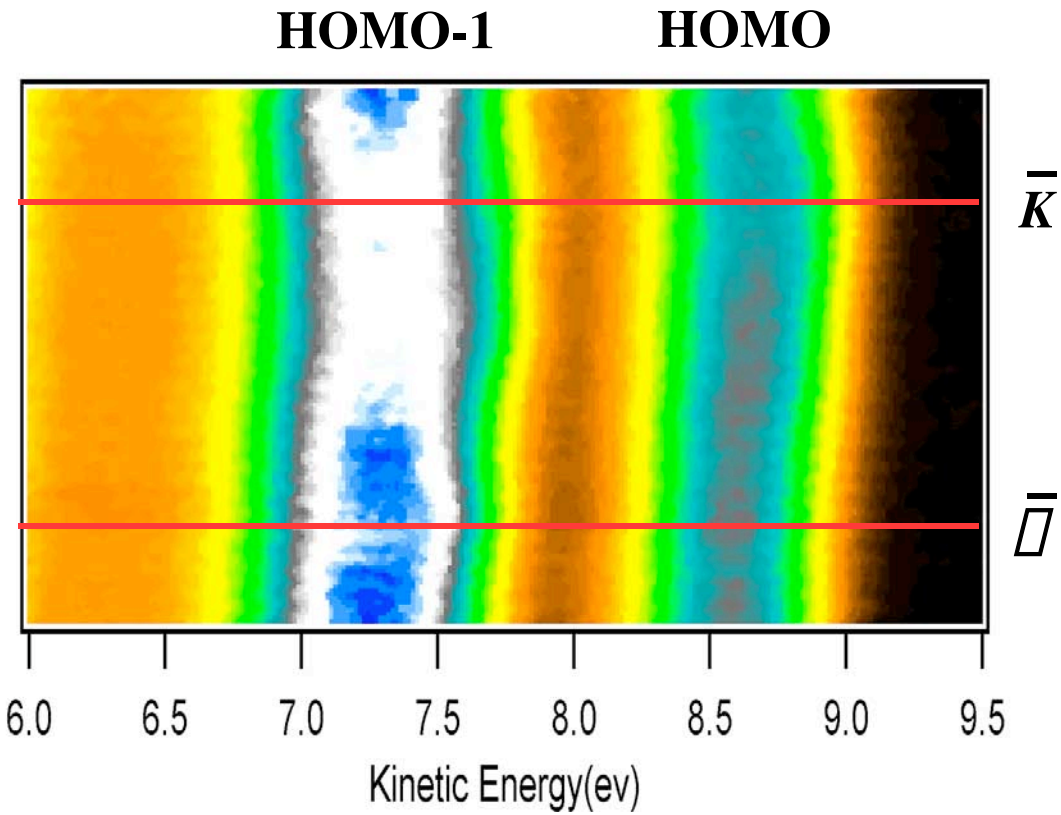

hν = 15 eV

HOMO dispersion apparently smaller than at 8 eV, but of the order of 0.2 eV ($K_{//}$ integration? Final state effects?)

C_{60}(111) multilayer

A. Goldoni et al.

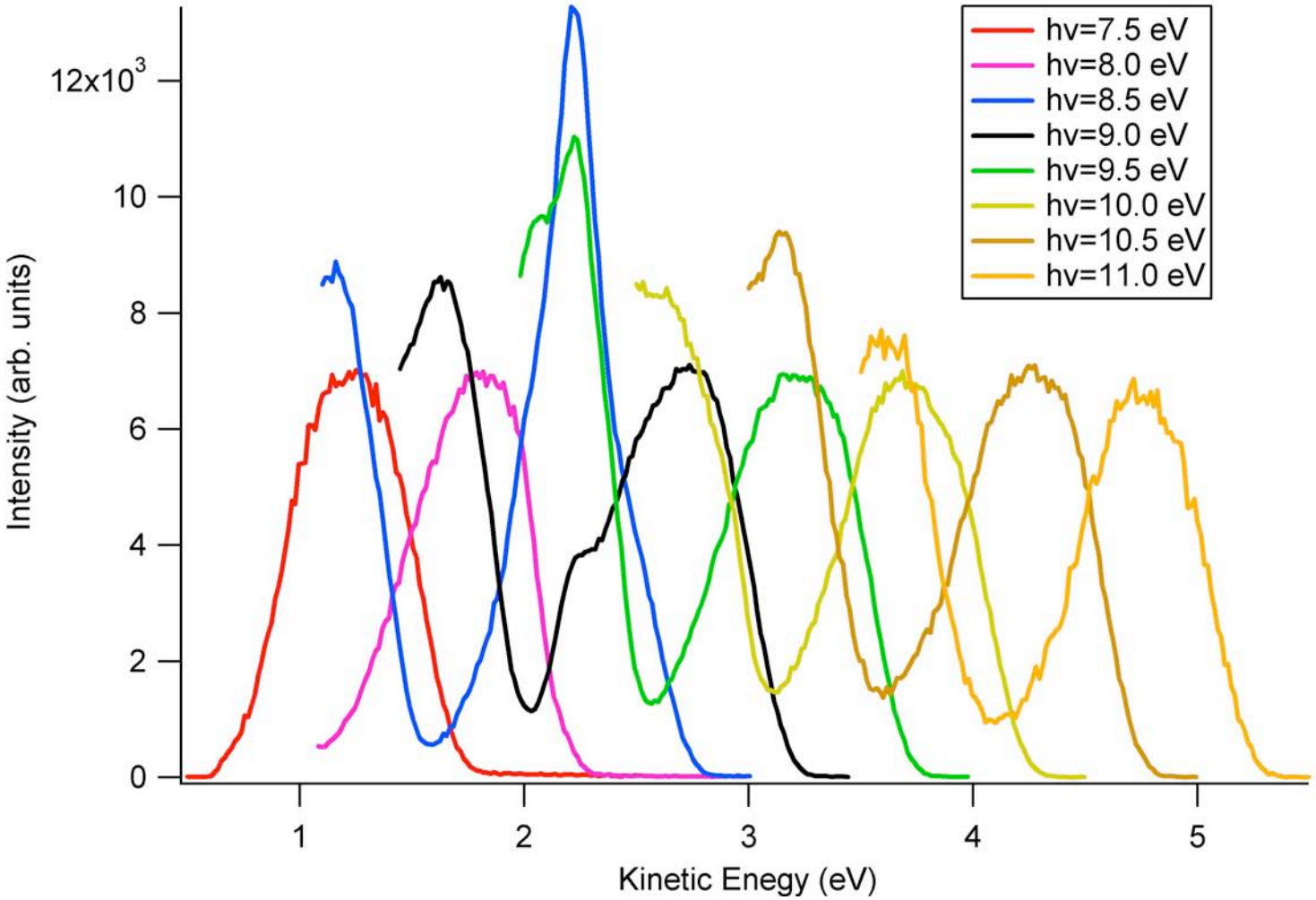

$C_{60}(111)$ multilayer

photoemission

inverse photoemission

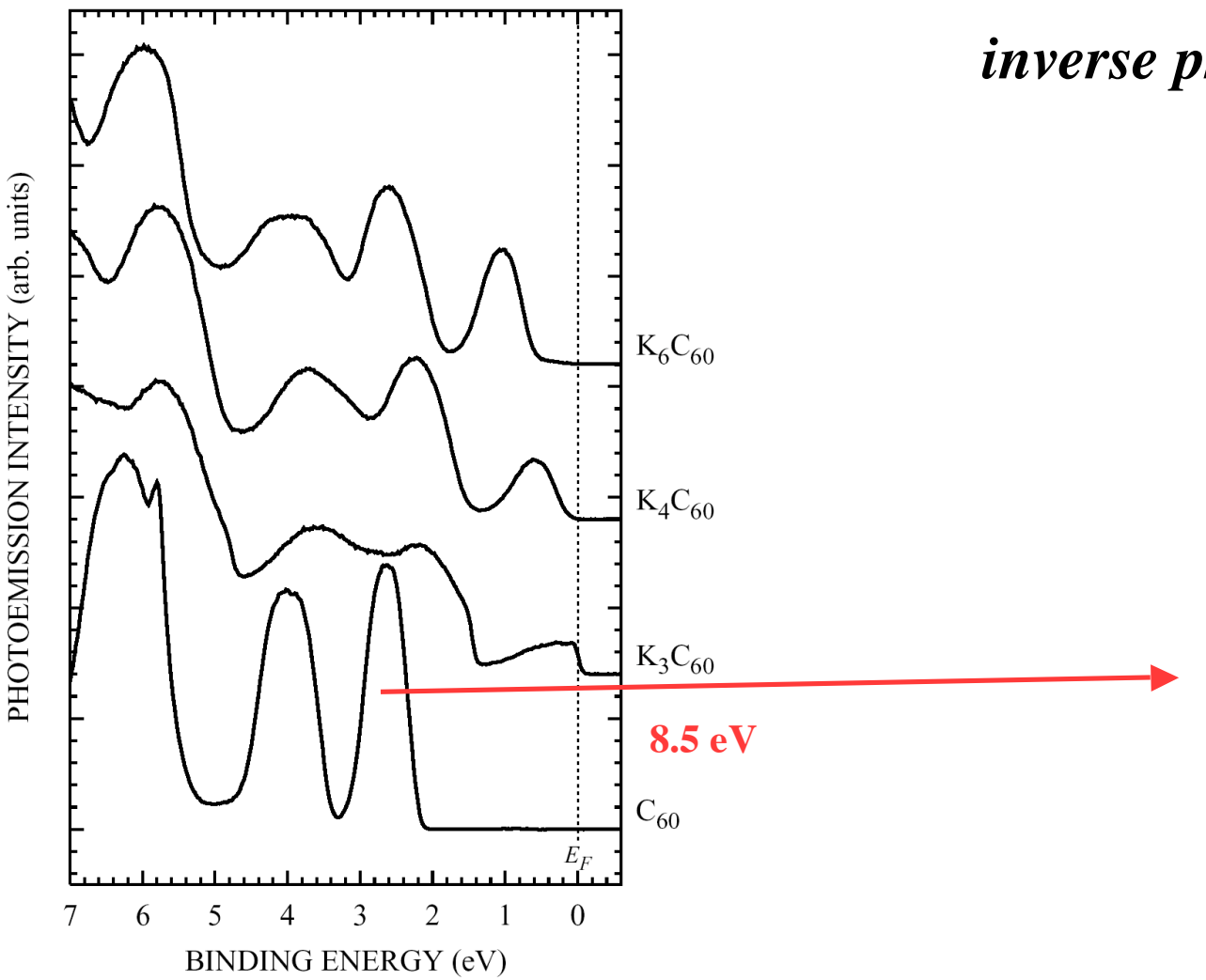

C_{60}(111) multilayer

A. Goldoni et al.

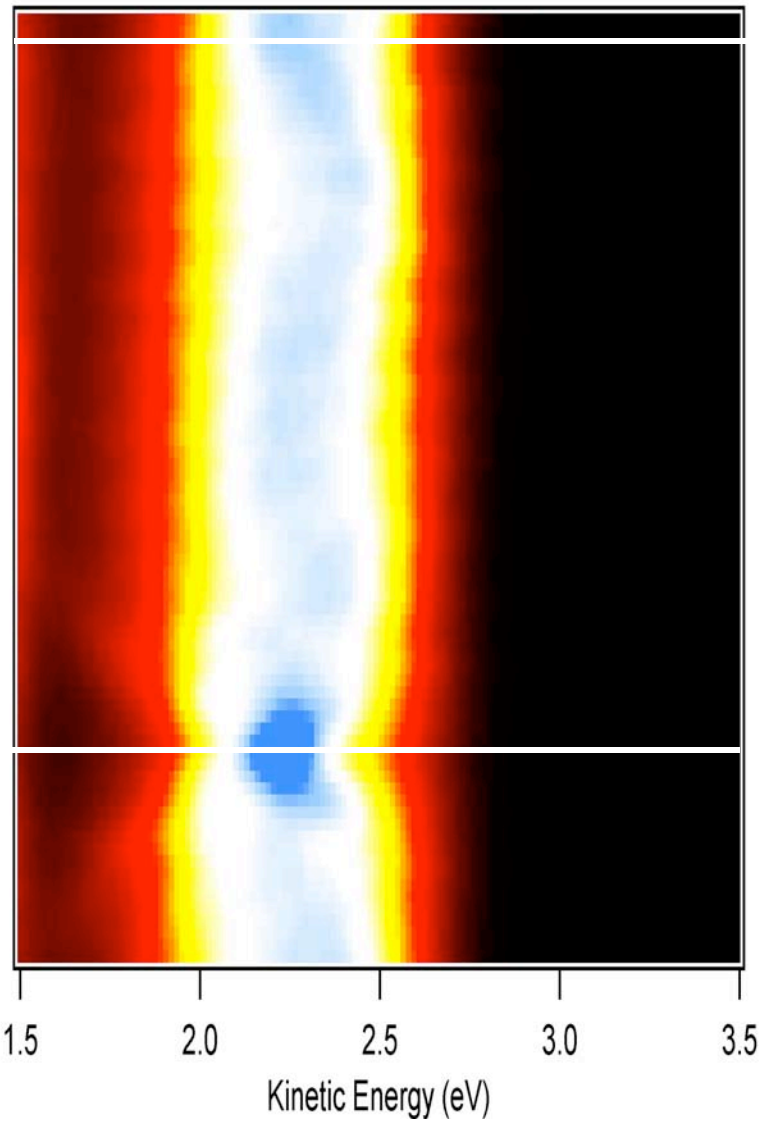

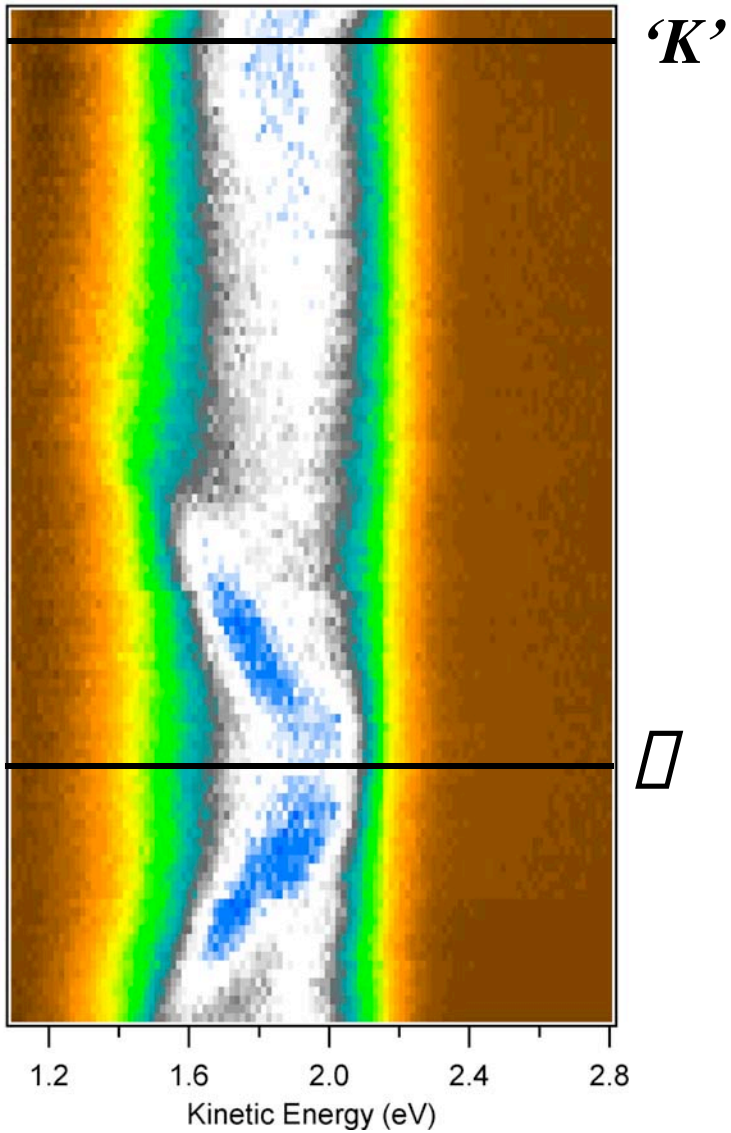

$Ca_{1-x}Sr_xVO_3$: angle-*integrated* photoemission

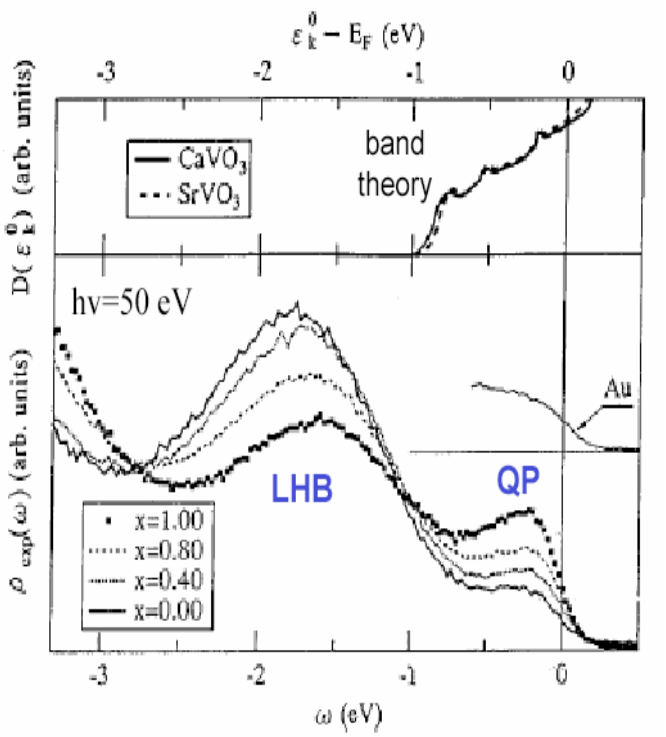

Inoue et al., PRL 1995

→ $CaVO_3$ more strongly correlated metal than $SrVO_3$?

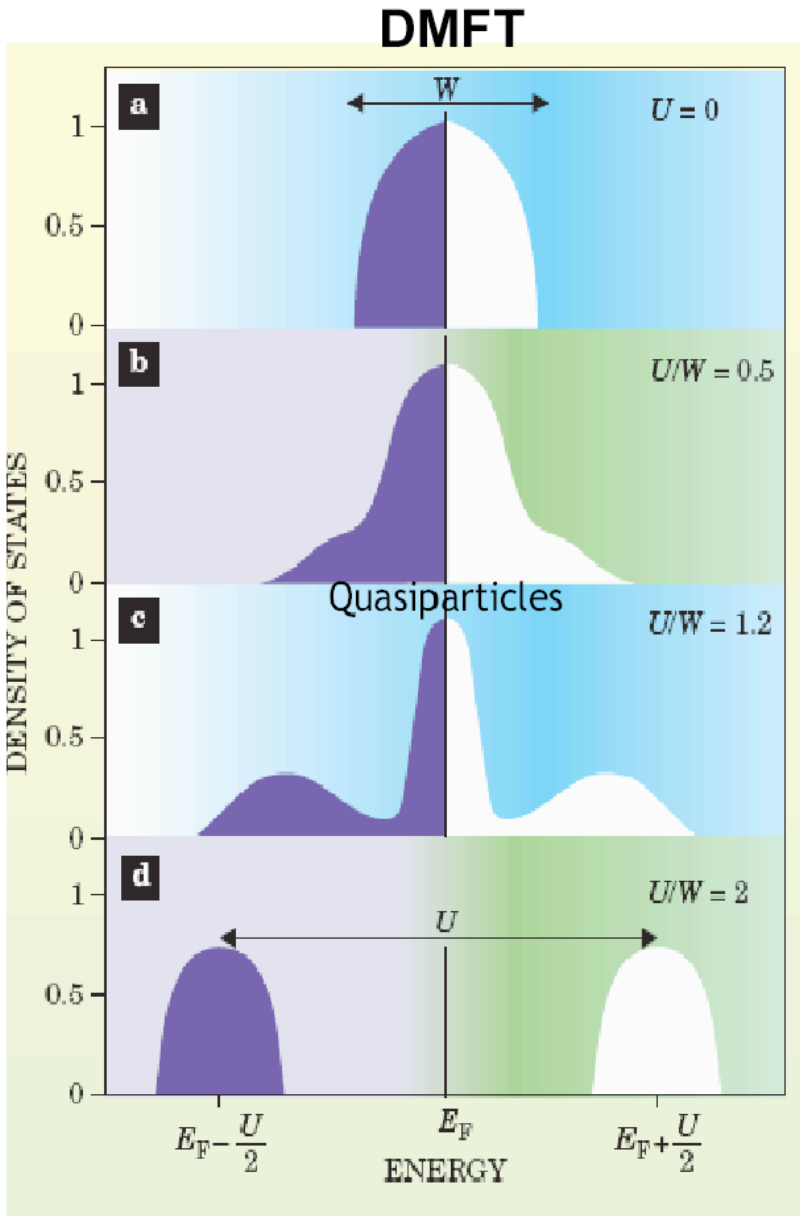

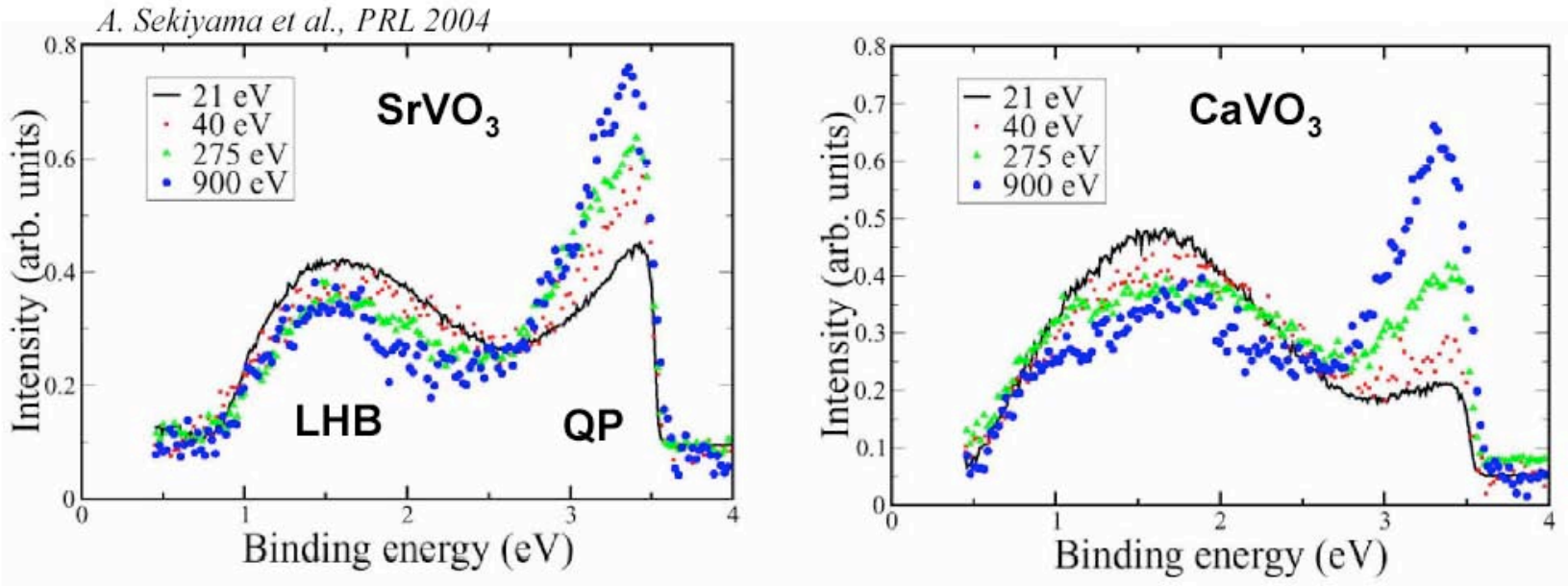

⇒ **at surface: reduced atomic coordination**

⇒ **effective bandwidth smaller:**
$W_{surf} < W_{bulk}$

⇒ **surface stronger correlated:**
$U / W_{surf} > U / W_{bulk}$

⇒ **surface effect stronger for $CaVO_3$, but in bulk ~ identical for all compositions**

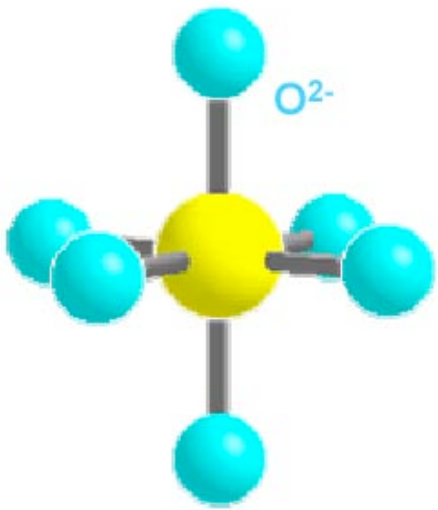

A. Sekiyama et al., PRL 2004

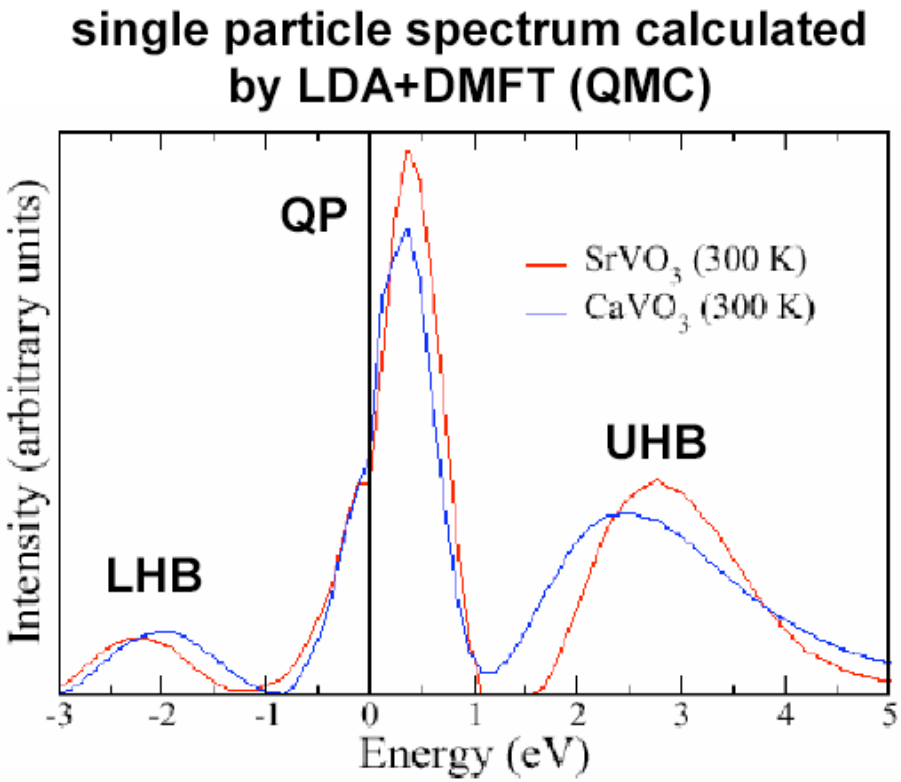

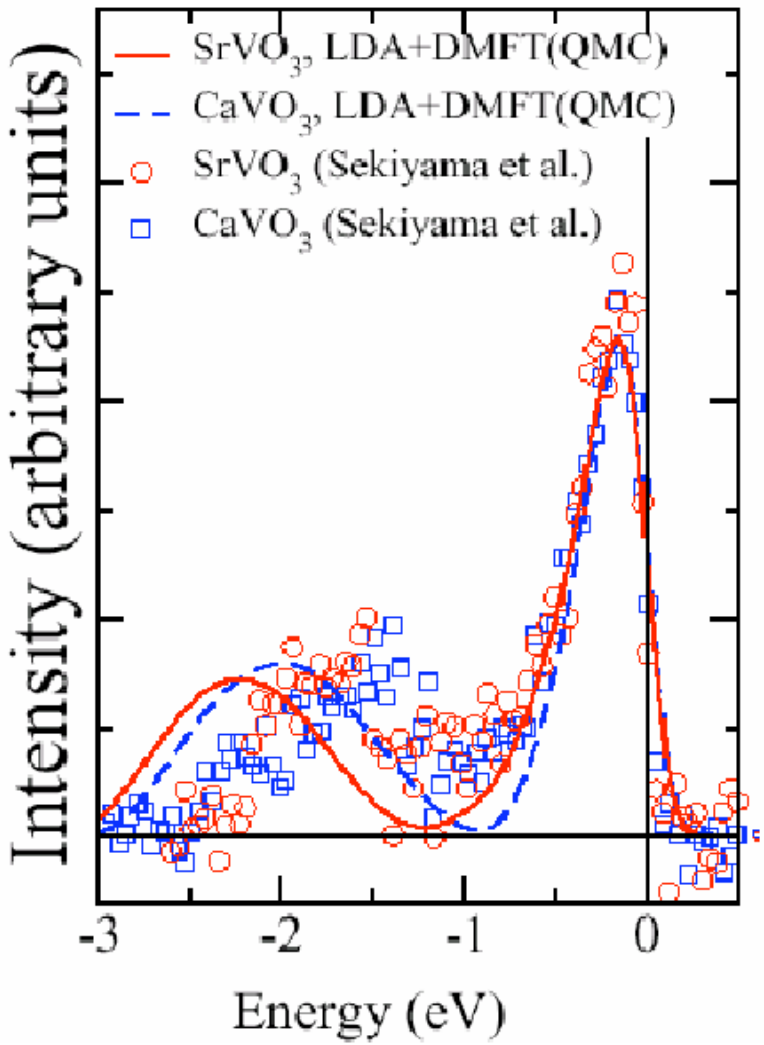

Good agreement, everything seems understood

- Incoherent peak becomes weak in SX PES
- $CaVO_3$ and $SrVO_3$ spectra are similar in SX PES

What happens in the bulk sensitive spectra using VUV laser ?

- More bulk sensitive
- much higher resolution

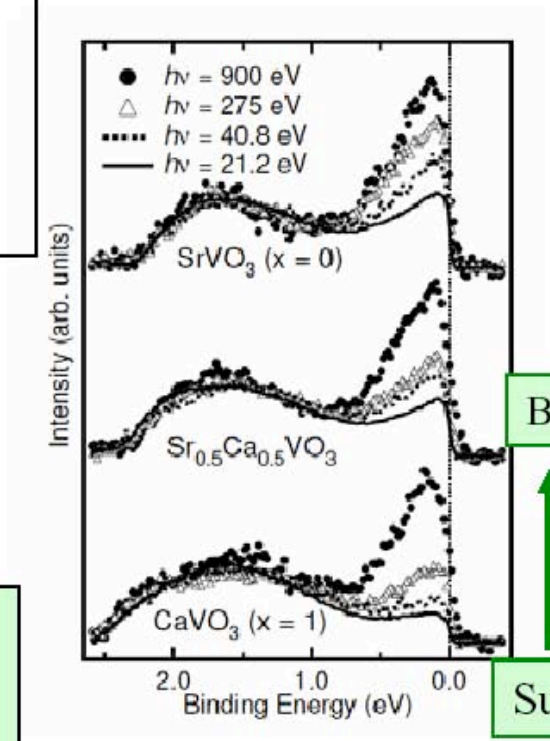

Photon-energy dependence of the V 3d spectral weights for $Sr_{1-x}Ca_xVO_3$. The V 3d spectra are normalized by the integrated intensities of the incoherent part ranging from 0.8 to 2.6 eV.

Sekiyama, PRL(2004)

Bulk

Surface

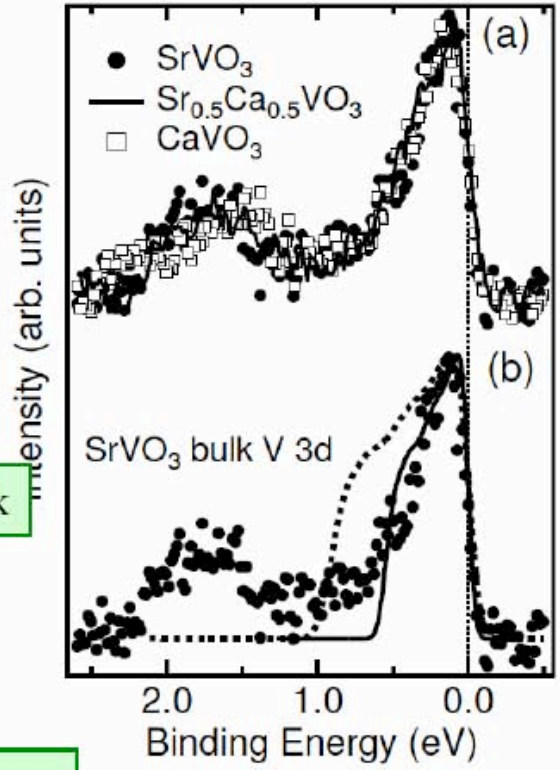

(a) Bulk V 3d spectral functions of $SrVO_3$ (closed circles), $Sr_{0.5}Ca_{0.5}VO_3$ (solid line) and $CaVO_3$ (open squares).
(b) Comparison of the experimentally obtained bulk V 3d spectral function of $SrVO_3$ (closed circles) to the V 3d partial density of states for $SrVO_3$ (dashed curve) obtained from the band-structure calculation, which has been broadened by the experimental resolution of 140 meV. The solid curve shows the same V 3d partial density of states but the energy is scaled down by a factor of 0.6.

Excitation energy dependence of coherence peak

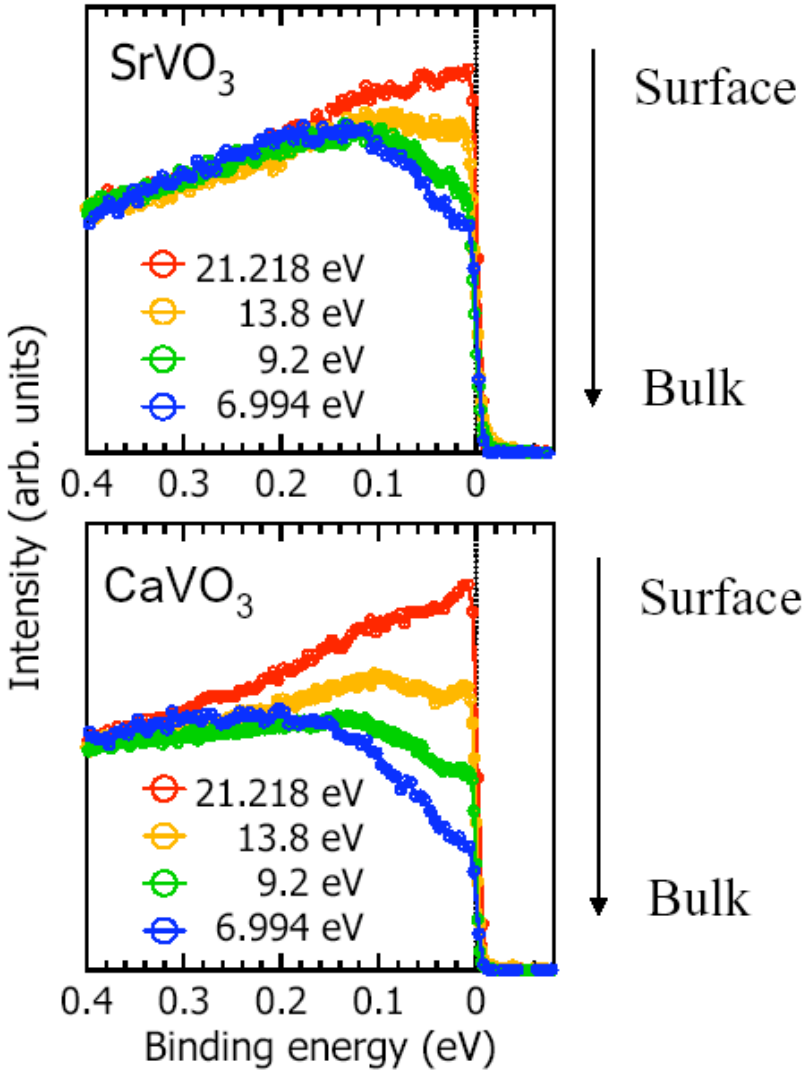

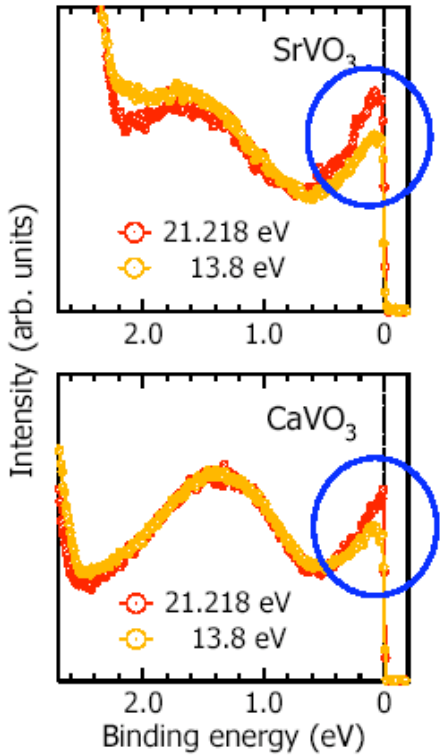

Contrary to the SX spectra, coherent peaks become weaker

What happens?

Other problems:

- Magnetic fields must be screened very well
- The total reflection angle for bulk state emission can be reached

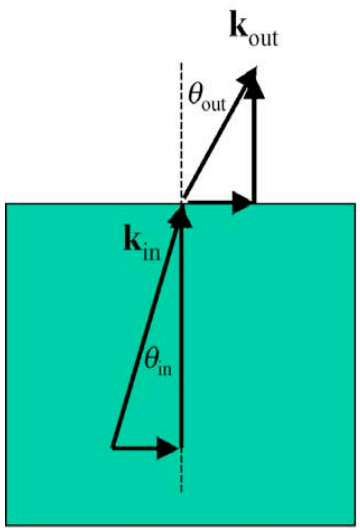

Kinematic relations

$$k_{out} = \sqrt{\frac{2m}{\hbar^2} E_{kin}}$$

$$k_{in} = \sqrt{\frac{2m}{\hbar^2} (E_{kin} + V_0)}$$

$$k_{out,\parallel} = k_{in,\parallel} \equiv k_{\parallel}$$

"Snell's Law"

$$k_{\parallel} = \sin\theta_{out} \sqrt{\frac{2m}{\hbar^2} E_{kin}} = \sin\theta_{in} \sqrt{\frac{2m}{\hbar^2} (E_{kin} + V_0)}$$

Critical angle for emission

$$(\sin\theta_{out})_{\max} = \sqrt{\frac{E_{kin}}{E_{kin} + V_0}}$$

- Large Brillouin zones cannot be mapped completely

SPIN POLARIZATION: HOW TO MEASURE and SOME EXAMPLES

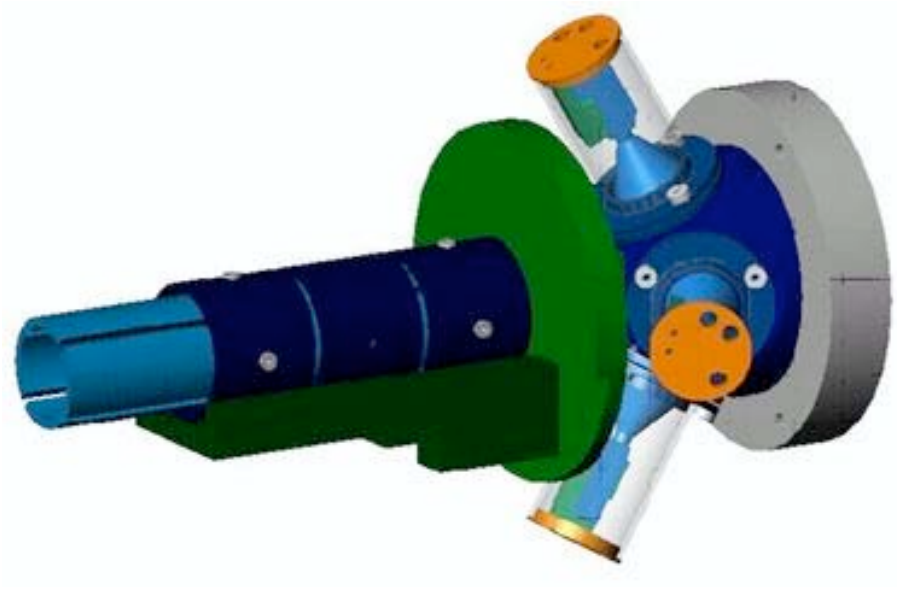

The Mott detector: measuring the electron spin polarization

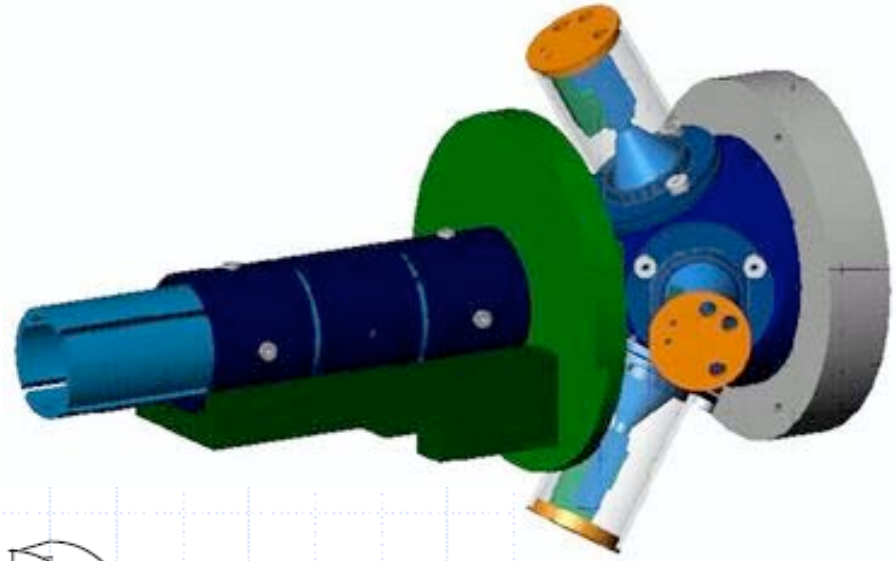

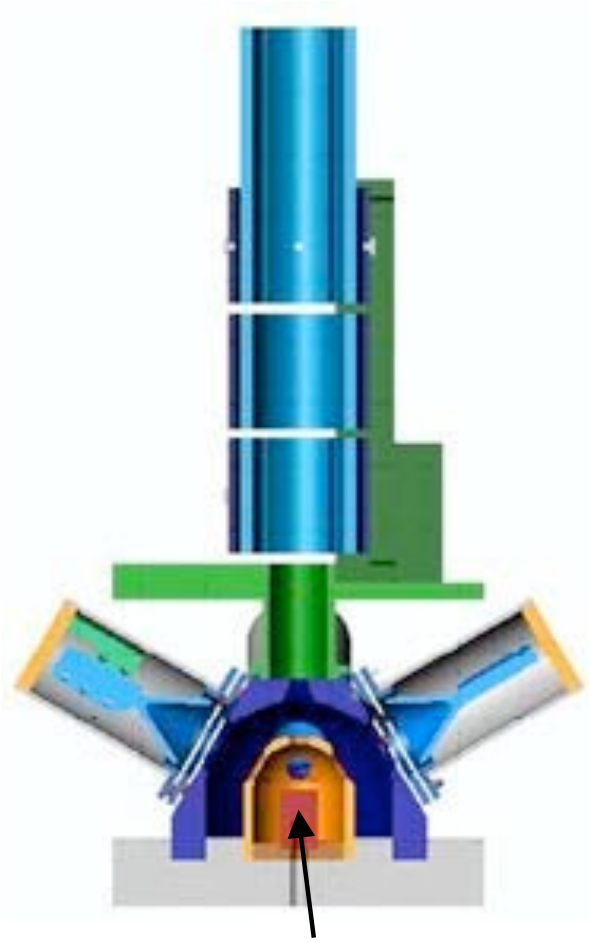

Gold foil

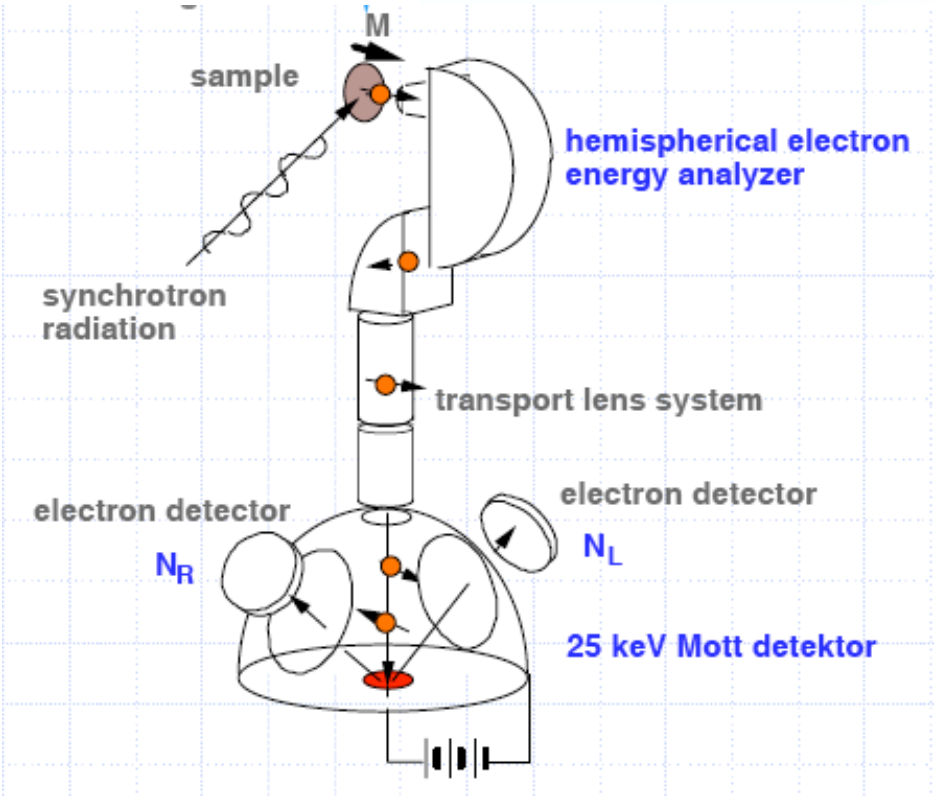

Gold foil is used because of its high Z, it is non-reactive and because thin gold, films which reduce multiple scattering, are easy to produce.

The presence of a spin-orbit term in the scattering potential introduces a spin dependence in the scattering cross section. Two detectors at exactly the same scattering angle to the left and right of the foil count the number of scattered electrons.

$$\underbrace{\frac{e\hbar^2}{4M^2c^2}\frac{1}{r}\frac{\partial V}{\partial r}}_{\xi(r)}\underbrace{(\vec{r}\times\vec{p})\cdot\vec{\sigma}}_{(\vec{L}\cdot\vec{S})}$$

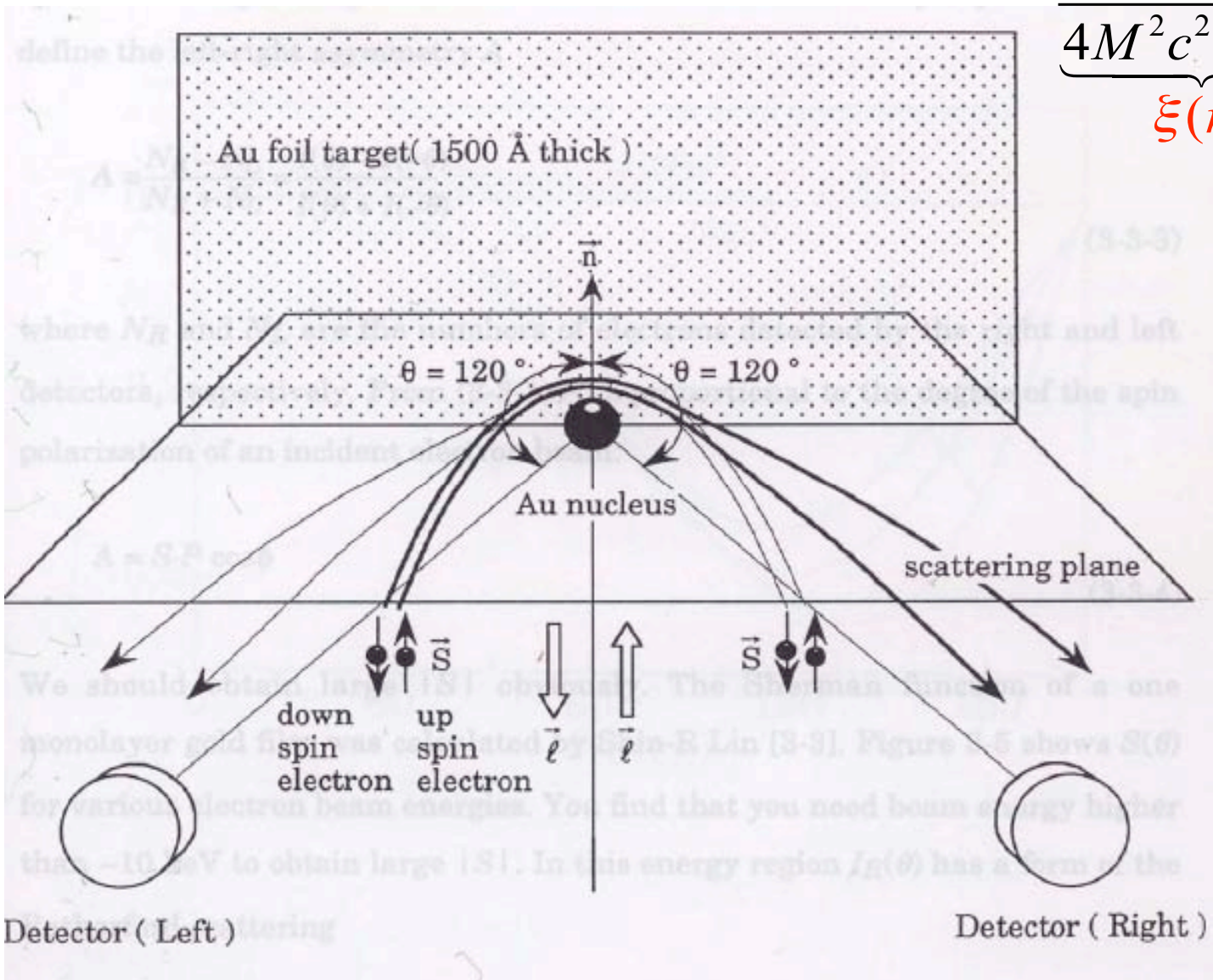

$$\boldsymbol{\mu}_{\text{spin}} = -g_s\mu_B\mathbf{s}$$

$$\boldsymbol{\mu}_{\text{orb}} = -\mu_B\mathbf{l}$$

$$A = S\cdot P_{ol}$$

$$A = \frac{I^{right} - I^{letf}}{I^{right} + I^{left}}$$

$$P_{ol} = \frac{N_\uparrow - N_\downarrow}{N_\uparrow + N_\downarrow}$$

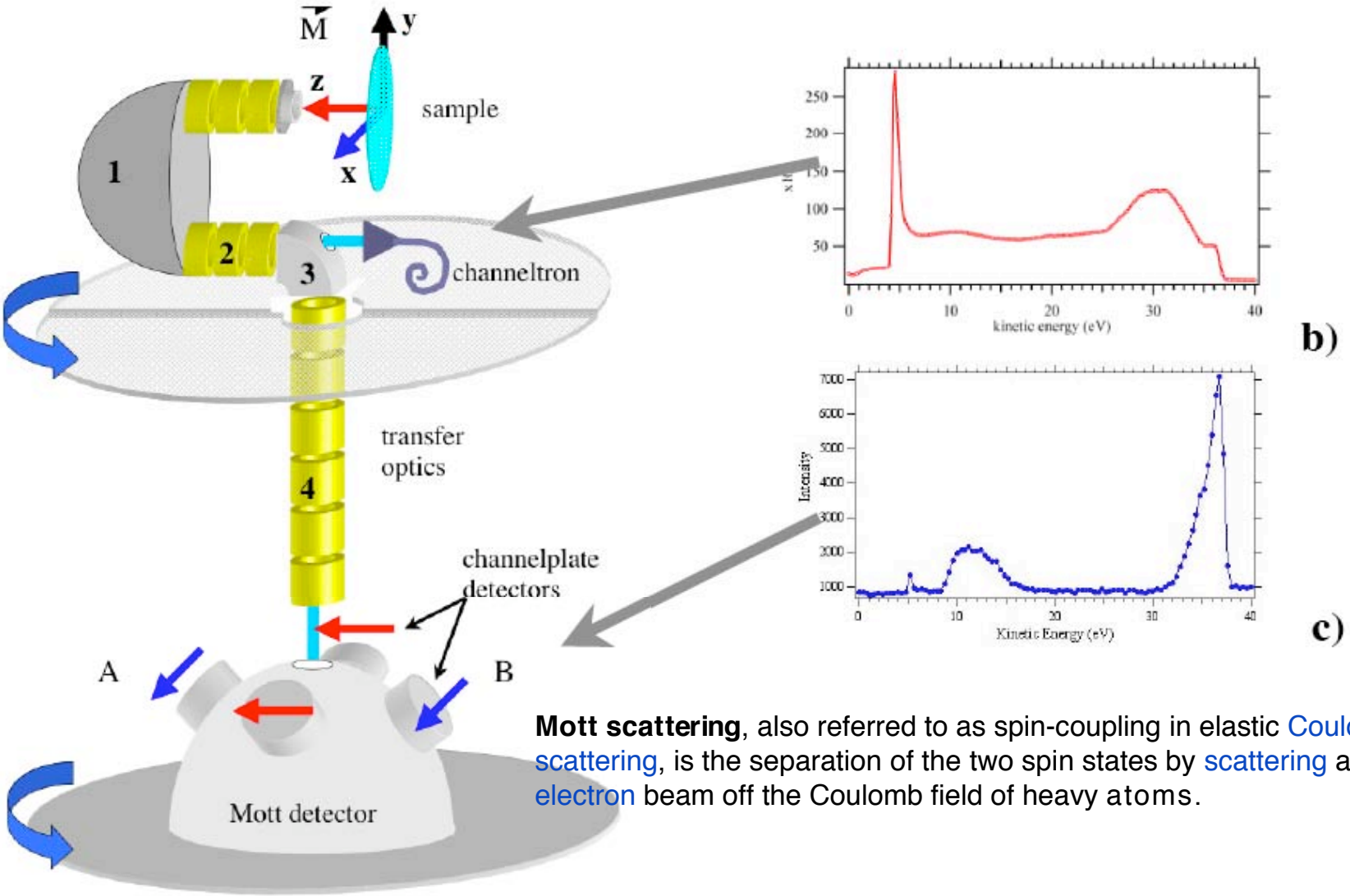

Mott scattering, also referred to as spin-coupling in elastic Coulomb scattering, is the separation of the two spin states by scattering an electron beam off the Coulomb field of heavy atoms.

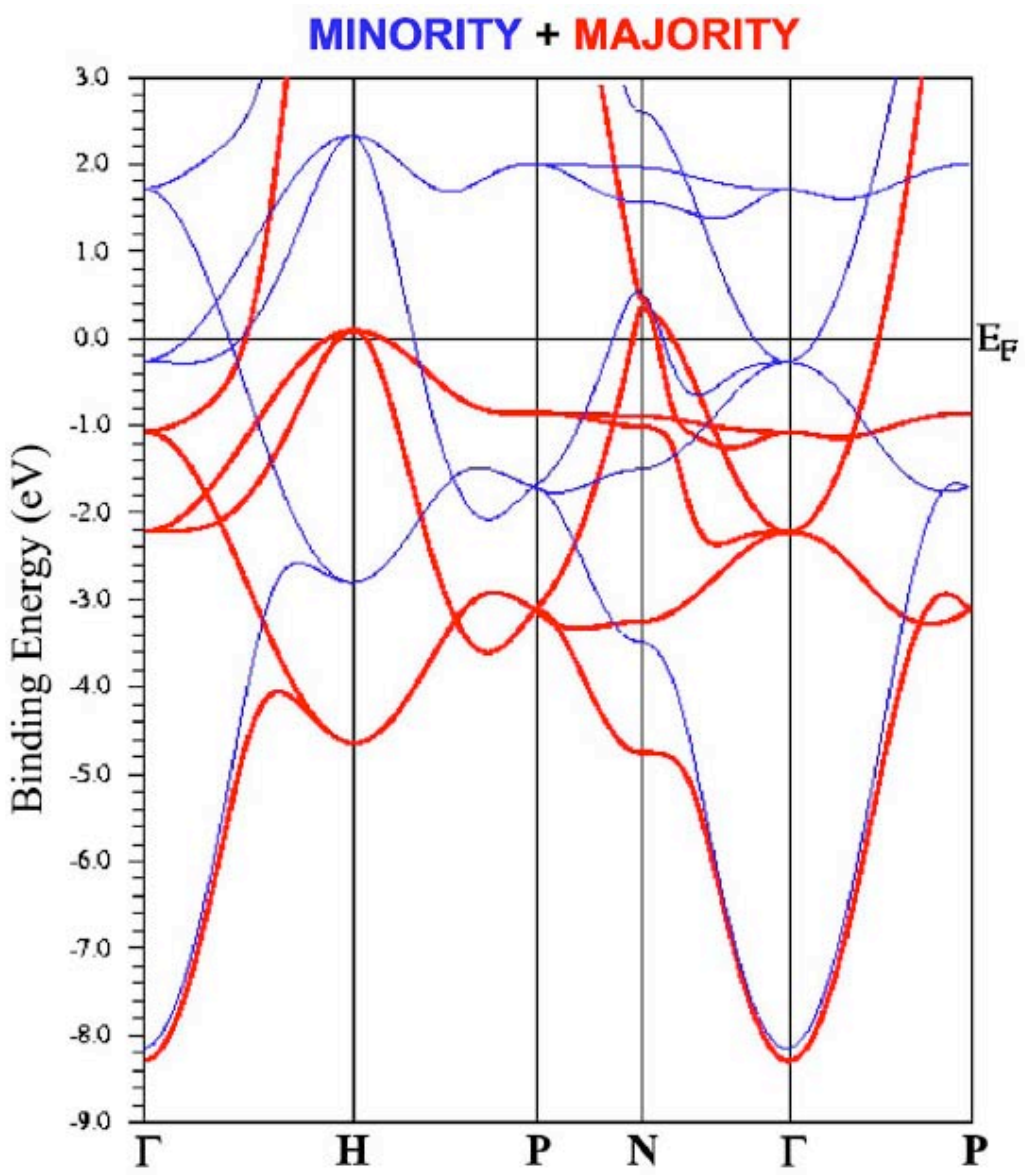

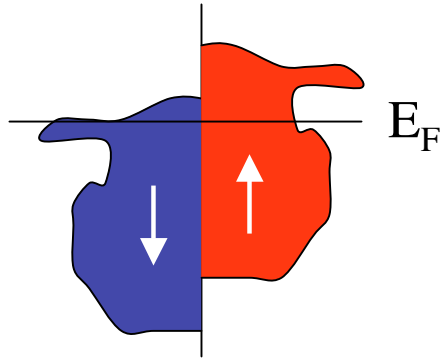

"in-plane" polarization in ferromagnetic iron films

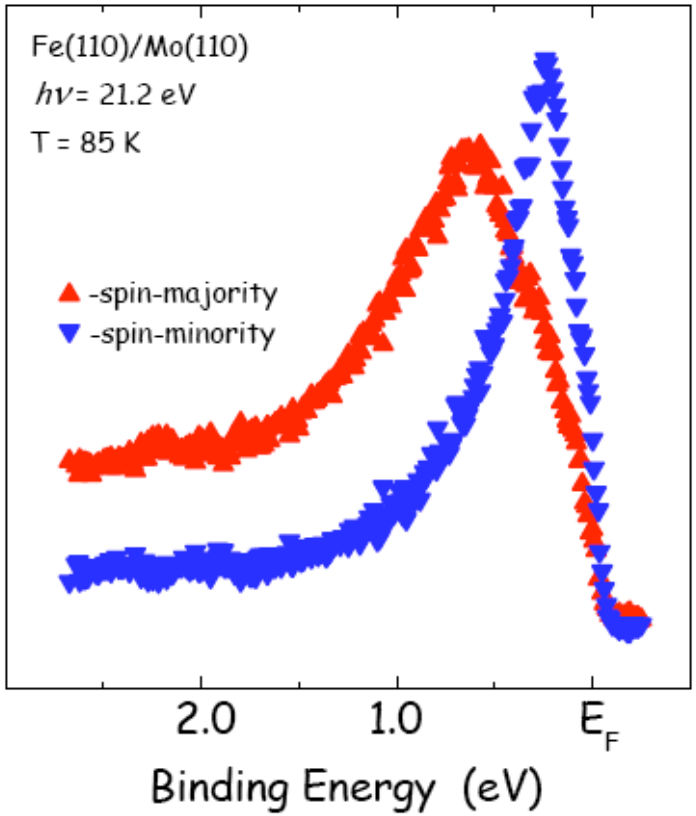

J. Osterwalder et al, (2005)

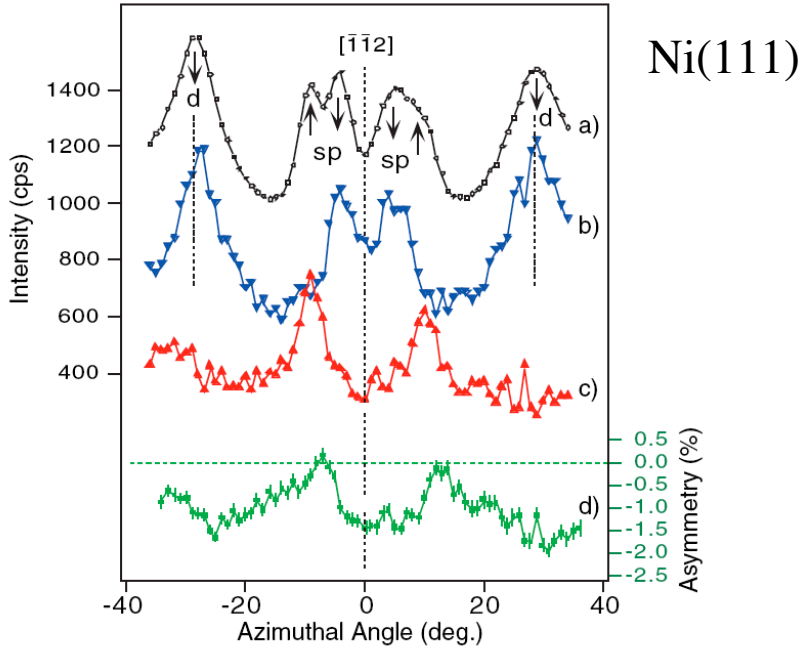

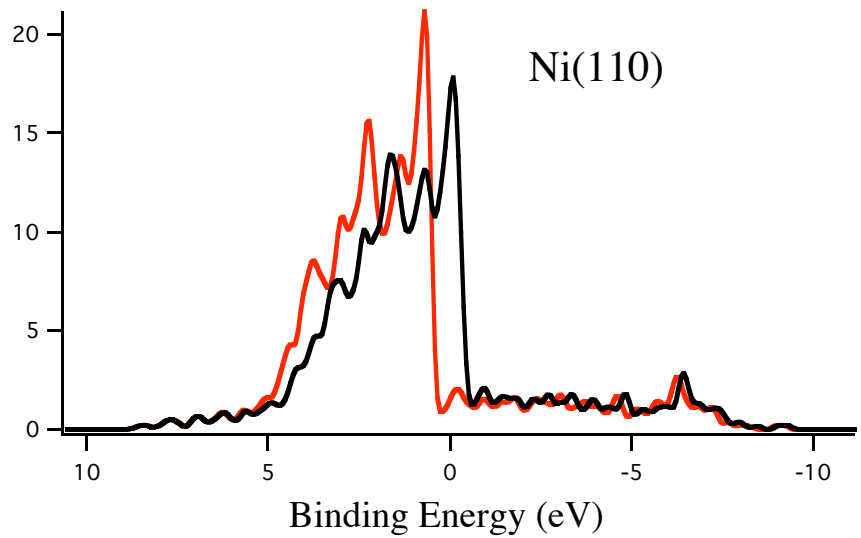

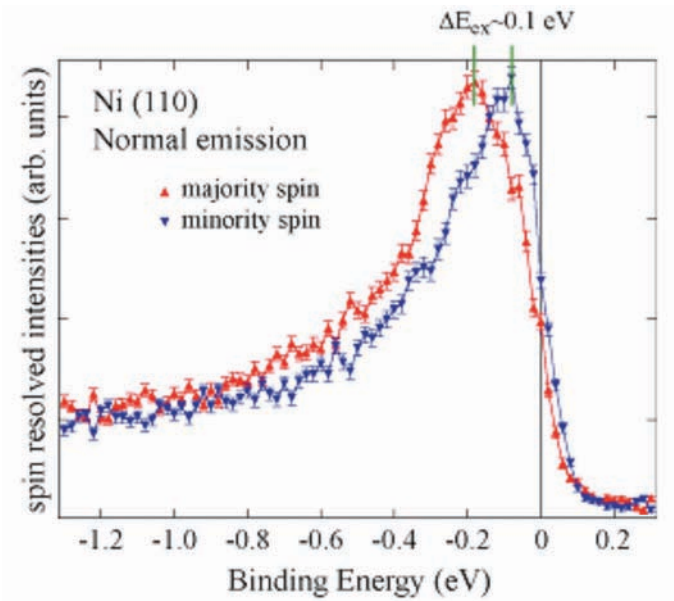

Rashba-Spin-Orbit Effect at Metal Surface States

J. Osterwalder et al, (2005)

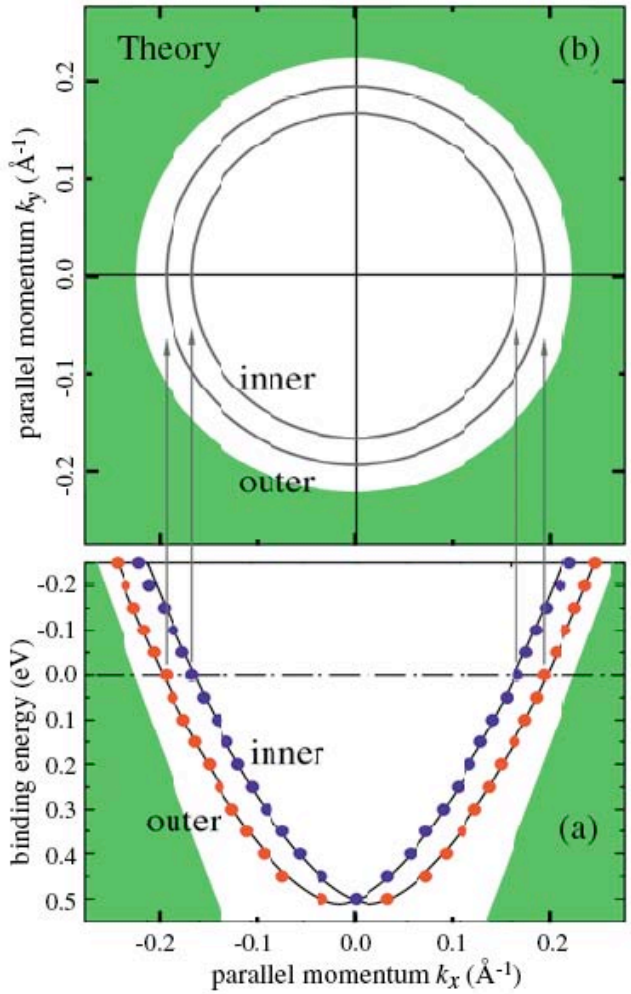

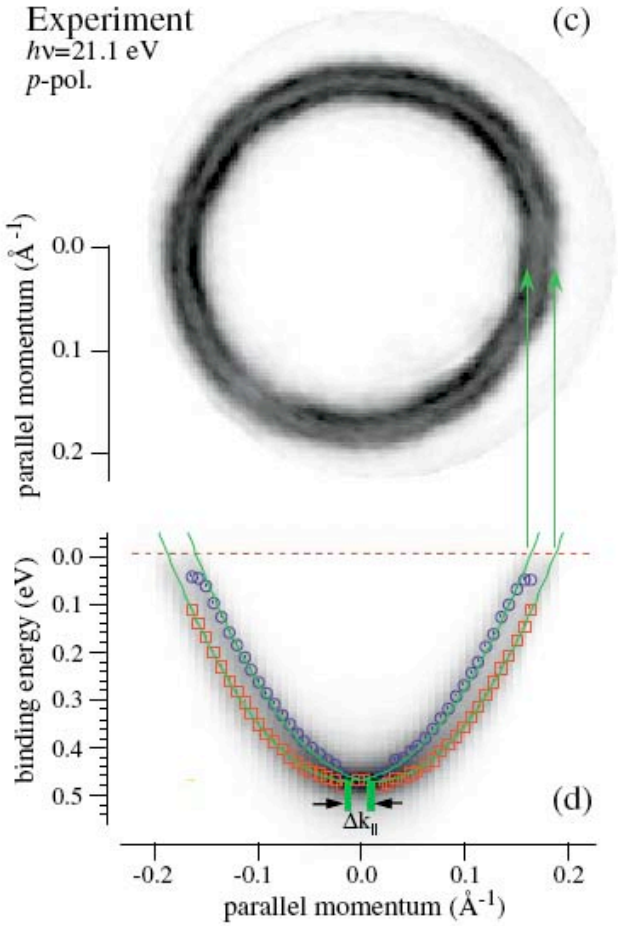

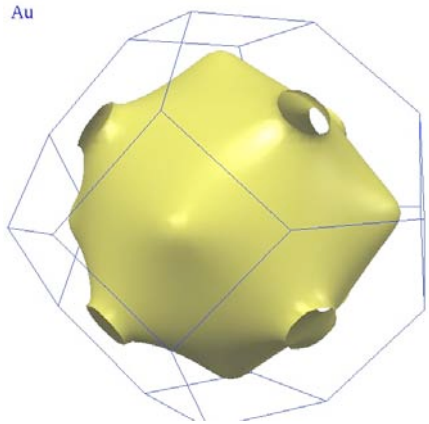

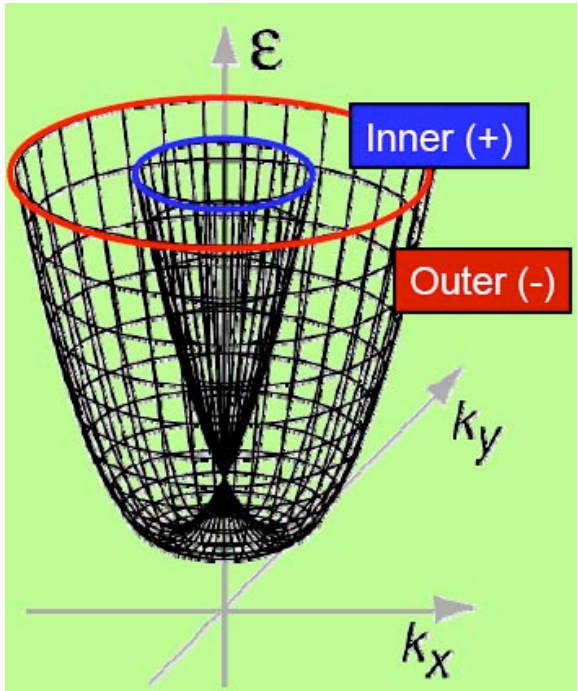

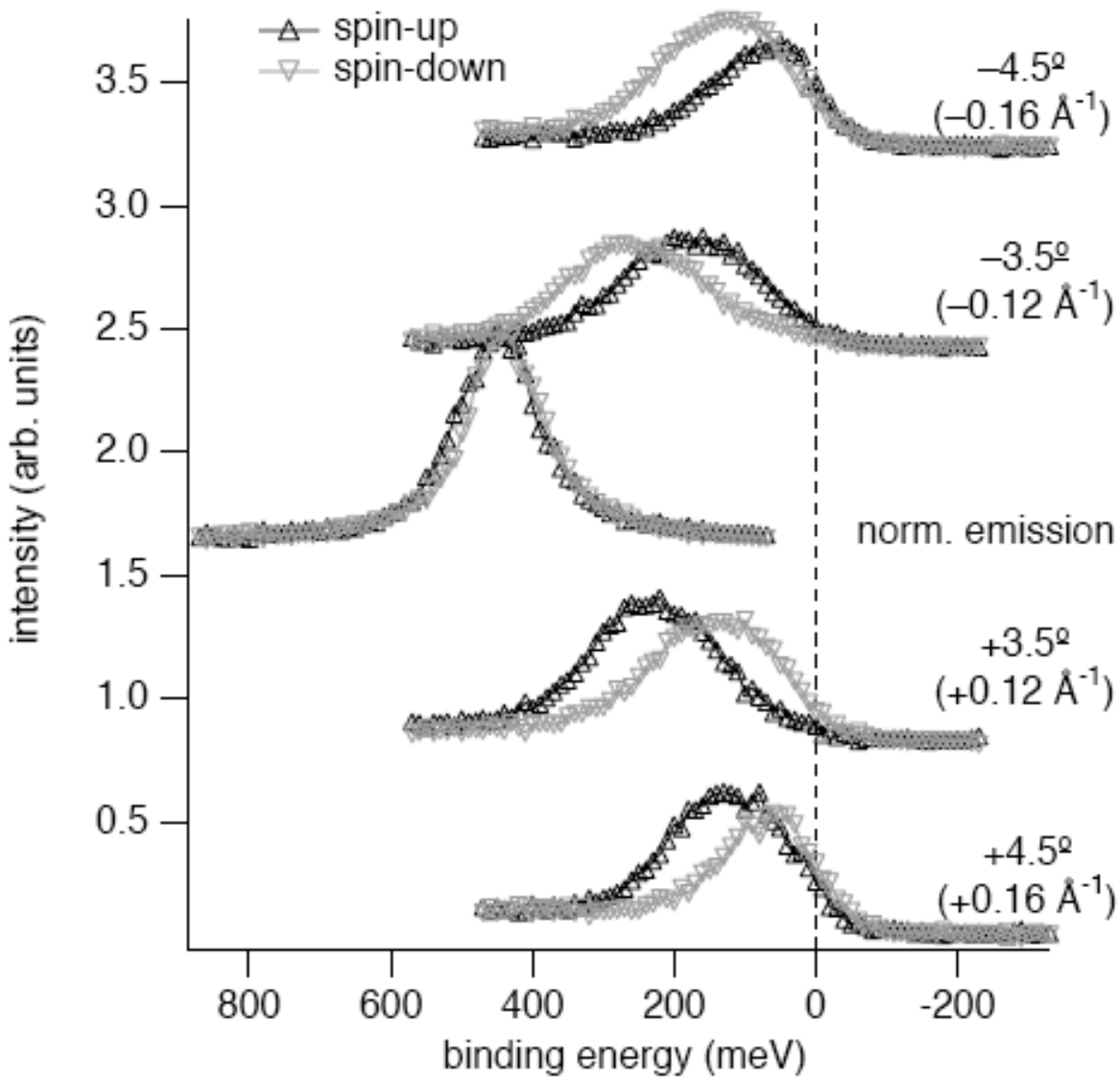
spin-up
spin-down
3.5
3.0
2.5
2.0
1.5
1.0
0.5
intensity (arb. units)
–4.5º
(–0.16 Å^{-1})
–3.5º
(–0.12 Å^{-1})
norm. emission
+3.5º
(+0.12 Å^{-1})
+4.5º
(+0.16 Å^{-1})
800
600
400
200
0
-200
binding energy (meV)

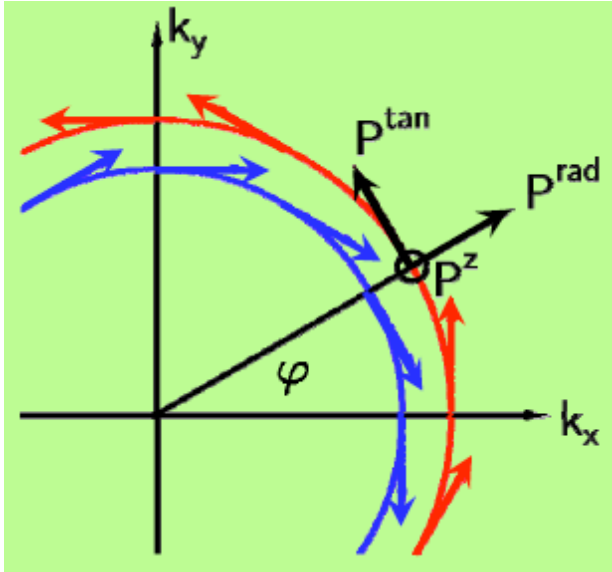
k_y
P^{tan}
P^{rad}
P^z
φ
k_x

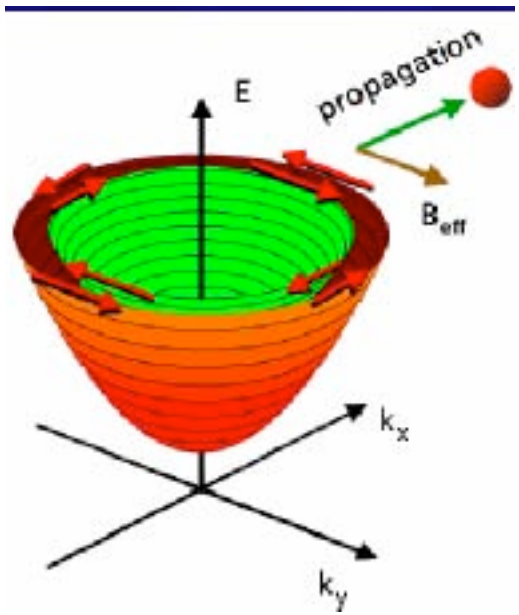
E
propagation
B_{eff}
k_x
k_y

Schematic diagram of near-gap optical transition for circularly polarized light

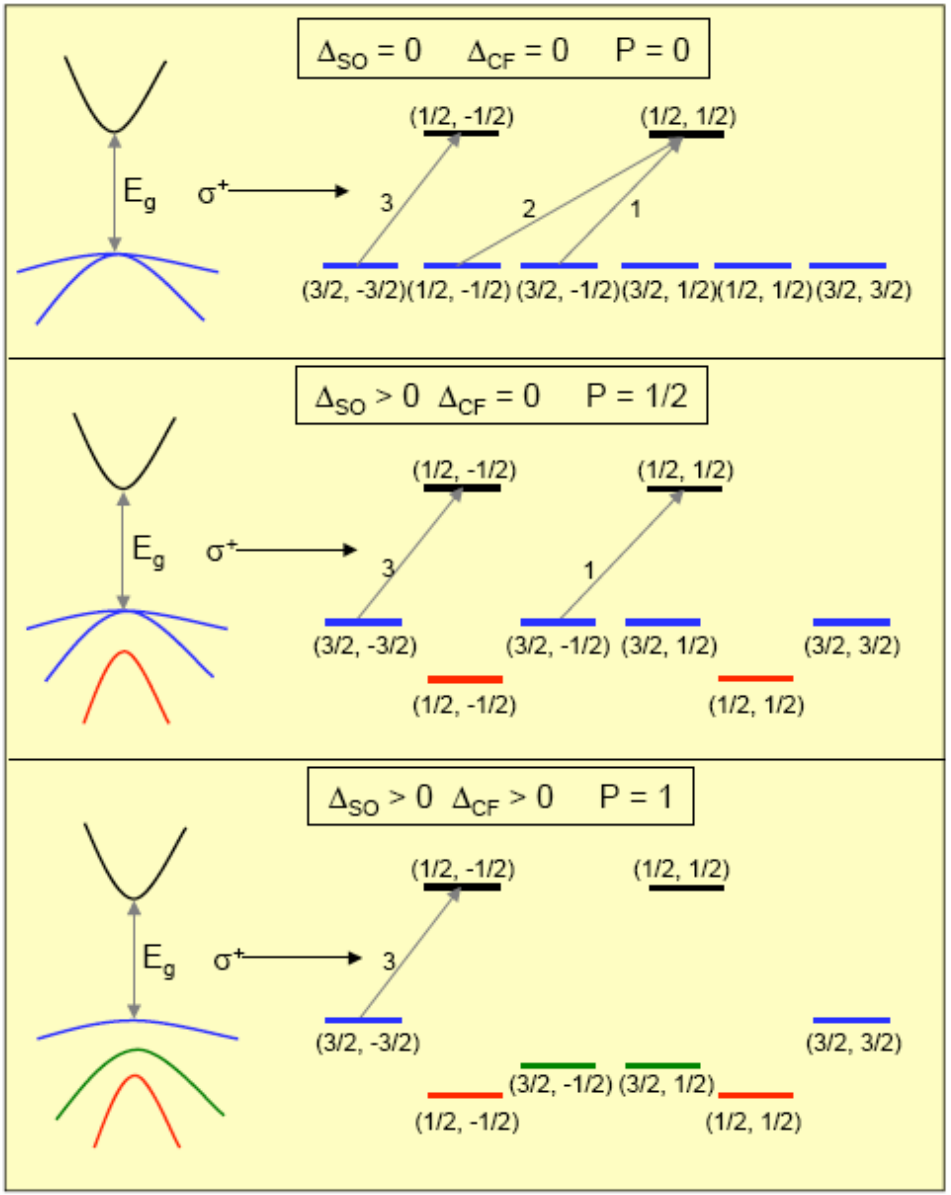

$$P = \frac{|I\downarrow - I\uparrow|}{|I\downarrow + I\uparrow|}$$

$$I = \left|\langle \Psi_f | H_{\text{int}} | \Psi_i \rangle\right|^2$$

$$H_{\text{int}} = X + iY \quad \text{for } \sigma^+ \text{ light}$$

Ideal material for SPES application

- Direct band gap
- Large spin-orbit splitting
- Large and positive crystal field splitting

Crystal Field splitting: Compressive strain in GaAs

P. Saez et al, IEEE (1996)

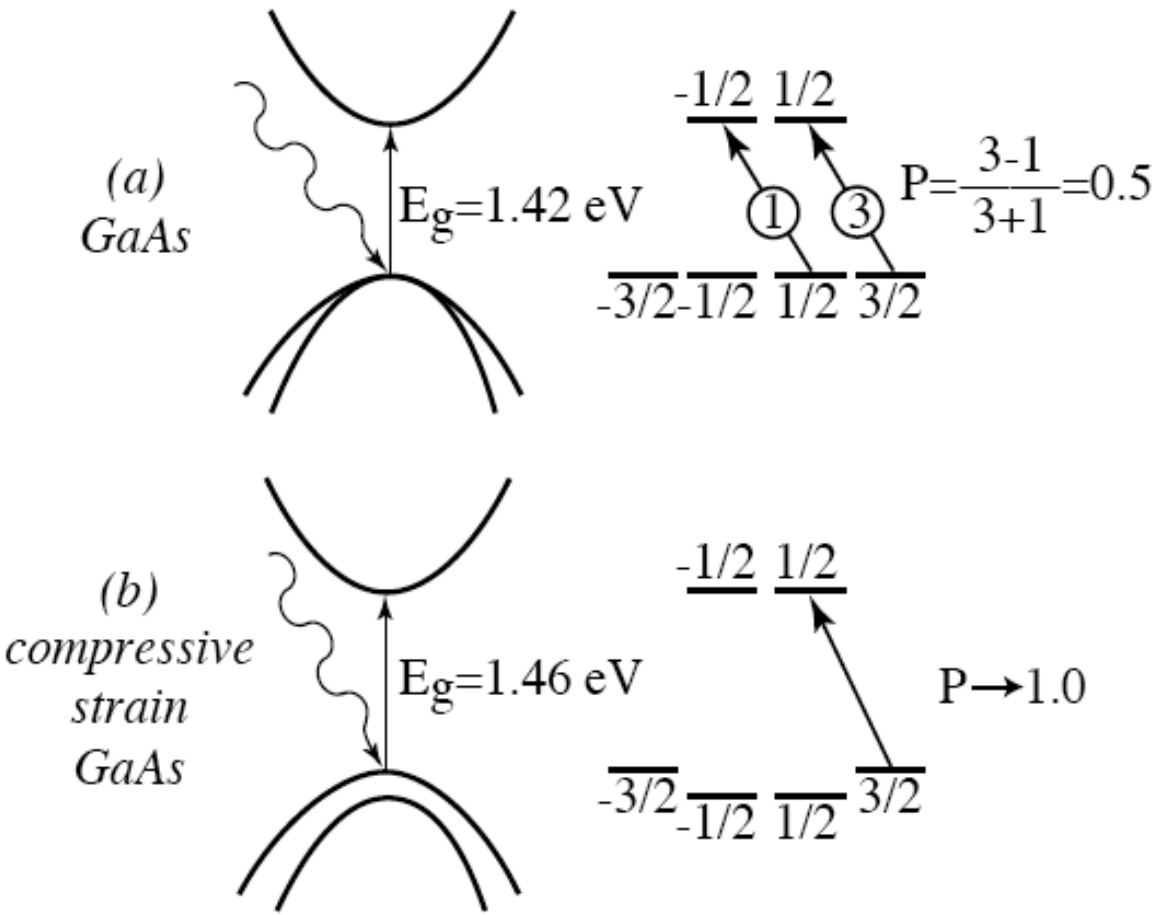

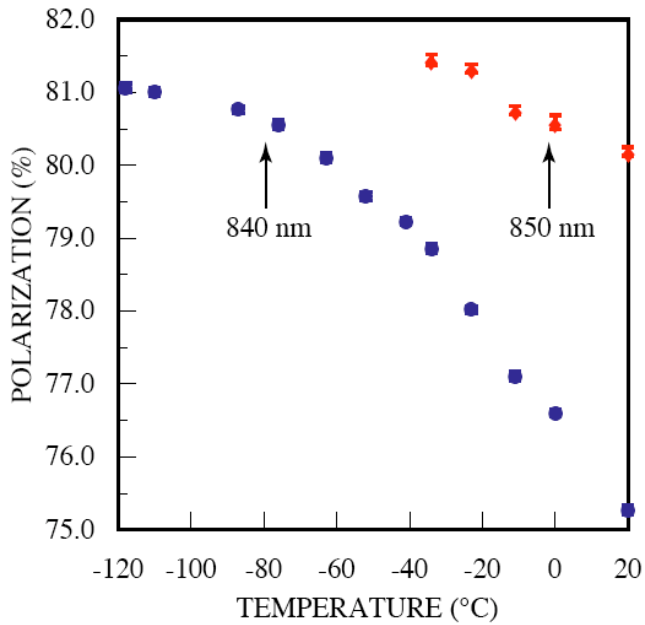

PES of GaAs and GaAs-based materials

- **Advantages:**

◆moderate even high polarization: *P* ~90% @ QE 0.5%

◆high brightness: 10^5 A/cm^2 · sr

◆good beam quality: small energy spreading etc.

◆polarization direction can be easily changed by reversing the helicity of the incident light

- **Disadvantages:**

◆*P* is only 20— 35% for bulk GaAs

◆low QE for strained superlattice GaAs-based material

◆Cs and O_2 activation to get "negative electron affinity" every hundreds of hours